Dissertation

Gesine Schmidt

Secondary Metabolites in the Arctic Sponge *Haliclona viscosa* – Spatial and Temporal Variation

Von der Fakultät für Lebenswissenschaften
der Technischen Universität Carolo-Wilhelmina
zu Braunschweig
zur Erlangung des Grades einer
Doktorin der Naturwissenschaften
(Dr. rer. nat.)
genehmigte

Dissertation

von Gesine Schmidt
aus Pößneck

Secondary Metabolites in the Arctic Sponge *Haliclona viscosa* — Spatial and Temporal Variation

Von der Fakultät für Lebenswissenschaften
der Technischen Universität Carolo-Wilhelmina
zu Braunschweig
zur Erlangung des Grades einer
Doktorin der Naturwissenschaften
(Dr. rer. nat.)
genehmigte
D i s s e r t a t i o n

von Gesine Schmidt
aus Pößneck

1. Referent: Prof. Dr. Thomas Lindel
2. Referent: PD Dr. Matthias Köck

eingereicht am: 30.06.2010
mündliche Prüfung (Disputation) am: 13.08.2010

Druckjahr 2010

Vorveröffentlichungen der Dissertation

Teilergebnisse aus dieser Arbeit wurden mit Genehmigung der Fakultät für Lebenswissenschaften, vertreten durch den Mentor der Arbeit, in folgenden Beiträgen vorab veröffentlicht:

Publikationen

1. G. Schmidt, A. Grube, M. Köck (2007). Stylissamides A-D — New Proline-Containing Cyclic Heptapeptides from the Marine Sponge *Stylissa caribica*. *Eur. J. Org. Chem.*, 4103-4110.

2. G. Schmidt, C. Timm, M. Köck (2009). New Haliclamines E and F from the Arctic Sponge *Haliclona viscosa*. *Org. Biomol. Chem.*, *7* (15), 3061-3064.

Tagungsbeiträge

1. A. Grube, G. Schmidt, M. Köck (2007). New Cyclic Heptapeptides and Pyrrole-Imidazole Alkaloids from the Caribbean Sponge *Stylissa caribica*. Poster PO36, Book of Abstracts pg. 110, 12$^{\text{th}}$ International Symposium on Marine Natural Products, February 4-9, Queenstown, New Zealand.

2. G. Schmidt (2007). Conformational Studies on Stylissamides, Cyclic Heptapeptides from *Stylissa caribica*. Talk, 5$^{\text{th}}$ European Conference on Marine Natural Products, September 15-22, Ischia, Naples, Italy.

3. G. Schmidt, A. Grube, S. Frickenhaus, M. Köck (2007). Conformational Studies on Stylissamides, Cyclic Heptapeptides from *Stylissa caribica*. Poster P44, Book of Abstracts pg. 141, 5$^{\text{th}}$ European Conference on Marine Natural Products, September 15-22, Ischia, Naples, Italy.

4. G. Schmidt (2008). MALDI – Characterizing the Chemistry of Sponge Powder. Talk, Bahamas Cruise.

5. G. Schmidt, C. Cychon, M. Köck (2008). Secondary Metabolites in Marine Sponges; Qualitative and Quantitative Variation over Time. Poster, AWIPEV-Workshop Bremen, Germany.

6. G. Schmidt (2009). Secondary Metabolites in the Arctic Sponge *Haliclona viscosa*; Spatial and Temporal Variation. Talk, May 21, Oldenburg, Germany.

7. G. Schmidt and M. Köck (2009). Study of the MS-Fragmentation of the Haliclamines. Poster PC18, Book of Abstracts pg. 89, 6th European Conference on Marine Natural Products, July 19-23, Porto, Portugal.

8. C. Cychon, G. Schmidt, M. Köck (2009). MALDI-TOF-MS, a Suitable Method for Metabolite Screening? Poster PC25, Book of Abstracts pg. 96, 6th European Conference on Marine Natural Products, July 19-23, Porto, Portugal.

Jeder dumme Junge kann einen Käfer zertreten. Aber alle Professoren der Welt können keinen herstellen.

(Arthur Schopenhauer)

Contents

Glossary

3-APA 3-alkyl pyridinium- or 3-alkyl tetrahydropyridine alkaloid

ACN acetonitrile

ArW Arctic Water

AW Atlantic Water

BuOH *n*-butanol

CID collision induced dissociation

cPro *cis*-proline

DAD diode array detector

DCM dichloromethane, methylene chloride

DGGE denaturing gradient gel electrophoresis

DMSO dimethylsulfoxide

DNA desoxyribonucleic acid

EI electron impact ionisation

ELSD evaporative light scattering detector

ESI electrospray ionisation

EGC East Greenland Current

EIC extracted ion chromatogram

ESC East Spitsbergen Current

EtOH ethanol

HCCA α-cyano-4-hydroxycinnamic acid

HMBC heteronuclear multiple bond correlation

HPLC high performance liquid chromatography

HRMS high resolution mass spectrometry

LCMS liquid chromatography – mass spectrometry

LCMS/MS liquid chromatography – tandem mass spectrometry

MALDI matrix-assisted laser desorption/ionisation

MeOH methanol

MS mass spectrometry

NAC North Atlantic Current, "Gulf Stream"

NMR nuclear magnetic resonance

TOF time of flight mass spectrometer

PI peak integral (given in % relative to the monoisotopic peak)

Pyr pyridine

rDNA ribosomal desoxyribonucleic acid

RP-TLC reversed phase thin layer chromatography

S salinity

SCUBA self-contained underwater breathing apparatus

T temperature

TAW Transformed Atlantic Water

TFA trifluoroacetic acid

THP tetrahydropyridine

TLC thin layer chromatography

tPro *trans*-proline

WSC West Spitsbergen Current

1 Introduction

All living organisms produce so-called natural products, bioactive chemicals or metabolites that are essential for the organisms' survival.[1] The natural products are divided into primary and secondary metabolites.[2] Primary metabolites include, among others, amino acids, sugars, and enzymes, compounds that are needed for the growth and reproduction of cells and whole organisms.[3] They are produced by the same biochemical pathways in all organisms.[4] Secondary metabolites, on the other hand, are metabolites that are not directly involved in the organism's survival. However, they often possess biological activity thus giving the organisms an advantage over competitors and may therefore promote survival. They are often species- or genus specific[5], which, together with the high biodiversity of organisms producing secondary metabolites like plants, animals, fungi, bacteria, has lead to a wide variety of different secondary metabolites.

The organisms that produce bioactive or otherwise interesting secondary metabolites have always fascinated humans. Their use can be dated back to the hunters in Stone Age Europe who knew e.g. about the toxicity of banewort (*Atropa belladonna*) and henbane (*Hyoscamus niger*) and used their plant saps as arrow poison.[6] Chinese, Indian, Egyptian and Celtic traditional medicines know treatments based on plant, fungi or animal products that contain bioactive secondary metabolites and exact reports about the preparation of remedies still exist today as some of the oldest written records.[7] Also the monastery gardens that developed in Medieval Europe are a testimony of the profound knowledge about medicinal plants and their remedy usage which had been collected and exchanged during travels throughout the known world.[8]

But natural products are not only interesting for their medicinal uses. Organic colors like indigotin (**1**) from the tree *Indigofera tinctoria*, Tyrian purple (**2**) obtained from the marine snails *Murex brandaris* and *M. trunculus*, carminic acid (**3**, E120) produced by the cactus-dwelling scale insect *Dactylopius coccus*, and crocin (**4**) from the saffron flower *Crocus sativus* have become inherent parts of human life as fabric dyes and food additives; natural rubber as well as the development of vulcanization techniques and synthetic rubber as a substitute has strongly promoted the automobile industry; insect pheromones play a role in insect attractants/repellents used in agriculture[9] or human households[10] and, more recently, in the development of pest-resistant genetically modified organisms.[11,12]

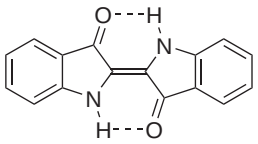

Indigotin (**1**)

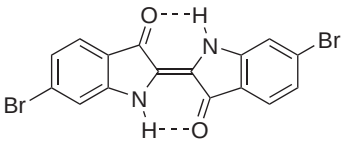

Tyrian Purple (**2**)

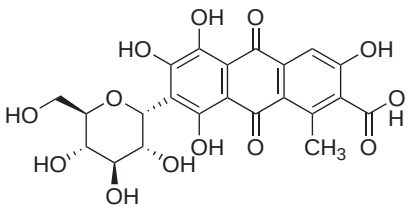

Carminic Acid (**3**)

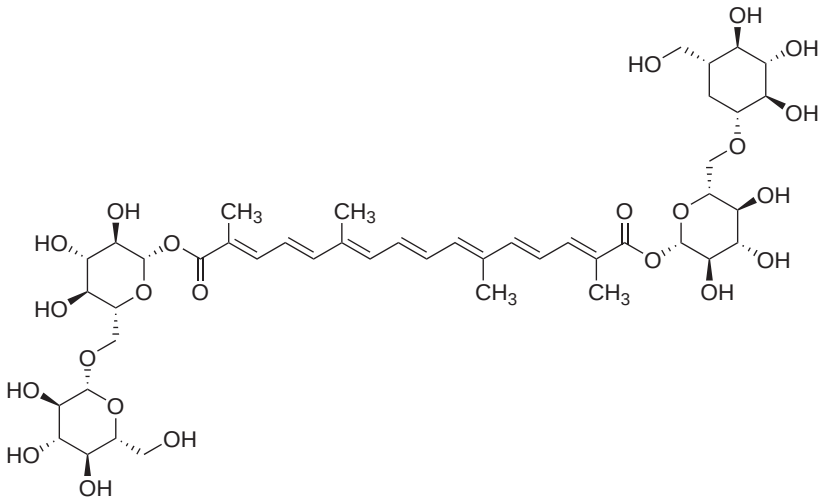

Crocin (**4**)

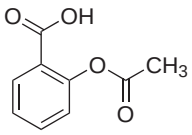

ASA (**5**)

Until the beginning of the 19th century however, little was known about the active ingredients in the organisms of use. One of the early successes in natural product research was the isolation and structure elucidation of salicin in 1828 from the bark of the white willow (*Salix alba*)[13] which had been known for its pain killing and fever reducing properties. Conversion of salicin to salicylic acid and later

into acetylsalicylic acid (**5**, ASA) yielded a potent analgesic and antipyretic remedy known under the trade name Aspirin™. Other famous natural product-derived drugs are morphine (**9**),[14] quinine (**7**),[15] cocaine (**8**),[16] the penicillins (**6**),[17] and cardiac glycosides like digoxin (**10**, digitalis).[18] But although Aspirin™ is the most widely used analgesic and antipyretic drug in the world since 1899, the complete process of isolation (1828)[13], characterisation (1869)[19] and the finding of its mode of action (1975)[20] took more than 100 years. However, with the progress in the field of chemistry, analytical methods improved in scope and sensitivity and today, the process of isolation and structure elucidation may take less than a year while at the same time natural resources can be preserved.[21]

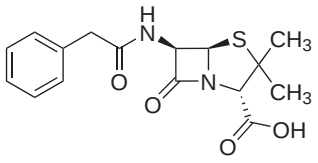

Penicillin G (**6**)

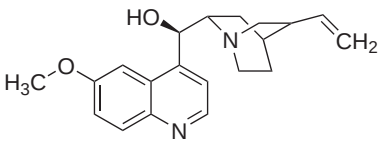

Quinine (**7**)

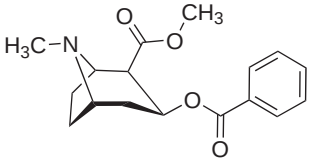

Cocaine (**8**)

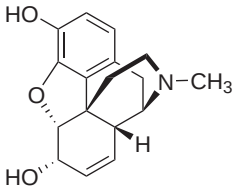

Morphine (**9**)

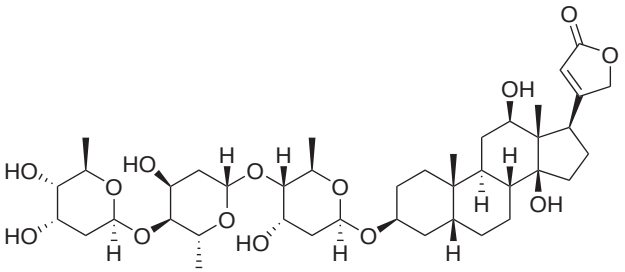

Digoxin (**10**)

After the isolation of bioactive compounds had concentrated on terrestrial plant, fungi and animal sources to elucidate the active component of traditional remedies, the focus was expanded to marine sources in the 1970s.[22] This trend went along with the development of the self-contained underwater breathing apparatus (SCUBA) which allowed observation and directed selection of organisms from under the water surface. Research in the marine sector concentrated on sessile organisms, based on the theory that sessile organisms like sponges, soft corals, ascidians, bryozoans, gorgonians etc., in contrast to mobile ones, have a stronger need to produce bioactive compounds to defend themselves against predators since they cannot escape or hide.[23] Many sessile marine organisms however, live in symbiosis with other organisms like bacteria or algae, and in many cases it was shown that e.g.

symbiotic bacteria instead of the host sponge produce the active metabolites.[24–27] This mutualistic relationship provides a benefit for both partners; the host is chemically protected against predators by metabolites produced by the symbiont while the symbiont is mechanically protected by the body structure of the host.

The finding that microscopic symbionts produce secondary metabolites promoted a new field of study, the isolation of secondary metabolites from bacteria, microscopic fungi or algae. While sessile organisms cannot be exploited from natural sources in industrially utilizable amounts and are often not suited for cultivation, many microscopic organisms can be cultured under laboratory conditions and the metabolites can thus be produced in the desired quantities.[28]

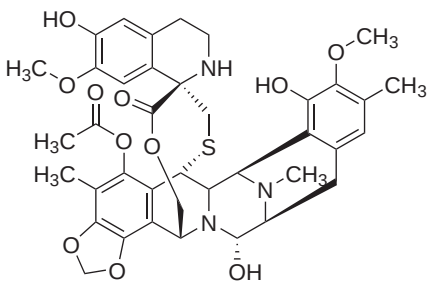

Ecteinascidine-743 (**11**)

In cases where cultivation in a laboratory is not possible, synthetic preparation of the secondary metabolites can supply material for industrial purposes or preclinical and clinical trials. Synthesis, however, is still a major challenge since many natural products possess complex structures with often multiple stereogenic centers or ring systems and develop the desired bioactivity only with stereochemical specificity. This may be one of the reasons why relatively few marine natural products have found their way into pharmaceutical use. However, a few examples exist that have successfully passed clinical trials and have been approved by the medical authorities; ziconitide (Prialt™, ω-conotoxin MVIIA),[29,30] the toxin of the marine cone snail *Conus magus* was accepted as an analgesic in 2004, and ecteinascidine 743 (**11**, Yondelis™, ET-743, trabectedine),[31,32] from the ascidian *Ecteinascidia turbinata*, was approved as an anti-cancer drug in 2007. Several others are currently in clinical trials, most of them as anti-cancer drugs.[33]

1.1 Sponges

Sponges (phylum Porifera) as a very diverse group of sessile aquatic organisms that often live in densely inhabited environments evoked the interest of scientists already at an early stage of marine natural products research. After nearly 40 years of investigation, they are today thought to contain the largest diversity of marine natural products.[34]

Sponges represent the simplest and most primitive of multicellular animals. Their cells are specialized for different functions, such as support, feeding, or reproduction, but they do not form complex organ structures like the cells of higher animals. They are mostly[1] filter-feeding animals that draw water into their central cavity through numerous tiny pores (ostia, Figure 1.1) all over the body surface, and expel it through the outlet vents (oscula), which are more obvious and fewer in number. Constantly beating flagellated cells (choanocytes) that sit in the cavity walls create the water current and at the same time strain fine food particles from the water that nourish the sponge. Tiny needles (spicules) of calcite or silicate, or fibers of a horny material (spongin) stiffen the body.[37,38] Sponges that possess calcite spicules belong to the class Calcarea while those that contain silicate spicules belong to the Hexactinellidae or Demospongiae; Demospongiae build the largest and most diverse group and contain approximately 85% of the recent species.[38] They are found in all oceans as well as in freshwater.

Sponges can defend themselves by physical or chemical means. Large or barbed spicules effectively deter feeding action imposed on sponges e.g. by fishes and turtles.[39] However, many sponge species do not possess apparent physical defenses but still assert themselves well against predators. An alternative to physical defenses are physical compensation mechanisms like high growth-, "healing-", or reproduction rates to compensate for the loss of tissue imposed by predators. Low nutritional value of the tissue makes some sponge species less susceptible to spongivores.[40] In addition, sponges accumulate a large amount of potentially pathogenic microorganisms in their body by their filter feeding activity. Since microorganisms are unaffected by

1 Exceptions from this filter-feeding life style are the carnivorous sponges that are found in deep caves or the deep ocean. These sponges are passively captivating prey by means of filaments covered with spicules, then engulf the entire prey with their own body and digest the organic material. An example is *Asbestopluma hypogea* found in a cave in Brittany, France.[35,36]

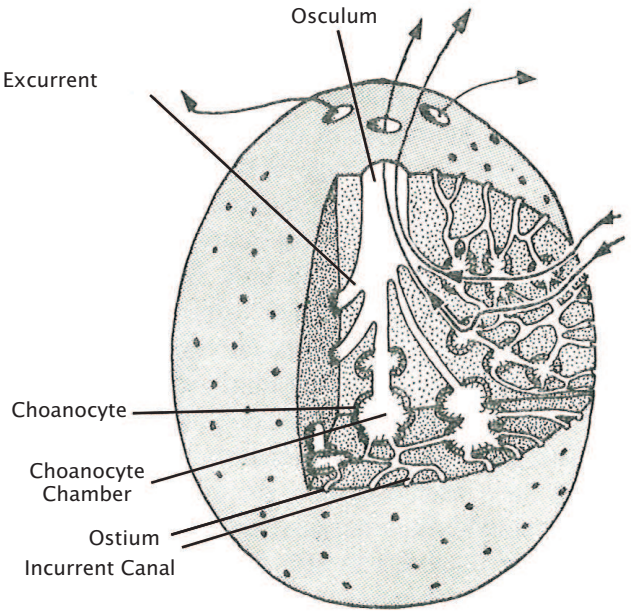

Figure 1.1 Schematic body plan of a sponge of the class Demospongiae; arrows indicate the direction of the water flow; modified from P.R. Bergquist (1978).[37]

physical defenses, many species produce antimicrobial or feeding deterrent secondary metabolites to counter the risk of infection and to fortify physical defenses.[41] In fact, sponges have been the major source of new secondary metabolites isolated from the marine environment since the beginning of natural products research.[42] Many of these compounds exhibit high pharmacological potential as antitumor agents, antibiotics, anti-inflammatory agents, etc.,[43] but scientists have also focused on revealing their ecological roles.[44,45]

Since the most densely populated areas are located in the tropics, the hypothesis has shaped that predation pressure is higher in the tropics than in temperate areas and consequently that tropical sponges[46] as well as e.g. holothurians[47] and algae[48,49] are chemically better defended than temperate ones. However, there are also examples that contradict this hypothesis,[50] which indicates that defense strategies cannot be generalized but that each species must be considered according to its habitat and predator-prey relationship.

1.2 Secondary metabolites as environmental markers

As a consequence, secondary metabolites may not only be appreciated for their pharmaceutical potential but also be used as environmental markers. On one hand, the metabolite composition of an organism is often genus- or species specific [51–53]; secondary metabolites can therefore be consulted to identify organisms to the genus or species level given that detailed information is available on the secondary metabolites present or absent in the species. While several studies examine the potential of secondary metabolites as chemotaxonomic markers (e.g. the works of Ciminiello et al. on Verongida sponges [54–62]), comparatively few studies address the spatial and temporal variation in composition and concentration of secondary metabolites in sponges [63] and the influence of environmental factors. [64,65] This information however, is equally important to estimate the value of specific marker compounds.

On the other hand, most authors discuss the presence of secondary metabolites on the basis of biotic factors such as predator-prey relationship, competition and antifouling [66] while there are also multiple abiotic factors to consider. Such factors can be the light intensity, salinity, water temperature, currents that transport nutrients and food particles, sediment load etc. which may have strong effects on the organism's metabolism. For example, low light intensity seems to stimulate several sponge species to produce more toxic metabolites. [67,68] At the same time the metabolite quantity changes with season [68] which might be linked to the reproductive or nutrition status of the sponge. Lindquist and Hay [69] as well as McClintock and Baker [70] report several Caribbean and Antarctic sponge larvae to be unpalatable to fish. Since the larvae do not contain morphological defense structures they conclude that the larvae must be chemically defended. This invites speculation on secondary metabolites contained already in sponge eggs which would be present in the "mother" sponge body. High sediment rates influence the pumping rate in the sponge *Aplysina lacunosa* and since most of the vital activities of a sponge, such as feeding, respiration and release of sexual products depend upon a water flow, sediment load in the water can strongly influence the organism's fitness and energy available to produce secondary metabolites. [71]

If the metabolite production is influenced by environmental parameters then the qualitative and/or quantitative metabolite composition is expected to change

with changing environmental conditions. Therefore, the monitoring of secondary metabolites of key species can give information about the condition of the organisms and can be used, together with other parameters and observations, as an indicator for change happening in the ecosystem.

The aim of this thesis is to investigate the differences in secondary metabolites of the sponge species *Haliclona viscosa* between two different habitats, the Orkneys and Spitsbergen; at the same time, the study addresses variations of the metabolites between different years and within the year. Since taxonomic differentiation of *Haliclona* species is difficult, the investigation tests various chemical, taxonomical and biological methods to answer the question whether the populations of sponges identified as *Haliclona viscosa* in the Orkneys and Spitsbergen are the same species. The chemical analysis also involves the identification of new secondary metabolites.

2
Summary and Outlook

In the course of this thesis, a total of 67 *Haliclona* individuals assigned to four different *Haliclona* groups[1] from Spitsbergen and the Orkneys were subject to a compound screening. None of the Orkney samples and only two of the Spitsbergen specimens yielded 3-alkyl pyridinium- or 3-alkyl tetrahydropyridine alkaloids (3-APAs). Since the identification of *Haliclona* individuals to the species level can be difficult, different chemical and biological approaches tried to supplement classical taxonomic identification of the sponges. Thin layer chromatography was a helpful tool to identify 3-APA containing individuals in proximity to the sampling site. Matrix assisted laser desorption/ionization mass spectrometry (MALDI-MS) also proved to be useful to identify 3-APA containing *Haliclonas* by a fast and universal crude extract screening, but both methods were unsuitable for sponges with low abundance of secondary metabolites. In addition, structure elucidation by MALDI-MS was hampered by the limits of the method in small molecule research and taxonomic identification of sponges was difficult by the absence of comparative databases. A study to overcome these difficulties is in progress. In the future, the usage of other environmental markers such as e.g. sponge specific sterols should be considered.

The sponge identification by biological methods concentrated on the direct phylogenetic relationship of the sampled sponge individuals and on the composition of the bacterial community. This study was performed by external researchers.

1 Since the species assignment is difficult in the *Haliclona* sponges examined for the present thesis, sponges were arranged in taxonomic "groups" according to important, though not necessarily diagnostic, taxonomic characteristics.

While the results for the direct relationship of the sponges are still in progress, DNA studies of the *Haliclona* sponges from Spitsbergen yielded a relationship with other *Haliclonas* sampled in cold water. Further identification was not possible due to limited database entries. The bacterial community was found to reflect the habitat in which the sponge lived, with predominantly sediment-associated bacteria for *Haliclonas* that had been samples in turbid water, and clearly sponge-associated bacteria in *Haliclona* that lived in oceanic environments. The similarities and differences observed for the bacterial community of the different *Haliclona* groups was reflected in their chemical profiles obtained by chromatographic methods.

Investigation of the compound variation in *Haliclona viscosa* from Spitsbergen between 1999 and 2009 showed a significant change in the metabolite composition between 2001 and 2003. All *H. viscosa* sponges sampled before 2003 contained 3-alkyl pyridinium compounds while the specimens collected in 2003 and 2009 almost only contained 3-alkyl tetrahydropyridine alkaloids. The results were discussed in view of environmental factors but could not be manifested due to lack of environmental data from the sampling area. To extend our knowledge on the mechanisms underlying the production of 3-APAs in *Haliclona viscosa*, the sampling in the Kongsfjord should be extended over the period of the presented thesis. The aim should be on sampling several individuals at different times within a year, e.g in early spring and later autumn as well as the sampling of multiple 3-APA containing individuals from the fjord. Also the monitoring of one sponge individual over several years should be considered.

The metabolite screening of *Haliclona viscosa* yielded 21 3-alkyl pyridinium alkaloids whose structure was unknown before (haliclocyclin C, haliclamine K and J, dehydro-haliclamine J, dehydro-viscosaline E_1, viscosamine D, dehydro-viscosamine C and D) or had previously been suggested and could be refined or confirmed (haliclocyclin F_1, haliclamine E and F, dehydro-haliclamine C, D, F, ambidehydro-haliclamine F and didehydro-haliclamine D, viscosaline B_1, B_2, E_1 and E_2, viscosamine B). The structure identification of haliclamines based on a mass spectrometric fragmentation study of the haliclamines that forms part of this thesis and is enclosed in manuscript form to be published (page 183). New viscosalines and viscosamines were identified by evaluation of the high resolution mass spectra of a known viscosaline and viscosamine, and the observations concerning their fragmentation behavior are described in the presented thesis. Structure elucidation of 3-APAs that contain double bonds in the alkyl chains is in progress, as is the

structure elucidation of still unknown 3-APAs in the crude extract eluting before 12 min and after 23 min.

The identification of a number of haliclamines, one viscosaline and two viscosamines with unsaturated alkyl chains confutes the hypothesis that *Haliclona* sponges in warmer waters yield more 3-APAs with unsaturated alkyl chains. Although the screening revealed viscosamines with longer chains than had been published from warmer waters, the hypothesis that alkyl chains tend to be longer in cold water *Haliclonas* cannot be confirmed or rejected for the lack of comparative organisms.

In the progress of developing a method that allows metabolite screening of different sponges by MALDI-MS, the Caribbean sponge *Stylissa caribica* was found to possess previously unknown compounds which were identified as the new cyclic heptapeptides stylissamides A-D. The stylissamides are very rich in proline and especially stylissamide B shows an interesting combination of amino acids, with three out of four prolines being arranged consecutively. Imposed by this configuration, the NMR signals of the stylissamides overlapped strongly but the structure elucidation could finally be achieved by a combination of extensive NMR and MS experiments.

Zusammenfassung und Ausblick

Im Rahmen dieser Arbeit wurden 67 einzelne *Haliclona* Schwämme, die vier verschiedenen Gruppen[2] aus Spitzbergen und den Orkneys zugeordnet wurden, einem Metabolitenscreening unterzogen. Keine der Orkney- und nur zwei der Spitzbergenproben enthielten 3-Alkylpyridinalkaloide (3-APAs). Da die Identifizierung von *Haliclona* Schwämmen bis zur Artebene schwierig sein kann, wurde die klassisch-taxonomische Identifizierung der Schwämme durch chemische und biologische Methoden unterstützt. Dünnschichtchromatographie erwies sich als nützliche Methode, um Individuen schon in der Nähe der Probennahmestelle (d.h. nicht erst im möglicherweise weit entfernten Analyselabor) auf das Vorhandensein von 3-APAs zu untersuchen. Massenspektrometrie, die Matrix-unterstützte Laser Desorption/Ionisation als Ionisierungsmethode verwendet (MALDI-MS), zeigte sich ebenfalls als nützliche Methode, um durch ein schnelles und universelles Screening des Rohextrakts 3-

2 Da die Artzuordnung in den untersuchten *Haliclona*-Schwämmen schwierig ist, wurden die Schwämme taxonomischen "Gruppen" zugeordnet. Die Gruppenzuordnung stützte sich auf taxonomisch wichtige, ggf. aber nicht diagnostische, Charakteristika.

APA beinhaltende Organismen zu identifizieren. Beide Methoden waren jedoch ungeeignet, Schwämme mit generell niedriger Menge an Sekundärmetaboliten zu klassifizieren. Zusätzlich war die Strukturaufklärung mit Hilfe von MALDI-MS erschwert, da die Methode für kleine Moleküle nicht optimal ist, und für die taxonomische Identifizierung von Schwämmen entsprechende Datenbanken fehlen. Eine Studie ist in Arbeit, die die Überwindung dieser Schwierigkeiten zum Ziel hat. Für zukünfige Studien sollte in diesem Zusammenhang auch die Verwendung anderer Umweltindikatoren, wie zum Beispiel die Zusammensetzung schwammspezifischer Sterole, in Betracht gezogen werden.

Die Schwammidentifizierung durch biologische Methoden konzentrierte sich auf die direkten phylogenetischen Verwandtschaften der untersuchten Schwämme und auf die Zusammensetzung ihrer Bakteriengemeinschaften. Dieser Teil der Studie wurde von externen Wissenschaftlern durchgeführt. Die Ergebnisse zum gegenseitigen Verwandtschaftsverhältnis der Schwämme sind noch in Arbeit, die DNA Studien zeigten aber eine enge Verwandtschaft mit anderen Kaltwasser-*Haliclonas*. Eine genauere Identifizierung war aufgrund fehlender Datenbankeinträge nicht möglich. Die Bakteriengemeinschaft spiegelte den Standort wider, an dem der Schwamm lebte. In Schwämmen, die aus schwebstoffreichem Wasser entnommen wurden, überwogen Sediment-assoziierte Bakterien, während Schwämme, die von Stellen stammten, die von ozeanischem Wasser geprägt waren, auch Schwamm-assoziierte Bakterien zeigten. Die Ähnlichkeiten und Unterschiede, welche die Bakteriengemeinschaften der verschiedenen *Haliclona*-Gruppen aufwiesen, wurden in den chemischen Profilen der Rohextraktchromatogramme dieser Schwämme wiedergefunden.

Die Untersuchung der Metaboliten-Variabilität in *Haliclona viscosa* von Spitzbergen zwischen 1999 und 2009 ergab eine deutliche Veränderung der Metabolitenzusammensetzung zwischen 2001 und 2003. Alle vor 2003 gesammelten *H. viscosa* besitzen 3-Alkylpyridinalkaloide während in den Proben aus 2003 und 2009 fast ausschließlich 3-Alkyltetrahydropyridine zu finden sind. Diese Ergebnisse werden mit Hinblick auf beeinflussende Umweltfaktoren diskutiert, eine abschließende Klärung konnte aber wegen mangelnder Umweltdaten von den Probennahmestellen nicht erzielt werden. Um unser Wissen über die zugrundeliegenden Mechanismen der 3-Alkylpyridinalkaloid-Produktion in *Haliclona viscosa* zu vertiefen, sollte die Beprobung von Schwämmen im Kongsfjord über den Zeitraum der vorgelegten Arbeit ausgedehnt werden. Ziel sollte es sein, eine jährliche Probennahme durchzuführen, bei der mehrere 3-Alkylpyridinalkaloid-enthaltende Schwämme zu mehreren Zeit-

punkten des Jahres, z.B. im frühen Frühjahr, Sommer, und späteren Herbst beprobt werden. Auch das Beobachten eines einzelnen Schwammindividuums über mehrere Jahre wäre sinnvoll.

Das Metabolitenscreening in *Haliclona viscosa* ergab 21 3-Alkylpyridinalkaloide, deren Struktur vormals unbekannt war (Haliclocyclin C, Haliclamine K und J, dehydro-Haliclamin J, dehydro-Viscosalin E_1, Viscosamin D, dehydro-Viscosamin C und D), oder deren Struktur suggeriert war und nun weiterenwickelt oder bestätigt werden konnte (Haliclocyclin F_1, Haliclamine E und F, dehydro-Haliclamine C, D, F, ambidehydro-Haliclamine F und didehydro-Haliclamine D, Viscosalin B_1, B_2, E_1 und E_2, Viscosamin B). Die Strukturaufklärung der Haliclamine basierte auf einer Studie zur massenspektrometrischen Fragmentierung der Haliclamine, die auch Teil dieser Arbeit ist und in einreichbarer Manuskriptform beigelegt wird (Seite 183). Die neuen Viscosaline und Viscosamine wurden durch die genaue Analyse von hochauflösenden Massenspektren eines bekannten Viscosalines und Viscosamines identifiziert. Die neuen Beobachtungen zum Fragmentierungsverhalten dieser Verbindungen sind Teil dieser Arbeit. Die Strukturaufklärung von 3-APAs mit ungesättigten Seitenketten ist in Arbeit, genauso wie die Aufklärung der noch unbekannten Verbindungen, die im Rohextrakt vor 12 min und nach 23 min eluieren.

Die Identifizierung einer Reihe von Haliclaminen, eines Viscosalines und eines Viscosamines mit ungesättigten Alkylketten widerlegte die Hypothese, dass Schwämme in wärmeren Gewässern vermehrt 3-APAs mit ungesättigten Alkylketten produzieren. Obwohl auch Viscosamine mit längeren Ketten als bisher bekannt und publiziert waren, gefunden wurden, konnte die These von längeren Alkylketten in kaltem Wasser aufgrund mangelnder Vergleichsorganismen weder belegt noch widerlegt werden.

Während der Entwicklung einer MALDI-MS-Methode die zum Metabolitenscreening in verschiedenen Schwämmen angewandt werden kann, wurden in dem karibischen Schwamm *Stylissa caribica* vier neue Verbindungen gefunden, die als zyklische Heptapeptide, Stylissamide A-D, identifiziert wurden. Die Stylissamide sind sehr reich an Prolin. Vor allem Stylissamid B zeigt eine interessante Verknüpfung der Aminosäuren, da hier drei von vier Prolinen hintereinander angeordnet sind. Die dadurch stark überlappenden NMR Signale gestalteten die Strukturaufklärung schwierig; sie war aber schließlich durch vertiefende NMR und MS Experimente erfolgreich.

3
Haliclona viscosa

A bioactivity screening in sessile or slow-moving Arctic invertebrate species in the Kongsfjord, Spitsbergen yielded a sponge, *Haliclona viscosa*, whose crude extract was significantly feeding deterrent to the Arctic amphipod *Anonyx nugax* and the North Sea starfish *Asterias rubens*[72]. It also inhibited the growth of five bacterial strains that had been isolated from the vicinity of the sponge[73] and a number of bacteria used in general bioactivity screening assays[74].

Haliclona viscosa belongs to the order Haplosclerida, class Demospongiae. Members of the order Haplosclerida are widely distributed around the world and form an important element of marine sessile shallow- as well as deep water communities. Among taxonomists they are known to be one of the most difficult and unstable groups of the Demospongiae.[75] Reasons for this are the few characters which are available for taxonomic identification, their variability (and assigned taxonomic weight), and the number of species involved.[76] This is especially true for most species of the genus *Haliclona*, where growth form is highly variable while spicule form and arrangement is highly homogeneous.[77] Therefore, most publications on new secondary metabolites isolated from *Haliclona* do not identify the sponge to the species level and instead use the paraphrase "*Haliclona* sp." Since the genus comprises numerous species, this noncommittal classification complicates evaluation of the findings in terms of ecological relevance or interspecific variation.

The identification of *H. viscosa* represented the first report of the species in the Arctic. The main distribution area of *H. viscosa* is located around the British Isles and the west coast of France, but some specimens were also collected on the west coast of Portugal and in the eastern Mediterranean.[78] The occurrence of *Haliclona viscosa* around the Orkneys, a much better accessible place than the

Arctic, stimulated an examination of the Orkneys specimen's secondary metabolites in hope of finding more organisms with similar bioactive metabolites.

However, a comparison of the secondary metabolites of the Arctic *H. viscosa* with the same species collected around the Orkneys showed large differences in the metabolite quality and quantity (Figure 3.1). A comparison of a second *Haliclona* species that was also reported from both geographic locations, *Haliclona rosea*, did not yield such differences; although the main metabolites present in the Arctic *Haliclona viscosa* were absent from the crude extracts of *H. rosea*, the crude extracts of *H. rosea* from both locations were similar. In addition, the Arctic *H. viscosa* showed variation of its metabolites between different sampling years while individuals from the Orkneys and *Haliclona rosea* from both locations did not show such variations (not shown).[79]

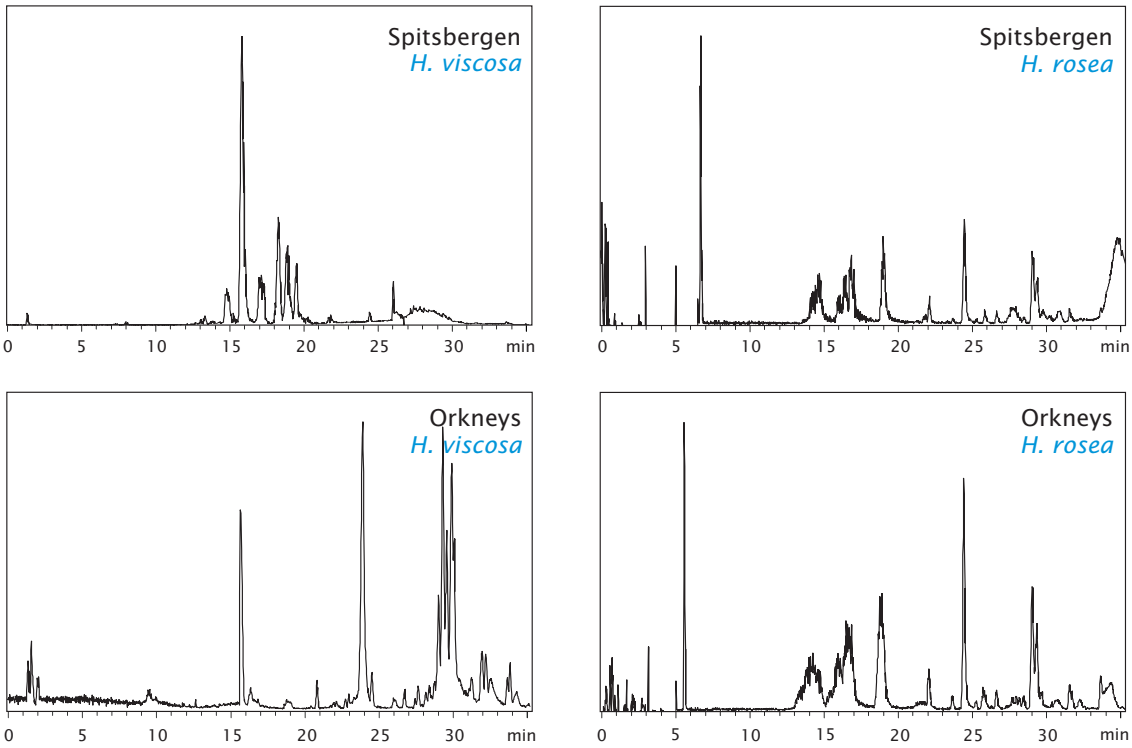

Figure 3.1 Metabolite variation in the sponge species *Haliclona viscosa* and *H. rosea* with place of origin. Modified from Köck (2006).[79]

The reason for the differences of secondary metabolites in *Haliclona viscosa* between the geographic locations has not been addressed yet, but the different environments the organisms were sampled in suggest an influence of environmental conditions. This concept is supported by the observed variation of the metabolites with year. An

alternative is a misidentification of the Arctic specimen or phenotypic/population differences between the habitats.

The *n*-butanol fraction of the crude extract of the Arctic *Haliclona viscosa* contained a number of 3-alkyl pyridinium- and 3-alkyl tetrahydropyridine alkaloids (both termed 3-APA)[1] that were identified as responsible for the observed bioactivity. 3-APAs are well known from different Haplosclerid sponges and are not confined to a geographic region. They consist of a pyridinium or tetrahydropyridinium moiety that is connected, usually in 1- and/or 3-position, to an alkyl chain of variable length. These compounds are arranged as open, cyclic or polycyclic structures. The open and cyclic compounds form monomers, dimers, trimers and polymers.

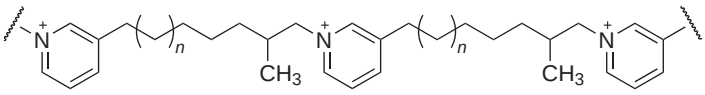

12

Figure 3.2 Halitoxin (**12**, $n = 3, 4, 5$).

The first 3-alkyl pyridinium- or 3-alkyl tetrahydropyridine alkaloid, halitoxin (**12**), a linear polymeric 3-APA with branched alkyl chains, was isolated in 1978 by Schmitz et al.[80] from different *Haliclona* species that were later reclassified to the genus *Amphimedon*. The finding was followed in 1982 by the isolation of petrosin (**13**), a bis-quinolizidine alkaloid, from the sponge *Petrosia* (=*Neopetrosia*) *seriata*[81] and the related xestospongins A-D in 1984.[82] The first member of the structurally rather complex manzamines, manzamine A (**14**) from *Haliclona* sp., was elucidated in 1986[83] while at the same time the sarains 1-3 (**15**-**17**) were identified in *Reniera* (= *Haliclona*)[78] *sarai*. All of the above mentioned compounds are cytotoxic and ichtyotoxic and stimulated an enforced search for similar compounds, represented today by the large number of more or less complex structures identified from five different sponge orders[2] from around the world. However, the largest

1 According to IUPAC nomenclature, the tetrahydropyridine nomenclature is different from the pyridinium nomenclature leaving the tetrahydropyridine alkaloids isolated from *Haliclona* to be 1,5-alkyl substituted. Although false, the 3-alkyl tetrahydropyridine concept is maintained throughout this thesis for agreement with previously published tetrahydropyridine and 3-alkyl pyridinium compounds.

2 Order Haplosclerida (compounds reported from six families: Chalinidae, Petrosiidae, Niphatidae, Callyspongiidae, Halichondriidae and Phloeodictyidae), Astrophorida (*Stelletta maxima*), Lithistida (*Theonella swinhoei*), Dictyoceratida (*Ircinia* sp.) and Poecilosclerida (*Echinochalina* sp.).

number of 3-APAs is reported from sponges of the order Haplosclerida with the genera *Haliclona*, *Amphimedon* and *Xestospongia* being most often studied and thus revealing most of the compounds. Most of the 3-APAs display at least moderate biological activity of various kinds.

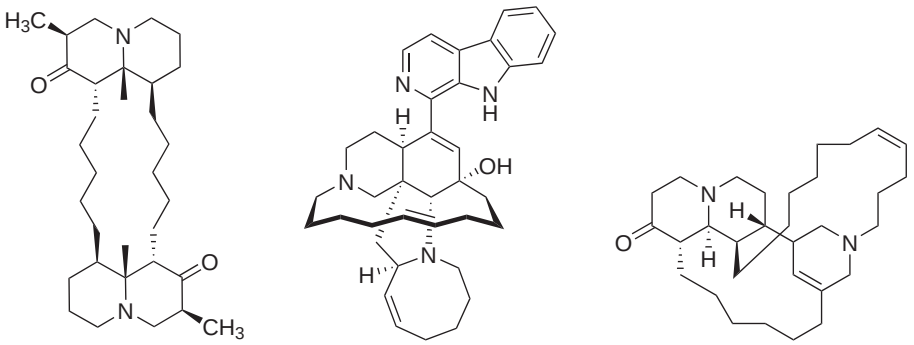

13 **14** **15**

Figure 3.3 Petrosin (**13**), Manzamine A (**14**) and Sarain 1 (**15**).

3.1 Known 3-APAs isolated from *Haliclona* sp.

In *Haliclona*, six linear 3-alkyl pyridinium compounds have been isolated so far. Viscosaline C (**18**)[3] was isolated from the Arctic sponge *Haliclona viscosa* and combines two 1,3-linked alkyl pyridines with the amino acid β-alanine.[74] Another two viscosalines, B and E[4], from the same sponge, are described in the dissertation thesis of Christoph Timm, prepared in the research group of M. Köck.[84] Viscosalines B and E possess alkyl chains of unequal length and therefore exist in two isomeric constitutions each, B_1 (**19**), B_2 (**20**), E_1 (**21**) and E_2 (**22**), with the β-alanine moiety connected to either the longer or the shorter chain (Figure 3.4). The sixth linear compound is a poly 3-alkyl pyridinium salt (**23**, Poly-APS), a polymer of variable size, isolated from a Mediterranean *Haliclona sarai*[85] and, very recently, also from *Haliclona* sp. from the Pacific coast of Guatemala.[86]

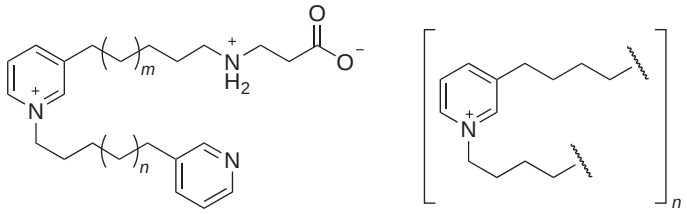

18-22 **23**

Figure 3.4 Viscosaline C (**18**, $m = n = 9$), B_1 (**19**, $m = 9$, $n = 8$), B_2 (**20**, $m = 8$, $n = 9$), E_1 (**21**, $m = 10$, $n = 9$), E_2 (**22**, $m = 9$, $n = 10$) and Poly-APS (**23**, $n = 29$, 99).

All other 3-APAs isolated from *Haliclona* are cyclic or polycyclic compounds. Of the cyclic monomers, only one true 3-APA, haliclocyclin F (**24**)[5] has been isolated, again from the Arctic sponge *Haliclona viscosa*.[87] Another monomeric compound, haliclocyclin F_1 (**25**) with a C_{14} alkyl chain that carries a double bond, was identified but could not be isolated.[84] Besides this, a 1,3-alkyl trihydropyrimidine monomer

3 Published as "viscosaline" (**18**), termed "C" later[84] for the similarity in chain lengths with cyclostellettamine C (**33**) and the identification of additional viscosalines with different alkyl chain lengths.

4 Viscosalines B and E were present in crude extract fractions formerly termed X2 and X4, respectively.

5 Published without a name as a "monomeric, cyclic 3-APA" that contains a C_{14} alkyl chain; however, naming is necessary due to the identification of additional monomeric 3-APAs in the crude extract of *Haliclona viscosa* (see Section 3.3.1).

with a branched alkyl chain, haliclorensin B (**26**), was isolated from a Madagascan *Haliclona tulearensis* together with a number of azecane derivatives.[88–90]

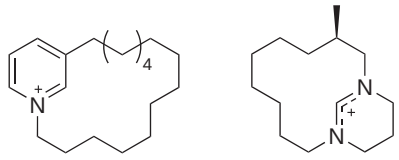

24 **26**

Figure 3.5 The monomeric 3-APAs haliclocyclin F (**24**) isolated from *Haliclona viscosa* and haliclorensin B (**26**) from *H. tulearensis*.

The cyclic dimers can be arranged by their degree of unsaturation. The haliclamines form the simplest, i.e. least unsaturated structures, with two tetrahydropyridines connected in 1- and 3-position by two alkyl chains of variable length. To date, six naturally occurring haliclamines are known; haliclamines C-F (**27-30**), isolated from the Arctic *Haliclona viscosa*, contain saturated alkyl chains[91,92] while haliclamines A (**31**) and B (**32**), isolated from *Haliclona* sp. from Hiburi-jima, Japan, contain mono- and/or bis-unsaturated alkene chains.[93] Four additional haliclamines with double bonds in the alkyl chains are mentioned in the dissertation thesis of C. Timm[84] but not further elucidated. They are haliclamine/C_{20}/1, haliclamine/C_{21}/1, haliclamine/C_{22}/1 and haliclamine/C_{22}/2 where nomenclature follows the concept "<compound name>/<total length of the alkyl chains>/<number of double bonds>".[84]

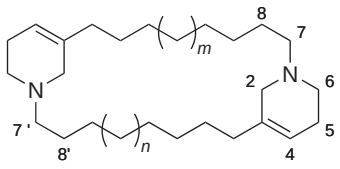

27-32

Figure 3.6 Haliclamines C-F (**27**: $m = 2$, $n = 4$, **28**: $m = 3$, $n = 4$, **29**: $m = 2$, $n = 3$, **30**: $m = 4$, $n = 4$) and haliclamines A (**31**, $m = 2$, $n = 5$, $\Delta_{9,9'}$) and B (**32**, $m = 2$, $n = 5$, $\Delta_{9,9',14'}$).

Cyclostellettamines are structurally similar to the haliclamines but possess pyridinium moieties instead of the tetrahydropyridines in haliclamines. Cyclostellettamine C (**33**) with saturated alkyl chains was identified in the Arctic *H. viscosa*[84] and several additional cyclostellettamines were isolated from other, non-*Haliclona* sponges. Cyclostellettamine-like compounds with monounsaturated alkyl chains are represented by cyclohaliclonamine A (**34**, $n = 1$) which was isolated from *Haliclona* sp. from Bise Island, Japan,[94] an unnamed cyclostellettamine derivative isolated from *Haliclona* sp. from the Pacific coast of Guatemala (**39**)[86] and njaoaminium A-C (**40-42**) which stem from a *Reniera* (=*Haliclona*) sp. from Tanzania.[95]

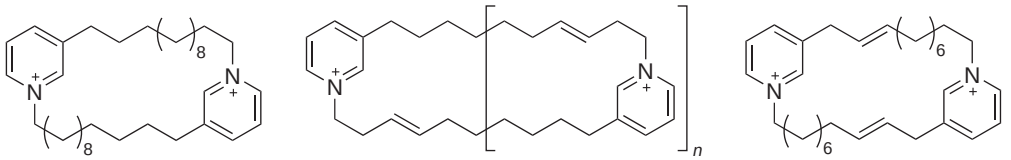

33 **34-38** **39**

Figure 3.7 Cyclostellettamine C (**33**), cyclohaliclonamines A-E (**34-38**, $n = 1 - 5$) and a cyclostellettamine derivative from Guatemala (**39**).

While the chains in cyclostellettamine C (**33**) contain 13 methylene groups, the compound **39** reported from Guatemala contains 11 methylene/methyne groups and cyclohaliclonamine A (**34**) and njaoaminium A-C (**40-42**) possess chains of ten methylene/methyne groups. Additionally, njaoaminium B (**41**) and C (**42**) contain methyl side chains in the interconnecting alkyl chains and cyclohaliclonamine A (**34**) and njaoaminium A (**40**) differ in the position of the double bond.

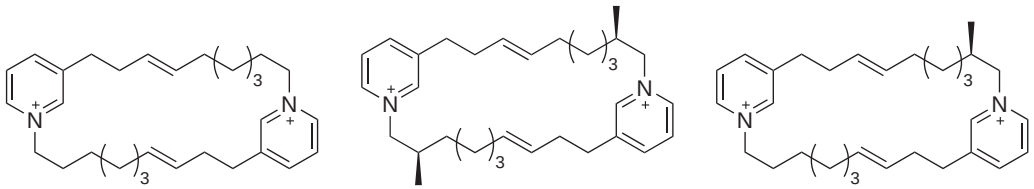

40 **41** **42**

Figure 3.8 Njaoaminium A-C (**40-42**).

Cyclic trimers are represented by viscosamine C (**43**)[6] that contains three saturated alkyl chains of 13 methylene groups each and was isolated from *H. viscosa* from the Arctic,[96] as well as a viscosamine that contains saturated alkyl chain with a total of 38 methylene groups.[84] Two derivatives with monounsaturated alkyl chains are represented by the unnamed compound **44** from *Haliclona* sp. from the Pacific coast of Guatemala[86] and cyclohaliclonamine B (**35**, $n = 2$) from *Haliclona* sp. from Bise Island, Japan.[94] The two derivatives differ in the position of the double bond. All four compounds are different in the length of the alkyl chain; viscosamine C (**43**) contains the longest chains of 13 methylene groups while compound **44** and cyclohaliclonamine B (**35**) possess chains of 11 and 10 methylene/methyne groups,

6 Originally published as "viscosamine", but termed viscosamine C (**43**) for the presence of additional viscosamines in the crude extract of *H. viscosa*.

respectively. The yet unidentified viscosamine from the Arctic *H. viscosa* contains alkyl chains of unequal length, probably 12/13/13.

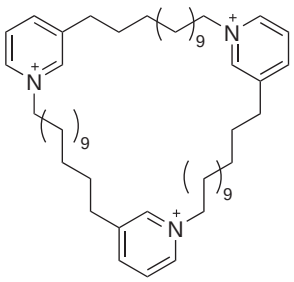

43

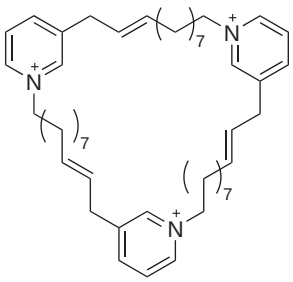

44

Figure 3.9 Viscosamine C (**43**) and a derivative from Guatemala (**44**).

In addition to the cyclic dimeric cyclohaliclonamine A (**34**) and the trimeric cyclohaliclonamine B (**35**), three more members of the cyclohaliclonamines are reported, cyclohaliclonamines C-E (**36-38**, $n = 3 - 5$). They form tetrameric, pentameric and hexameric macrocycles that are unprecedented among the 3-APAs in *Haliclona*.[94] All of them possess alkyl chains of 10 methylene/methyne groups and a double bond in the last but third bond of the alkyl chain.

Halicyclamine A (**45**),[97] haliclonacyclamines A-D (**46-49**)[98,99] and 22-hydroxyhaliclonacyclamine B (**50**)[100] are tetracyclic 3-APAs that are related to the haliclamines. They can be seen as haliclamines in which the double bond of one tetrahydropyridine is used to connect the two azacycles. The haliclonacyclamines A-D (**46-49**) and 22-hydroxyhaliclonacyclamine B (**50**), in contrast to halicyclamine A (**45**), lack the double bond in the second tetrahydropyridine, resulting in two interconnected piperidine moieties. All haliclonacyclamines possess one C_{10} and one C_{12} alkyl chain but differ in the number and position of double bonds in these chains. Halicyclamine A (**45**) and 22-hydroxyhaliclonacyclamine B (**50**) were isolated from *Haliclona* sp. from Biak and Flores Island, Indonesia, while haliclonacyclamines A-D (**46-49**) were isolated from *Haliclona* sp. from Heron Island, Australia.

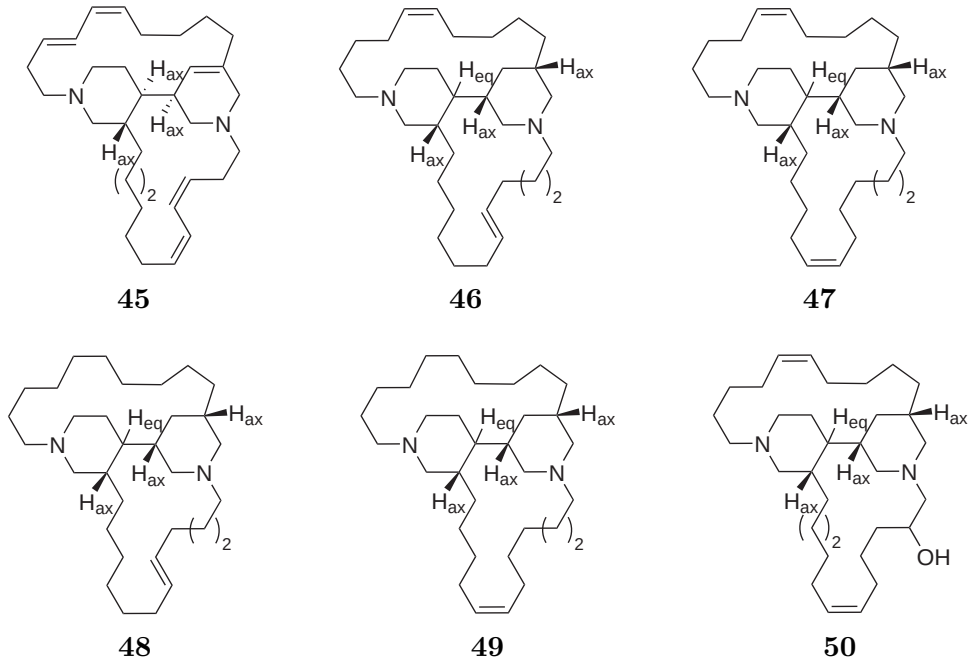

45 **46** **47**

48 **49** **50**

Figure 3.10 Halicyclamine A (**45**), haliclonacyclamines A-D (**46-49**) and 22-hydroxyhaliclonacyclamine B (**50**).

Similar to halicyclamine A (**45**) and the haliclonacyclamines A-D (**46-49**) are the sarains-1 to -3 (**15-17**) and isosarain-1 (**51**) isolated from *Haliclona sarai* from the Bay of Naples, Italy. Sarains-1 to -3 (**15 - 17**) and isosarain-1 (**51**) consist of a quinolizidine moiety connected to a tetrahydropyridine moiety. The tetrahydropyridine is connected in 1- and 3-position to two alkyl chains that are, in turn, connected to the quinolizidine in *meta*-position to the nitrogen. They differ in the length of one of the alkyl chains and the number and position of the double bond therein.

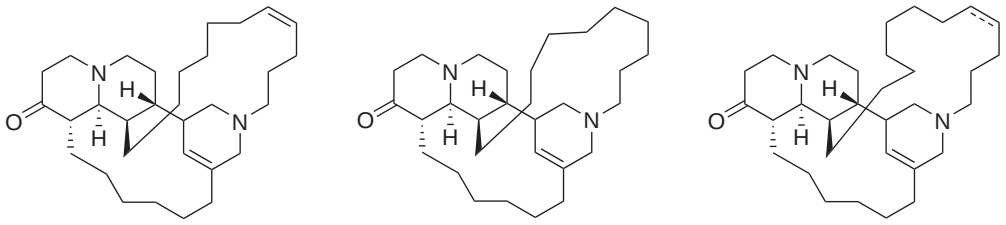

15 **16** **17**

Figure 3.11 Sarains 1-3 (**15-17**) and isosarain-1 (**51**). The position of the double bond in the alkyl chain of sarain-3 (**17**) is not determined.

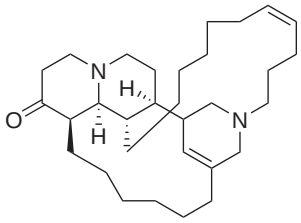

51

Figure 3.12 Isosarain-1 (**51**)).

Haliclonin A (**52**) constitutes the next step in complexity of the 3-APA compounds present in *Haliclona*. It was recently isolated from a *Haliclona* sp. from Jeju Island, Korea[101] and provides a novel skeletal class with two condensed rings.

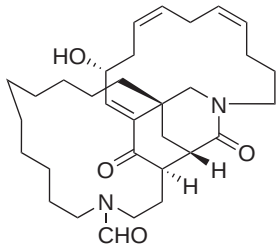

52

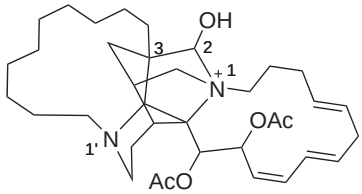

53

Figure 3.13 Haliclonin A (**52**) and Sarain-A (**53**).

An even more complex condensed ring system is represented by sarain A (**53**). It is characterized by a central tetracyclic cage in the middle of two cyclic alkyl chains.[102] Two structurally similar sarains, sarain B and C, were isolated from the same sponge, *Haliclona sarai*, with sarain B containing "[...] an additional carbon atom and double bond" in the alkyl chain between N1' and C3 while sarain C "[...] is the superior homolog of Sarain B".[102]

The most complex 3-APAs isolated from *Haliclona* sponges are the manzamines. They are β-carboline alkaloids with intricate nitrogen-containing polycyclic systems. The complexity of the compounds and their biological activity fired the search for new examples of the manzamine family resulting today in a large number of manzamines published from different Haplosclerid sponges. Yet only four, manzamines A-C (**14**, **54**, **55**) and Y (**56**),[83,103,104] are reported from *Haliclona* sp. They are, as most manzamine alkaloids (Table A.5), isolated from sponges collected in the Okinawa prefecture, Japan. The joint occurrence of manzamines in different sponge genera led to the assumption that commensal bacteria instead of the host sponge produce these types of secondary metabolites,[104] but this hypothesis was not assessed yet.

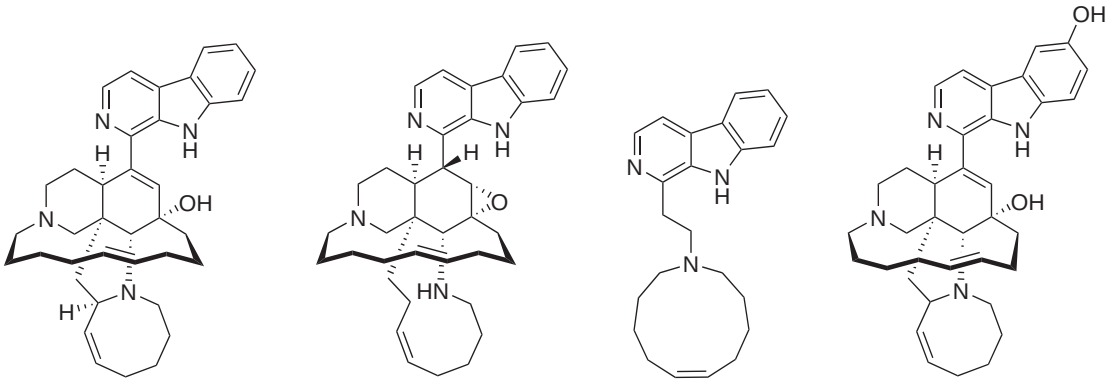

14 **54** **55** **56**

Figure 3.14 Manzamines A (**14**), B (**54**), C (**55**), and Y (**56**).

Looking at the distribution of 3-APAs in a global context, sponges from the Western Pacific yielded the largest number of 3-APAs and the highest structural diversity (Table 3.1 and A.5, Figure A.1). However, it must be noted that the type of structure published and the area of origin are influenced by the scope, interest and methods of the individual researcher operating in a defined geographic area. The high number of compounds reported from the Western Pacific is therefore reflected in the "trends in geographic distribution of collection sources" for all marine natural products published.[42]

With the 3-APAs in *Haliclona*, there seems to be a trend for shorter alkyl chains with increased water temperature. Similarly, the structural complexity seems to increase with increasing water temperature. In addition, it must be noted that the cyclic dimeric 3-alkyl tetrahydropyridines are represented by the rather large number of haliclamines while cyclostellettamine C (**33**) is the only cyclic dimeric 3-alkyl pyridinium compound found in *H. viscosa* to-date.

Table 3.1 3-Alkyl pyridinium and 3-alkyl tetrahydropyridine alkaloids reported from sponges of the genus *Haliclona*, sorted by geographic region (Is. = Island, w/ DB = with double bonds).

Nr[a]	Geographic Area[b]	Compound	Sponge
1	SJM, Kongsfjord	Viscosaline C (**18**) [74]	*H. viscosa*
		Viscosaline $B_{1/2}$ (**19**, **20**), $E_{1/2}$ (**21**, **22**) [84]	*H. viscosa*
		Haliclocyclin F, F_1 (**24**, **25**) [84,87]	*H. viscosa*
		Haliclamine C-F (**27-30**) [91,92]	*H. viscosa*
		Haliclamine/C_{20}/1, Haliclamine/C_{21}/1 [84]	*H. viscosa*
		Haliclamine/C_{22}/1, Haliclamine/C_{22}/2 [84]	*H. viscosa*
		Cyclostellettamine C (**33**) [84]	*H. viscosa*
		Viscosamine C (**43**) [96]	*H. viscosa*
		Viscosamine/C_{38}/0 [84]	*H. viscosa*
2	SVN, North. Adriatic	Poly-APS (**23**) [85]	*H. sarai*
3	ITA, Bay of Naples	Sarain-1 (**15**), -2 (**16**), -3 (**17**) [105]	*H. sarai*
		Isosarain-1 (**51**) [102,106]	*H. sarai*
		Sarain-A (**53**), -B, -C [107]	*H. sarai*
4	JPN, Hiburi-jima	Haliclamines A (**31**), B (**32**) [93]	*Haliclona* sp.
	JPN, Bise Is.	Cyclohaliclonamine A-E (**34-38**) [94]	*Haliclona* sp.
5	KOR, Jeju Is.	Haliclonin A (**52**) [101]	*Haliclona* sp.
6	JPN, Manzamo Is.	Manzamine A (**14**) [83]	*Haliclona* sp.
		Manzamine B (**54**), C (**55**) [103]	*Haliclona* sp.
	JPN, Iriomote Is.	Manzamine A-C (**14**, **54**, **55**), Y (**56**) [104]	*Haliclona* sp.
7	IDN, Biak	Halicyclamine A (**45**) [97]	*Haliclona* sp.
8	IDN, Flores Is.	22-Hydroxyhaliclonacyclamine B (**50**) [100]	*Haliclona* sp.
9	AUS, Heron Is.	Haliclonacyclamine A (**46**), B (**47**) [98]	*Haliclona* sp.
		Haliclonacyclamine A-D (**46-49**) [99]	*Haliclona* sp.
10	GTM, Pacific coast	Cyclostellettamines w/ DB (**39**) [86]	*Haliclona* sp.
		Viscosamine w/ DB (**44**) [86]	*Haliclona* sp.
		Poly-APS (**23**) [86]	*Haliclona* sp.
11	TZA, Pemba Is.	Njaoaminium A-C (**40-42**) [95]	*Reniera* sp.
12	MDG, Salary Bay	Haliclorensin B (**26**) [90]	*H. tulearensis*

[a] Numbers refer to geographic regions as denoted in Figure A.1.
[b] Country codes: AUS = Australia, GTM = Guatemala, IDN = Indonesia, ITA = Italy, KOR = Korea, MDG = Madagaskar, SVN = Slovenia, SJM = Svalbard & Jan Mayen, TZA = Tanzania.

3.2 Bioactivity of *Haliclona viscosa* secondary metabolites

This observation is interesting with regard to the bioactivity of the compounds. In the original bioactivity screening of sessile or slow moving Arctic invertebrates, the *n*-butanol fraction of the Arctic *Haliclona viscosa* crude extract showed feeding deterrence[72,108] and antimicrobial activity[73,74]

The 3-alkyl pyridinium and 3-alkyl tetrahydropyridine alkaloids present in the *n*-butanol fraction are responsible for the bioactivity and in the course of that study, several of the metabolites were isolated or synthesized and tested as pure compounds. The isolated viscosaline C (**18**) was identified as the compound that deterred feeding in *Anonyx nugax* and *Asterias rubens* while the 3-alkyl tetrahydropyridine alkaloids haliclamines C (**27**) and D (**28**) were not feeding deterrent.[73] Viscosaline C (**18**) inhibited the growth of four out of five bacterial strains isolated from the sponge's habitat and haliclamines C (**27**) and D (**28**) inhibited two of the five bacterial strains.[73]

The compounds were also tested for growth inhibition in different gram-positive (gram+) and gram-negative (gram–) bacteria, yeasts and fungi as well as for cytotoxicity on mouse fibroblasts L929.[84,87] To test the influence of alkyl chain length, size of the macrocycle and number of charges on the bioactivity, synthetic compounds were included that were not identified in natural crude extracts. While most compounds were not active against the yeasts and fungi, all compounds with alkyl chain lengths longer than eight methylene groups inhibited gram+ and gram– bacteria and were cytotoxic against mouse fibroblasts.[84]

A review about the known 3-alkyl pyridinium and 3-alkyl piperidine alkaloids states that 3-APA monomers, dimers and trimers possess greater antimicrobial activity, while higher polymers show more pronounced cytolytic, cytotoxic and antifouling activities, but not as an absolute rule.[109] This is confirmed by Timm,[87,110] where antimicrobial activity of cyclic compounds decreased with increasing oligomerization and/or total number of charges. Cyclic monomeric 3-APAs showed the highest activity. Compounds with equal size of the macrocycle but higher number of charges (pyridinium moieties) showed decreased antimicrobial activity. The relationship between cytotoxicity and antimicrobial activity was negatively correlated; i.e. the most cytotoxic compound viscosamine C (**43**) showed the least antimicrobial activity while the highest antimicrobially active compound, the synthetic cyclic monomer

haliclocyclin C (**57**, C_{13} alkyl chain), was least cytotoxic. This is in accordance with the findings of Anan et al. (1996) of the macrocyclic monomeric 3-APA with a C_{13} alkyl chain (see Section 3.3) being less cytotoxic than cyclostellettamine C (**33**).[111] Linear 3-APAs with fully saturated alkyl chains or terminal methylene groups showed no antimicrobial and low cytotoxic activity but addition of a terminal amino or hydroxyl group resulted in significantly heightened activity.[87]

In addition, the alkyl chain length influenced the cytotoxicity and antimicrobial activity; longer chains resulted in increased activity.[110] On the other hand, 3-alkyl tetrahydropyridines proved to be less active than 3-alkyl pyridinium compounds of equal chain length.[84,87]

The bioactivity of 3-APAs with unsaturated chains was not tested in this series since natural or synthetic haliclamines and cyclostellettamines with unsaturated alkyl chains were not at hand. However, 3-APAs with unsaturated alkyl chains like the cyclohaliclonamines A-E (**34-38**)[94], njaoaminium A (**40**)[95] and the cyclostellettamine (**39**) and viscosamine (**44**) from Guatemala[86] as well as haliclamines A (**31**) and B (**32**)[93] were tested for cytotoxicity on different cell lines by the respective authors.

Although the results cannot be directly compared for the use of different cell types as basis for the cytotoxicity assays, the 3-alkyl pyridinium alkaloids with unsaturated alkyl chains show low general cytotoxicity on the tested cell lines whereas the haliclamines A (**31**) and B (**32**) are significantly toxic against mouse fibroplasts. The cyclostellettamine and viscosamine isolated from a *Haliclona* sp. from Guatemala showed IC_{50} values of $>20\,\mu g\ ml^{-1}$ against murine macrophage J774.A1[86] while Haliclamine A and B were significantly cytotoxic against L1210 cells (1.5 and $0.9\,\mu g\ ml^{-1}$) and P388 mouse leukemia cells (0.75 and $0.39\,\mu g\ ml^{-1}$, respectively).[93]

This seems to reverse the finding of haliclamines with saturated alkyl chains being less cytotoxic than cyclostellettamines; the addition of double bonds seems to increase their cytotoxic potential more than double bonds in cyclostellettamines. Haliclamine B (**32**) with one mono- and one bisunsaturated alkyl chain was significantly more cytotoxic than haliclamine A (**31**) with two mono-unsaturated alkyl chains.[93]

The mode of action for cytotoxic, antimicrobial, enzyme inhibitory and receptor modulating activity in 3-APAs has not been studied, yet.[109] An exception is the cause for the cytolytic activity which has been addressed for halitoxin (**12**) and Poly-APS (**23**). Due to their positively charged pyridinium ring and the aliphatic

moieties which are reminiscent of the "polar head" and "nonpolar tails" of detergents, Poly-APS (**23**) produces discrete membrane lesions with an average diameter of 5.8 nm which results in moderate haemolytic activity.[112] By assuming a similar mode of action in halitoxin (**12**) and taking into account the increase in activity with increasing molecular weight, this explains the strong haemolytic activity, lethality to mice,[80,113] irreversible membrane potential depolarization and action potential inhibition of halitoxin (**12**).[109] However, cytolysis has not yet been reported for linear monomers and cyclic compounds and it is uncertain whether these compounds have not been tested or were tested and did not possess e.g. haemolytic activity.

3.3 New secondary metabolites in *Haliclona viscosa*

Sample volumes in the Spitsbergen sponge samples are limited by the small size of the individuals, their slow growth rate and the attention to sustainable sampling in the fragile Arctic ecosystem. Small sample volumes hinder the isolation of compounds in the quantities required for structure elucidation by nuclear magnetic resonance (NMR). Thus only the major secondary metabolites in *Haliclona viscosa* were isolated and identified by the combination of high resolution mass spectrometry (HRMS) and NMR. Two previous dissertation theses prepared by Christian Volk[114] and Christoph Timm[84] in the Köck working group concentrated on the isolation and structure elucidation of secondary metabolites from *Haliclona viscosa*.

To date, five different structural classes are known among the 3-APAs contained in the Arctic *Haliclona viscosa*; 3-alkyl pyridinium alkaloids are represented by the linear, open viscosalines, macrocyclic monomeric haliclocyclins, the macrocyclic dimeric cyclostellettamine C (**33**) and macrocyclic trimeric viscosamines; the cyclic dimeric haliclamines are the only representatives of 3-alkyl tetrahydropyridines (Section 3.1). The difference among the members of each structural class is only in the length of the alkyl chain and the number of double bonds therein.

Haliclamine C (**27**) and D (**28**) constitute the major components in the crude extracts of all *H. viscosa* samples obtained so far, with exception of the year 2001, and were first identified by C. Volk.[91] Other compounds isolated by him are viscosaline C (**18**),[74] cyclostellettamine C (**33**) and viscosamine C (**43**).[96]

Several additional compounds were identified in the thesis of C. Timm. Since the quantity of these compounds was too low to allow their isolation, C. Timm relied on synthetic preparation of the proposed structures and compared their chemical properties (retention times, masses, UV data) to those of the natural products in the crude extract. In this manner, he isolated the monomeric, cyclic haliclocyclin F (**24**)[87] and found haliclocyclin F_1 (**25**), two new viscosalines, B and E, one haliclamine, haliclamine/C_{23}/0 with saturated alkyl chains, four haliclamines with unsaturated alkyl chains, haliclamine/C_{20}/1, haliclamine/C_{21}/1, haliclamine/C_{22}/1 and haliclamine/C_{22}/2[84] as well as one viscosamine with a total of 38 methylene groups (Table 3.2).[84]

The present thesis uses a chromatographic method that achieves better separation of compound peaks in high performance liquid chromatography (HPLC) compared

Table 3.2 3-APAs in *Haliclona viscosa* published prior to the presented thesis. The compounds are sorted according to their affiliation with structural class.

linear/cyclic	Pyr/THP[a]	oligomer	compound name	alkyl chains	DB
linear	Pyr	dimer	viscosaline B_1 (**19**)	12/13	0
			viscosaline B_2 (**20**)	13/12	0
			viscosaline C (**18**)	13/13	0
			viscosaline E_1 (**21**)	13/14	0
			viscosaline E_2 (**22**)	14/13	0
cyclic	Pyr	monomer	haliclocyclin F (**24**)	14	0
			haliclocyclin F_1 (**25**)	14	1
cyclic	Pyr	dimer	cyclostellettamine C (**33**)	13/13	0
cyclic	Pyr	trimer	viscosamine B (**80**)	12/13/13	0
			viscosamine C (**43**)	13/13/13	0
cyclic	THP	dimer	haliclamine C (**27**)	9/11	0
			haliclamine D (**28**)	10/11	0

[a] Pyr = pyridinium, THP = tetrahydropyridine, DB = double bonds, 12/13 = number of methylene groups in each of the two alkyl chains.

to previous analyses (no raw data available, for comparison see dissertation thesis of C. Timm[84]). Improved compound peak resolution consequently leads to better differentiation and higher detailedness of compound-specific mass spectra in HRMS thus facilitating the structure elucidation of compounds. Despite the improved chromatographic separation, the large number of similar 3-APAs in the crude extract of *H. viscosa* hinders the complete baseline-separation of chromatographic peaks; several of the 3-APAs still co-elute or overlap. While compounds of the same compound class but with different chain lengths can be separated well (Figure 3.17), compounds associated with different compound classes may elute in one chromatogram peak. Although this results in superimposed mass spectra, compounds of different compound classes can confidently be recognized by their exact mass, characteristic molecular ions and fragmentation pattern, even inside the same mass spectrum.

This is exemplified in the identification of haliclocyclin C (**57**, Section 3.3.1) which has a singly charged molecular ion $[M]^+$ of $m/z = 260$. This compound was previously included in a fraction that contained cyclostellettamine C (**33**), haliclocyclin F_1 (**25**) and a new viscosamine 12/13/13 (fraction X7 in the dissertation thesis of C. Timm[84]) as the major metabolites. Since cyclostellettamine C (**33**) shows a doubly charged molecular ion $[M]^{2+}$ of $m/z = 260$, the ions of the two compounds were superimposed and were thus not differentiated. However, both compounds are clearly separated in the LC analysis used for the presented thesis and thus distinguishable

in the MS spectrum. As before in the thesis of C. Timm however, the quantity and purity of the analytes achieved by preparative chromatography prevents informative results by NMR experiments.

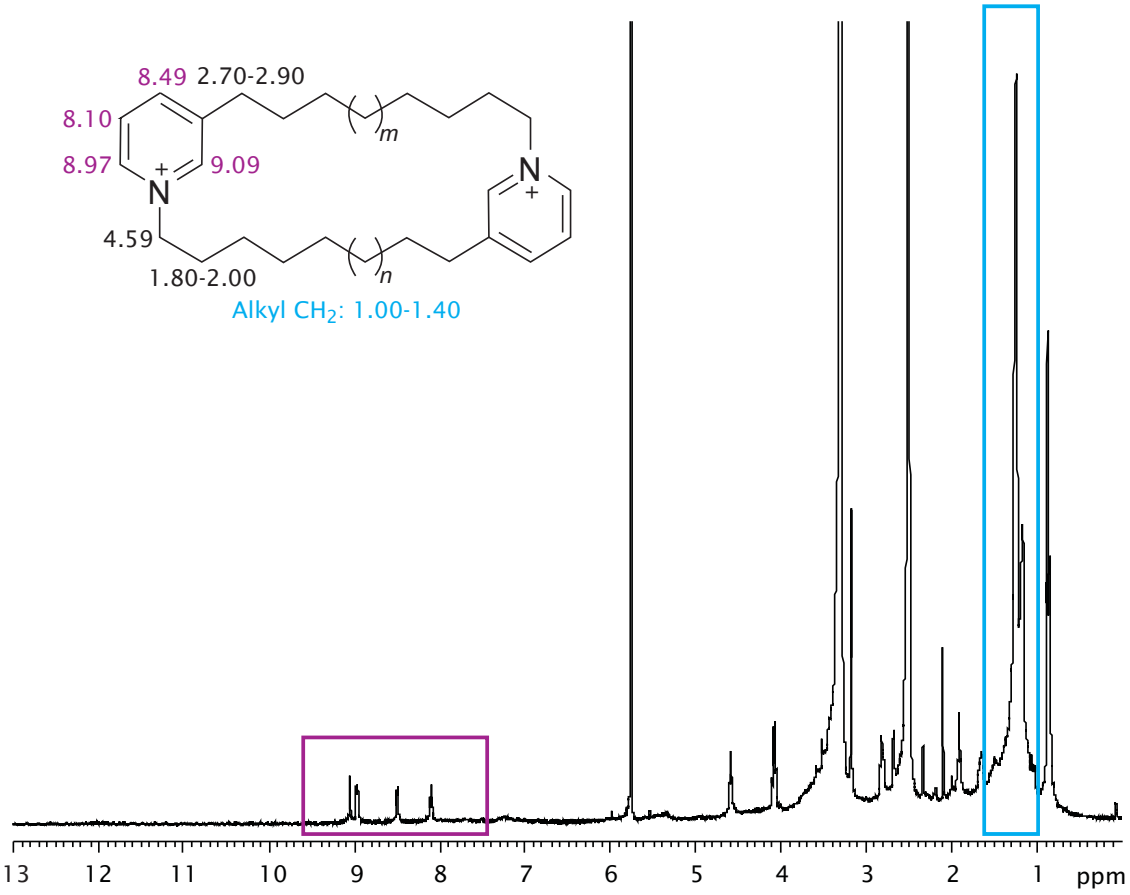

Figure 3.15 ^{1}H-NMR spectrum of a crude extract fraction (1.5 mg) obtained from the sponge *Pachychalina* sp. in DMSO-d_6. Alkyl chain methyl groups are marked in blue and aromatic hydrogen are marked in purple. Modified from Grube et al. (2005).[115]

In addition, the repetitive 3-alkyl pyridinium or tetrahydropyridine motif in 3-APAs causes NMR spectra to show only one structural unit of the molecule and the large number of similar methylene units results in a strong overlap of the aliphatic protons. NMR spectra are thus not ideally suited to distinguish large numbers of structurally very similar 3-APAs. An example for this constitutes a crude extract fraction (1.5 mg) obtained from the Brazilian sponge *Pachychalina* sp. The fraction contains eleven different cyclostellettamines (A-F and G, H, I, K and L) as well as ingenamide G,[116] but the NMR spectrum of the complete fraction only indicates the presence of one cyclostellettamine substructure (Figure 3.15). While it is possible

to determine from NMR spectra, whether the compounds present contain pyridine or tetrahydropyridine moieties, the number of different compounds and their chain lengths cannot be deduced.

In these cases it is advantageous to use liquid chromatography – mass spectrometry (LCMS) and liquid chromatography – tandem mass spectrometry (LCMS/MS) methods to identify the natural compounds, e.g. directly in the crude extract. In the 1.5 mg crude extract fraction of *Pachychalina* sp. mentioned above, Oliveira et al.[116] succeeded in identifying twelve compounds by applying LCMS methods. Thus, liquid chromatography mass spectrometry constitutes the basic method for obtaining information about the chain length, number of double bonds, and connectivity of the substructures in 3-APAs, especially where only small amounts of sample are available.

However, for mass spectrometry to be a useful tool in identifying different 3-APA compound classes and the constitution of their members, detailed knowledge about the compound class specific ion- and MS-fragmentation pattern is essential. This is especially true where all structure assignments of new 3-APAs in *H. viscosa* base on high resolution mass spectra and fragmentation of the full scan spectrum. A large part of the presented thesis therefore concentrates on the fragmentation of different 3-APAs.

The MS fragmentation of 3-alkyl pyridinium alkaloids is different from the fragmentation of 3-alkyl tetrahydropyridine alkaloids. Fragmentation of 3-alkyl pyridinium alkaloids like the cyclostellettamines is described by Grube et al.[117] The MS fragmentation of 3-alkyl tetrahydropyridines, haliclamines, is described in detail in manuscript 1 (page 183).

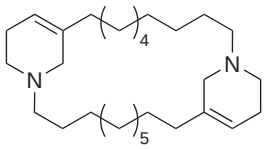

Haliclamine E
(**29**)

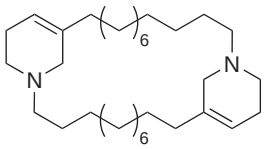

Haliclamine F
(**30**)

Figure 3.16 New haliclamines with saturated alkyl chains published as part of the presented thesis.

For the presented thesis, four new haliclamines with saturated chains are identified in the crude extract of *Haliclona viscosa* by HPLC-HRMS experiments. Two of

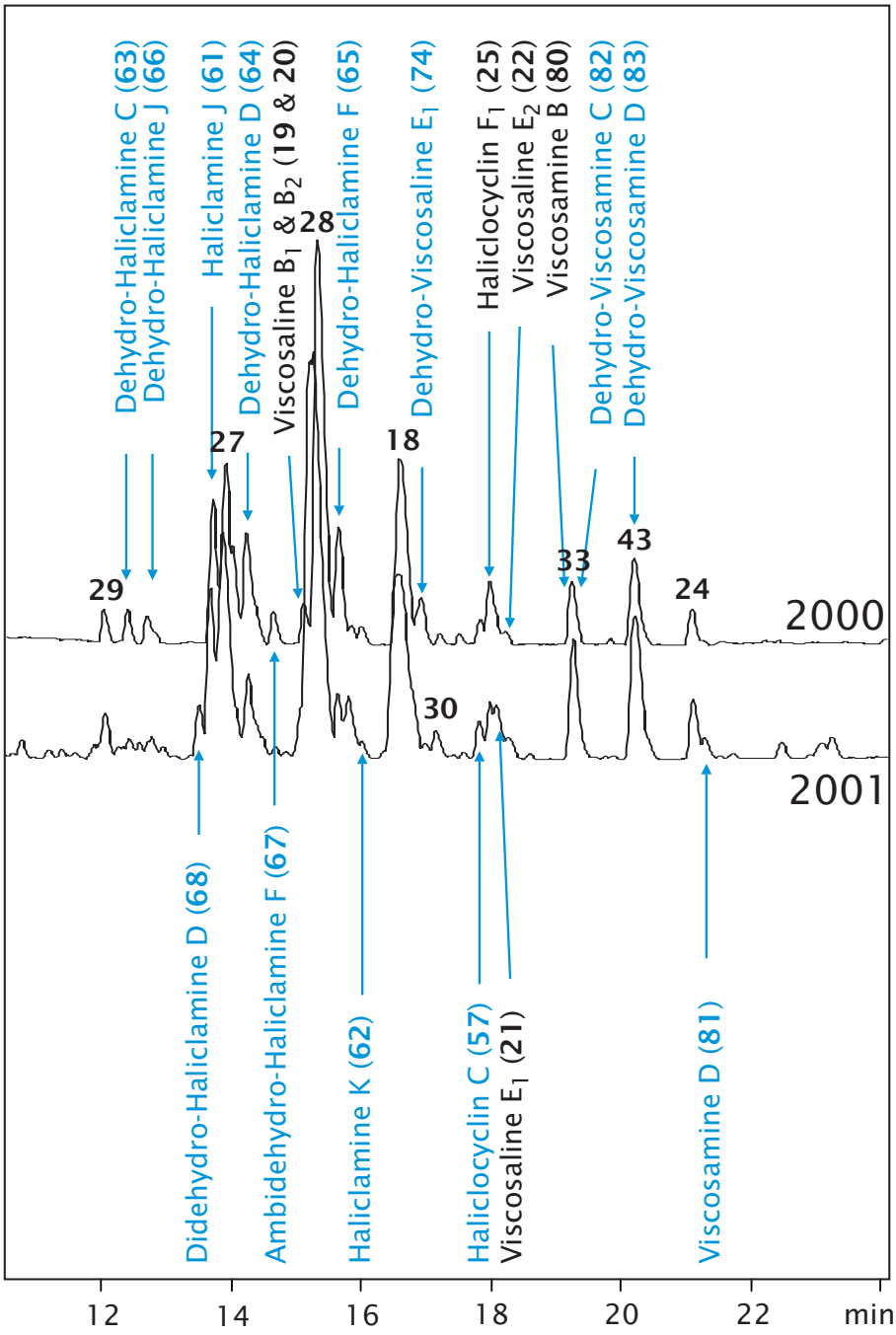

Figure 3.17 Secondary metabolites in *Haliclona viscosa*. Blue – newly identified as part of the presented thesis. Black – previously known compounds[84] whose structure was refined. Compounds are included in two exemplary crude extract base peak chromatograms ($m/z = 50 - 1000$) from the years 2000 and 2001. Several new compounds coelute with the published compounds given in black numbers.

them, haliclamines E (**29**) and F (**30**), are published in cooperation with C. Timm (see publication 1 on page 161). Another two, haliclamines J (**61**) and K (**62**),[7] are included in manuscript draft form but the final confirmation by synthetic products is still missing (see manuscript 2 on page 223). In addition to the first report of the cyclic monomer haliclocyclin C (**57**) from a natural source, two additional new haliclamines J (**61**), and K (**62**) with saturated alkyl chains, two new haliclamines with unsaturated chains, one viscosaline and three additional viscosamines are identified in the crude extract of *Haliclona viscosa* while at the same time knowledge about the structures of previously identified haliclamines with unsaturated alkyl chains and viscosalines is expanded. To differentiate between new and known compounds, new compounds are marked by an asterisk in the compound description in Section 3.3.1-3.3.6.

As mentioned before, the structure elucidation or refinement of new or known compounds builds almost exclusively on mass spectrometric experiments but it uses a different method or instrument parameters than previous analyses. This leads to slightly different mass spectra in both viscosalines and viscosamines and is therefore discussed again using previously reported compounds as an example to allow direct comparison.

3.3.1 Monomeric 3-alkyl pyridinium alkaloids

The cyclic monomeric 3-APAs haliclocyclins F (**24**) and F_1 (**25**), were first reported from the Arctic sponge *Haliclona viscosa* in the dissertation thesis of C. Timm. Haliclocyclin F (**24**, Figure 3.18) was published in 2008 and represented a novel structural class among the naturally occurring 3-APAs.[87] The haliclocyclins are the only compounds known to-date in the crude extract of the sponge that are characterized solely by a singly charged molecular ion. Owing to their single nitrogen, no multiply charged ions or fragments are expected, nor observed (Figure 3.18).

The second cyclic monomer, haliclocyclin F_1 (**25**), is unpublished yet and since no spectrometric data are given in Timm's thesis, the results obtained from this compound are presented here (Figure 3.19). It elutes at a retention time of 17.8 min,

7 Haliclamines G (12/12), H (13/13) and I (11/14) are synthetic haliclamines that are not yet reported from nature.[92]

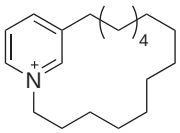

24

	peak	m/z	mol. form.	Δm
C	$[M]^+$	274.2523	$C_{19}H_{32}N$	9.6 ppm

C: compound mass

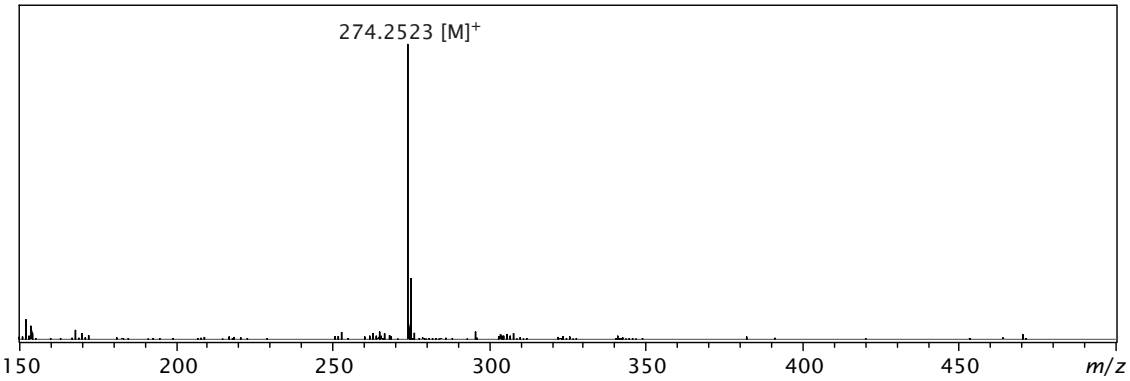

Figure 3.18 Structural formula, compound mass and high resolution mass spectrum for the peak at 20.5 min, identified as haliclocyclin F (**24**).

close to a third cyclic monomer, haliclocyclin C (**57**) and a viscosaline (see Section 3.3.5).

The mass of the singly charged molecular ion $[M]^+$ is $m/z = 272.2370$ which yields a molecular formula of $C_{19}H_{30}N$. The mass is two mass units lower than compound **24** and suggests that a monomeric cyclic 3-APA with an alkyl chain of 14 methylene units contains a double bond in the chain.

The position of the double bond inside the alkyl chain cannot be determined purely by HRMS analysis of crude extracts. Mass spectrometric analysis of double bonds in alkyl chains is difficult by H-shifts that happen prior to the cleavage and hamper an exact localization.[118] A solution to this problem may be the immobilization of the double bond by e.g. oxidative addition of dimethyl disulphide[119] or ethanethiol[120] to transform the double bond to its 1,2-bis-thiomethyl or -thioethyl derivative, respectively. Induced by charge localization at either sulphur atom, the molecular ions of dimethyl disulphide and ethanethiol are susceptible to α-cleavage at the former double bond position. This results in sulphonium ions that should be readily identified in the mass spectrum.[118] For 3-APAs this method would have to be tested for its suitability since also the double bonds inside the pyridine (Pyr) or tetrahydropyridine (THP) moiety might be oxidized. Determination of the position of

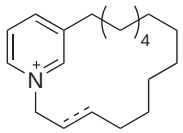

25

	peak	m/z	mol. form.	Δm
C	$[M]^+$	272.2370	$C_{19}H_{30}N$	1.1 ppm

C: compound mass

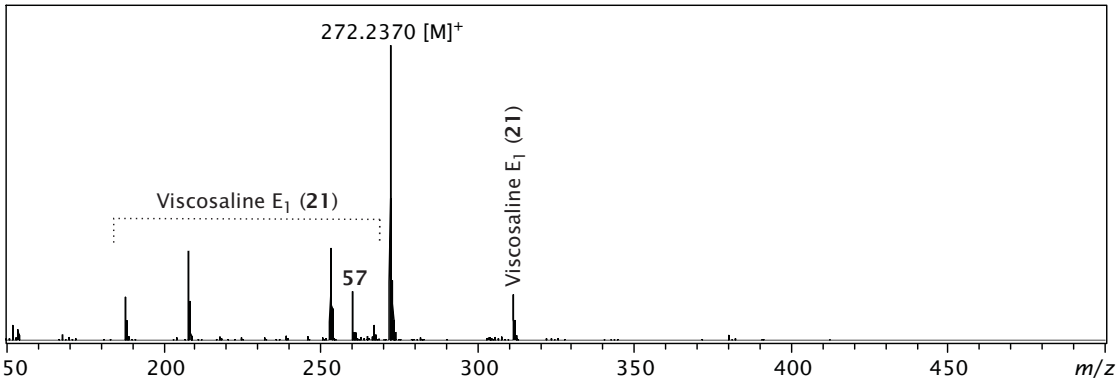

Figure 3.19 Structural formula, compound mass and high resolution mass spectrum of the peak at 17.8 min, identified as haliclocyclin F_1 (**25**). The exact position of the double bond is not determined, yet.

the double bond in haliclocyclin F_1 (**25**) as well as its chromatographic confirmation by comparison with the synthetic analogue is in progress.

In the known 3-APAs with unsaturated alkyl chains, a single/the first double bond is separated by one or two methylene groups from the 3-position of the Pyr/THP moiety or by two to five methylene groups from the nitrogen in 1-position. Multiple double bonds usually occur in conjugation.

Haliclocyclin C (**57**)*[8]

At almost the same retention time as haliclocyclin F_1 elutes a third cyclic monomer, compound (**57**), that is previously unreported from natural sources. It is identified by a diagnostic singly charged molecular ion $[M]^+$ at $m/z = 260.2368$ while no doubly or triply charged molecular ions are present. The molecular ion assigns the formula $C_{18}H_{30}N$. The mass corresponds to the doubly charged molecular ion of cyclostellettamine C (**33**) but for its charge. The molecular formula is consistent with a pyridine moiety connected to an alkyl chain of 13 methylene groups. To

8 * New compounds or previously known compounds whose structure could be refined are marked with an asterisk.

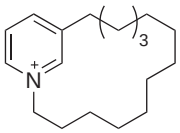

57

	peak	m/z	mol. form.	Δm
C	$[M]^+$	260.2368	$C_{18}H_{30}N$	1.9 ppm

C: compound mass

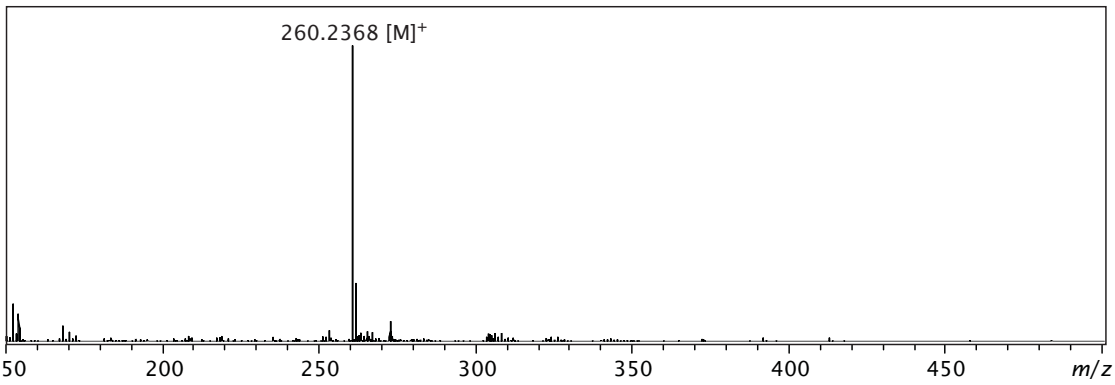

Figure 3.20 Structural formula, compound mass and high resolution mass spectrum for the peak at 17.8 min, identified as haliclocyclin C (**57**).

satisfy the molecular formula, the pyridine can be attached to an open alkyl chain that carries a terminal methylene group or a double bond inside the chain. The other option is that the alkyl chain is attached, possibly in 1- and 3-position (to follow the example of the other 3-APAs in *H. viscosa*), to the pyridine thereby forming a macrocycle as is known from haliclocyclin F (**24**).

The macrocycle **57** was synthesized in 1996 by Anan and coworkers[111] for the structural comparison between **57** and the then newly synthesized cyclostellettamine C (**33**) as well as for comparison of the bioactivity between the two compounds. In addition, the macrocyclic monomer **57** was synthesized by Timm[87] to examine the effect of the chain length on the bioactivity of 3-alkyl pyridinium alkaloids. Therefore, it is available for a comparison of retention times between the compound in the crude extract of *H. viscosa* and the pure, synthetic compound.

The synthetic monomer, haliclocyclin C (**57**), elutes at the same retention time as the natural compound **57** in the crude extract. The HPLC-HRMS analysis of the synthetic compound **57** yields the mass $m/z = 260.2360$ $[M]^+$ which corresponds to the molecular formula $C_{18}H_{30}N$ with a mass accuracy of 4.9 ppm. The chromatographic analysis of a mixture of the crude extract and the synthetic haliclocyclin C (**57**) results in increased intensity of the compound peak in the crude extract

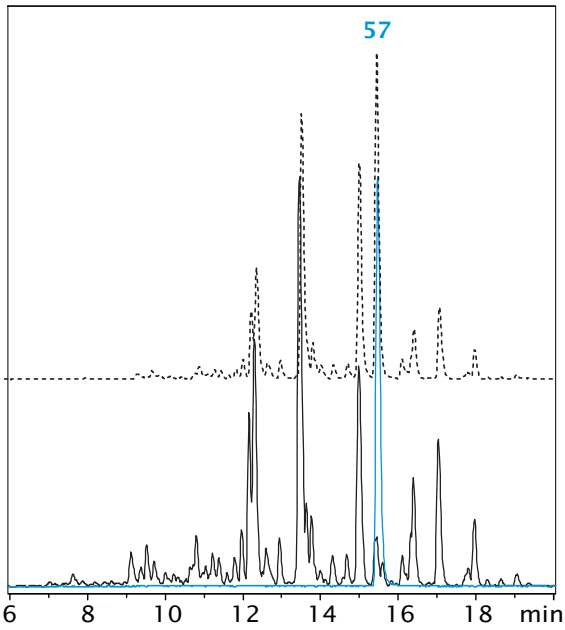

Figure 3.21 Overlay of the HPLC-HRMS base peak chromatogram of the crude extract of a *Haliclona viscosa* sample from 2000 (black), the synthetic Haliclocyclin C (**57**, blue), and a mixture of both (dotted line). Due to the use of different chromatographic methods, the retention times deviate from the original analysis.

(Figure 3.21). Thus, it can be concluded that the natural compound **57** very likely has the same structure as the synthetic haliclocyclin C (**57**, see manuscript on page 217). This is the first report of the macrocyclic monomer **57** from natural sources.

3.3.2 Haliclamines with saturated alkyl chains

Haliclamines and cyclostellettamines with saturated alkyl chains can be recognized in HRMS by their fragments that constitute the mass equivalent of a THP or Pyr moiety connected to one alkyl chain (see Grube et al.[117] and manuscript 1 on page 183). Consequently, two fragments are expected in compounds with chains of different length. In non-fragmentation mode, the fragments are usually of low intensity but nevertheless clearly present.

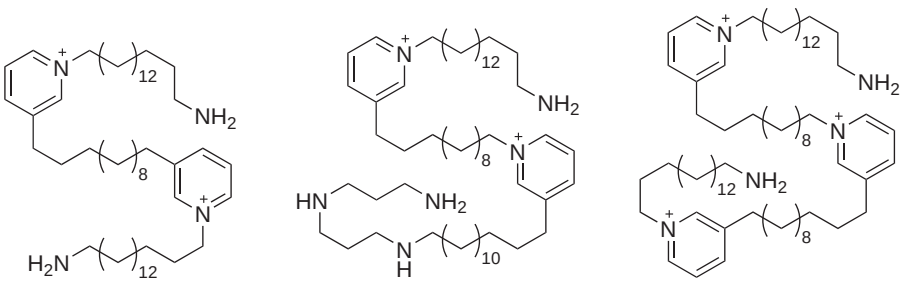

Figure 3.22 Pachychalines A-C (**58-60**).

When relying almost exclusively on mass spectrometric results, considerations regarding the connectivity of the alkyl chains in 3-APAs should be performed. Most 3-APAs published to-date are head-to-tail linked pyridinium or tetrahydropyridine compounds; however, there are also examples for head-to-head and tail-to-tail linked naturally occuring pyridinium alkaloids. The pachychalines A-C (**58**-**60**) isolated from *Pachychalina* sp. from the Caribbean are linear 3-(aminoalkyl) pyridinium salts with head-to-tail, head-to-head and tail-to-tail linked pyridinium moieties.[121]

The molecular mass of head-to-tail linked 3-APAs is not distinguishable from head-to-head or tail-to-tail linked structures. However, if the fragmentation in head-to-head and tail-to-tail linked compounds bases on the same mechanisms as observed in head-to-tail linked pyridinium and tetrahydropyridine compounds, the three can be distinguished by their fragments. The fragmentation of 3-alkyl pyridinium compounds in in-sourcecollision induced dissociation (CID) experiments builds on three different fragmentation reactions; Hofmann fragmentation, onium reaction and McLafferty rearrangement. 3-Alkyl tetrahydropyridine fragmentation is dominated by the retro-Diels-Alder reaction (Figure 3.23).

In the 3-alkylpyridinium compounds, all three fragmentation reactions lead to fragments of the same mass and thus cannot be distinguished in MS experiments. In the case of the cyclostellettamines, the major fragments comprise the mass equivalent of a pyridine moiety connected to either alkyl chain. This first fragmentation step may then be followed by cleavage of the alkyl chain, but the highest intensity fragments constitute pyridine moieties with "intact" alkyl chains (Figure 3.23).[117]

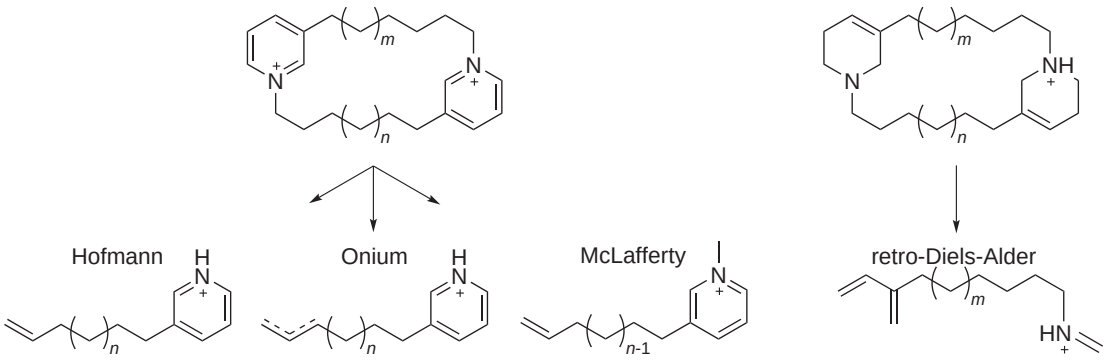

Figure 3.23 Proposed main fragments of head-to-tail linked cyclostellettamines (fragment masses for $n = 4$: $m/z = 204$, $n = 5$: $m/z = 218$, $n = 6$: $m/z = 232$, $n = 7$: $m/z = 246$, $n = 8$: $m/z = 260$) and haliclamines (all cyclostellettamine fragment masses by $m/z = 4$ higher).

Similar fragmentation mechanisms in tail-to-tail linked 3-alkyl pyridinium alkaloids would lead to a fragment that consists of two pyridine moieties interconnected in 3-position by an alkyl chain. Timm synthesized a head-to-tail and a tail-to-tail linked viscosaline, subjected it to fragmentation experiments and confirmed that head-to-tail linked viscosalines were distinguishable from tail-to-tail linked viscosalines by their mass (Figure 3.24, for viscosaline fragmentation see Section 3.3.5).[84] While the head-to-tail linked viscosaline C (**18**) showed a Pyr + alkyl chain type fragment at $m/z = 260$, fragmentation of the tail-to-tail linked viscosaline resulted in a fragment of $m/z = 339$, corresponding to two pyridine moieties connected by an alkyl chain, as well as the aminoalkyl fragment $m/z = 198$.

Fragmentation of cyclostellettamine C (**33**) which has the same chain lengths as viscosaline C (**18**) is expected to result in the same fragment $m/z = 339$. In contrast to the tail-to-tail linked viscosaline however, tail-to-tail linked cyclostellettamines would not show the aminoalkyl fragment that, in viscosaline C (**18**), derives from cleavage of the amino-acid carrying alkyl chain (Figure 3.25). In macrocyclic dimers, tail-to-tail linked compounds are the equal of head-to-head linked compounds. Differences may be seen in linear or trimeric and polymeric cyclic pyridinium alkaloids but the fragmentation of these compounds has not been examined, yet.

Tetrahydropyridines can probably be distinguished in the same way. The tetrahydropyridine fragmentation results in methylene-iminium ions (manuscript 1, page 183). In the case of tail-to-tail linked tetrahydropyridines, this fragmentation mech-

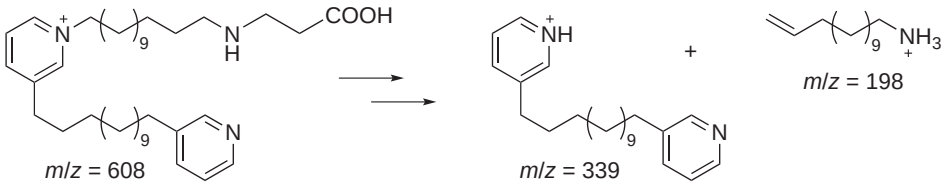

Figure 3.24 Fragmentation of tail-to-tail linked viscosaline C (**18**). Modified from Timm.[84]

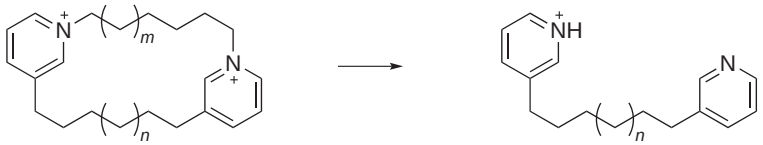

Figure 3.25 Proposed fragmentation for tail-to-tail linked cyclostellettamines. Fragment masses for $n = 4$: $m/z = 283$, $n = 5$: $m/z = 297$, $n = 6$: $m/z = 311$, $n = 7$: $m/z = 325$, $n = 8$: $m/z = 339$.

anism most likely results in fragments that contain two nitrogen atoms and are thus discernible from their head-to-tail linked analogs by exact mass (Figure 3.26). However, this proposed fragmentation needs to be experimentally confirmed.

Since the njaoaminiums B (**41**) and C (**42**) represent examples of 3-APAs with branched alkyl chains,[95] also the possibility of methyl (and other homologously) branched alkyl chains should be considered in this context. The molecular mass of compounds with branched C_n alkyl chains does not differ from those with straight C_{n+1} alkyl chains. However, the fragmentation pattern is different by favoured cleavage in proximity to the branch which allows the determination of the position of e.g. methyl branches by mass spectrometric methods. In contrast to double bonds, the position of methyl branches is stable inside an alkyl chain. Direct σ-cleavage leads to a relative (though not diagnostic) increase in intensity of the charge-retaining fragment mass peak while α-cleavage leads to loss of C_nH_{2n} and C_nH_{2n+1} fragments.[122]

None of the proposed fragments for tail-to-tail linked pyridinium or tetrahydropyridine alkaloids are observed in the compound peaks resulting from LC-MS analysis of the crude extract, nor is chain branching specific fragmentation observed in the compounds. Therefore, the identification of new compounds bases on the known structure of 3-APAs in *Haliclona viscosa*, i.e. head-to-tail linked compounds with unbranched alkyl chains.

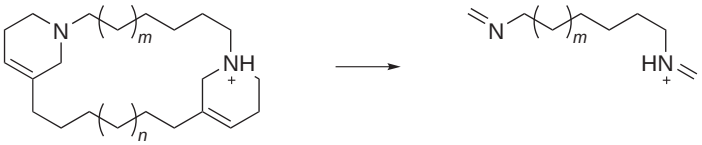

Figure 3.26 Proposed fragmentation for cyclic dimeric tail-to-tail linked haliclamines. Fragment masses for $m = 4$: $m/z = 183$, $m = 5$: $m/z = 197$, $m = 6$: $m/z = 211$, $m = 7$: $m/z = 225$, $m = 8$: $m/z = 239$.

Haliclamine J (**61**)* — haliclamine 10/10 (0/0)

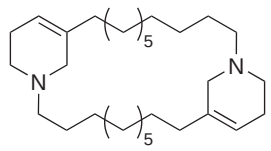

61

	peak	m/z	mol. form.	Δm
C	$[M+H]^+$	443.4370	$C_{30}H_{56}N_2$	2.3 ppm
C	$[M+2H]^{2+}$	222.2225	$C_{30}H_{57}N_2$	3.7 ppm
$F_{1/2}$	$[M+H]^+$	222.2225	$C_{15}H_{28}N$	3.7 ppm
F_3	$[M+H]^+$	400.3949	$C_{28}H_{50}N$	2.7 ppm
F_4	$[M+H]^+$	414.4104	$C_{29}H_{52}N$	2.4 ppm

C: compound masses, F: fragment masses

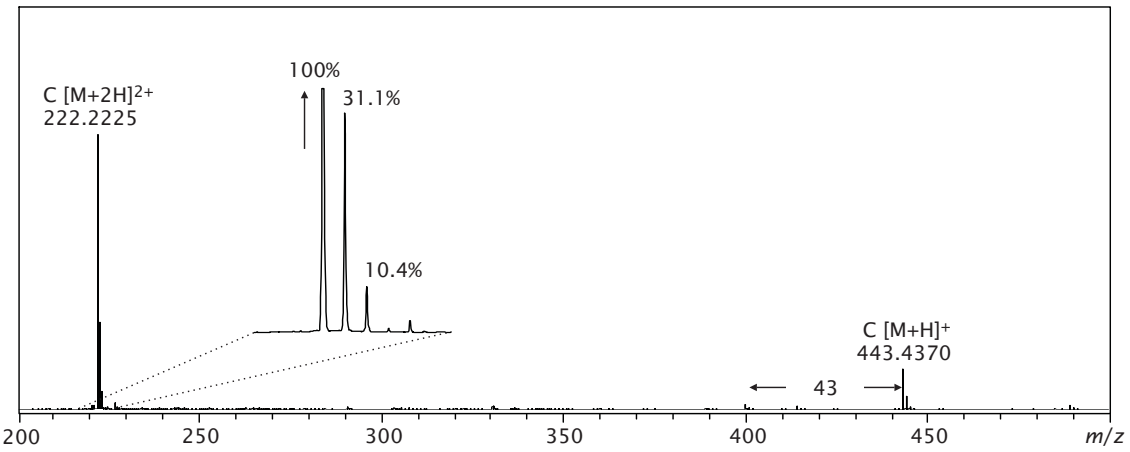

Figure 3.27 Structural formula, compound and fragment masses and high resolution mass spectrum for the peak at 13.8-14.0 min, identified as haliclamine J (**61**). $F_{1/2}$ = THP + alkyl chain type fragments, F_3 and F_4 = fragments derived from loss of *N*-methylene methanamine and methanimine, respectively.

Compound **61** at a retention time of 13.8-14.0 min shows a singly charged pseudomolecular ion $[M+H]^+$ at $m/z = 443.4370$ and a doubly charged pseudomolecular ion $[M+2H]^{2+}$ at $m/z = 222.2225$ corresponding to the molecular formula $C_{30}H_{55}N_2$ [M]. The same molecular formula and similar masses are assigned to haliclamine C (**27**), but **27** elutes at a retention time of 14.0-14.2 min. Haliclamine C (**27**) contains two alkyl chains of 9 and 11 methylene groups, respectively. The high resolution mass spectrum of haliclamine C (**27**) shows mass peaks of two fragments F_1 at $m/z = 208.2090$ and F_2 at $m/z = 236.2331$ which represent the mass equivalent of a THP moiety connected to either alkyl chain. In the mass spectrum of compound **61** the fragments superimpose with the doubly charged pseudomolecular ion peak which suggests the alkyl chains to be of equal length of 10 methylene groups. This is supported by the observed relative isotope peak intensity (PI, given in % relative to the

monoisotopic peak) of the doubly charged pseudomolecular ion which deviates from the calculated PI as well as the observed isotope pattern (see inlay in Figure 3.27). While the calculated isotope PI is 100 : 33.3 : 5.5, the observed PI is 100 : 31.1 : 10.4. The increase in intensity of the X+2 isotope peak of the doubly charged ion is caused by an underlying X+1 isotope peak of the singly charged fragment $F_{1/2}$. The X+2 isotope peak of $F_{1/2}$ consequently lies at $m/z = 224.2244$. Both results suggest that compound **61** should be a haliclamine 10/10 with saturated alkyl chains (0/0).

Apart from the main fragments that constitute the mass equivalent of a THP moiety connected to either alkyl chain, the mass spectrum shows incipient fragmentation that is discussed in manuscript 1 (page 183). The fragment F_3 that derives from loss of *N*-methylene methanamine ($\Delta m/z = 43$) is present at $m/z = 400.3949$ while the fragment F_4 that emerges from loss of methanimine ($\Delta m/z = 29$) is present at very low intensity at $m/z = 414.4104$.

Haliclamine K (**62**)* — haliclamine 10/12 (0/0)

Compound **62** elutes at 17.0-17.3 min and shows a singly charged pseudomolecular ion $[M+H]^+$ at $m/z = 471.4699$ and a doubly charged pseudomolecular ion $[M+2H]^{2+}$ at $m/z = 236.2385$. This corresponds to a molecular formula of $C_{32}H_{60}N_2$ [M], the same as has been established for haliclamine F (**30**) which elutes at a retention time of 16.8-17.0 min. With the alkyl chains of haliclamine F (**30**) being of equal length of 11 methylene groups the fragments that represent the THP moiety connected to an alkyl chain concur with the doubly charged pseudomolecular ion. In the mass spectrum of compound **62** however, two fragment peaks are visible at $m/z = 222.2218$ and $m/z = 250.2538$. They correspond to fragments that carry alkyl chains of 10 and 12 methylene groups, respectively.

The fragment masses that correspond to the loss of *N*-methylene methanamine (F_3) and methanimine (F_4) are visible at $m/z = 428.4253$ and $m/z = 442.4423$, respectively. Both new haliclamines with saturated alkyl chains must be confirmed by further chromatographic, MS and NMR experiments (manuscript draft on page 223).

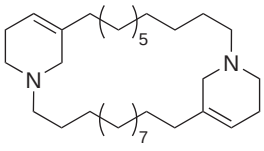

62

	peak	m/z	mol. form.	Δm
C	$[M+H]^+$	471.4699	$C_{32}H_{61}N_2$	5.5 ppm
C	$[M+2H]^{2+}$	236.2385	$C_{32}H_{62}N_2$	5.2 ppm
F_1	$[M+H]^+$	222.2218	$C_{15}H_{28}N$	0.7 ppm
F_2	$[M+H]^+$	250.2538	$C_{17}H_{32}N$	3.5 ppm
F_3	$[M+H]^+$	428.4253	$C_{30}H_{54}N$	0.5 ppm
F_4	$[M+H]^+$	442.4423	$C_{31}H_{56}N$	3.6 ppm

C: compound masses, F: fragment masses

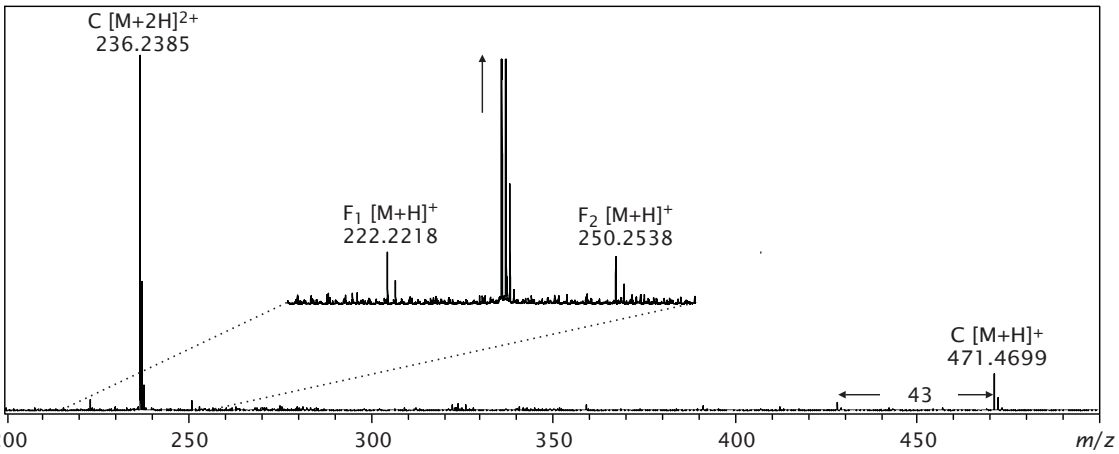

Figure 3.28 Structural formula, compound and fragment masses and high resolution mass spectrum for the peak at 17.0-17.3 min, identified as haliclamine K (**62**). $F_{1/2}$ = THP + alkyl chain type fragments, F_3 and F_4 = fragments derived from loss of *N*-methylene methanamine and methanimine, respectively.

3.3.3 Haliclamines with monounsaturated alkyl chains

Similar to haliclamines with saturated alkyl chains, double bonds may be assigned to either THP + alkyl chain type fragment by the mass of the double bond carrying fragment being two mass units lower than the corresponding fragment with saturated chains.

Dehydro-Haliclamine C (**63**)* — haliclamine 9/11 (0/1)

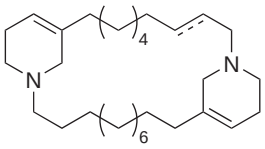

63

	peak	m/z	mol. form.	Δm
C	$[M+H]^+$	441.4214	$C_{30}H_{53}N_2$	2.5 ppm
C	$[M+2H]^{2+}$	221.2146	$C_{30}H_{54}N_2$	3.6 ppm
F_1	$[M+H]^+$	208.2090	$C_{14}H_{26}N$	4.5 ppm
F_2	$[M+H]^+$	234.2228	$C_{16}H_{28}N$	5.0 ppm
F_3	$[M+H]^+$	398.3794	$C_{28}H_{48}N$	3.2 ppm
F_4	$[M+H]^+$	412.3938	$C_{29}H_{50}N$	3.7 ppm

C: compound masses, F: fragment masses

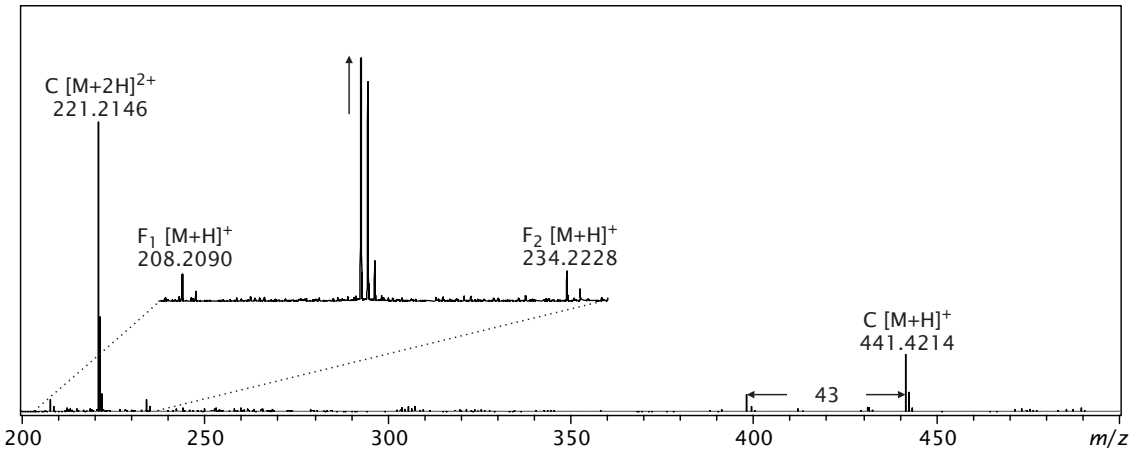

Figure 3.29 Structural formula, compound and fragment masses and high resolution mass spectrum for the peak at 12.7-12.8 min, identified as dehydro-haliclamine C (**63**). $F_{1/2}$ = THP + alkyl chain type fragments, F_3 and F_4 = fragments derived from loss of *N*-methylene methanamine and methanimine, respectively. The exact position of the double bond is not determined, yet.

Compound **63** elutes at a retention time of 12.7-12.8 min. Its molecular mass is by two mass units lower than the mass of haliclamine C (**27**) and J (**61**) and suggests that the compound contains an additional double bond. With an additional double bond, either chain fragment can be by two mass units lower than those of haliclamine C (**27**) and J (**61**), resulting in possible fragment peaks at $m/z = 208\,\&\,234$ for haliclamine 9/11 (0/1), $m/z = 206\,\&\,236$ for haliclamine 9/11 (1/0) and $m/z = 220\,\&\,222$ for haliclamine 10/10 (1/0). In the mass spectrum of compound **63**, two distinct fragment peaks are visible at $m/z = 208.2090$ and $m/z = 234.2228$. This corresponds to alkyl chains of 9 and 11 methylene units with a double bond in the $(CH_2)_{11}$ alkyl chain.

Dehydro-Haliclamine D (**64**)* — haliclamine 10/11 (0/1)

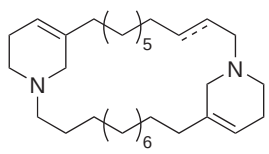

64

	peak	m/z	mol. form.	Δm
C	$[M+H]^+$	455.4384	$C_{31}H_{55}N_2$	5.2 ppm
C	$[M+2H]^{2+}$	228.2229	$C_{31}H_{56}N_2$	5.5 ppm
F_1	$[M+H]^+$	222.2224	$C_{15}H_{28}N$	3.6 ppm
F_2	$[M+H]^+$	232.2221	$C_{16}H_{28}N$	1.9 ppm
F_3	$[M+H]^+$	412.3938	$C_{29}H_{50}N$	5.1 ppm
F_4	$[M+H]^+$	426.4089	$C_{30}H_{52}N$	1.2 ppm

C: compound masses, F: fragment masses

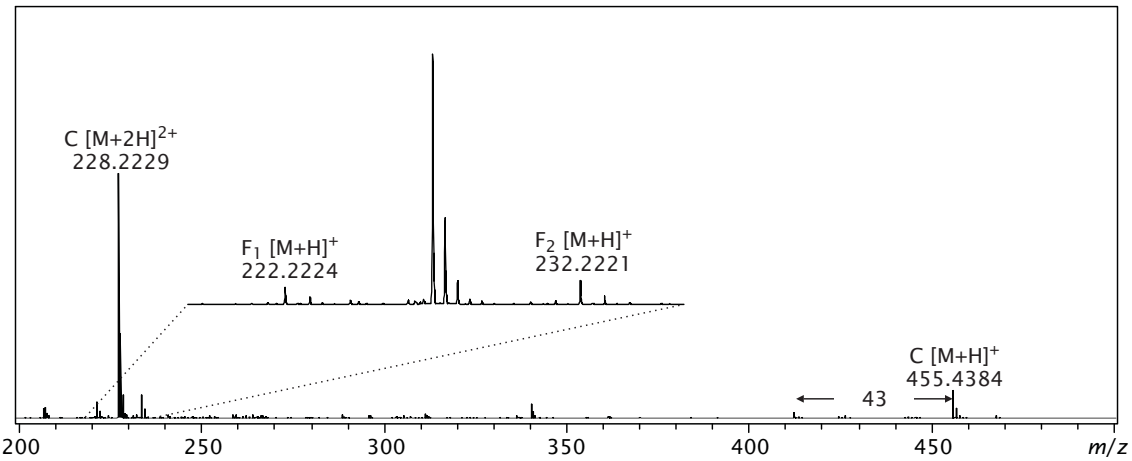

Figure 3.30 Structural formula, compound and fragment masses and high resolution mass spectrum for the peak at 14.3-14.5 min, identified as dehydro-haliclamine D (**64**). $F_{1/2}$ = THP + alkyl chain type fragments, F_3 and F_4 = fragments derived from loss of *N*-methylene methanamine and methanimine, respectively. The exact position of the double bond is not determined, yet.

Compound **64** elutes at a retention time of 14.3-14.5 min and shows a molecular mass that is two mass units lower than that of haliclamine D (**28**) or of a potential haliclamine 9/12. The mass suggests a double bond in one of the chains. This would result in fragment peaks at $m/z = 222\,\&\,234$ for haliclamine 10/11 (0/1), $m/z = 220\,\&\,236$ for haliclamine 10/11 (1/0), $m/z = 208\,\&\,244$ for haliclamine 9/12 (0/1) or $m/z = 206\,\&\,248$ for haliclamine 9/12 (1/0). The fragments observed in the mass spectrum of compound **64** are $m/z = 222.2224$ and $m/z = 234.2221$ and therefore correspond to a haliclamine with alkyl chains of 9 and 11 methylene groups of which the $(CH_2)_{11}$ alkyl chain contains a double bond.

Dehydro-Haliclamine F (**65**)* — haliclamine 11/11 (1/0)

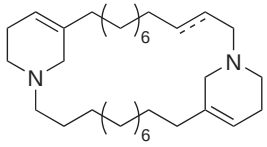

65

	peak	m/z	mol. form.	Δm
C	$[M+H]^+$	469.4537	$C_{32}H_{57}N_2$	4.5 ppm
C	$[M+2H]^{2+}$	235.2310	$C_{32}H_{58}N_2$	6.4 ppm
F_1	$[M+H]^+$	234.2222	$C_{16}H_{28}N$	2.6 ppm
F_2	$[M+H]^+$	236.2331	$C_{16}H_{30}N$	9.7 ppm
F_3	$[M+H]^+$	426.4094	$C_{30}H_{52}N$	4.7 ppm
F_4	$[M+H]^+$	440.4200	$C_{31}H_{54}N$	11.6 ppm

C: compound masses, F: fragment masses

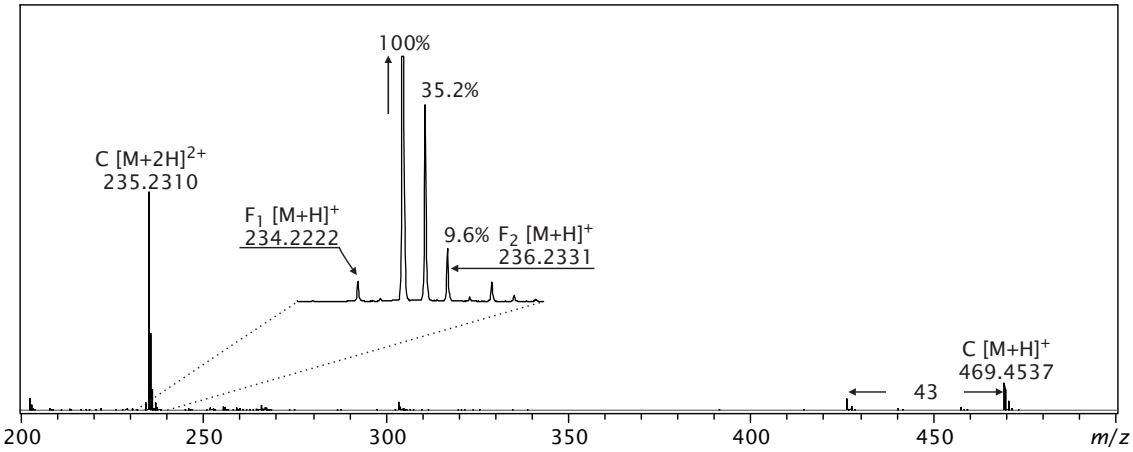

Figure 3.31 Structural formula, compound and fragment masses and high resolution mass spectrum for the peak at 15.8 min, identified as dehydro-haliclamine F (**65**). $F_{1/2}$ = THP + alkyl chain type fragments, F_3 and F_4 = fragments derived from loss of *N*-methylene methanamine and methanimine, respectively. The exact position of the double bond is not determined, yet.

Compound **65** elutes at a retention time of 15.8 min and has a molecular mass that is two mass units lower than that of haliclamine F (**30**) and K (**62**). Compound **65** shows fragment peaks at $m/z = 234.2222$ and $m/z = 236.2331$, with the latter being overlaid by the doubly charged pseudomolecular ion but clearly identified by the peak pattern (figure 3.31) and the elevated X+2 isotope peak of the doubly charged pseudomolecular ion (PI calcd. 100 : 35.6 : 6.4; found 100 : 35.2 : 9.6). Fragment peaks that correspond to haliclamine 10/12 (1/0, $m/z = 220\,\&\,250$) or haliclamine 10/12 (0/1, $m/z = 222\,\&\,248$) are missing.

Dehydro-Haliclamine J (**66**)* — haliclamine 10/10 (1/0)

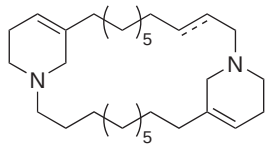

66

	peak	m/z	mol. form.	Δm
C	$[M+H]^+$	441.4216	$C_{30}H_{53}N_2$	2.9 ppm
C	$[M+2H]^{2+}$	221.2155	$C_{30}H_{54}N_2$	7.6 ppm
F_1	$[M+H]^+$	220.2076	$C_{15}H_{26}N$	7.4 ppm
F_2	$[M+H]^+$	222.2203	$C_{15}H_{28}N$	5.9 ppm
F_3	$[M+H]^+$	398.3796	$C_{28}H_{48}N$	3.6 ppm
F_4	$[M+H]^+$	412.3898	$C_{29}H_{50}N$	9.7 ppm

C: compound masses, F: fragment masses

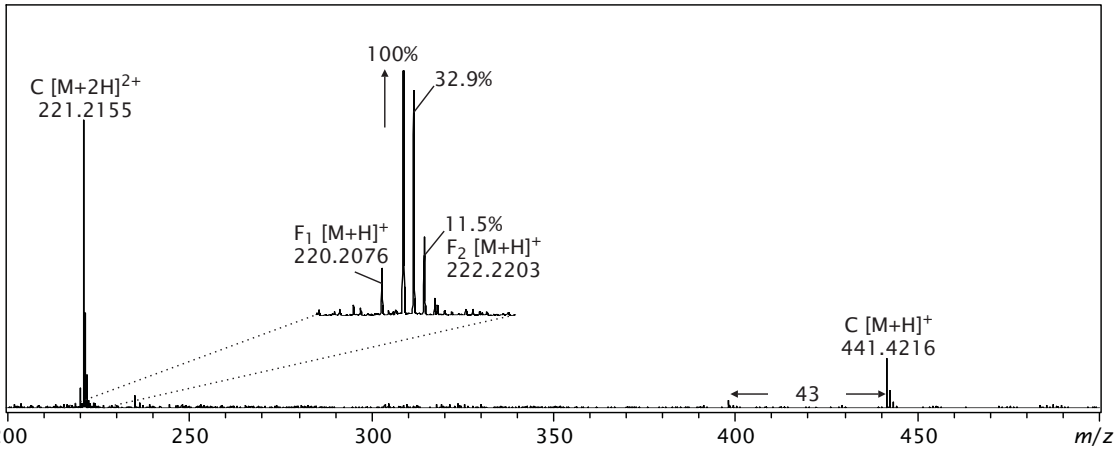

Figure 3.32 Structural formula, compound and fragment masses and high resolution mass spectrum for the peak at 13.0 min, identified as dehydro-haliclamine J (**66**). $F_{1/2}$ = THP + alkyl chain type fragments, F_3 and F_4 = fragments derived from loss of *N*-methylene methanamine and methanimine, respectively. The exact position of the double bond is not determined, yet.

Compound **66** elutes at a retention time of 13.0 min and shows very similar molecular masses as dehydro-haliclamine C (**63**) which results in the same molecular formula of $C_{30}H_{52}N_2$ [M] as for dehydro-haliclamine C (**63**). Since dehydro-haliclamine C (**63**) is assigned to the peak at 12.7-12.8 min, this new compound **66** is likely to represent haliclamine 9/11 (1/0) or haliclamine 10/10 (1/0). Haliclamine 9/11 (1/0) requires fragment peaks of $m/z = 206\,\&\,234$ and while $m/z = 236.2234$ can be found, the $m/z = 206$ peak is missing. Haliclamine 10/10 (1/0) requires fragment peaks of $m/z = 220\,\&\,222$. Both can be found in the compound spectrum; $m/z = 220.2076$ and $m/z = 222.2203$. However, the $m/z = 222$ peak is overlaid by the doubly charged pseudomolecular ion. A comparison of the peak intensities between the calculated and the effective doubly charged pseudomolecular ion yields a significantly

enlarged X+2 doubly charged pseudomolecular ion isotope peak; instead of an isotope PI ratio of 100 : 33.8 : 5.5, the doubly charged pseudomolecular ion shows an isotope ratio of 100 : 32.9 : 11.5. Thus compound **66** is assigned as the haliclamine 10/10 (1/0) isomer.

Ambidehydro-Haliclamine F (**67**)* — haliclamine 11/11 (1/1)

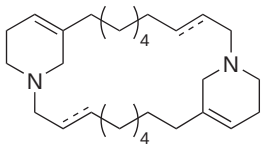

67

	peak	m/z	mol. form.	Δm
C	$[M+H]^+$	467.4376	$C_{32}H_{55}N_2$	3.5 ppm
C	$[M+2H]^{2+}$	234.2222	$C_{32}H_{56}N_2$	2.3 ppm
$F_{1/2}$	$[M+H]^+$	234.2222	$C_{16}H_{28}N$	2.3 ppm
F_3	$[M+H]^+$	424.3960	$C_{30}H_{50}N$	5.3 ppm
F_4	$[M+H]^+$	438.4087	$C_{31}H_{52}N$	1.8 ppm

C: compound masses, F: fragment masses

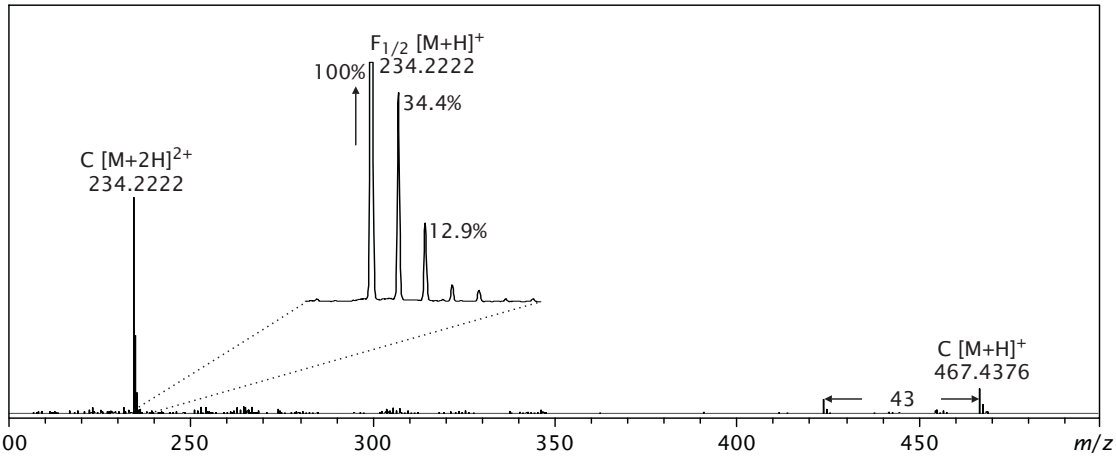

Figure 3.33 Structural formula, compound and fragment masses and high resolution mass spectrum for the peak at 14.7-14.8 min, identified as ambidehydro-haliclamine F (**67**). $F_{1/2}$ = THP + alkyl chain type fragments, F_3 and F_4 = fragments derived from loss of *N*-methylene methanamine and methanimine, respectively. The exact position of the double bonds is not determined, yet.

Compound **67** elutes at a retention time of 14.7-14.8 min. The molecular mass of the compound mass lies four mass units below the mass of haliclamine F (**30**) and K (**62**) and suggests two double bonds. They may be located one in each alkyl chain or both in either alkyl chain, leaving a number of possibilities for fragment masses; $m/z = 236\,\&\,232$ for haliclamine 11/11 (0/2), $m/z = 234\,\&\,234$ for haliclamine 11/11 (1/1), $m/z = 218\,\&\,250$ for haliclamine 10/12 (2/0), $m/z = 222\,\&\,246$ for haliclamine

10/12 (0/2), and 220 & 248 for haliclamine 10/12 (1/1). None of these masses can be found in the compound spectrum with the exception of $m/z = 234.2222$ which constitutes the doubly charged pseudomolecular ion. However, the peak pattern and the peak integrals confirm that a singly charged peak representing the molecular formula $C_{16}H_{28}N$ underlies the pseudomolecular ion (PI calcd. 100 : 35.9 : 6.3, found 100 : 34.4 : 12.9, X+2 isotope peak at $m/z = 236.2234$). Compound **67** can therefore be assigned as haliclamine 11/11 with a double bond in each alkyl chain.

3.3.4 Haliclamines with bisunsaturated alkyl chains

Didehydro-Haliclamine D (**68**)* — haliclamine 10/11 (0/2)

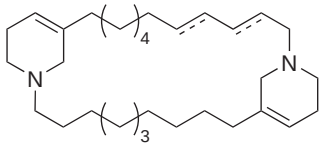

68

	peak	m/z	mol. form.	Δm
C	$[M+H]^+$	453.4164	$C_{31}H_{53}N_2$	8.7 ppm
C	$[M+2H]^{2+}$	227.2095	$C_{31}H_{54}N_2$	13.7 ppm
F_1	$[M+H]^+$	222.2187	$C_{15}H_{28}N$	13.1 ppm
F_2	$[M+H]^+$	232.2048	$C_{16}H_{26}N$	19.4 ppm
F_3	$[M+H]^+$	410.3738	$C_{29}H_{48}N$	10.6 ppm
F_4	$[M+H]^+$	424.3901	$C_{30}H_{50}N$	8.6 ppm

C: compound masses, F: fragment masses

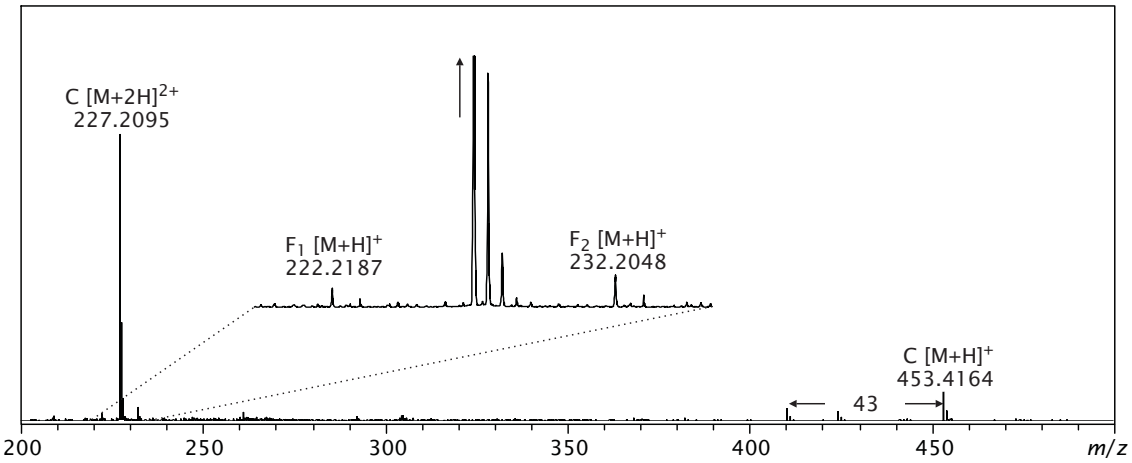

Figure 3.34 Structural formula, compound and fragment masses and high resolution mass spectrum for the peak at 13.8 min, identified as didehydro-haliclamine F (**68**). $F_{1/2}$ = THP + alkyl chain type fragments, F_3 and F_4 = fragments derived from loss of *N*-methylene methanamine and methanimine, respectively. The exact position of the double bonds is not determined, yet.

Compound **68** that is present at low abundance in *Haliclona viscosa* sampled in 1999 and in the 2009 cave sample elutes at a retention time of 13.8 min. The molecular masses correspond to the molecular formula $C_{31}H_{52}N_2$ [M] and lie four mass units lower than the molecular mass of haliclamine D (**28**). Four mass units difference suggest the presence of two additional double bonds which, as before, may be located together in either alkyl chain or one in each chain. This leaves the fragment masses $m/z = 220\,\&\,234$ for haliclamine 10/11 (1/1), $m/z = 218\,\&\,236$ for haliclamine 10/11 (2/0), and $m/z = 222\,\&\,232$ for haliclamine 10/11 (0/2) as possibilities for compound **68**. While neither $m/z = 220$ nor $m/z = 234$, $m/z = 218$ and $m/z = 236$ can be observed in the compound mass spectrum, the masses $m/z = 222.2187$ and $m/z = 232.2048$ are present. They represent a saturated alkyl chain of 10 methylene units and a bisunsaturated alkyl chain of 11 carbons. This defines the compound as haliclamine 10/11 (0/2).

3.3.5 Viscosalines

In addition to viscosaline C (**18**) which was originally reported by Volk under the name "viscosaline" but later termed "C" for its corresponding chain lengths to cyclostellettamine C (**33**), Timm[84] suggests two additional viscosalines, viscosaline B and E which each occur in two isomeric constitutions, B_1 (**19**), B_2 (**20**), E_1 (**21**) and E_2 (**22**).[123]

Timm does not succeed in differentiating the constitutional isomers in HPLC-HRMS experiments since the chromatographic separation is not successful. Also the mass spectrometric analysis of synthetically prepared isomers does not give unambiguous results in the context of assigning the position of the alkyl chains. His final discrimination of the four viscosalines builds on a derivatization approach; he derivatizes the synthetically prepared isomers prior to MS measurement which allows him to determine isomer-specific fragments. Derivatization of the viscosaline B- and E-containing fractions of the *H. viscosa* crude extract and subsequent HPLC-HRMS measurement yields baseline separated compound peaks which each show isomer-specific fragments. From this he draws the conclusion that both isomers of viscosaline B and E are present in the crude extract. Achim Grube, a former PhD student in the Köck research group, later succeeds in separating and differentiating the underivatized, synthetic isomers by HPLC.[123]

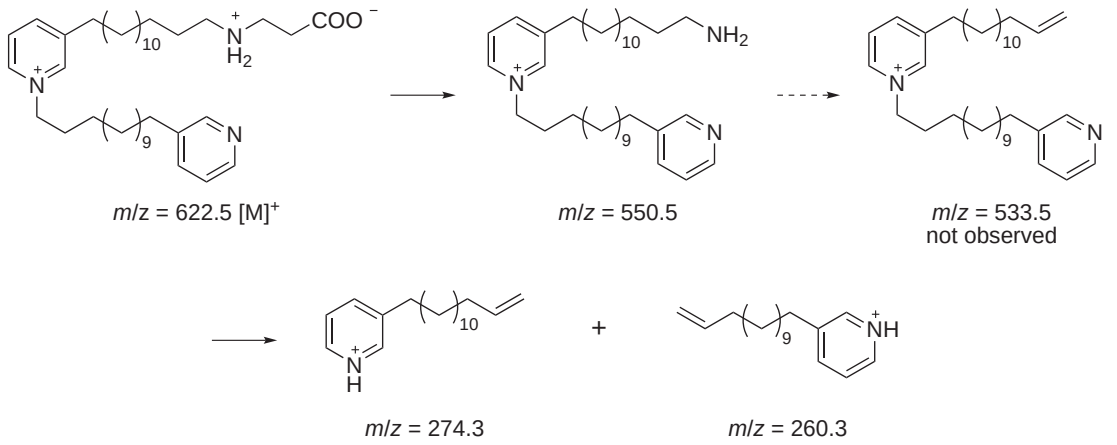

Figure 3.35 Proposed fragmentation of viscosaline E_1 (**21**) under CID-MS conditions in an ion trap mass spectrometer.[123]

Grube also investigates the fragmentation pattern of the synthetic viscosalines under CID-MS^n conditions in an ion trap mass spectrometer. He states that fragmentation of the singly charged molecular ion results in an initial loss of $m/z = 72$ which he attributes to a simultaneous loss of CO_2 and ethene. Subsequently, a fragmentation into the Pyr + alkyl chain type fragments also observed during fragmentation of the cyclostellettamines (Figure 3.35) occurs for which a neutral loss of NH_3 ($m/z = 17$) has to proceed.[117] However, with both Pyr + alkyl chain type fragments of viscosalines with dissimilar chain lengths co-existing in the same mass spectrum it is not possible to assign the position of the two alkyl chains.

In a different approach he uses a reduced trap drive level (analogous to in-source-CID, see Section 3.3.2 and manuscript 1 on page 183) which results in increased fragmentation prior to the entrance of the ions into the ion trap. Thus, a number of fragments become visible in the full scan spectrum apart from the Pyr + alkyl chain type fragments that aid in structure assignment. In viscosaline E_1 (**21**), a doubly charged $m/z = 281.8$ derives from the singly charged precursor $m/z = 622.5$ by an α-cleavage inside the amino acid moiety. This unusual event of a doubly charged progeny emerging from a singly charged precursor is explained by the nature of the precursor; it persists as a zwitterion and carries an additional charged pyridinium nitrogen; cleavage of the negatively charged part of the zwitterion results in the double positively charged ion $m/z = 281.8$ (Figure 3.36). Accordingly, the fragment $m/z = 281.8$ may occur in two different forms in which the charges are located at different nitrogen atoms .

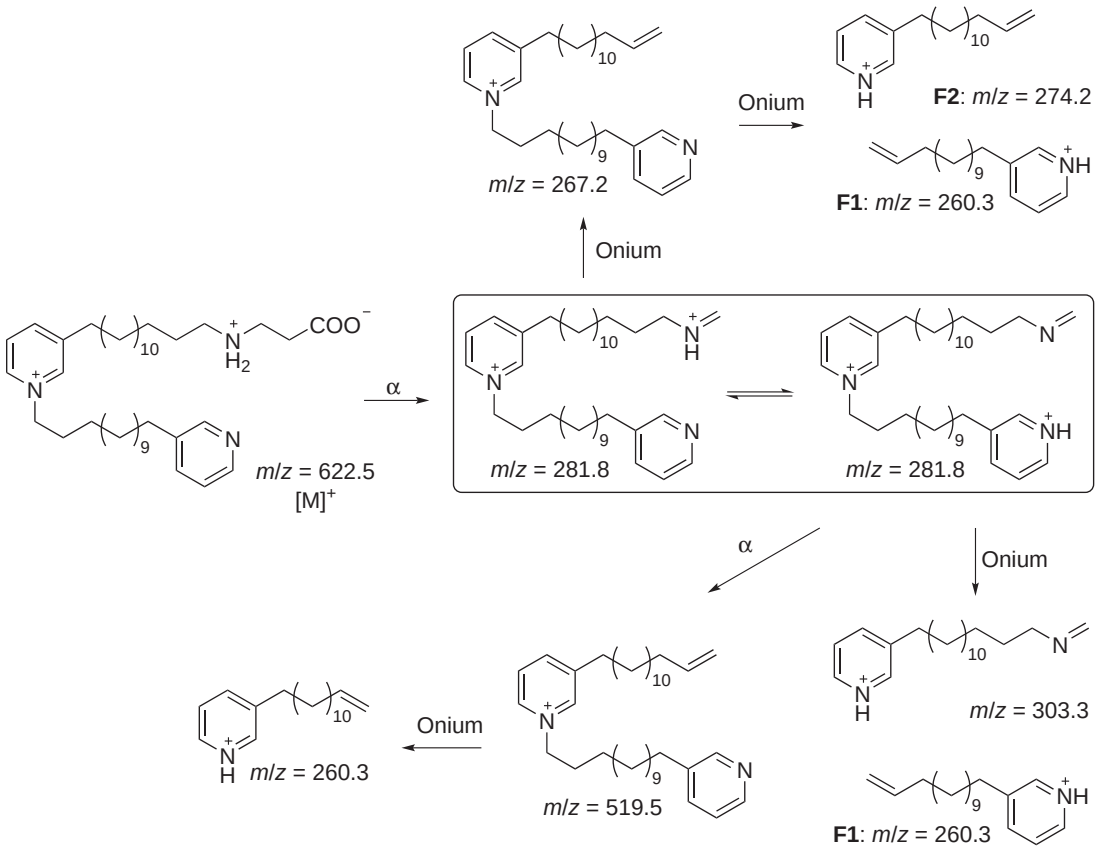

Figure 3.36 Proposed fragmentation of viscosaline E_1 (**21**) under in-source-CID + MS^n conditions in an ion trap mass spectrometer. Modified from Timm et al. [123]

Trapping and fragmentation of the doubly charged $m/z = 281.8$ of viscosaline E_1 (**21**) results in the singly charged fragments $m/z = 260.3$, $m/z = 303.3$ and $m/z = 519.5$. Of these fragments, only $m/z = 303.3$ is a characteristic fragment by which the constitution of the viscosalines can be assigned. This fragment represents a pyridine moiety connected in position 3 to an imine-carrying C_{14} alkyl chain; the imine derives from α cleavage inside the amino acid residue. This fragment is characteristic for viscosaline E_1 (**21**) where the amino acid connecting alkyl chain carries 14 methylene groups (Figure 3.36). The corresponding singly charged imine fragments for C_{13} and C_{12} alkyl chains are $m/z = 289.2$, $m/z = 275.3$, respectively. [123]

It should be noted, however, that this fragmentation (as well as any other fragmentation method used to differentiate the viscosaline isomers), still requires a preceding separation of the isomers.

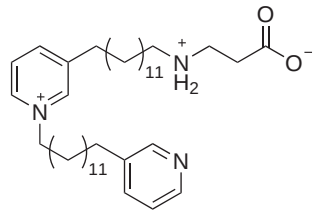

18

	peak	m/z	mol. form.	Δm
C	$[M]^+$	608.5172	$C_{39}H_{67}N_3O_2$	3.7 ppm
C	$[M+H]^{2+}$	304.7621	$C_{39}H_{68}N_3O_2$	3.2 ppm
C	$[M+2H]^{3+}$	203.5130	$C_{39}H_{69}N_3O_2$	15.6 ppm
F_1	$[M+H]^{2+}$	260.2376	$C_{36}H_{60}N_2$	1.3 ppm
F_2	$[M+H]^{2+}$	274.7509	$C_{37}H_{63}N_3$	22.3 ppm
F_2	$[M+2H]^{3+}$	183.5018	$C_{37}H_{64}N_3$	1.3 ppm

C: compound masses, F: fragment masses

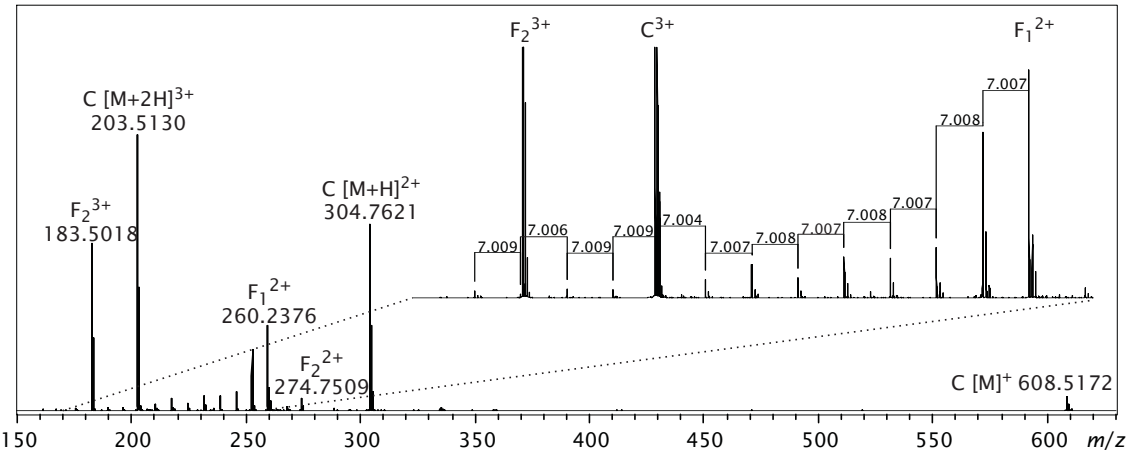

Figure 3.37 Structural formula, compound and fragment masses and high resolution mass spectrum for viscosaline C (**18**). The region important to determine the alkyl chain cleavage is expanded. F_1 = fragment mass derived from β-alanine loss, F_2 = fragment masses derived from acetate loss. The decreasing mass accuracy with decreasing m/z is due to instrument and method settings.

By improvement of the chromatographic separation within the presented thesis it is possible to discriminate the constitutional isomers viscosaline B_1 (**19**) and B_2 (**20**) as well as E_1 (**21**) and E_2 (**22**) already in the crude extract, without prior derivatization, and without tandem mass spectrometry experiments. By the use of a "softer" fragmentation method than in the original publication of viscosaline C (**18**) and Timm's thesis, the compounds show a slightly different fragmentation pattern which is helpful in discriminating the isomers. The most apparent difference to the published mass spectrum is an observable alkyl chain cleavage in the chain that carries the amino acid residue. This cleavage is important when determining the length of the alkyl chain that carries the amino acid. It is especially helpful in viscosalines with dissimilar chain lengths or when determining the alkyl chain

affiliation of a possible double bond. This new fragmentation pathway is discussed again in the following for viscosaline C (**18**).

Viscosaline C (**18**) elutes at a retention time of 16.4-16.8 min. It is one of the major compounds in *H. viscosa* samples. The HRMS (ESI+) spectrum of viscosaline C (**18**) shows a number of characteristic peaks. On one hand, the singly, doubly and triply charged molecular ions assign the molecular formula $C_{39}H_{66}N_3O_2$ ([M], Figure 3.37).

In addition, the spectrum shows a doubly charged fragment F_1 at $m/z = 260.2376$, and a corresponding singly charged ion at $m/z = 519.4665$ present at very low intensity. The fragment $m/z = 260$ could be mistaken for an overlaid cyclostellettamine C (**33**) peak. Since cyclostellettamine C (**33**) elutes at a different retention time, the fragment peak can be assigned to viscosaline C (**18**) that has lost the β-alanine unit; this is achieved by an α-cleavage inside the amino acid to split off acetate, followed by an onium reaction to yield fragment **69** (Figure 3.39). Starting at the doubly charged fragment F_1, the fragments of a successive loss of 14 mass units (typical for alkyl chain cleavage) are clearly visible as the doubly charged $m/z = 253.2304$, $m/z = 246.2237$, $m/z = 239.2148$, etc. This alkyl chain cleavage can be followed, though at lower intensity than the molecular and main fragment masses, to the doubly charged $m/z = 176.1472$ which corresponds to 3-methyl-1-(13-(pyridinium-1-yl)tridecyl)pyridinium (**70**).

Another characteristic fragment, F_2, constitutes the triply charged $m/z = 183.5018$ (**71**). This fragment represents viscosaline C (**18**) in which acetate is lost from the β-alanine carrying alkyl chain by an α-cleavage. The corresponding doubly charged fragment is visible at $m/z = 274.7509$ (Figure 3.37). A cleavage of the second alkyl chain is not observed; splitting off the pyridinium moiety, probably by an α-cleavage,

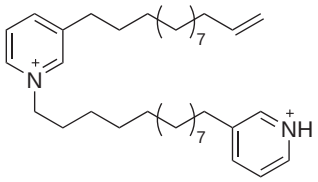

69, F_1
$m/z = 260.2376$

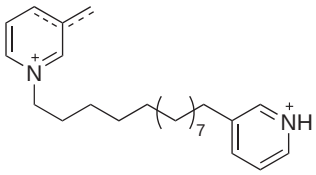

70, $m/z = 176.1472$

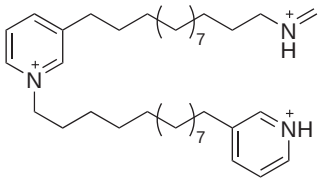

71, F_2
$m/z = 183.5018$

Figure 3.38 Structure of fragments in the MS-spectrum of viscosaline C (**18**).

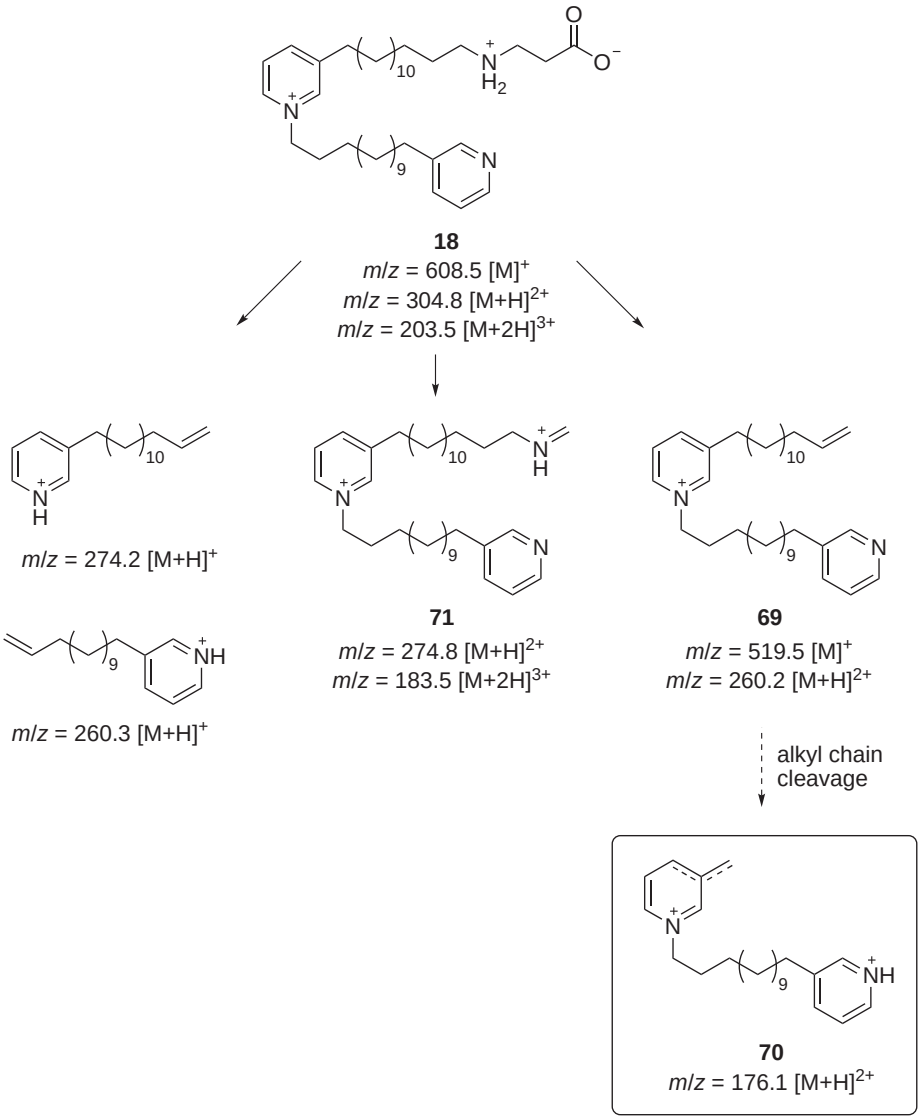

Figure 3.39 Proposed fragmentation pathway of viscosaline C (**18**) under in-source-CID conditions.

would result in a loss of $m/z = 92$ leading to the fragments $m/z = 530$ $[M]^+$ and $m/z = 265$ $[M+H]^{2+}$. These fragments are not present in the spectrum.

Cleavage of one 3-alkyl pyridine moiety results in a singly charged fragment **72** at $m/z = 349$ which is present as $m/z = 349.2833$ ($C_{21}H_{37}N_2O_2$, $\Delta m = 4.8$ ppm) in the spectrum at very low intensity. Thus it can be concluded that the cleavage of the amino acid carrying alkyl chain is the predominant fragmentation process under the applied instrument settings.

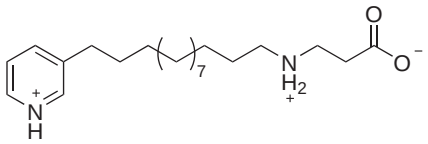

72, $m/z = 349.2833$

Figure 3.40 Proposed fragment that derives from loss of a 3-alkyl pyridine moiety.

Viscosaline B_1 (**19**) — viscosaline 12/13 (0/0)

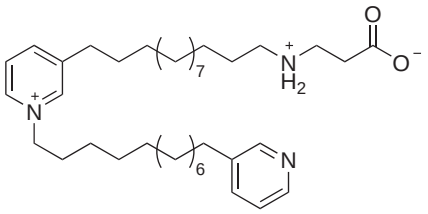

19

	peak	m/z	mol. form.	Δm
C	$[M]^+$	594.4949	$C_{38}H_{64}N_3O_2$	7.4 ppm
C	$[M+H]^{2+}$	297.7529	$C_{38}H_{65}N_3O_2$	1.5 ppm
C	$[M+2H]^{3+}$	198.8413	$C_{38}H_{66}N_3O_2$	16.7 ppm
F_1	$[M+H]^{2+}$	253.2294	$C_{35}H_{58}N_2$	0.3 ppm
F_2	$[M+H]^{2+}$	267.7386	$C_{36}H_{61}N_3$	15.3 ppm
F_2	$[M+2H]^{3+}$	178.8354	$C_{36}H_{62}N_3$	22.3 ppm

C: compound masses, F: fragment masses

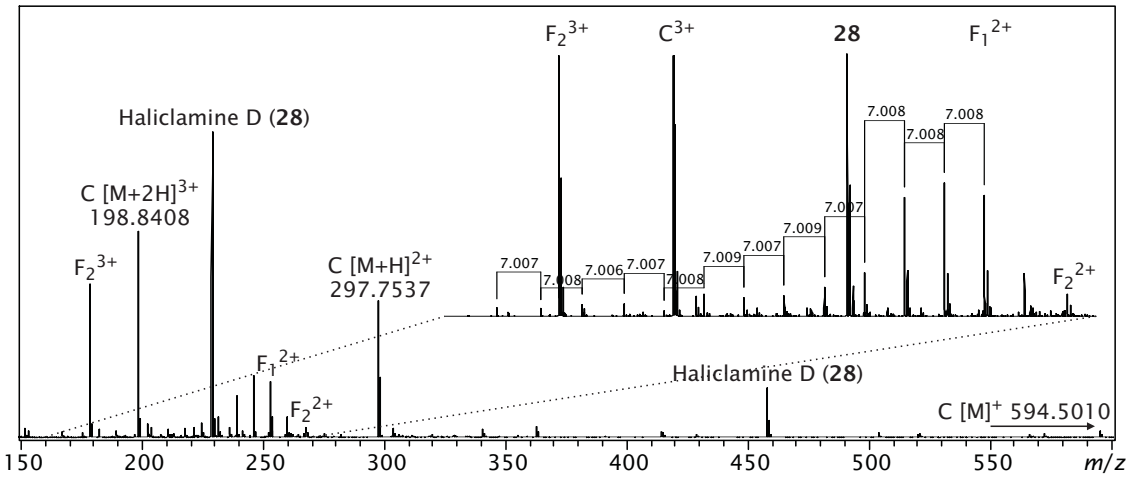

Figure 3.41 Structural formula, compound and fragment masses and high resolution mass spectrum for viscosaline B_1 (**19**). The region important for determining the alkyl chain cleavage is expanded. F_1 = fragment mass derived from β-alanine loss, F_2 = fragment masses derived from acetate loss.

Compound **19** elutes at a retention time of 15.2 min and is overlaid by haliclamine D (**28**). The molecular masses (see Figure 3.41) yield a molecular formula of $C_{38}H_{63}N_3O_2$ which is by CH_2 lower than viscosaline C (**18**). This suggests a viscosaline with one chain shortened by one methylene group as compared to viscosaline C (**18**).

Two constitutional isomers are supposable in this case; one is a viscosaline 12/13 (**19**, viscosaline B_1), where the chain that connects the two pyridinium moieties contains 12 methylene groups while the alkyl chain that carries the β-alanine moiety is 13 methylene groups long; the other is a viscosaline 13/12 (**20**, viscosaline B_2) where the pyridinium moiety connecting chain carries 13 methylene units and the β-alanine carrying chain comprises 12 methylene groups. Both isomers are difficult to distinguish in mass spectra since the fragments that result from loss of an acetate- or the cleavage of the β-alanine moiety lead to fragments of equal mass in both isomers. The only mass by which the isomers can be distinguished is the fragment **73** which should be a doubly charged $m/z = 169.1$ ($n = 6$) in viscosaline B_1 and a doubly charged $m/z = 176.1$ ($n = 7$) in viscosaline B_2.

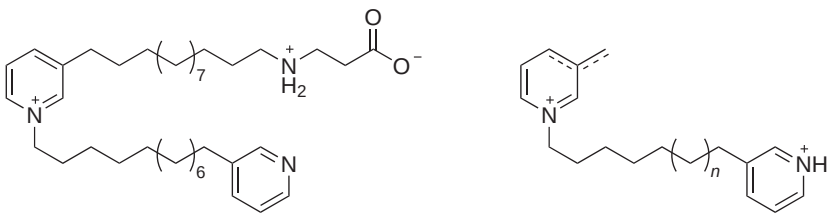

19 **73**

Figure 3.42 Viscosaline B_1 (**19**) and the doubly charged fragment **73** that derives from alkyl chain cleavage of the F_1 fragment.

The doubly charged fragment that emerges from the loss of a β-alanine unit by α cleavage and onium reaction is present at $m/z = 253.2294$. From there, the alkyl chain fragmentation can be followed to a doubly charged $m/z = 169.1$ which assigns viscosaline 12/13 (0/0). This does not rule out the possibility of a viscosaline 13/12 (0/0) being contained in the same spectrum, since its fragments would superimpose with those of compound **19**, but it can be stated that viscosaline 12/13 (0/0) is present in the chromatogram peak.

The fragments that results from the loss of an acetate moiety, $m/z = 267.7386$ $[M+H]^{2+}$ and $m/z = 178.8354$ $[M+2H]^{3+}$ are also clearly visible in the spectrum.

Viscosaline B_2 (**20**) — viscosaline 13/12 (0/0)

The extracted ion chromatogram (EIC) for $m/z = 594.5$ (Figure 3.44) returns a second compound in close proximity to compound **19** at a retention time of 15.3 min. Compound **20** is also overlaid by haliclamine D (**28**). The molecular masses (see Figure 3.43) yield a molecular formula of $C_{38}H_{63}N_3O_2$ which is the same as compound

19. From the retention time and the similarity in molecular masses (see Figure 3.41) it is reasonable to expect that this is the isomer to **19**, viscosaline 13/12 (0/0).

The doubly charged onium fragment lies at $m/z = 253.2321$. From there, the alkyl chain cleavage can be followed to $m/z = 176.1466$ $[M+H]^{2+}$ but not to $m/z = 169.1$ $[M+H]^{2+}$. This rules out a viscosaline 12/13 and, as expected, assigns viscosaline 13/12 (**20**).

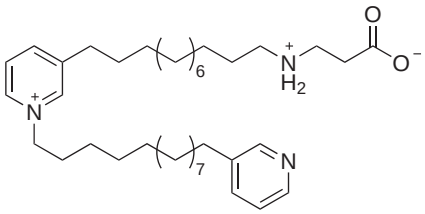

20

	peak	m/z	mol. form.	Δm
C	$[M]^+$	594.5010	$C_{38}H_{64}N_3O_2$	2.8 ppm
C	$[M+H]^{2+}$	297.7537	$C_{38}H_{65}N_3O_2$	1.5 ppm
C	$[M+2H]^{3+}$	198.8408	$C_{38}H_{66}N_3O_2$	14.2 ppm
F_1	$[M+H]^{2+}$	253.2321	$C_{35}H_{58}N_2$	1.7 ppm
F_2	$[M+H]^{2+}$	267.7429	$C_{36}H_{61}N_3$	0.5 ppm
F_2	$[M+2H]^{3+}$	178.8348	$C_{36}H_{62}N_3$	21.7 ppm

C: compound masses, F: fragment masses

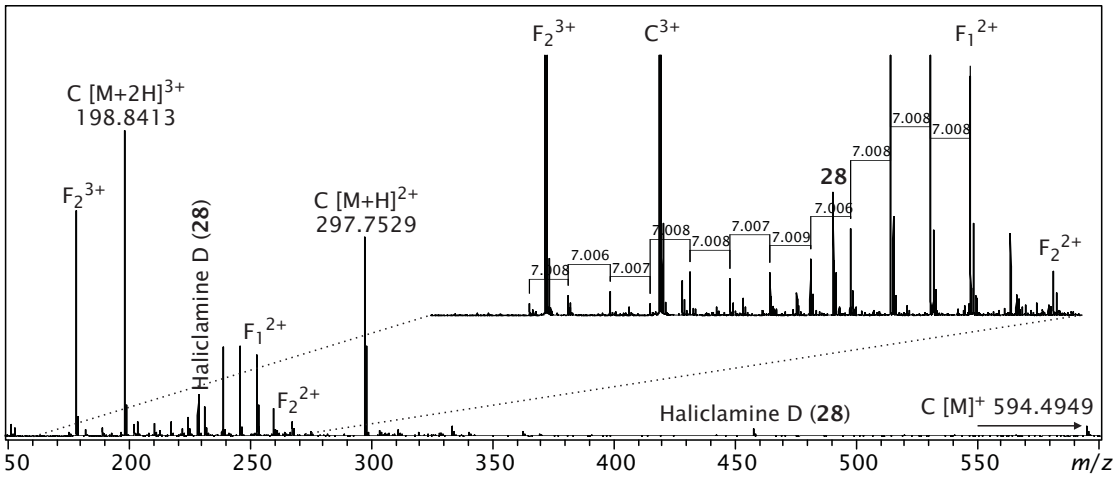

Figure 3.43 Structural formula, compound and fragment masses and high resolution mass spectrum for viscosaline B_2 (**20**). The region important for determining the alkyl chain cleavage is expanded. F_1 = fragment mass derived from β-alanine loss, F_2 = fragment masses derived from acetate loss.

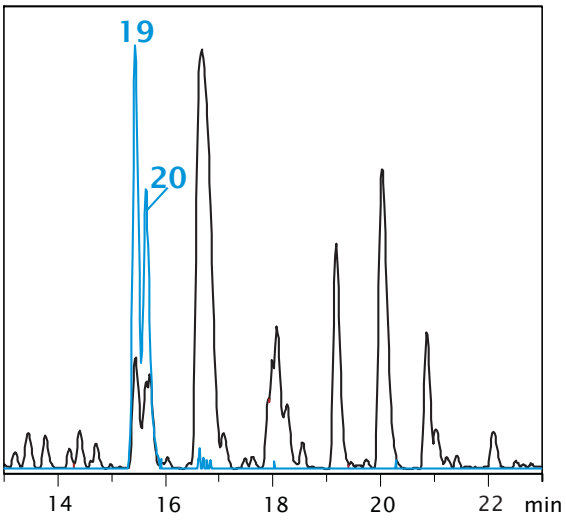

Figure 3.44 Extracted ion chromatogram of m/z = 594.5 (blue) for viscosalines B_1 (**19**) and B_2 (**20**) superimposed by the crude extract chromatogram of the 2001 sample of *Haliclona viscosa* (black). Both chromatograms are scaled to 100% intensity of the highest peak and do not reflect true compound intensities.

Viscosaline E_1 (**21**) — viscosaline 13/14 (0/0)

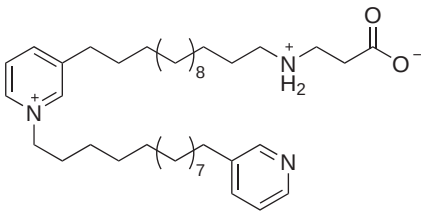

21

	peak	m/z	mol. form.	Δm
C	$[M]^+$	622.5315	$C_{40}H_{68}N_3O_2$	2.2 ppm
C	$[M+H]^{2+}$	311.7703	$C_{40}H_{69}N_3O_2$	4.5 ppm
C	$[M+2H]^{3+}$	208.1847	$C_{40}H_{70}N_3O_2$	14.4 ppm
F_1	$[M+H]^{2+}$	267.2457	$C_{37}H_{62}N_2$	2.1 ppm
F_2	$[M+H]^{2+}$	281.7587	$C_{38}H_{65}N_3$	1.2 ppm
F_2	$[M+2H]^{3+}$	188.1789	$C_{38}H_{66}N_3$	22.4 ppm

C: compound masses, F: fragment masses

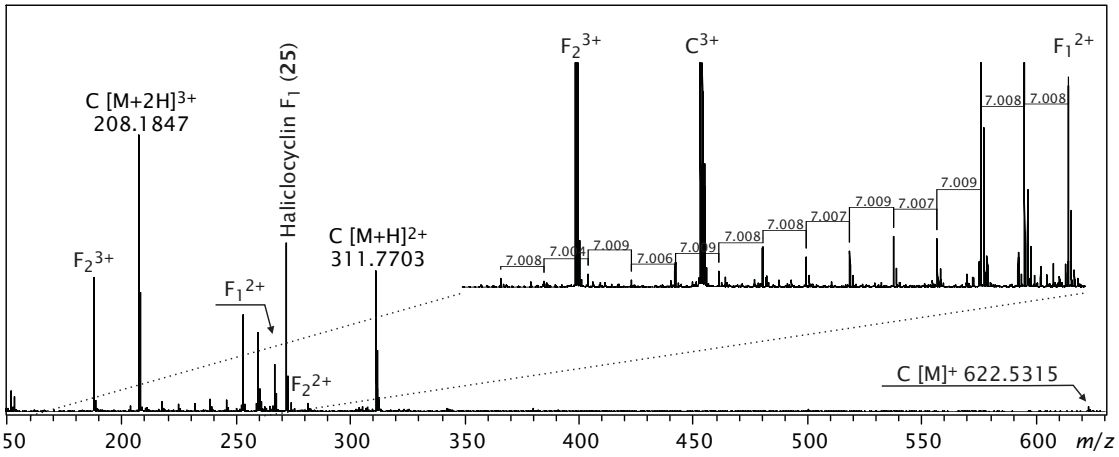

Figure 3.45 Structural formula, compound and fragment masses and high resolution mass spectrum for viscosaline E_1 (**21**). The region important for determining the alkyl chain cleavage is expanded. F_1 = fragment mass derived from β-alanine loss, F_2 = fragment masses derived from acetate loss.

Compound **21** elutes at a retention time of 18.0 min and coelutes with haliclocyclin F_1 (**25**). **21** is by one methylene group larger than viscosaline C (**18**).

Two constitutional isomers can be proposed for this compound; viscosaline 13/14 (0/0) and viscosaline 14/13 (0/0). The constitutional isomers can be distinguished by their **73**-type fragment which should have a mass of $m/z = 176.1$ $[M+H]^{2+}$ for viscosaline E_1 or $m/z = 183.1$ $[M+H]^{2+}$ for viscosaline E_2.

In the mass spectrum of compound **21** the alkyl chain cleavage can be followed to a doubly charged $m/z = 176.1472$, as before in viscosaline C (**18**). This does not eliminate the alternative of viscosaline E_2 (**22**) being contained in the same compound peak since a fragment at $m/z = 183$ $[M+H]^{2+}$ is part of the alkyl chain cleavage of viscosaline E_1 (**21**) but it can be concluded that the peak contains viscosaline E_1.

The fragments that results from the loss of an acetate moiety, $m/z = 281.7587$ $[M+H]^{2+}$ and $m/z = 188.1789$ $[M+2H]^{3+}$ are also clearly visible in the spectrum. The peak that emerges from the loss of a β-alanine unit by α-cleavage and onium reaction is present at $m/z = 267.2457$ $[M+H]^{2+}$.

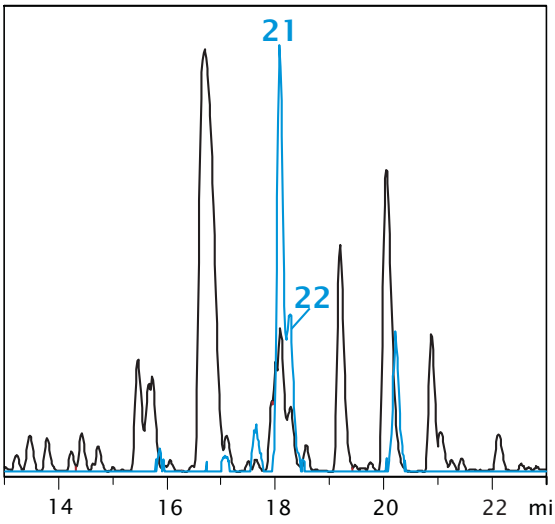

Figure 3.46 Extracted ion chromatogram of $m/z = 622.53$ (blue) for viscosalines E_1 (**21**) and E_2 (**22**) superimposed by the crude extract chromatogram of the 2001 sample of *Haliclona viscosa* (black). Both chromatograms are scaled to 100% intensity of the highest peak and do not reflect true compound intensities. The structure of the compounds at 17.6 min and 20.3 min could not be determined, yet.

Viscosaline E_2 (**22**) — viscosaline 14/13 (0/0)

The EIC of $m/z = 622.53$ (Figure 3.46) yields a second compound in close proximity to the peak of compound **21** at a retention time of 18.1 min. Apart from the singly charged molecular ion, also the doubly and triply charged molecular ions as well as the fragment ions have a similar mass as those observed in **21**. From the close retention time to the viscosaline 14/13 (0/0, **21**) and the similarity in masses it

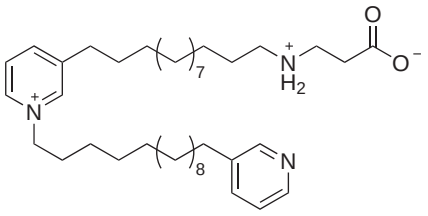

22

	peak	m/z	mol. form.	Δm
C	$[M+H]^+$	622.5234	$C_{40}H_{68}N_3O_2$	11.6 ppm
C	$[M+2H]^{2+}$	311.7653	$C_{40}H_{69}N_3O_2$	11.8 ppm
C	$[M+3H]^{3+}$	208.1805	$C_{40}H_{70}N_3O_2$	5.7 ppm
F_1	$[M+2H]^{2+}$	267.2458	$C_{37}H_{62}N_2$	2.7 ppm
F_2	$[M+2H]^{2+}$	281.7547	$C_{38}H_{65}N_3$	12.9 ppm
F_2	$[M+3H]^{3+}$	188.1709	$C_{38}H_{66}N_3$	2.3 ppm

C: compound masses, F: fragment masses

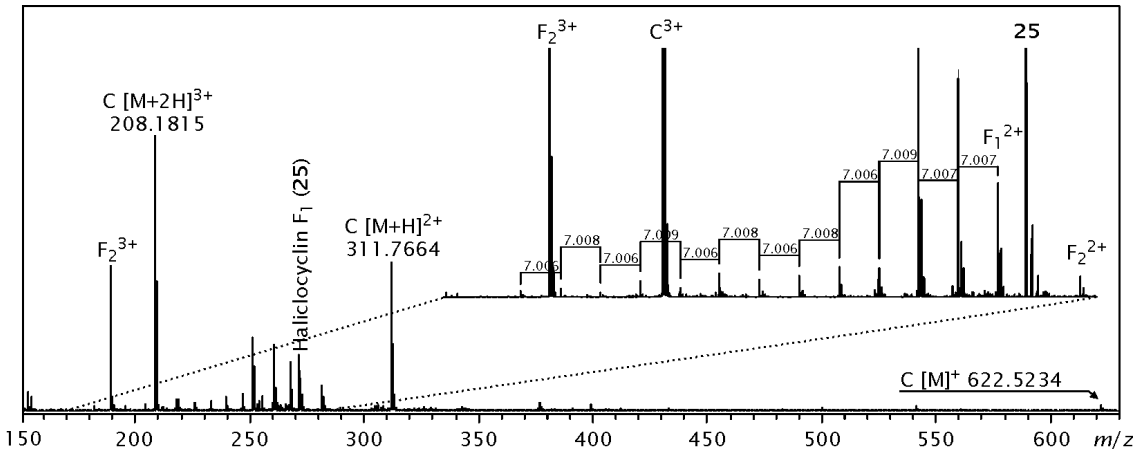

Figure 3.47 Structural formula, compound and fragment masses and high resolution mass spectrum for viscosaline E_2 (**22**). The region important for determining the alkyl chain cleavage is expanded. F_1 = fragment mass derived from β-alanine loss, F_2 = fragment masses derived from acetate loss.

is reasonable to expect that compound **22** is the constitutional isomer to **21**. It can be distinguished by the fragment **73** that derives from alkyl chain cleavage. The doubly charged fragment F_1 that arises from α-cleavage and subsequent onium reaction of the β-alanine unit is found at $m/z = 267.2458$. The alkyl chain cleavage emanating from this fragment can be followed to $m/z = 183.1512$ $[M+H]^{2+}$ but not to $m/z = 176.1$ $[M+H]^{2+}$. This rules out a viscosaline E_1 (**21**) and assigns viscosaline E_2 (**22**).

Dehydro-Viscosaline E_1 (**74**)* — viscosaline 13/14 (0/1)

Compound **74** elutes at a retention time of 17.7 min where it coelutes with haliclamine F (**30**). The characteristic molecular ion pattern and the $m/z = 7$ fragmentation indicates that the compound is a viscosaline. The molecular mass is two mass units lower than compound **21** and **22** which suggests a double bond in one of the alkyl

chains. The alkyl chain fragmentation can be followed from the doubly charged $m/z = 266.2367$ to a doubly charged ion at $m/z = 176.1482$ which assigns the viscosaline as a viscosaline 13/14 (0/1). Viscosaline 13/14 (1/0) would be given by a doubly charged fragment $m/z = 175.6$, viscosaline 14/13 (0/1) by $m/z = 183.2$ and viscosaline 14/13 (1/0) by $m/z = 182.7$. **74** constitutes a previously unreported compound.

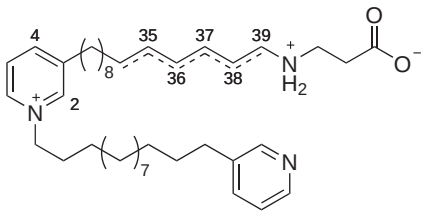

74

	peak	m/z	mol. form.	Δm
C	$[M]^+$	620.5130	$C_{40}H_{66}N_3O_2$	3.1 ppm
C	$[M+H]^{2+}$	310.7608	$C_{40}H_{67}N_3O_2$	0.9 ppm
C	$[M+2H]^{3+}$	207.5116	$C_{40}H_{68}N_3O_2$	8.3 ppm
F_1	$[M+H]^{2+}$	266.5116	$C_{37}H_{60}N_2$	2.0 ppm
F_2	$[M+H]^{2+}$	280.7502	$C_{38}H_{63}N_3$	8.3 ppm
F_2	$[M+2H]^{3+}$	187.5057	$C_{38}H_{64}N_3$	4.0 ppm

C: compound masses, F: fragment masses

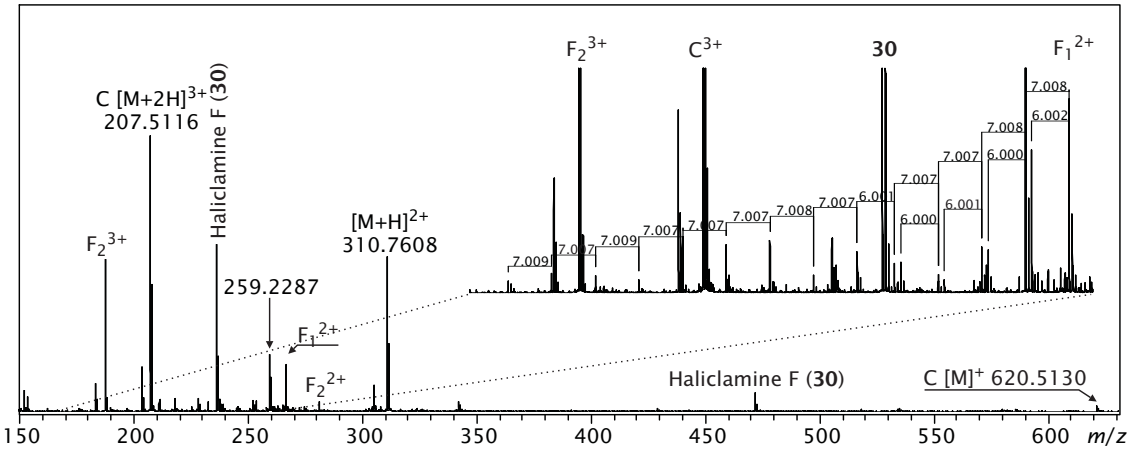

Figure 3.48 Structural formula, compound and fragment masses and high resolution mass spectrum for dehydro-viscosaline E_1 (**74**). The region important for determining the alkyl chain cleavage is expanded. F_1 = fragment mass derived from β-alanine loss, F_2 = fragment masses derived from acetate loss. Dashed bonds indicate the range for the likely position of the double bond.

By following the fragmentation steps of the alkyl chain which is represented by $\Delta m/z = 7.007$ (calcd.) steps for methylene groups in doubly charged compounds, the double bond can be identified by the $\Delta m/z = 5.999$ (calcd.) mass difference. While the H-shift mentioned above hinders the exact localization, it is possible to assign the range in which the doubly bond is likely to occur. The spectrum of compound **74** (Figure 3.48) displays four groups of doubly charged peaks that have a

distance of both $m/z = 7$ and $m/z = 6$ to their preceding or following alkyl cleavage peak group. Each group shows two doubly charged peaks that are 2 mass units (or $m/z = 1$) apart. The first group lies at $m/z = 260.2372$ and $m/z = 259.2287$, the second at $m/z = 253.2231$ and $m/z = 252.2217$, the third at $m/z = 246.2150$ and $m/z = 245.2077$ and the fourth at $m/z = 239.2068$ and $m/z = 238.2041$. The first pure $\Delta m/z = 7$ cleavage peak lies at $m/z = 232.2052$. This locates the double bond between position 34 and 39 (Figure 3.48). However, a significant shift in the intensity of the fragments occurs between $m/z = 259.2287$ and $m/z = 252.22174$. This suggests that the favoured fragmentation, which is probably promoted by the double bond, produces the fragment $m/z = 259$. This fragment corresponds an alkyl chain length of 13 methylene units and tentatively assigns the double bond to position $38 - 39$, i.e. in conjugation to the amide nitrogen. However, further mass spectrometric analysis and possibly derivatization of the double bond is necessary to give a clear picture, since also viscosalines with saturated alkyl chains show this shift in intensity of the fragments.

3.3.6 Viscosamines

Viscosamine C (**43**), termed "C" for its chain lengths that correspond to cyclostellettamine C (**33**), elutes at a retention time of 19.8 min. It is the most abundant of the viscosamines and was reported before.[96]

The most pronounced mass peak in the spectrum of viscosamine C (**43**) is the triply charged molecular ion $[M]^{3+}$ at $m/z = 260.2382$. In addition, the compound shows a number of characteristic fragment (F) and adduct/salt (A) peaks. Two doubly charged ions of almost equal intensity lie at $m/z = 390.2350$ and $m/z = 412.8512$. The sum formula assigned to the fragment ion F_1 at $m/z = 390$ holds one hydrogen more and one charge less than that of the molecular ion (Figure 3.49). This is reminiscent of the cyclostellettamine fragmentation under in-source-CID conditions, where one fragment contained one charge less than the precursor ion and one hydrogen more. In cyclostellettamines, this fragment appears only in orthogonal time of flight (oTOF) mass spectrometry measurements under concomitance of formic acid and is assigned as a reduced form of a Hofmann fragment (Figure 3.50).[117] Since the HPLC-HRMS measurements of *Haliclona viscosa* crude extracts use similar MS conditions, the same mechanism can be proposed for viscosamine

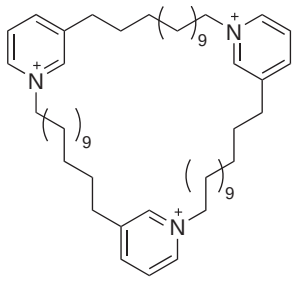

43

	peak	m/z	mol. form.	Δm
C	$[M]^{3+}$	260.2382	$C_{54}H_{90}N_3$	3.4 ppm
F_1	$[M+H]^{2+}$	390.8637	$C_{54}H_{91}N_3$	6.5 ppm
F_2	$[M+H]^{2+}$	389.8637	$C_{54}H_{89}N_3$	5.5 ppm
A_1	$[M+H]^{2+}$	412.8512	$C_{55}H_{91}N_3O_2$	4.9 ppm
A_2	$[M+H]^{2+}$	446.8519	$C_{56}H_{90}N_3F_3O_2$	7.1 ppm

C: compound masses, F: fragment, A: adduct/salt

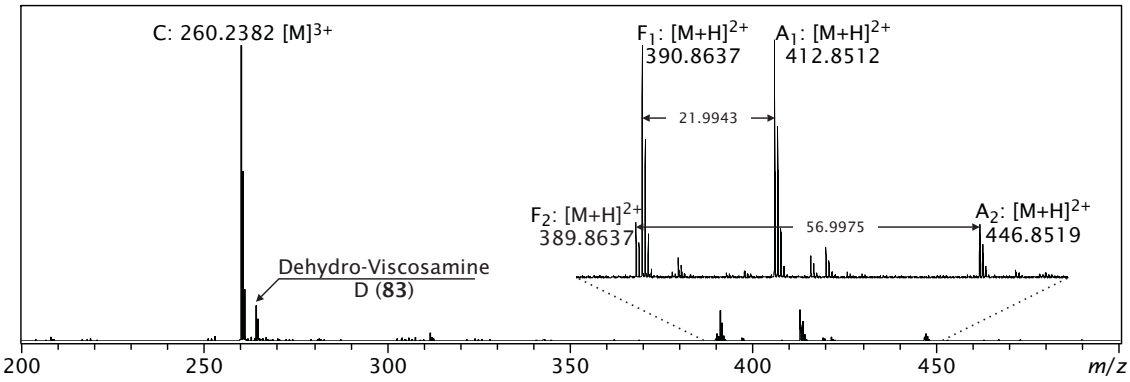

Figure 3.49 Structural formula, compound masses and high resolution mass spectrum for viscosamine C (**43**). The compound coelutes with dehydro-viscosamine D (**83**). The peak area of fragments and adducts/salts is expanded.

C (**43**) to explain the fragment at $m/z = 390$. It results in an opening of the macrocycle and the loss of one charge (**75**).

The mass difference between the doubly charged F_1 fragment ion $m/z = 390$ and the second doubly charged ion of similar intensity, A_1 at $m/z = 412$, is $m/z = 21.9943$. This correlates very well to CO_2 (calcd. $m/z = 21.9944$, $\Delta m = 3.0$ ppm). Carbon dioxide may be derived from reaction with the formic acid that is simultaneously involved in reduction of the Hofmann fragment to form **75**.[117] Formation of adduct ions is favoured in ESI-MS as compared to EI-MS due to the lower energy used for ionisation that increases the lifetime of the collision complex. While CO_2 adducts are not typical during LC-MS experiments and not stable in nature, Villiers et al.[124] have very recently isolated a CO_2 adduct of a nitrogen base for the first time. Similar to the structure described by Villiers et al., the pyridine nitrogen in **75** may be involved in binding CO_2, which would result in an adduct **76**.

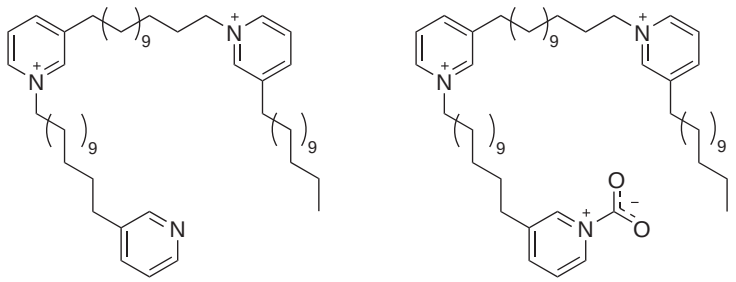

75 **76**

Figure 3.50 Viscosamine C fragment **75** derived from reduction of the Hofmann fragment **77** and possible CO_2 adduct (**76**).

The doubly charged ion at $m/z = 412$ also shows a mass difference of $m/z = 23.0029$ to a third characteristic doubly charged ion F_2 at $m/z = 389.8451$. The F_2 ion is two mass units lower than the F_1 ion and constitutes the Hofmann fragment **77** that is also observed in the related cyclostellettamines.[117,125] The mass difference of $m/z = 23$ can be attributed to formic acid (calcd. $m/z = 23.0022$) with a mass deviation of 30.8 ppm. Therefore it remains unresolved whether $m/z = 412$ is the CO_2 adduct of **75** or the formic acid salt of **77**, or both.

The formic acid salt **78** is supported by the presence of a fourth characteristic doubly charged ion A_2 at $m/z = 446.8519$ which is only present at very small intensity. A_2 shows a mass difference of $m/z = 56.9975$ to the F_2 ion which tentatively assigns a trifluoroacetic acid (TFA) salt (**79**, calcd. $m/z = 56.9959$) with an accuracy of 28.4 ppm.

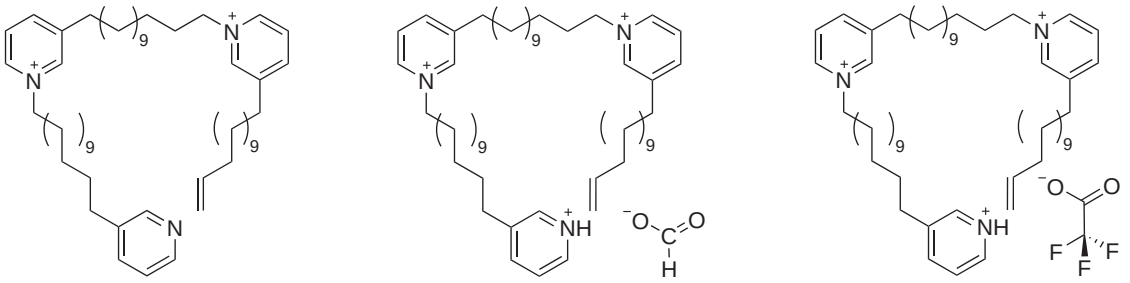

77 **78** **79**

Figure 3.51 Hofmann fragment (**77**) of viscosamine C and possible formic acid (**78**) and trifluoroacetic acid salt (**79**).

While formic acid is introduced into the sample during chromatographic separation, the presence of TFA is unresolved, yet. The crude extract had not been in contact

with TFA. Other ions that could be present in the instrument e.g. sodium formate clusters from calibration, do not satisfy the observed mass difference. If the observed ion is a TFA salt, it must be concluded that TFA is present as residual impurities in glassware or the instrument and thus contaminates the sample. However, that raises the question why TFA salts are not observed in the mass spectra of other 3-APAs identified in the same crude extract of *Haliclona viscosa*. Since TFA is unlikely to be the natural counterion of 3-APAs in the sponge, it is therefore reasonable to assume that the mass difference of $m/z = 56.9959$ derives from a different, yet unidentified counterion. For example, fumaric acid (M=116) which is a natural biosynthesis byproduct, is close in mass to the molecular mass of TFA. MALDI-MS is a method that requires little sample preparation and is therefore closer to showing the natural state of the molecule than other, laboratory-intensive sample processing methods. Thus, MALDI-MS could be a useful tool to elucidate the structure of the natural counterion. Until further results are available, the ion observed in the spectrum of the viscosamine C (**43**) must be regarded as the TFA salt.

The masses given in the original publication of viscosamine C (**43**) in part differ from the masses observed during LC-MS analysis of the *H. viscosa* crude extract.[96] These differences are due to different mass spectrometers used for the analysis and the workflow of isolating the compound. The original publication of viscosamine C (**43**) agrees in the triply charged molecular ion $[M]^{3+}$ at $m/z = 260$, the Hofmann fragment at $m/z = 389$ $[M+H]^{2+}$ and the TFA salt at $m/z = 446$ $[M+H]^{2+}$.[9] Instead of the formic acid salt it shows an acetic acid salt at $m/z = 419$ $[M+H]^{2+}$. The reduced Hofmann fragment at $m/z = 390$ $[M+H]^{2+}$ is not observed in the original publication.

9 It should be noted that in this case, TFA was introduced during chromatographic purification of the isolated compound.

Viscosamine B (**80**) — viscosamine 12/13/13 (0/0/0))

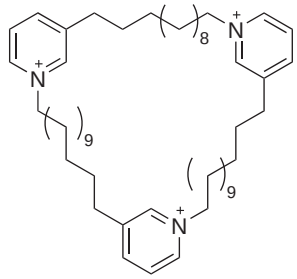

80

	peak	m/z	mol. form.	Δm
C	$[M]^{3+}$	255.5668	$C_{53}H_{88}N_3$	5.4 ppm
F_1	$[M+H]^{2+}$	383.8550	$C_{53}H_{89}N_3$	7.1 ppm
F_2	$[M+H]^{2+}$	382.8463	$C_{53}H_{87}N_3$	4.7 ppm
A_1	$[M+H]^{2+}$	405.8508	$C_{54}H_{89}N_3O_2$	8.8 ppm
A_2	$[M+H]^{2+}$	439.8459	$C_{55}H_{88}N_3F_3O_2$	11.4 ppm

C: compound masses, F: fragment, A: adduct/salt

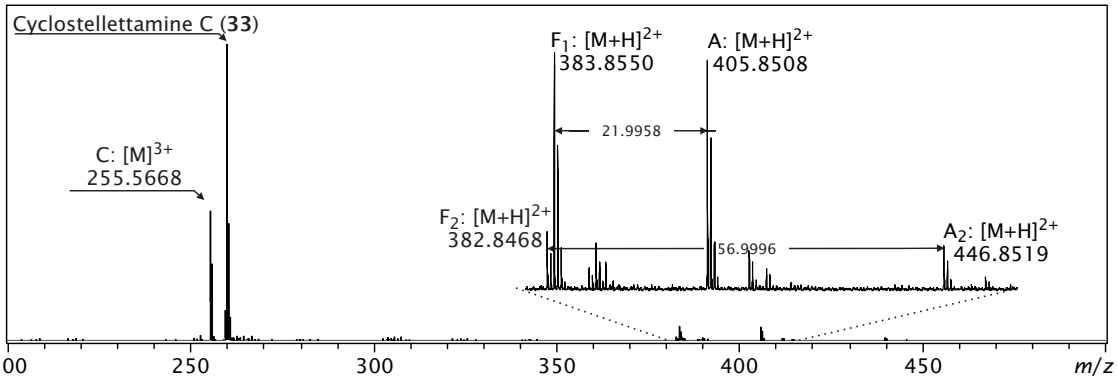

Figure 3.52 Structural formula, compound masses and high resolution mass spectrum of the peak at 18.9 min, identified as viscosamine B (**80**). The compound coelutes with cyclostellettamine C (**33**). The peak area of the fragments and adducts/salts is expanded.

The mass pattern of viscosamine C (**43**) can be found in a chromatogram peak that coelutes with cyclostellettamine C (**33**) at 18.9 min. The molecular mass is 14 mass units less than viscosamine C (**43**). This suggests that one alkyl chain is shortened by a methylene group. Also in this compound, the proposed carbon dioxide adduct is clearly visible at a distance of $m/z = 21.9958$ to the doubly charged molecular ion peak.

A compound of this mass was reported before by C. Timm as a viscosamine that contains 38 methylene groups in the alkyl chain.[84] Due to the absence of a fragmentation that can assign the alkyl chain length, the compound may be assigned as viscosamine 12/13/13 (0/0/0) but other alkyl chain lengths, e.g. 11/12/14, cannot be ruled out. To induce a fragmentation, the crude extract should be submitted

to higher fragmentation energies in the hope of producing Pyr + alkyl chain type fragments as are known from the cyclostellettamines. This work is in progress.

Viscosamine D (**81**)* — viscosamine 13/13/14 (0/0/0)

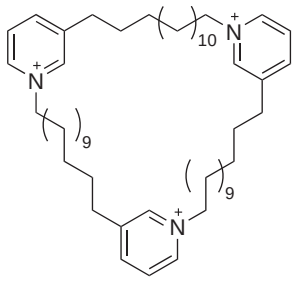

81

	peak	m/z	mol. form.	Δm
C	$[M]^{3+}$	264.9063	$C_{55}H_{92}N_3$	10.9 ppm
F_1	$[M+H]^{2+}$	397.8661	$C_{55}H_{93}N_3$	4.5 ppm
F_2	$[M+H]^{2+}$	396.8560	$C_{55}H_{91}N_3$	5.5 ppm
A_1	$[M+H]^{2+}$	412.8512	$C_{56}H_{93}N_3O_2$	5.8 ppm
A_2	$[M+H]^{2+}$	453.8543	$C_{57}H_{92}N_3F_3O_2$	5.0 ppm

C: compound masses, F: fragment, A: adduct/salt

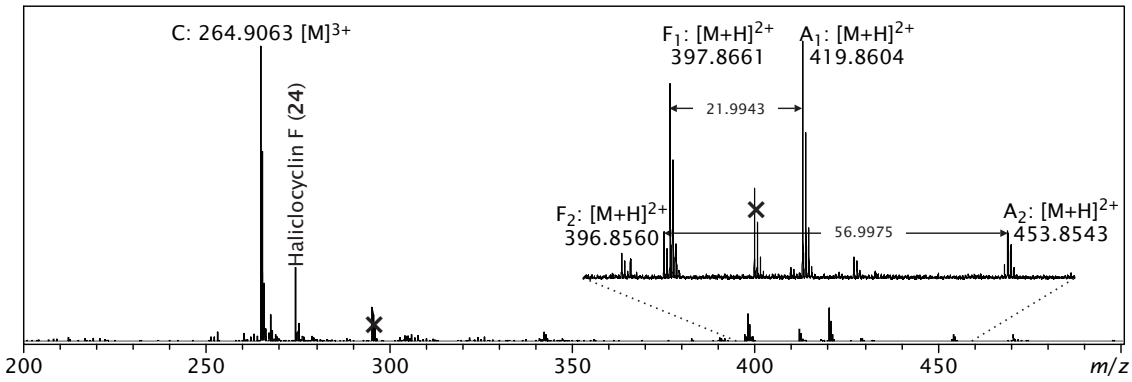

Figure 3.53 Structural formula, compound masses and high resolution mass spectrum of the peak at 19.8 min, identified as viscosamine D (**81**). The compound coelutes with viscosamine C (**43**). The peak area of the fragments and adducts/salts is expanded.

A new viscosamine can be discerned in a peak at 20.5 min. It is 14 mass units larger than viscosamine C (**43**) which indicates an additional methylene group in one of the alkyl chains (Figure 3.53). The proposed carbon dioxide adduct is visible at a distance of $\Delta m/z = 21.9943$ to the doubly charged molecular ion peak while the TFA salt is present at $\Delta m/z = 56.9975$ to the Hofmann fragment. As before, different chain lengths, e.g. 12/13/15, cannot be ruled out.

Dehydro-Viscosamine C (**82**)* — viscosamine 13/13/13 (0/0/1)

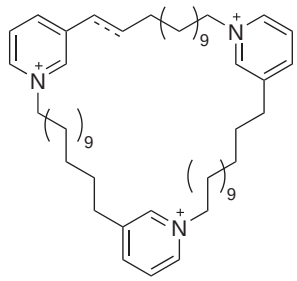

82

	peak	m/z	mol. form.	Δm
C	$[M]^{3+}$	259.5665	$C_{54}H_{88}N_3$	4.2 ppm
F_1	$[M+H]^{2+}$	389.8539	$C_{54}H_{89}N_3$	4.2 ppm
F_2	$[M+H]^{2+}$	388.8451	$C_{54}H_{87}N_3$	1.7 ppm
A_1	$[M+H]^{2+}$	411.8492	$C_{55}H_{89}N_3O_2$	4.9 ppm
A_2	$[M+H]^{2+}$	445.8492	$C_{56}H_{88}N_3F_3O_2$	6.9 ppm

C: compound masses, F: fragment, A: adduct/salt

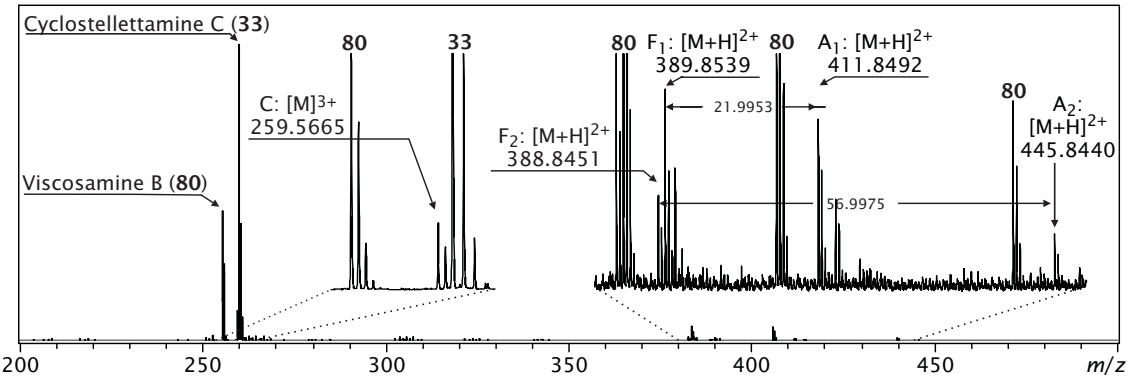

Figure 3.54 Structural formula, compound masses and high resolution mass spectrum of the peak at 18.9 min, identified as dehydro-viscosamine C (**82**). The compound coelutes with cyclostellettamine C (**33**) and viscosamine B (**80**). The peak area of the fragments and adducts/salts is expanded. The position of the double bond is not determined, yet.

With the knowledge about the mass- and fragment pattern of viscosamine C (**43**), a second new viscosamine can be identified in the mass spectrum of viscosamine B (**80**), but at much lower intensity (Figure 3.54).

Also this compound coelutes with cyclostellettamine C (**33**) at 18.9 min. The molecular mass is 2 mass units lower than viscosamine C (**43**). This suggests that one alkyl chain carries a double bond. The proposed carbon dioxide adduct is clearly visible at a distance of $m/z = 21.9953$ to the doubly charged molecular ion. With the compound being cyclo-symmetrical but for the double bond, it can be assigned as viscosamine 13/13/13 (0/0/1).

Double bonds in viscosamines were reported earlier; a *Haliclona* sp. from the Pacific coast of Guatemala yielded an unnamed viscosamine **44** with C_{11} alkyl chains

that contained three double bonds, one in each alkyl chain and assigned to the same position in each chain.[86]

Dehydro-Viscosamine D (**83**)* — viscosamine 13/13/14 (0/0/1)

A third new viscosamine (**82**) is visible in the mass spectrum of viscosamine C (**43**) at low intensity (Figure 3.55). Compound **83** shows a mass that is by 12 mass units larger than viscosamine C (**43**). This corresponds to the extension of one of the alkyl chains by a methylene group and the occurence of a double bond (Figure 3.55).

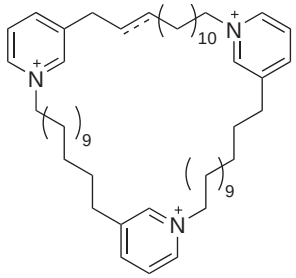

83

	peak	m/z	mol. form.	Δm
C	$[M]^{3+}$	264.2377	$C_{55}H_{90}N_3$	1.6 ppm
F_1	$[M+H]^{2+}$	396.8622	$C_{55}H_{91}N_3$	5.3 ppm
F_2	$[M+H]^{2+}$	395.8605	$C_{55}H_{89}N_3$	20.8 ppm
A_1	$[M+H]^{2+}$	418.8587	$C_{56}H_{91}N_3O_2$	5.8 ppm
A_2	$[M+H]^{2+}$	452.8416	$C_{57}H_{90}N_3F_3O_2$	3.2 ppm

C: compound masses, F: fragment, A: adduct/salt

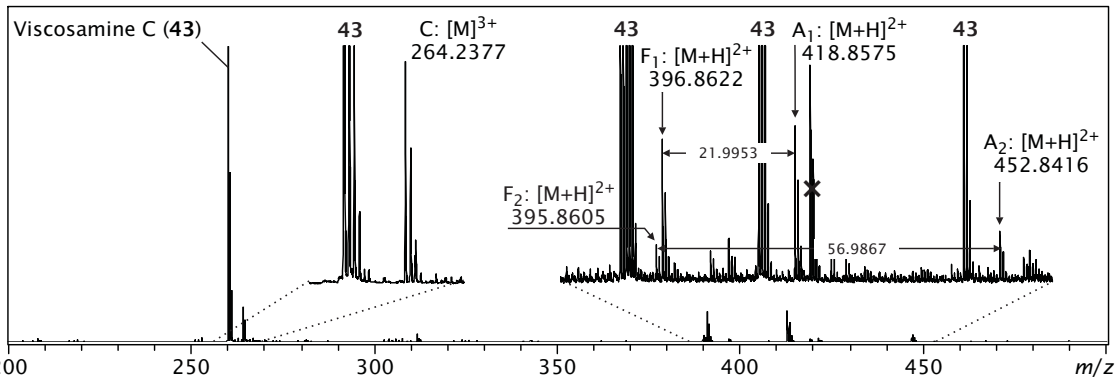

Figure 3.55 Structural formula, compound masses and high resolution mass spectrum of the peak at 19.8 min, identified as dehydro-viscosamine D (**83**). The compound coelutes with viscosamine C (**43**). The peak area of the fragments and adducts/salts is expanded. The position of the double bond is not determined, yet.

Also in this compound, the proposed carbon dioxide adduct A_1 is clearly visible at a distance of $m/z = 21.9952$ to the doubly charged molecular ion peak. The Hofmann fragment F_2 and the proposed TFA salt A_2 are discernible as well. With this information the compound can be assigned as viscosamine 13/13/14 (0/0/1).

In the present compound **83** and with the methods at hand, it is not possible to distinguish which chain carries the double bond. This leaves three possibilities for

the compound's constitution; viscosamine 13/13/14 (0/0/1), viscosamine 13/13/14 (0/1/0) and viscosamine (13/13/14 (1/0/0). In the haliclamines and viscosalines with dissimilar chain lengths that are proposed in this thesis, a double bond is always part of the longer alkyl chain. Until further experiments are performed it can be assumed that compound **83** constitutes a viscosamine 13/13/14 (0/0/1).

It must also be mentioned that due to the absence of fragments that constitute the mass equivalent of a pyridinium connected to an alkyl chain that were observed for cyclostellettamines the possibility persists that the compound is a viscosamine 12/13/15 (0/0/1). However, the observation of a co-elution pattern (see below, Section 3.3.7) assigns the compound as a viscosamine 13/13/14 (0/0/1).

3.3.7 Other observations

Several other observations result from the performed compound screening. The structures of all compounds that elute at retention times before 12 min and after 23 min are unidentified, yet, and under examination. The mass spectra of these compounds do not conform to the typical mass spectra of known of 3-alkyl tetrahydropyridines or pyridinium alkaloids although the masses detected in these compound peaks are similar to haliclamine masses. In haliclamines that possess unequal chain lengths, double bonds are found in the longer alkyl chain.

In addition, a clustering pattern is visible in the chromatogram analysis; by the current evaluation method, compounds with one methylene group difference in the alkyl chain elute with approximately 1 min difference in retention time. At the same time, compounds with saturated alkyl chains often coelute with compounds that possess one methylene group less in one of the chains but one double bond more. However, 3-alkyl tetrahydropyridines are well separated from 3-alkyl pyridinium alkaloids in the chromatogram with a change from tetrahydropyride to pyridinium happening at approximately 16 min retention time, correspondent to a solvent composition of 40 % acetonitrile and 60 % water. An exception from this are the viscosalines which coelute with the haliclamines (THP) but possess Pyr moieties. The reason for this is the amino acid which increases the polarity of the compounds.

In the absence of a mass spectrometric method, the observed clustering could be useful to predict the likely structure of the eluting compounds purely by chromatographic methods.

3.4 Sampling areas and *Haliclona* samples

During the sampling seasons of 2007-2009, two geographically distant sites were visited for sponge sampling: the Arctic Kongsfjord in the Spitsbergen archipelago and the temperate Orkneys, Great Britain. Both areas had been visited for sponge sampling between 1999 and 2003 by our working group. The most significant difference between the two sampling areas is in water temperature and the light regime. Both sites comprise similar fauna, with variation in the abundance and composition of species. The sessile fauna consists mainly of sea anemones, sea squirts, barnacles, bryozoans, molluscs, tube worms and sponges. The mobile fauna comprises snails, a large variety of crustaceans, brittle stars, sea stars and sea urchins, annelid worms and fishes.[126] In addition, the hard bottom is populated by a variety of brown and red macroalgae and their co-occurring fauna. Since sponges are filter feeders, also the planktonic organisms that fall prey to sponges should be mentioned; they comprise various microalgae, juvenile metazoans like copepod nauplii, bivalve veliger, Protozoa like ciliates, foraminifera and rotifers, (dino)flagellates, bacteria and viruses.[127,128]

3.4.1 Kongsfjord, Spitsbergen

Spitsbergen is the largest island of the Svalbard archipelago, located between 74-81° N and 010-035° E. Due to its northerly location, Spitsbergen is an Arctic island but it is characterized by comparably mild winters considering other territories at this latitude. The ocean around the island is dominated by two main water masses: relatively warm Atlantic Water (AW) and cold Arctic Water (ArW). Atlantic Water is contained in the West Spitsbergen Current (WSC), the northernmost branch of the warm North Atlantic Current (NAC, "Gulf Stream"). The WSC flows northward along the western continental slope of Spitsbergen (Figure 3.56). It carries heat and very saline water into high latitudes and occupies the upper ca. 600 m in the eastern Fram Strait. After circulating the Arctic basins as well as thorough mixing and cooling, the AW water emerges as ArW from the Arctic basins southward and flows along the east coasts of both Greenland (East Greenland Current, EGC) and Spitsbergen (East Spitsbergen Current, ESC). A small portion of the East Spitsbergen Current (ESC) turns north at the southern tip of Spitsbergen and follows the coast line northward. Since this part of the ESC flows on the shelf, it

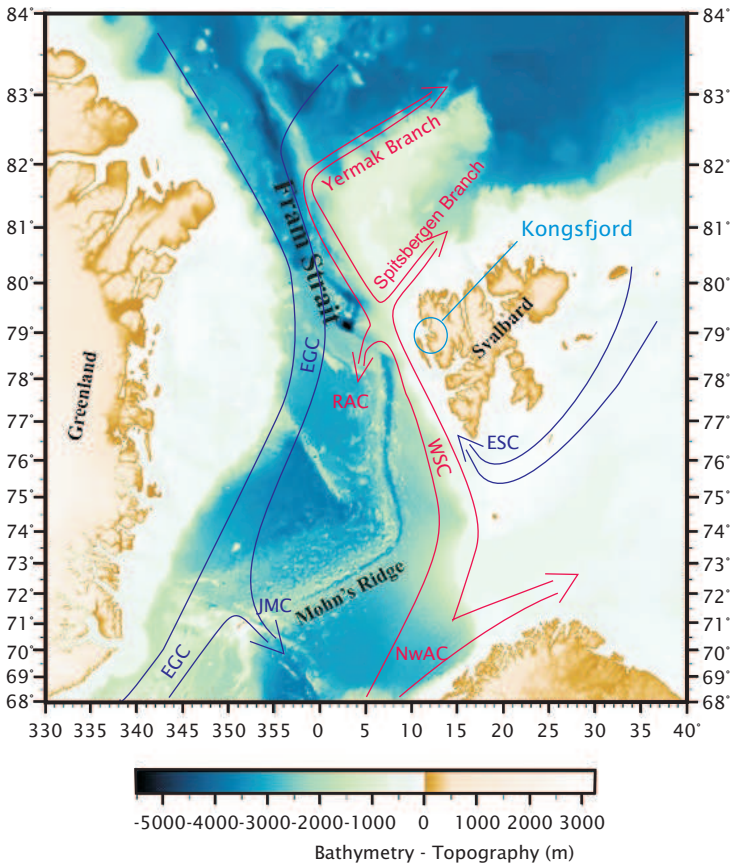

Figure 3.56 Map of Svalbard and the current system in the northern Atlantic. The green circle indicates the geographic location of the Kongsfjord. EGC East Greenland Current, ESC East Spitsbergen Current, WSC West Spitsbergen Current, RAC Return Atlantic Current, JMC Jan Mayen Current, NwAC Norwegian Atlantic Current. Changed from www.awi.de.

separates the WSC from direct contact with coastal Spitsbergen, which entails that the fjords on the western coast of Spitsbergen usually contain cool ArW.

The Kongsfjord is located on the north-western coast of Spitsbergen at about 79° N and 011° W. The fjord opens in north-westerly direction, stretches inland for about 20 km and is approximately 10 km wide at the mouth. It is separated into two main areas by the island Blomstrandhalvøya; the south-eastern, shallow (50-200 m) and rather protected part and the north-western, deeper (200-400 m) and more exposed part (Figure 3.57).[129]

The wind system, the general shape of the fjord and other physical parameters of the area like fresh water input and light regime determine the circulation pattern, salinity, temperature, sea ice expansion, water transparency etc. Tides have an amplitude of only about 1 m, therefore almost no tidal currents occur in the inner, and weak currents in the mouth part of the fjord. However, with winds blowing from the West or katabatic winds from the glaciers some areas can be exposed to heavy wave action.

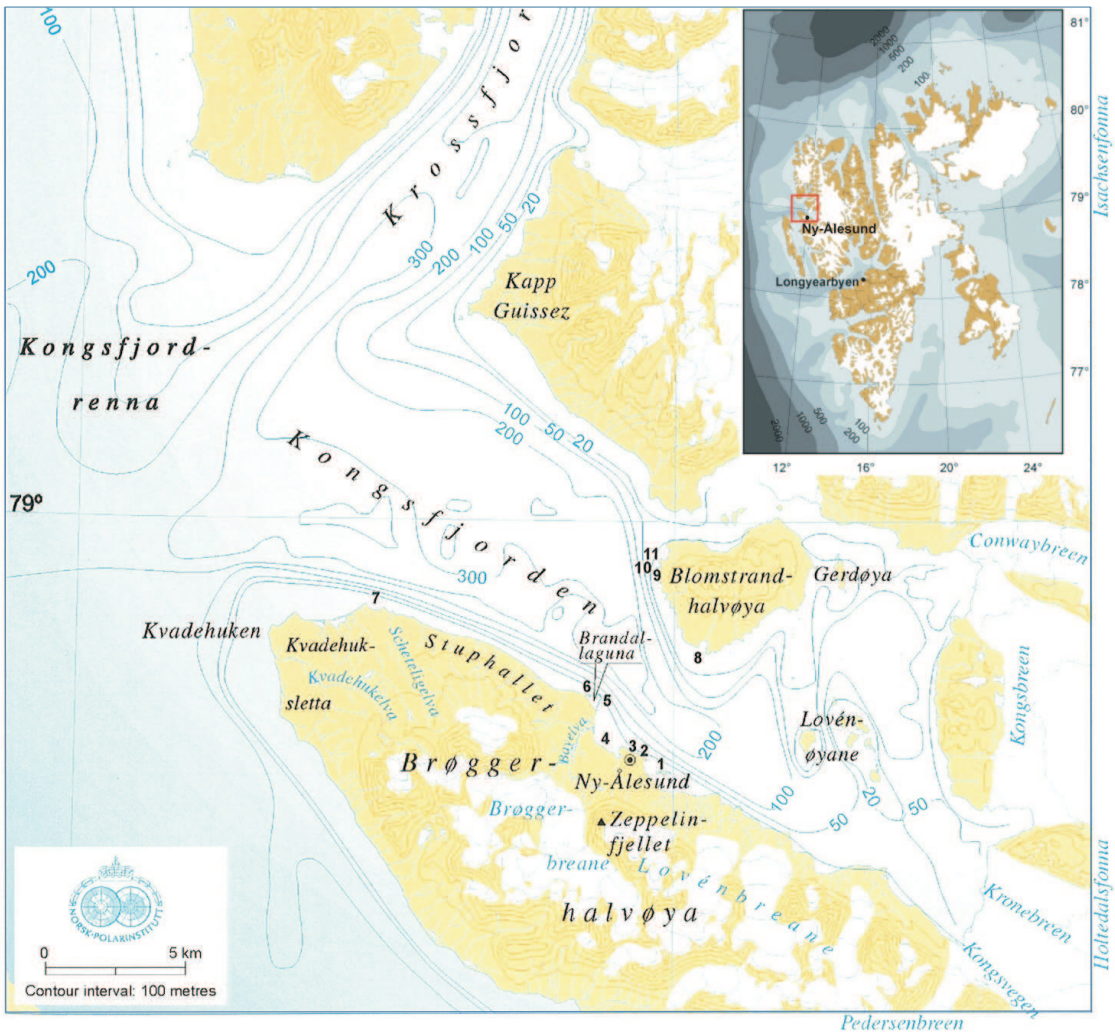

Figure 3.57 Kongsfjord bathymetric map. The sampling areas Kongsfjordneset, Hansneset Cave, Hansneset Step are marked with the numbers 7, 9, and 10, respectively. Source: Norsk Polarinstitutt.

The inner part of the fjord is surrounded by five glaciers that contribute a considerable amount of fresh water to the fjord by calving events or ablation. Other sources of fresh water are melting snow and sea ice as well as summer rainfalls. The fresh water input creates a very stable stratification in spring and summer with a brackish water layer of only a few meters thickness that has a salinity of about 30-33 psu and even below 28 psu close to river mouths and glaciers in the inner part of the fjord. This brackish layer is separated by a strong halocline from the underlying salty water masses and their circulation and shows an own circulation that is influenced by wind forcing. The autumn cooling destabilizes the stratification.[129]

The fresh water that results from melting snow and calving glaciers also carries large amounts of suspended matter and therefore undergoes fast heating from solar radiation (from the winter low of ca. –1.8°C to the summer high of 4-6°C). In the subjacent water masses, temperatures can be as high as 4°C in summer but show large interannual fluctuation. The reason for this is the oscillation of the WSC that especially influences the deeper water masses.[130] Usually, the water that enters the Kongsfjord is Transformed Atlantic Water (TAW) that differs significantly from the water in the core of the WSC (temperature (T) > 3°C, salinity (S) > 34.9 psu). The TAW is a result of mixing of AW with shelf water (ArW) which produces water of decreased temperature and salinity (T > 1°C, S > 34.7 psu). In winter 2006, a strong and long-lasting northerly wind in combination with the Ekman drift resulted in an upwelling of warm and very saline AW from the WSC core that intruded almost the complete Kongsfjord and led to anomalous high temperatures of about 8°C in the fjord in winter.[131] This winter time warming also had a large impact on the ice cover, causing the thinnest and least ice in the fjord observed during the preceding decade.[132] The warming also had an impact on the winter zooplankton community in the fjord by advection of species that are usually only found in warmer waters.[133] Since such winter time warming phenomena happen periodically in the Kongsfjord, the fjord is considered a sub-Arctic fjord in constrast to other fjords at the same latitude.[127]

The seasonal light regime in the Kongsfjord area is significantly different from the temperate Orkneys. The period of polar night ranges from October 28 to February 14 and the midnight sun shines from April 21 to August 21. During the period of midnight sun, the irradiance from the sun at nighttime is only slightly smaller than during daytime. This results in considerable photostress for all shallow water organisms. In contrast, the period of polar night does not allow any photosynthetic processes and phytoplankton as a food resource may be depleted in this period. Suspended matter introduced by melt water influences both the irradiance of UV and visible light penetrating the water column and may attenuate the photostress imposed during summer. The clearest waters and consequently the deepest euphotic zones are found in early spring at the mouth of the fjord, furthest away from the main freshwater sources. While the euphotic zone reaches down to approximately 33 m in the outer parts of the fjord it may be less than 1 m close to a glacier front.[129]

In the Kongsfjord, three places with hard bottom substrate are known to host a rich hard bottom fauna and are regularly visited by divers for sponge sampling: Hansneset Step, Hansneset Cave and Kongsfjordneset.

Hansneset Step

Hansneset Step (N 78° 59.147', E 011° 57.715') lies on the foot of a number of sizeable semi-submerged rocks that are located about 100 m from the western coast of the island Blomstrandhalvøya. From a level area at about 6 m depth (high tide) directly below the rocks stretches a wall down to approximately 12 m. There it levels into a first step that is horizontally tilted in south-westerly direction. From this step a less angular slope stretches to 18 m to a second step. Sponge sampling in the 2008 and 2009 sampling season was exclusively performed between the 6 m platform and the 18 m step. In spring and summer, the steps are overgrown by a large variety of marine macroalgae. Sponges can be found between these macroalgae as well as on the walls. On the steep walls, sponges seem to be more abundant[10] and are more easily accessed than on flat areas. Two types of *Haliclona* sponges co-occur in Hansneset Step: the purple, elastic form (Figure 3.58, approximately three-four individuals per square meter) and, to a much lesser extent, the white, soft form (no picture from Hansneset step available, 0.1 individuals per square meter). The purple form may grow in large cushions with many chimneys and cover considerable parts of the wall while the white-fragile form usually consists of not more than one or two chimneys.

Figure 3.58 The substrate in Hansneset Step is interspersed with small holes and ridges that give the place a reef-like structure. Macroalgae are dominant. Sponges grow in small patches between the algae and are often covered by sediment or algae exudates. Photo: M. Schwanitz.

10 Abundance values are estimated. As flat areas are strongly overgrown by macroalgae, the sponge population on the flat parts is not easily visible and may thus be underestimated.

Hansneset Cave

Hansneset Cave is a semi-submerged cave at the western coast of Blomstrandhalvøya. It is located approximately 100 m from Hansneset Step, i.e. within vision range. The cave is approximately 8 m wide and 9 m high at the mouth, of which 6 m lie below the water line (high tide). It reaches approximately 15 m into the rock. The floor is even, but slightly ascending towards the inner part, and covered with boulders which show sign of being moved regularly (by waves, ice bergs, etc.) since little overgrowth can be seen on them. The walls on both sides are concave and well overgrown. At the inner end of the northern wall lies a niche in about 1-2 m depth. The rear wall is vertical, in places overhanging and tapers to a niche in the south-eastern corner.

A B

Figure 3.59 (A) Hansneset Cave above the water. (B) Typical underwater fauna in the cave. Photos: M. Schwanitz.

The entrance part of the cave is covered with algae but with decreasing light intensity the algae density diminishes rapidly towards the inner part. A distinct zonation can be observed with leaved algae growth reaching about half way into the cave. Their lower boundary limit has been determined as lying at the 0.7% irradiance line (visible spectrum) as compared to the surface irradiance.[134,135] Further back, only encrusting red algae can be found. However, they are strongly overgrown by bryozoans, actinia, ascidians and sponges. Sponge density is highest in the rear part and the niches, i.e. the darkest parts of the cave. They grow from about 1 m water depth (ice scouring line) down to about 1 m above the floor (boulder scouring line) and cover large parts of the wall. The sponge fauna in the cave at Hansneset was thorougly examined by M. Assmann; the predominant sponge species

is *Halichondria panicea*, and, according to his observations, only *Haliclona excelsa* as a representative of the genus *Haliclona* is found in the cave.[136]

Kongsfjordneset

On Kongsfjordneset (N 78° 58.635', E 011° 29.454', waypoint 84[11]), a steep wall is located about 500 m from the coast and runs for several hundred meters parallel to the coast line in a north-westerly direction. Between the shore and the wall exists a gradual slope of bare rock that is in some places covered with dense stands of macroalgae. This slope turns into a steep wall in about 10 m depth and forms a step in about 30 m depth. It continues to larger depths beyond that. In the upper part of the wall, patches of brown algae overhang the rock face and cover the sessile macrofauna of mainly actinians and ascidians (Figure 3.60). Sponges grow in small patches of two-three chimneys with a density of about one-three individuals per square meter. Larger sponge patches are rare and increasingly found in greater depths. Four different sponge groups can be found on this spot: the purple, elastic group, the white soft group, the brown stiff group, and the white, elastic group. Sponge cushions with more than three chimneys have only been observed of the purple, elastic and the white, elastic group.

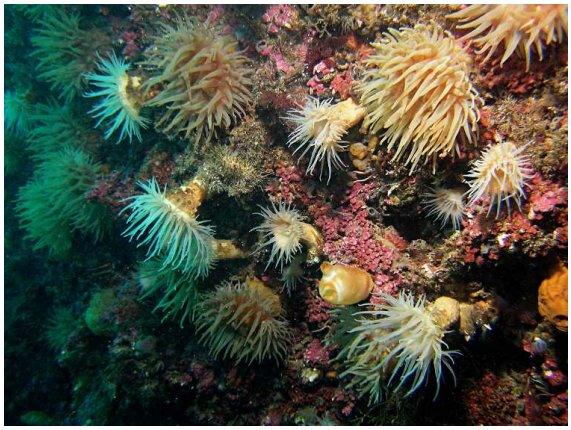

Figure 3.60 Underwater scenery at Kongsfjordneset. Actinians and ascidians are abundant at this site. Photo: M. Schwanitz.

3.4.2 Great Britain, Orkneys

The Orkney Islands are an archipelago of approximately 100 islands that lie north of Great Britain, separated from the Scottish mainland by the 10-13 km wide Pentland

11 Waypoint determined by the AWI polar diving operation supervisor, Max Schwanitz.

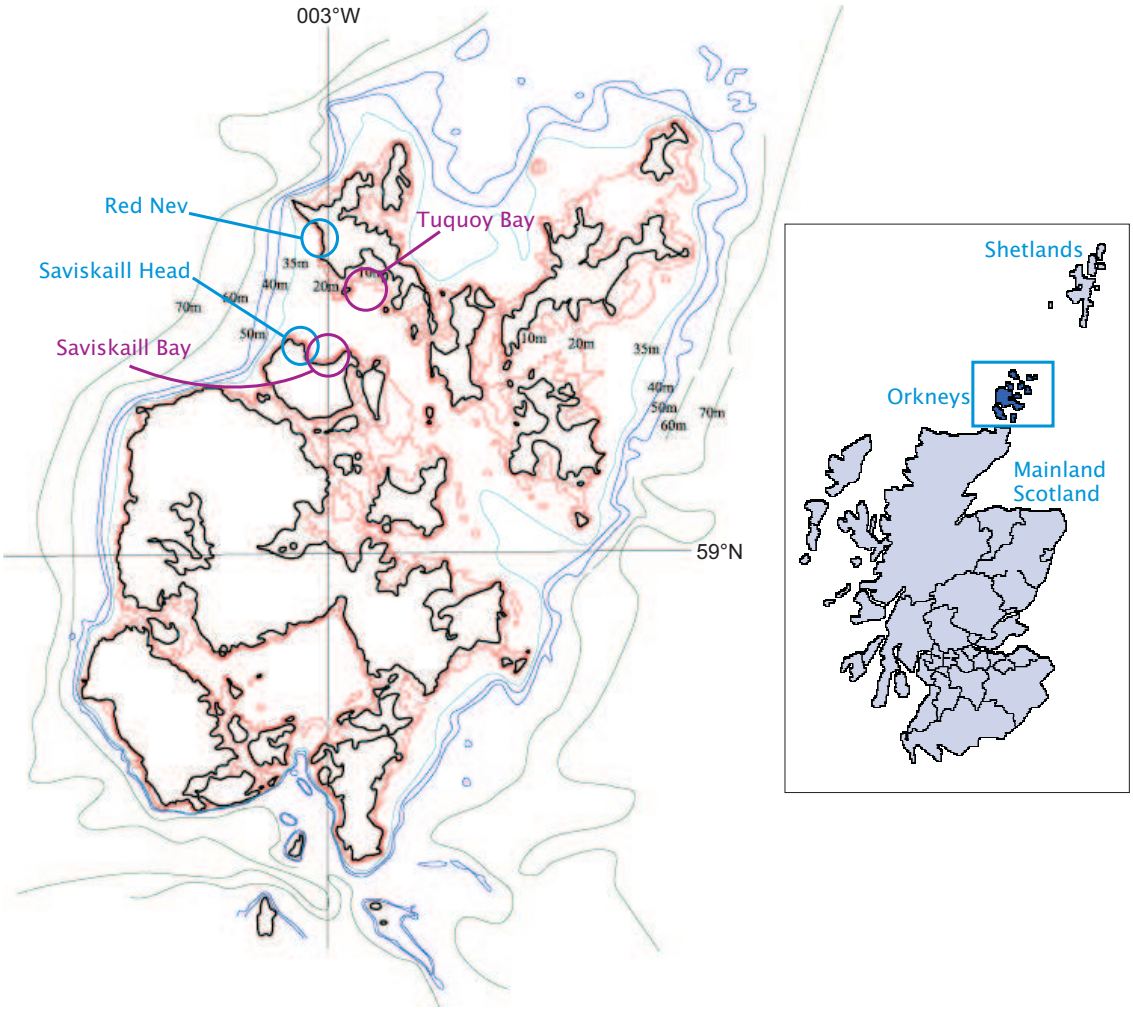

Figure 3.61 Map of the Orkney Islands, Great Britain. Colored lines indicate the bathymetry. The section shows mainland Scotland and the Orkney- and Shetland Islands for orientation. Green circles mark the sponge sampling areas. Changed from http://www.fettes.com/orkney/bathymetry.htm.

Firth. They are situated on the European continental shelf at approximately 59° N and 003° W. The ocean around the archipelago is influenced by the Atlantic Water (AW) of the North Atlantic Current (NAC, "Gulf Stream") that after crossing the Atlantic in easterly direction is deflected to the North by the continental slope and the Ireland-Britain island barrier. Water depths between the islands rarely exceed 30 m but quickly drop to larger depths along the west coasts. Off the east coast they reach the average depth of 70 m of the continental shelf further away from the islands (Figure 3.61). The amplitude of the tide is approximately 3-4 m which results in very strong tidal currents between the islands (~2 m s^{-1}). The west coast of the

archipelago is dominated by clear Atlantic waters and strong waves that build up by wind forcing over the Atlantic. The east coast, in contrast, is influenced by the more turbid waters of the North Sea. Also the coastal constitution differs between the East and the West; the western coast consists mainly of steep cliffs, sometimes of several hundred meters height while the eastern coast is characterized by shallow shores. Under water, the bottom west of the islands is characterized by coarse sand and gravel while the East is dominated by sands and mud.[137] Therefore, the west coast offers better possibilities to sample hard bottom fauna than the east coast.

Water temperatures range between 7 and 15°C owing to the influence of the Atlantic Water. In contrast to the Arctic Kongsfjord, they rarely fall below 7°C even during winter time cooling. In winter, the water masses are well mixed, but a thermocline establishes in late spring. Its strength is dependent on the heat input and the turbulence generated by tides and the wind. On the other hand, the salinity does not show strong fluctuations and ranges between 34.5 and 35.3 psu.[137] This is due to the lack of major tributaries that empty close to the archipelago and the area being solely influenced by waters of marine origin.

The steep cliffs of the western coasts were picked for fauna examinations during the 2007-2009 "R/V Heincke" expeditions. Among them, two locations stood out as suitable sites for sponge sampling: Red Nev (Westray) and Saviskaill Head (Rousay). They are sites where tidal current speeds are very high, hence they yield a rich hard bottom fauna that is typical for temperate areas (e.g. Naylor (2005)).[138] Red Ned was previously visited for sponge sampling during a scientific cruise in 2001 and 2003. At that time, also two other places, Saviskaill Bay and Tuqouy Bay, were visited for sponge sampling.[139] These two sites, which lie to the East and across Westray Firth relative to Saviskaill Head, respectively (Figure 3.61), were shortly visited for sponge sampling between 2007 and 2009 but yielded, probably due to their more sheltered location and in part sandy bottom, significantly less sponges than e.g. Saviskaill Head.

Red Nev

Red Nev (N 59° 18', W 003° 01') represents a number of semi-submerged caves on the island of Westray. The caves are extremely exposed to waves and diving is only possible after several days of calm weather. The water depth inside the caves is

approximately 8 m.[12] Due to the wave action, the fauna layer inside the caves is at maximum 1.5 cm thick and consists mainly of ascidians, brittle stars, crustaceans and sponges but compared to Saviskaill Head rather few cnidarians (S. Fuhrmann, pers. commun.). Being set back into the cliff front and reaching rather deep, the caves are poorly illuminated and the flora is constricted to encrusting red algae while the macroalgae are confined to the cave entrance.

Saviskaill Head

Saviskaill Head (N 59° 12', W 003° 03') is an exposed cape on the northern coast of Rousay, overlooking Westray Firth. The cape is exposed to strong tidal currents that allow diving only during turning tides and in calm weather. The steep, in parts overhanging cliff falls to a 10 m wide step in 30 m depth from where it continues to 50 m depth and beyond. The upper meters are densely covered by a macroalgae forest (Figure 3.62A). Below, a large variety of hard bottom fauna is found, with different Anthozoa species (e.g *Alcyonium digitatum* and *Actinia equina*) being the most abundant larger animals. Sponges are also rather abundant on this cliff (Figure 3.62B). The macroalgae stalks are often covered by *Halichondria panicea*

A B

Figure 3.62 Underwater scenery at Saviskaill Head. A: Algae forest with dense epibiont growth; 11 m depth. B: Fauna on the vertical wall; the soft coral *Alcyonium digitatum* is abundant at the site; 14 m depth; Photo: G. Schmidt (A) and M. Wehkamp (B).

12 More detailed information about the caves is not available since sampling occasions are extremely rare and are solely used for sampling, not mapping.

and *Esperiopsis fucorum* (Figure 3.62A) while other sponges like *Pachymatisma johnstoni*, *Cliona celata*, *Myxilla incrustans*, and *Haliclona* sp. occur deeper, where the algae cover is not as dense or lacking completely.

Haliclona sponges sampled at these two locations do not differ considerably in their morphology. The organisms sampled in Red Nev are generally thinner cushions and greyish in color, but their microstructure does not deviate significantly from sponges collected in Saviskaill Head. In general, they resemble the purple type observed in the Kongsfjord but grow in significantly larger cushions.

3.4.3 *Haliclona* samples

Sponges were collected in three subsequent years between 2007 and 2009. In 2007, sponges were only collected from around the Orkneys while both the Orkneys and Spitsbergen were visited for sponge sampling in 2008 and 2009. Due to bad weather conditions during the expeditions to the Orkneys in 2007 and 2008, the divers could not access Red Nev hence the majority of *Haliclona* sponges from the Orkneys in these two years originated from Saviskaill Head. A total of 11 *Haliclona* individuals were sampled around the Orkneys and 56 partial organisms from the Kongsfjord, Spitsbergen. For sustainability reasons, only a small piece of each Spitsbergen individual was sampled to determine the presence of 3-APAs, prior to the collection of a larger subsample from 3-APA containing individuals.

Two morphologically different groups of sponges that belong to the genus *Haliclona* were found at the two Orkney sampling sites and four different groups were found in the Kongsfjord. The group in this context refers to color and haptics of the sponge, but one has to be aware that sponge color is not a confident identification feature as it may be highly variable. The haptics on the other hand is a character determined by the way the spicules are arranged and is considered more confident than color. The growth form, i.e. whether the sponge grows branches, erect chimneys or forms rather flat cushions, is also highly variable and strongly dependent on the habitat, exposure to currents etc. Since the individuals inside a group showed strong variation in growth form (e.g. Figure 3.63), the growth form was not considered when assigning groups.

The sponges could not be identified to the species level purely by classical taxonomical methods. Therefore, it remains uncertain whether the groups belong into one species or are indeed different species. All sponges were examined by light mi-

croscopy, identified as belonging to the genus *Haliclona*, and then grouped according to their microscopic characteristics. These groups corresponded to their most obvious characteristics, color and haptics. To give a more accurate picture about the phylogenetic relationship of the groups, they are currently under genetical investigation by external researchers. Justification for grouping the individuals notwithstanding the uncertainty of characters like color and haptics in *Haliclona* is given by the correlative appearance of these characters with microscopic characteristics and chemical profiles.

In her dissertation thesis, Heike Lippert states that only two *Haliclona* species, *H. viscosa* and *H. rosea*, occur in the Kongsfjord,[108] while Michael Assmann reports a third species, *H. excelsa*, from the cave at Hansneset.[136] Since the presented thesis finds four groups, species names are assigned only tentatively to these groups.

The purple, elastic *Haliclona*

The purple *Haliclona* has a soft, elastic texture. The sponge is found from approximately 6-24 m depth where it grows in cushions of 8-20 chimneys. The cushions are usually 2-3 cm thick with elevated oscula. In few cases at protected sites the oscula sit on pronounced chimneys which can reach 6 or more centimeters in height. Oscula have a diameter of 0.5-1 cm. A thin membrane perforated by a hole much smaller than the osculum stretches over the osculum opening after the sponge is preserved in alcohol, but is not observed in living organisms. The surface of the sponge is visibly perforated by ostia and has a smooth feel. The sponge is found primarily in Hansneset but also in Kongsfjordneset (Spitsbergen) where the organisms reach sizes of 2-3 chimneys. Similar organisms are present in Saviskaill Head (Orkneys) where large individuals reach cushions sizes of 20-30 chimneys. Since the purple form from the Orkneys and the purple form from Spitsbergen show no visible difference, the representatives of both areas are combined into one group (Figure 3.63).

The skeleton contains no ectosome and consists of paucispicular[13] primary tracts connected by irregularly scattered, unispicular secondary tracts (Figure 3.64). Spicules are slender, pointed oxea, 140-170 µm × 4-7 µm. Spongin is scarce and, if present, found at the nodes of the spicule net.

The sponge is mainly found on vertical walls, but also among macroalgae fastholds and can be covered by sediment. When removed from the water and squeezed, the

13 Paucispicular in this context is defined as bundles of 2-4 spicules beside each other.

A B C

Figure 3.63 The purple, elastic *Haliclona*. (A) Reference picture of the GS 07/21 individual from Saviskaill Head (Orkneys) in the lab prior to conservation. (B) Reference picture of the GS 09/05 individual from Hansneset (Spitsbergen) in the lab prior to conservation; square length = 0.5 cm. (C) A purple *Haliclona* sponge in its habitat at Hansneset. Pictures by G. Schmidt (A) C. Cychon (B) and M. Schwanitz (C).

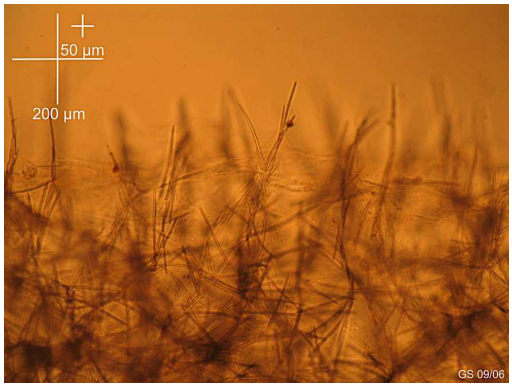

Figure 3.64 Microscopic image of the spicule arrangement in a purple *Haliclona* showing the surface and sub-surface area of a longitudinal section at 10× magnification, size reference is given in the upper left corner.

sponge gives away purple-stained, cell-containing water and an acrid smell, but does not excrete slime. The purple pigmentation reaches well into the sponge interior and fades to a brown coloring towards the base of the sponge. The organism loses all color in alcohol. The description of this sponge and its abundance fits well to the species *Haliclona rosea*.

In few cases in Spitsbergen specimen parts of the sponge tissue were observed to have lost all color resulting in translucent areas in the organism. These parts were more fragile than the surrounding tissue and no pigments or other structures were observed inside the cells in these areas. This phenomenon is evocative of bleaching in *Haliclona* sp. and other sponges in Australian waters[140] and the Caribbean.[141]

The white, elastic *Haliclona*

Two different groups of white *Haliclona* sponges grow in the Kongsfjord. One of them has an elastic consistency and retains its form well when taken out of the water. The sponge's surface appears coarse, an effect which is probably due to the ostia being rather large and clearly visible. Only one individual was found of this group but it was incomparably larger (Figure 3.65A) than any other *Haliclona* sponge observed in the sampled area. The sponge is slightly slimy and exerts an acrid smell when manipulated; it is extremely slimy when extracted by chemical methods. As in the purple, elastic *Haliclona*, a thin membrane stretches over the osculum as soon as the sponge is taken out of the water (Figure 3.65B). The sponge also carried a large number of eggs at the time of sampling that were not present in any other sponge in the area. It was found on a vertical wall in a ditch facing the main current direction, situated at ca. 16 m depth (high tide) at Kongsfjordneset and covered an area of about half a square meter. Despite its robust white outer color the tissue is increasingly brownish towards the base of the sponge. It turns completely white in alcohol.

The skeleton is arranged in paucispicular primary and unispicular secondary tracts which get increasingly disorderly towards the base of the sponge. It contains no

A B C

Figure 3.65 The white, elastic *Haliclona*. (A) The organism at its habitat at Kongsfjordneset (Spitsbergen), reference number GS 09/23; the yellow marker cable tie in the lower right corner of the picture, attached to an orange flag, has a width of ca. 0.5 cm. (B) The same organism in the lab prior to conservation; length of a square's edge = 0.5 cm. (C) Microscopic image of the spicule arrangement showing the surface and sub-surface area of a longitudinal section at 10× magnification, size reference is given in the upper left corner. Pictures by M. Schwanitz (A), C. Cychon (B) and G. Schmidt (C).

ectosome, mega- or microscleres. Spicules are oxea or slightly spatulate flanged, nearly tornote, with a size of 150-180 µm × 6-9 µm. Spongin belts the nodes of the spicule net but is scarce elsewhere. Except for its color, slime excretion and egg masses the sponge strongly resembles the purple *Haliclona*. However, it forms a separate group because of the difference in chemical profile. Sponges with a similar chemical profile were previously named *Haliclona viscosa*. The spicule arrangement of *H. viscosa* type species examined at the Zoölogisch Museum in Amsterdam, Netherlands, shows strong resemblance to the spicule arrangement of the white, elastic sponge sampled in the Kogsfjord.

The white, soft *Haliclona*

The other white *Haliclona* is extremely soft, and offers almost no resistance when squeezed. Under water it easily regains its form after being squeezed whereas it subsides easily if handled above the water. It grows in pads of 3-4 but rarely more chimneys erect on vertical walls, usually in small ditches that offer protection from currents (Figure 3.66A). The sponge was observed from about 10 to 24 m depth in Kongsfjordneset and, less abundantly, at Hansneset Step. The sponge can be covered with considerable amounts of sediment, especially at Hansneset Step.

The oscula usually sit on chimneys which may reach heights of 4-6 cm and are, if well developed, about 1 cm in diameter. The oscula have diameters of 0.5-0.8 cm. No contraction is observed, and the oscula are not covered by membranes as described for the purple and the other white *Haliclona*. Under water, the ostia are not as easily visible as in the preceding two sponges.

The surface of the sponge has a velvety feel. The tissue is stringy when torn apart and excretes no slime. A thin layer of white-pigmented cells is visible directly under the surface and gives the exterior a white flocculent look (Figure 3.66B). This white layer washes out when the sponge is manipulated. The sponge tissue away from the extremities is increasingly brownish in color but turns white in alcohol.

The sponge has no ectosome. Unispicular primary tracts are crossed by irregular, unispicular secondary tracts. They are arranged orderly towards the surface and increasingly irregular towards the base (Figure 3.66C). Spicules are thick oxea, 130-170 µm × 9-11 µm, no megascleres or microscleres are present. Spicules are bonded by small amounts of spongin at the nodes of the spicule net.

A B C

Figure 3.66 The white, soft *Haliclona*. (A) The organism in its habitat at Kongsfjordneset (Spitsbergen); the height of the largest chimney is approximately 4 cm. (B) A different organism of the same group in the lab prior to conservation; length of a square's edge = 0.5 cm. (C) Microscopic image of the spicule arrangement showing the surface and sub-surface area of a longitudinal section at 10× magnification, size reference in the upper left corner. Pictures by M. Schwanitz (A), C. Cychon (B) and G. Schmidt (C).

Figure 3.67 A white, soft *Haliclona* from the Kongsfjord with a "sick" area; GS 09/04.

Only two *Haliclona* species with unispicular primary tracts, *H. cinerea* (Grant 1826)[142] and *Reniera* (=*Haliclona*) *rufescens* (Lambe 1892),[143] were reported to-date from North Atlantic waters. *Haliclona cinerea* is described as one of the softest *Haliclona* species, which fits well to the description of the white, soft *Haliclona*, but it does not, as reported from *H. cinerea*, show slime strands when pulled apart. In addition, the spicules of the sampled sponges are too thick and the color does not fit well to be assigned to *H. cinerea*. The *Haliclona rufescens* type was unfortunately examined as a dried sponge, therefore no assertion can be made for its softness. Though reported from the Pacific, the type was collected from cold water Kamtchatka

(60° 30' N)[143] and the spicule size fits well to the white, soft *Haliclona* collected in the Kongsfjord.

Similar to the purple, elastic *Haliclona*, several members of the white, soft *Haliclona* were found in the Kongsfjord that seemed to have lost all color (Figure 3.67) resulting in sickly-looking, slightly translucent and very fragile areas within the organism.

The brown, stiff *Haliclona*

This form is found exclusively in Hansneset cave (Spitsbergen) where it grows in small patches of 2-5 oscula. The sponge is confined to the back wall of the cave and the niches where least light is present (Figure 3.68A). This habitat represents the most densely overgrown habitat in terms of sponge density and competition for space can be assumed to be high (Page 83).

The sponge has a rather brittle feel which is intensified when the sponge is preserved in alcohol, and shows oscula on low-mounded elevations. It excretes no slime. The sponge is of a same brown color throughout in contrast to the other sponge groups that have different outer and inner colors (Figure 3.68B), but as the other sponges it turns white in alcohol.

A B C

Figure 3.68 The brown, stiff *Haliclona*. (A) The organism in its habitat at Hansneset cave (Spitsbergen); white arrows indicate the *Haliclona* among a neighboring sponge, possibly *Halichondria genitrix*; the arrow length represents 7 cm in the field. (B) A brown *Haliclona* in the lab prior to conservation (reference GS 09/27); length of a square's edge = 0.5 cm. (C) Microscopic image of the spicule arrangement showing the surface and sub-surface area of a longitudinal section at 10× magnification, size reference in the upper left corner. Pictures by M. Schwanitz (A), C. Cychon (B) and G. Schmidt (C).

Spicules are slender oxea, 150-170 µm × 4-7 µm. They are arranged in pauci- or polyspicular[14] primary tracts interconnected by unispicular secondary tracts (Figure 3.68C). In general, the skeleton seems much more compact and dense which is the probable cause for the sponge's stiffness. The sponge contains no ectosome, mega- or microscleres. Spongin is routinely present at the nodes of the spicule net but scarcely elsewhere.

The only *Haliclona* species reported from the Hansneset cave is *H. excelsa*.[136] *Haliclona excelsa* was recently reclassified to *Isodictya palmata*. However, *I. palmata* shows a significantly different growth form than the sponges sampled in the cave, none of which grew antler-shaped branches. While, *I. palmata* grows in boreal and sub-Arctic North Atlantic, has a yellow-brown color and a firm consistency, all of which fits to the description of the brown, stiff *Haliclona*, *I. palmata* is reported to contain palmate isochelae which were not observed in the brown, stiff *Haliclona*.

14 Polyspicular tracts in this context contain 4-8 spicules in parallel.

3.5 Annual variation in *Haliclona viscosa*

3.5.1 Interannual variation 1999-2009

The white, elastic sponge *Haliclona viscosa* shows variation in its metabolites between different years. The variation can be divided into two components; (a) presence/absence of specific compound classes and (b) presence/absence of single compounds inside a compound class.

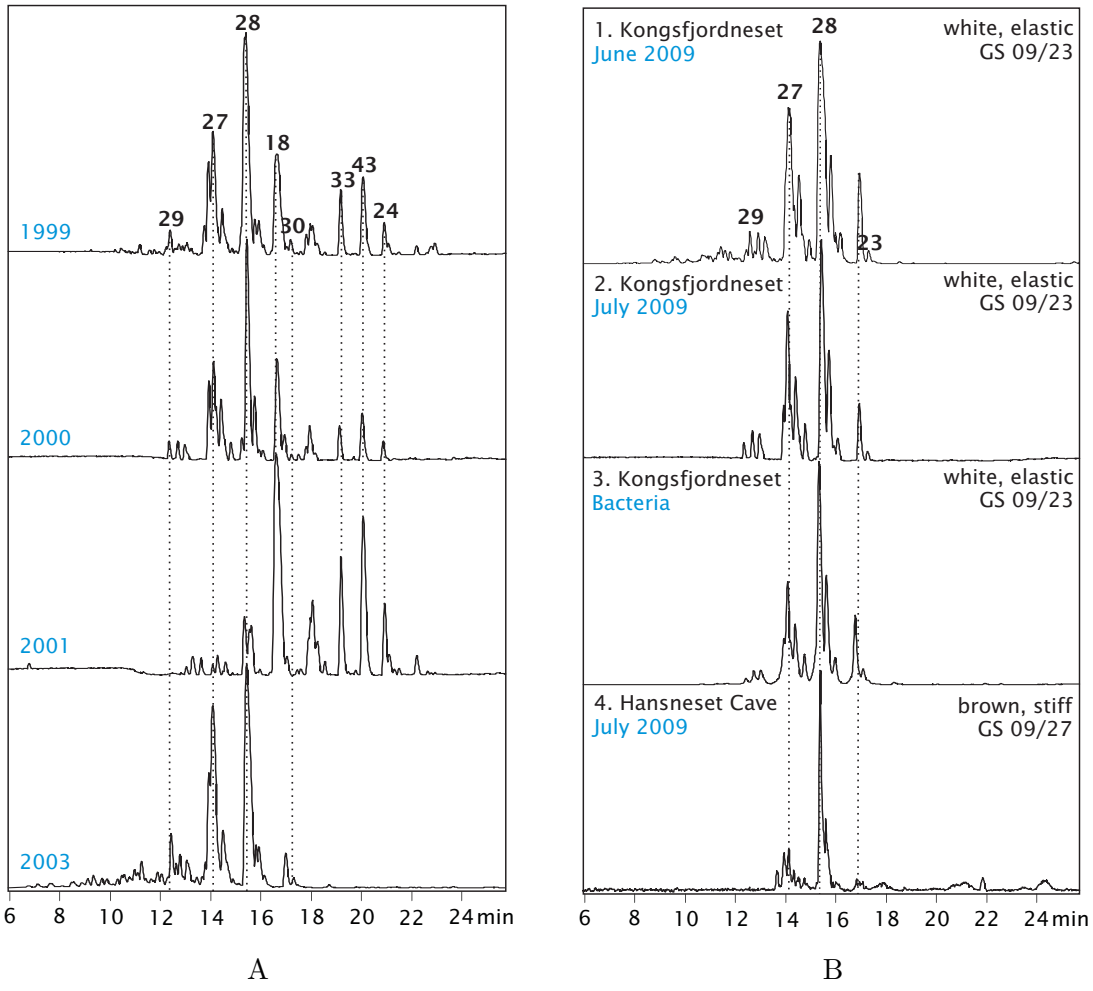

Figure 3.69 Base peak chromatograms ($m/z = 50 - 1000$) of *Haliclona viscosa* crude extracts. A: Interannual metabolite variation in *H. viscosa* between 1999 and 2003. B: Metabolite variation in *H. viscosa* in 2009; (1) crude extract of the GS 09/23 individual sampled in June and (2) in July; (3) crude extract chromatogram of GS 09/23-associated bacteria; (4) crude extract chromatogram of a brown, stiff individual from Hansneset Cave. Numbers denote previously published secondary metabolites. Dotted lines are inserted for orientation.

Presence/absence of compound classes is most conspicious between the years 2001 and 2003. This is most obvious with 3-alkyl tetrahydropyridines. Haliclamines C (**27**) and D (**28**) are the major metabolites in most years but they are almost absent in 2001 (Figure 3.69A). The same is true for other haliclamines which show very low abundance in normal years but even less in 2001. Instead, the 3-alkyl pyridinium alkaloids are more prevalent in 2001, with viscosaline C (**18**) and viscosamine C (**43**) being the major metabolites. Consequently, viscosamine C (**43**) and viscosaline C (**18**) were isolated from the 2001 extract and published in 2003[96] and 2004,[74] respectively. In contrast, the haliclamines prevail in the 2003 and 2009 extracts and almost no 3-alkyl pyridinium alkaloids are present in these two years.

Variation inside a compound class is exemplified by Haliclamine K (**62**) which is present in the 2003 and 2009 samples (see manuscript on page 223) but not present in 2001 and only present in very small quantities in 1999 and 2000. In 2001, all haliclamines with double bonds are absent.

An interesting observation is that most compound classes, haliclocyclins, haliclamines, viscosalines and viscosamines, consist of several members with varying alkyl chain lengths. An exception from this is cyclostellettamine C (**33**). It is present in all samples obtained before 2003 but does not have any analogues with shorter or longer chains in the crude extract of *H. viscosa* although the co-occurrence of different cyclostellettamines is known from other Haplosclerid sponges.[116]

The change in the metabolite composition between 2001 and 2003 suggests a change in environmental factors since the competitive habitat of neighboring sessile organisms is not subject to rapid changes. However, few environmental monitoring programs exist to-date in the Kongsfjord area. They record oceanographic data like salinity, temperature and currents along the main axis of the fjord but not close to the sampling sites and with too low resolution in the sponge sampling depth. Other environmental factors like the water transparency, nutrient availability and plankton composition are not recorded on a regular basis. Without these data, the correlation of secondary metabolite changes with environmental parameters is highly speculative. However, the speculation is necessary in view of a continued study of the secondary metabolite variation in the sponge genus *Haliclona* to determine the environmental parameters that should be recorded to allow a better picture.

On one hand, the variation in the compound classes produced by the sponge can be due to the nutrient uptake varying between the years or between seasons in which the sponge is sampled. The C:N:P ratio (Redfield ratio = 106:16:1), i.e. the

availability of carbon, nitrogen and phosporus, strongly influences the appearance of e.g. plankton blooms which form in early spring as soon as the water temperature rises to allow high metabolic rates and stratification of the water column increases. At that time, nutrient levels in the upper water layer are high from winter time overturn of the water column. Due to high abundance of organisms that use the nutrients for growing, the stratified layer soon depletes in N while C is never and P rarely depleted. Minor blooms also occur in early autumn, i.e. after the first mixing events (storms) when the water temperature is still high.[144]

Before a phytoplankton bloom, the nutrients are available as dissolved organic or inorganic matter that can be taken up through cell membranes. During the bloom, the availability of nutrients for a sponge is given by the planktonic organisms that the sponge can filtrate from the water. After the bloom however, the water column might be depleted in both nutrients and food particles possibly resulting in a change of secondary metabolite biosynthesis. For example, if nitrogen is depleted, fewer compounds may be synthesized that require the incorporation of many nitrogen entities. In the case of the 3-APAs this may be indicated by longer alkyl chains or a shift from trimeric to dimeric compounds. The strong presence of viscosalines and viscosamines in 2001 may therefore be a sign for high nutrient levels. Since phytoplankton and zooplankton contain different nutrient ratios, the change may also be due to a change in food source by advected food species. Therefore, the sampling season and site may be important for the 3-APA content and composition in *Haliclona viscosa*.

Nutrient-dependent secondary metabolite production is known e.g. from plants (e.g. Bryant et al. 1987)[145] and microorganisms.[146–148] In the marine environment, few studies exist that test the influence of nutrient enrichment or depletion on the secondary metabolism of organisms. One example is the soft coral *Sarcophytum ehrenbergi* that was shown to lower its stress metabolite (terpene) content with elevated nutrient levels. However, the response is attributed to decreased interspecific competitiveness in the nutrient enriched environment, not to the initial nutrient availability.[149]

On the other hand, variation in secondary metabolites can be due to an adjustment to the defensive need of the sponges. Since sponges are only observed to be under spatial competition in Hansneset Cave, and only one individual from Hansneset Cave in 2009 shows low abundance of 3-APAs, the metabolites are presumably not used for competitive defense against other sponge species. However, they may be used

against potentially infectious microorganisms, as is indicated by the antimicrobial activity of viscosaline C (**18**) and the haliclamines C (**27**) and D (**28**).

Since haliclamines display lower cytotoxicity than cyclostellettamines and viscosamines,[84] a shift of the compound composition towards haliclamines can indicate a lower need for defense as well as a lower fitness to produce energetically "costly" secondary metabolites. This is observed in the samples collected in 2003 and 2009 which contain almost exclusively haliclamines, few viscosalines at low concentration, no cyclostellettamine C (**33**) and no viscosamines (Figure 3.69). However, haliclamines with double bonds probably balance the decrease in biological activity between 3-alkyl pyridinium and 3-alkyl tetrahydropyridine compounds.

Haliclamines with double bonds were more diverse and abundant in 2003 and 2009 than e.g. in the crude extract from a 2001 individual. The sponge sampled in 2009 carried large numbers of eggs at the time of sampling. This may be an indication that the sponge produces more haliclamines to protect the eggs from predation, or the eggs themselves are chemically defended. The compounds may also serve as a cue to signal larvae release. Two studies addressed the chemical defense of marine invertebrate larvae and concluded that the larvae must be chemically defended since they are unpalatable to fish but do not contain physical defense mechanisms.[69,70]

A possible chemical defense of sponge larvae may also be the reason why no 3-APAs were found in the other sponge groups present in the Kongsfjord. The individuals in these groups were generally much smaller than the *Haliclona viscosa* found at Kongsfjordneset and did not contain eggs. Whether this is a seasonal or a maturity phenomenon cannot be resolved at this time.

The compound class variation may also be due to sponge individuality. From each of the sampling years, only one sample of *Haliclona viscosa* exists. Today it is not possible to ascertain, whether different organisms were pooled to form one sample or whether each sample consists of a single individual. In 2009, only one large individual was found at Kongsfjordneset that was readily identified by its 3-APA content by thin layer chromatography (Section 3.7.1). The organism was large enough to have lived at the site for several years and might have been the source for previous samples, e.g. the 2003 sample. The crude extract of the latter shows strong similarity to the extract of the 2009 sample, but it remains speculation whether these results are due to the samples having the same origin. The hypothesis of individual variation is supported by a second individual (GS 09/27) with lower 3-APA content that was identified by HPLC methods later (Figure 3.69B4).

3.5.2 Seasonal variation 2009

In 2009, a thin layer chromatography method was used to screen for 3-APA containing individuals. For this purpose, small pieces of sponges were sampled under water and the remaining organisms were marked with cable ties (Figure 3.65A). The identified individual was sampled again and the crude extracts of both sampling periods were compared.

The *Haliclona viscosa* individual sampled from Kongsfjordneset in 2009 shows a shift in its metabolite composition between the first and the second sampling. Compounds that elute before 12 min are absent in the second sampling (Figure 3.69B). Whether this change is due to a seasonal change, i.e. production of 3-APA biosynthetic precursors earlier in the season and accumulation of the educts later, or due to the damage inflicted by the sampling process and the animal's response to it cannot be determined. The observed shift poses the question, whether the 3-alkyl pyridinium alkaloids present only in the years 1999-2001 are due to a seasonal change and whether a later sampling of the 2009 individual would also yield 3-alkyl pyridinium compounds. Further sampling later in the year as well as the elucidation of the compounds that elute before 12 min is required to answer the question, but a review of the sampling times of the other *H. viscosa* sponges between 1999 and 2001 suggests that season does not play an important role. All sponges were sampled in approximately the same season, in late spring and summer (Table A.1).

In 2009, bacteria were isolated from the sponge and extracted. The resulting crude extract shows the same 3-APAs as are present in the extract obtained from the whole sponge. Although the possibility remains that a carryover of secondary metabolites was obtained during the extraction procedure, this result indicates that bacteria may be involved in the production of the secondary metabolites of *Haliclona viscosa*.

3.6 Secondary metabolite variation in different *Haliclonas*

The motivation for the presented study is the spatial and temporal variation of secondary metabolites observed in *Haliclona viscosa* from two different geographical locations, the Orkneys and Spitsbergen. These observations founded on approved *Haliclona viscosa* samples from both locations. During research for the presented thesis, the sampled *Haliclona* sponges could not be identified to the species level for lack of an experienced *Haliclona* taxonomist. Therefore, a combination of molecular genetics and different chemical methods tries to supplement taxonomic identification characteristics.

3.6.1 Intraspecific variation in *Haliclona*

The secondary metabolites found in a given *Haliclona* group at a given site do not show significant variation both in diversity and abundance (not shown). Of the four *Haliclona* groups obtained during the sampling seasons 2007-2009, the purple, elastic group is the only one that occurs in Spitsbergen and the Orkneys. It shows significant deviations of secondary metabolites between the different sampling sites.

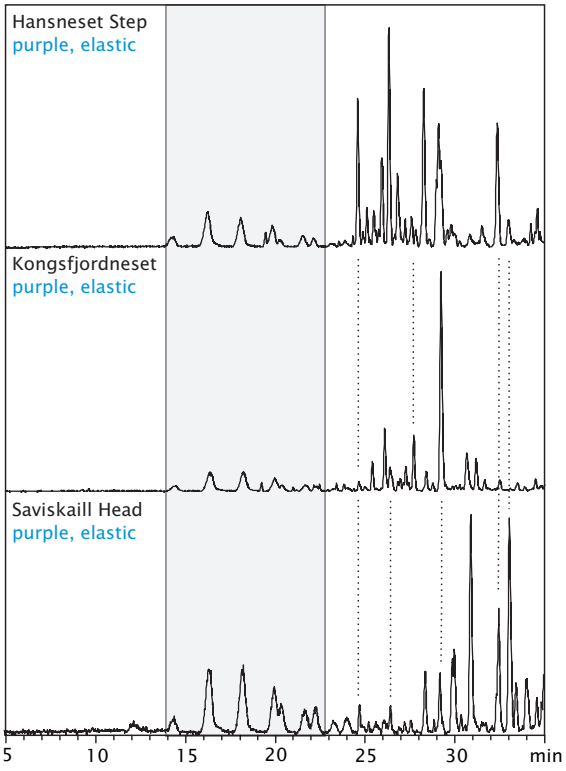

Figure 3.70 Comparison of base peak chromatograms ($m/z = 50 - 1000$) obtained from crude extracts of purple, elastic *Haliclona* specimens collected at different sites in the Kongsfjord, Spitsbergen (Hansneset Step and Kongsfjordneset) and the Orkney Islands (Saviskaill Head). Due to low concentration of the metabolites, column specific peaks are visible (shaded area) although the analysis uses the same chromatographic gradient as for *H. viscosa* samples (Figure 3.17 and 3.69). Chromatograms are scaled to 100 % intensity of the highest peak.

None of the sampled purple, elastic *Haliclonas* produces 3-alkyl pyridinium alkaloids. The compound peaks observed in Figure 3.70 invariably elute in high (>60%) acetonitrile (ACN) concentration or pure ACN (30-35 min) and therefore probably constitute primary metabolites like sterols, fatty acids and glycerolipids. The composition of these strongly nonpolar compounds in the purple, elastic *Haliclona* is significantly different between the two sampling sites Hansneset and Kongsfjordneset in Spitsbergen, and both are different from the sampling site in the Orkneys.

The lipid composition can give valuable information about the food source of an organism. While the lipids produced naturally in a given sponge species are assumed to be constant for all individuals of the species, different food sources or commensal organisms may influence the total lipid composition of an individual. For example, zooplankton has a different lipid composition than phytoplankton or bacteria. The coastal Kongsfjordneset is influenced by oceanic waters while Hansneset is located in the inner part of the fjord and is influenced by fresh water and sediment runoff from glaciers and rivers. The food sources may therefore be different between the two sites, with cold- and freshwater adapted food species in Hansneset whereas the food species in Kongsfjordneset may be advected by the currents passing off the western coast.

Since the structure of the highly nonpolar compounds in *Haliclona* was not examined during the study, no further assertion can be made towards the nature of the compounds. However, a closer examination in the future might yield valuable results in the chemotaxonomic identification since a similar approach has been assessed with sterols in other marine sponges.[150]

Sterols are used in all eukaryotic organisms as membrane constituents that modulate the passive movement of solutes across the membrane bilayer. Eukaryotic organisms that are not able to synthesize their own sterols require an exogenous source of the molecules. The greatest diversity of sterols is encountered among the most simply constructed eukaryotic organisms and sponges yield the most diverse array of sterols found in all marine invertebrate phyla. As physiological complexity increases from invertebrate to vertebrate, a progressive reduction in the number of sterols is found, along with an increasing occurrence of cholesterol. This has been related to the importance of cholesterol in the development of an increasingly complex nervous system.[53] Therefore it is not surprising to find a large diversity of sterols in a single sponge species and specific sterols may be used as chemotaxonomic marker compounds. On the other hand, if the composition of the nonpolar compounds

in the *Haliclonas* is assumed to be species or phenotype specific, all three purple, elastic *Haliclonas* should be different species or different phenotypes of the same species, respectively.

3.6.2 Interspecific variation in *Haliclona*

A comparison of interspecific metabolite variation of all *Haliclonas* sampled in the Kongsfjord yields very different results for the different *Haliclona* groups. Only the white, elastic sponge sampled at Kongsfjordneset and a brown, stiff *Haliclona* sampled in the cave at Hansneset contain 3-alkyl pyridinium- or 3-alkyl tetrahydropyridine alkaloids (3-APAs). These metabolites are discussed in detail in Section 3.3 and 3.5.

Haliclona samples obtained in the Kongsfjord

While the nonpolar compounds in the purple, elastic *Haliclona* vary between sites, the secondary metabolites between two *Haliclona* groups – the brown, stiff *Haliclona* sampled in 2008 in the cave at Hansneset and the white, soft *Haliclona* from Kongsfjordneset – are not markedly different. Taking into account the site difference described above for the purple, elastic *Haliclonas*, a difference would be expected for the white, soft and the brown, stiff sponge sampled at Kongsfjordneset and Hansneset, respectively. This contradicts the conclusion about the food source being responsible for the nonpolar metabolite composition given above for the purple, elastic *Haliclona*.

Since the white, soft and the brown, stiff *Haliclona* are morphologically very distant, there must be a different reason for the concurrence. Similar chemical defense mechanisms are unlikely since the brown, stiff *Haliclona* grows in a habitat with much higher sponge density than the white, soft *Haliclona* and would therefore be expected to produce different or more metabolites. One environmental factor that unites the two groups is light intensity. For the white, soft *Haliclona* light intensity is limited due to water depth while the cave overhang limits the light for the brown, stiff *Haliclona*. This would require commensal photosynthetic organisms that are involved in the metabolite production. The purple, elastic *Haliclona* sampled at Kongsfjordneset is subject to the same light limitation as the white, soft *Haliclona* and shows a similar metabolite composition although present in different relative compound intensities (Figure 3.71).

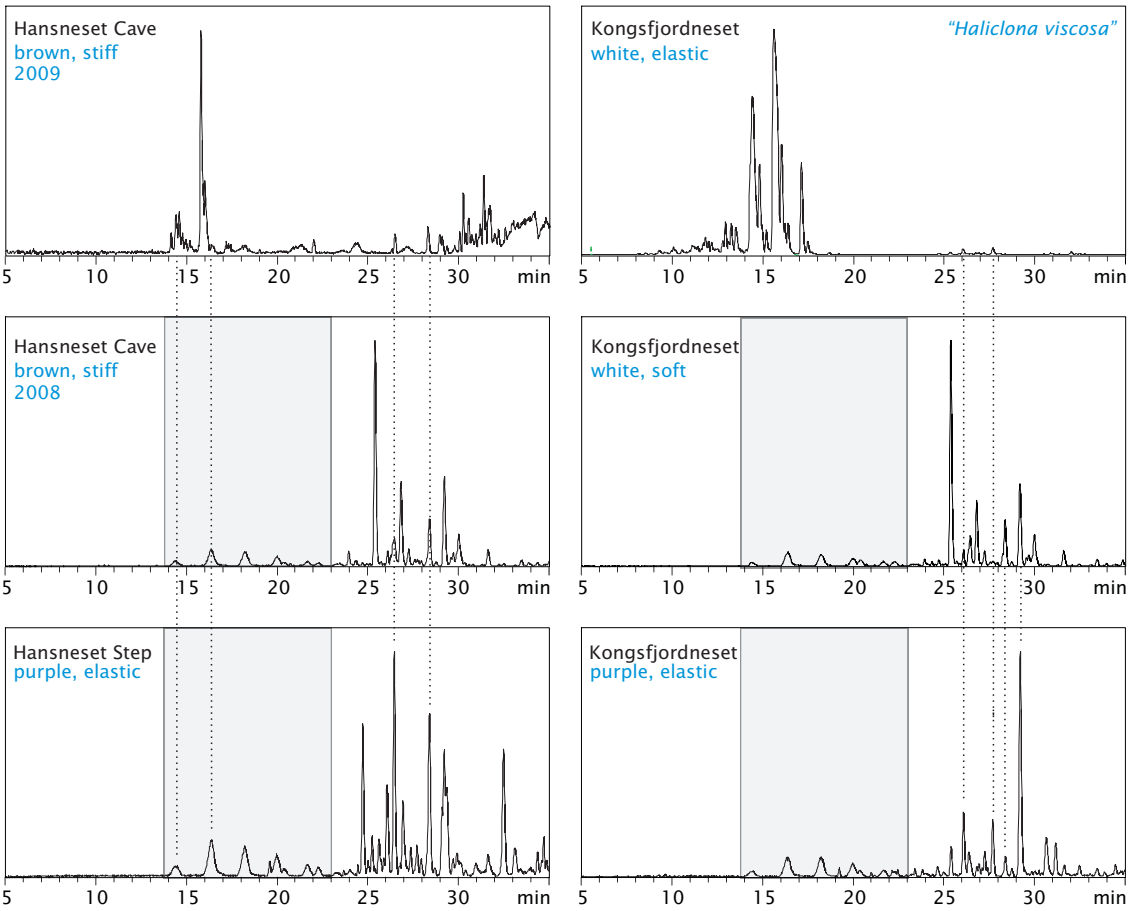

Figure 3.71 Comparison of base peak chromatograms ($m/z = 50 - 1000$) obtained from crude extracts of different *Haliclona* specimens collected in the Kongsfjord, Spitsbergen. The shaded areas mark column-specific peaks. The analysis uses the same chromatographic gradient as for *H. viscosa* samples (Figure 3.17 and 3.69). Chromatograms are scaled to 100 % intensity of the highest peak each, observable by varying intensity of the column-specific peaks.

A striking difference is observed between the two brown, stiff *Haliclonas* sampled in the cave at Hansneset in subsequent years. The individual sampled in 2009 shows 3-APAs at low intensity in addition to other metabolites also present in other *Haliclona* groups. The major compounds of the 3-APAs are haliclamine D (**28**) and dehydro-haliclamine F (**65**). The other 3-APAs in that sponge are unidentified, yet.

The difference between the two brown, stiff *Haliclonas* indicates that the 2009 individual may have been misclassified. A different possibility is that the production of the 3-APAs in that sponge has recently started suggesting that the appearance of

3-APAs is linked to the life stage of a sponge. This possibility is supported by the low intensity and diversity of 3-APAs in the individual.

Haliclona samples obtained from the Orkneys

Compound variation for the Orkney *Haliclona* groups is similar to the variation observed in the Spitsbergen "dark-dwelling" groups. The *Haliclona* from Saviskaill Head shows a similar compound composition as the *Haliclona* from Red Nev, but the compound intensity is significantly different. While the purple, elastic *Haliclona* was sampled from several meters depth, the grey, stiff *Haliclona* was sampled from the cave in Red Nev. The observed difference in metabolite intensity may thus be due to similar processes as in Spitsbergen, i.e. production of the metabolites by commensal photosynthetic organisms.

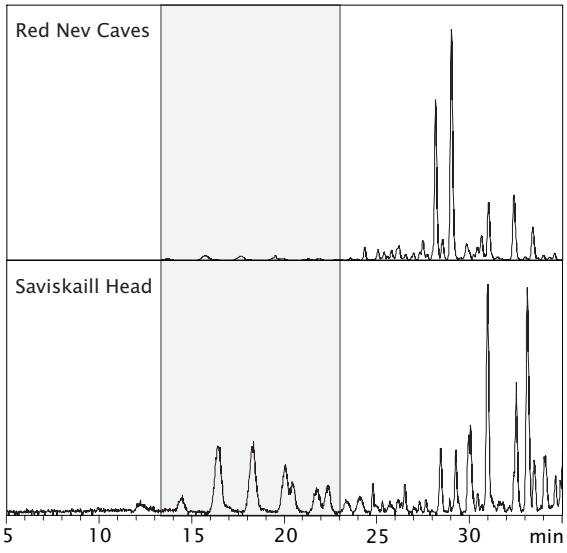

Figure 3.72 Comparison of base peak chromatograms ($m/z = 50 - 1000$) obtained from crude extracts of different *Haliclona* specimens collected around the Orkney Islands. The shaded area marks column-specific peaks. The analysis uses the same chromatographic gradient as for *H. viscosa* samples (Figure 3.17 and 3.69). Chromatograms are scaled to 100 % intensity of the highest peak each, observable by varying intensity of the column-specific peaks.

3.7 Alternative taxonomy

Several questions emerge from the results of the HPLC-HRMS screening:

1. Does a given sponge species always produce the same chemical compounds which can be used as a characteristic?
2. Are the compounds produced by the sponge itself or by associated bacteria?
3. If they are produced by associated bacteria, and if the bacteria are advected by the water currents drawn through the sponge body, would these compounds be found in other sponge species in the same habitat?
4. Does a given sponge species always contains the same bacteria composition which therefore can be used as an additional characteristic, or are bacteria ingested with food particles and thus strongly variable between different habitats?
5. Are there bacteria strains that are resident/invariable in a *Haliclona* species?
6. If bacteria are ingested would a similar bacteria composition be found in various *Haliclona* species that occupy the same habitat?

These questions cannot successfully be answered without trusted species identification. The few characteristics available for a taxonomic identification of *Haliclona viscosa* call for alternative methods to identify this sponge. For this purpose, several molecular biology and chemical taxonomy methods are available. Molecular biology offers the possibility to study the composition of associated bacteria or the sponge genome directly. Chemical taxonomy examines the compound composition produced by the sponge and/or the associated bacteria.

One of the most challenging tasks, before any further studies can be accomplished, is the sampling of the desired sponge. If the sponge is hard to identify by classical taxonomic methods, but possible to identify by its chemical fingerprint, there is large potential for a chemical "rapid test" that answers whether the desired sponge is found or not. After one season in Spitsbergen that did not yield any sponges that contained 3-APAs although they had been reported from the area earlier, a method was devised that allowed the quick, preliminary identification of 3-APA-containing individuals.

3.7.1 Thin layer chromatography

None of the *Haliclona*s obtained to-date from the Orkneys yielded 3-APAs. The absence of 3-APAs in Orkney samples, a result that transpired from examination of the sponges after return to the laboratory in Bremerhaven, was therefore not surprising. A preliminary study of each sponge's 3-APA content was deemed impossible during vessel-based expeditions since this requires the return to the sampling spot after a possible confirmation as well as the luck of finding the individual. Both requirements are not easily met considering the ships schedule and the dependence upon the weather and tides.

In contrast, the hard-substrate locations in the Kongsfjord are well known to the divers, less exposed to weather and tides, easily accessible and clearly arranged. Another advantage is the presence of a chemical lab at the research site in Ny-Ålesund. Reversed-phase thin layer chromatography (RP-TLC) was chosen for its speed, low requirements in chemical and technical equipment and low sponge crude extract consumption. On the RP-TLC plate, crude extracts were compared to a standard mixture of several synthetic cyclostellettamines and haliclamines (see Section 5).

By this method, one individual (identifier GS 09/23, Figure 3.73 no. 23) was identified in the 2009 samples that very likely contained 3-APAs as well as a number of unknown alkaloids. However, a second individual that was later shown to contain 3-APAs by HPLC experiments (identifier GS 09/27, Figure 3.73 no. 27) was not recognized. The reason for this may be a too-low crude extract application to the RP-TLC plate or the general low concentration and abundance of 3-APAs in that sponge.

3.7.2 Matrix assisted laser desorption/ionisation (MALDI)

The exact compound composition of a sponge can be a diagnostic feature in combination with classical taxonomic methods. However, the presence or absence of specific compounds alone should not decide over a species affiliation as long as the reason for presence or absence of compounds is not determined. Several chromatographic methods can be used to assign the chemical compounds of a sponge but the evaluation of classical chromatographic methods is rather time consuming. Next to these methods, a technique would be favorable that combines analytical

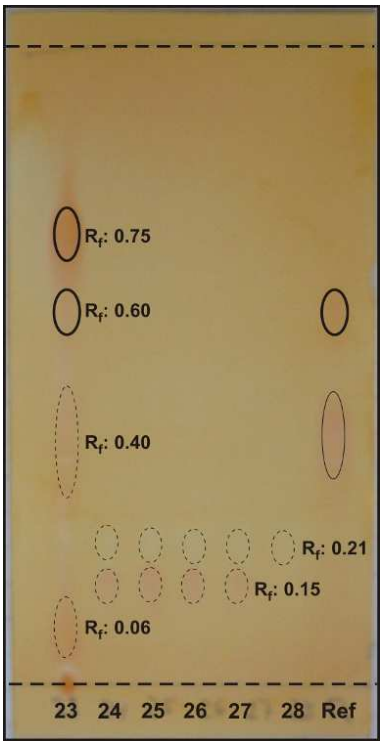

Figure 3.73 RP-TLC plate with crude extracts from various *Haliclona* individuals (no. 23-28) applied against a standard mixture (Ref) of cyclostellettamines and haliclamines.

precision and speed with a possibility to evaluate the results by a computerized algorithm which allows the high sample throughput and evaluation necessary to make a statement about ecological relevance of the findings. This possibility is given in a mass spectrometric analysis tool like MALDI mass spectrometry. MALDI-MS is a powerful method to analyze and characterize macromolecules like proteins[151], carbohydrates[152], oligonucleotides[153] and synthetic polymers.[154] It is also increasingly used to investigate bacteria with regard to their chemotaxonomy[155] and secondary metabolism.[156] For technical reasons however, MALDI-MS is not the method of choice for small molecules although a few reports exist (e.g. Grube et al.[157] and Cohen & Gusev, 2002[158]). In spite of that, MALDI-TOF-MS was applied to a subset of *Haliclona* crude extracts and yielded interesting results for the 3-alkyl pyridinium alkaloids.

The MALDI mass spectrum of the *Haliclona viscosa* sampled in 2003 shows two areas with numerous compound masses between $m/z = 420 - 500$ and $m/z = 640 - 740$ (Figure 3.74). The mass range at $m/z = 420 - 500$ correlates to haliclamines and cyclostellettamines, and a closer look into the mass pattern shows that the mass peaks are by 2 mass units apart (Figure 3.75). The clusters inside the mass range $m/z = 420 - 500$ have a mass difference of $m/z = 14$. This agrees with

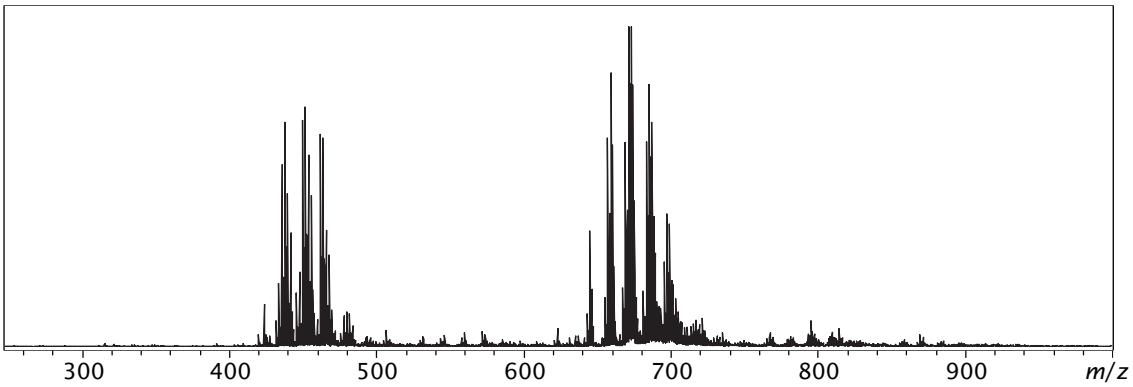

Figure 3.74 Typical MALDI-TOF-MS spectrum of a *Haliclona viscosa* specimen. The spectrum is uncalibrated.

the results obtained from HPLC-HRMS analysis where many compounds differ by the length of the alkyl chain ($m/z = 14$) and the number of double bonds ($m/z = 2$) but many more compound masses are visible in MALDI-MS than have been identified (including the identification suggestions in Section 3.3) by standard LC-MS techniques.

Although the observed masses in MALDI-MS correspond to computed masses of different cyclostellettamines and dehydro-cyclostellettamines, only cyclostellettamine C (**33**) was identified in *H. viscosa* crude extracts by LC-MS methods. However, the possibility is given that various cyclostellettamines cannot be identified by chromatographic methods due to their low concentration in the crude extract. The possibilities of LC-(ESI)-MS of assigning chain lengths and double bonds as well as compound abundance are not met by MALDI-MS which suggests that both methods should be used in parallel.

The masses at $m/z = 640 - 740$ are unexplained yet. A speculation is that they constitute salts of the haliclamines and cyclostellettamines. The mass difference between the first and the second mass range of approximately $m/z = 222$ points to the second mass range showing double TFA salts (M=114), but a reaction of the compounds with α-cyano-4-hydroxy cinnamic acid (HCCA, M=189) is also possible although the mass difference does not fit very well. Both counterions, TFA and HCCA are introduced into the sample as contents of the MALDI matrix solution. On the other hand MALDI-MS constitutes an analysis method that mirrors very closely the natural state of the sample since extensitve sample processing does not occur. In this manner, the natural counterions of the 3-APAs may be analyzed

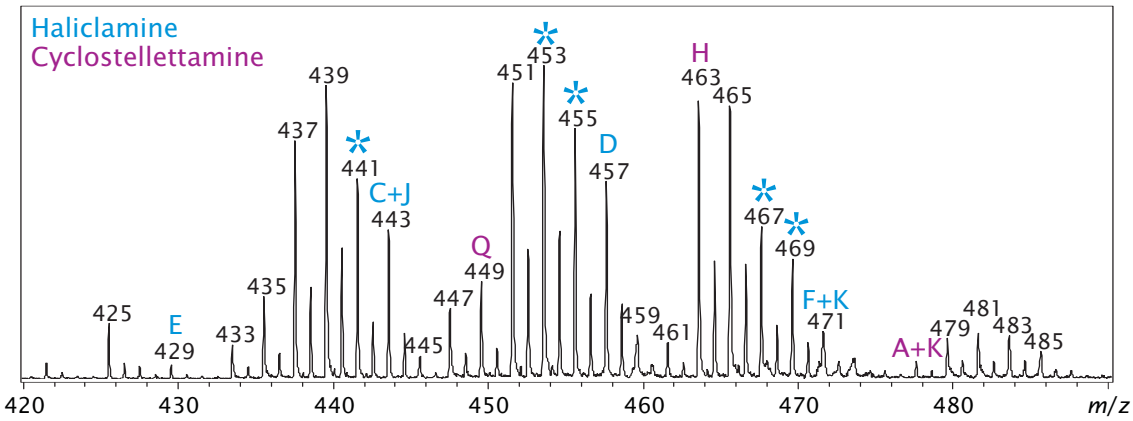

Figure 3.75 Detail of a typical MALDI-TOF-MS spectrum (Figure 3.74) of a *Haliclona viscosa* specimen. Known haliclamines and suggested cyclostellettamines are marked by the appropriate letter of their trivial names. Masses of compounds proposed in section 3.3 are marked with an asterisk. The spectrum is uncalibrated.

in the MALDI mass spectrum but it is uncertain whether the mass difference of $m/z = 222$ reflects a natural counterion or an artefact introduced during sample preparation.

Compound peaks for the monomeric 3-APAs, viscosalines and viscosamines are missing in the spectrum. This is due to the variation in compound class already observed in LC-MS analysis. For the MALDI-MS examination, the 2003 sample had to be chosen because it required raw material (dried sponge powder) which was no longer available for the samples of 1999, 2000 and 2001. The 2009 sample has not been examined, yet, but is expected to show similar results as the 2003 sample since 3-alkyl pyridinium alkaloids are absent in that sample as well. The usability of formerly prepared and dried crude extracts will have to be tested in the future.

Another interesting feature is that all compound masses detected in the MALDI-MS spectrum of *H. viscosa* are singly charged masses. In HPLC-ESI-MS, the singly charged molecular ions show very low intensity while doubly and triply charged masses prevail. This is a direct effect of the different ionization methods used for the analysis; ESI supports the formation of multiply charged ions, especially during LC-(ESI)-MS where chromatography provides a constant excess of acid. Although MALDI also enhances multiple charges, the effect seen here may be due to an early fragmentation happening in the haliclamines, e.g. due to the laser impact. By this, a doubly charged haliclamine might lose a charge without change in mass (e.g. by

a retro-Diels-Alder reaction) and may thus be seen only as a singly charged ion (Figure 3.76).

The mass peak intensities observed in MALDI-MS cannot be due to relative compound quantities in the crude extract; according to HPLC-MS analyses which give a much more accurate picture about relative abundances of different compounds, haliclamines C (**27**) and D (**28**) constitute the major metabolites in the examined *H. viscosa* individual (see Figure 3.69A-2003). However, the corresponding masses for **27** and **28**, $m/z = 443$ and $m/z = 457$, respectively, are not the highest mass peaks. Instead, the compound masses that, in theory, offer several structural possibilities (constitutional isomers) have higher mass abundance. For example, $m/z = 439$ may be a haliclamine C (**27**) or J (**61**) with two double bonds. This leaves five possibilities for chain length and double bond variation; haliclamine 9/11 (1/1), haliclamine 9/11 (2/0), haliclamine 9/11 (0/2), haliclamine 10/10 (1/1) and haliclamine 10/10 (0/2). All of them are supposable to occur in *H. viscosa*, as is suggested by the number of new structures proposed in part 3.3. The much lower $m/z = 441$ is occupied only by haliclamine C (**27**) and J (**61**), which supports this hypothesis.

On the other hand, the MALDI spectrum shows the mass equivalent of compounds that have not yet been identified as natural products from the sponge but are known as synthetic products. An example of this is cyclostellettamine Q at $m/z = 449$ that contains a C_{10} and a C_{11} alkyl chain. Cyclostellettamine Q is the pyridinium analogue of haliclamine D (**28**).

The other *Haliclona* groups sampled in the Kongsfjord and the Orkneys do not show a distinctive peak pattern (Figure 3.77). On one hand this is consistent with the results obtained during LC-MS analyses (Section 3.6), with low general abundance of secondary metabolites and strong variation in the visible peaks. On the other hand, the spectra do not show the, although small, similarities observed between the different *Haliclona* groups in chromatographic analyses. The peak pattern (Figure

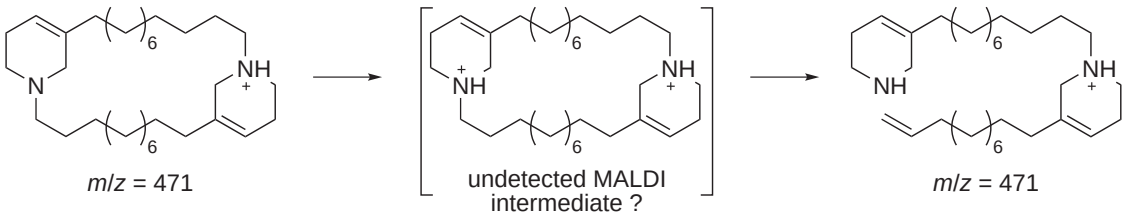

Figure 3.76 Proposed fragmentation of haliclamine F (**30**) in MALDI-MS

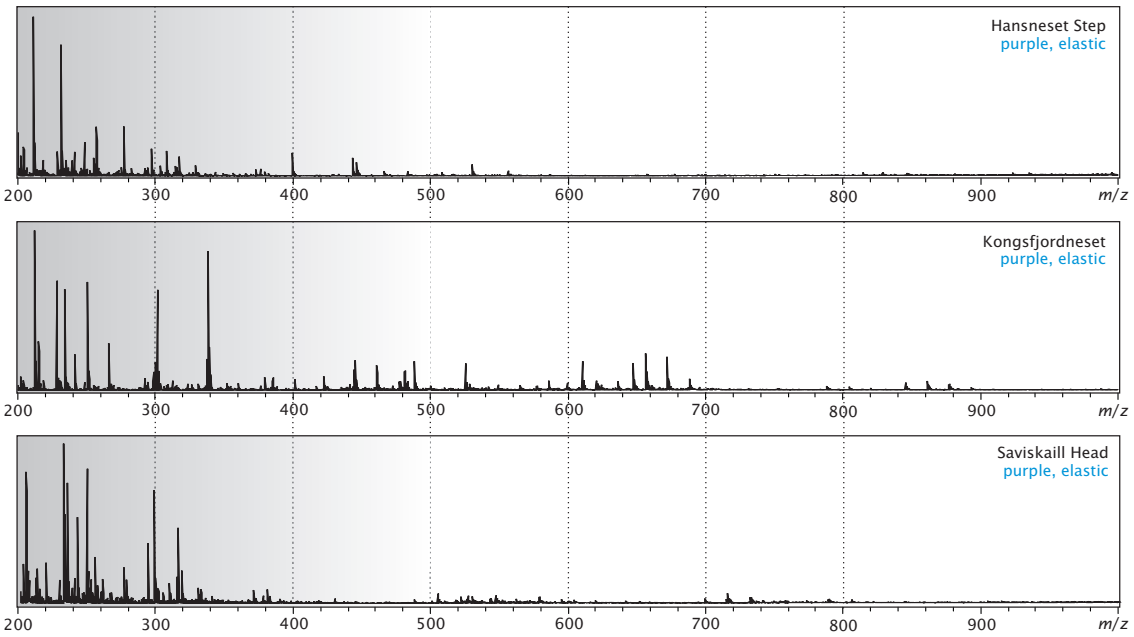

Figure 3.77 Comparison of MALDI-TOF-MS spectra obtained from analysis of the crude extract of purple, elastic *Haliclona* sponges from different sampling sites. The area shaded in grey can show unspecific matrix peaks and should be evaluated cautiously for species specific compounds. Dotted lines are inserted for orientation.

3.77-3.79) varies strongly even within the samples of one group (not shown). The method is not established enough to allow a clear statement about the visible peaks being matrix peaks, impurities from sample preparation or true species specific metabolites that change between organisms due to intra- or interspecific variation.

These results are elusive and not easily compatible with the informative results obtained for *Haliclona viscosa*. MALDI-MS poses several challenges for taxonomic applicability. One is the right choice of matrix as matrix peaks can overlie or congest with species specific analyte peaks. Another one is the use of laser energy that can easily lead to compound fragmentation. The distribution of the analytes inside the sample spot is a third challenge that can give a false picture on the compounds contained in a sample. Adduct ions of Na^+ and K^+ frequently occur in MALDI-MS, possibly enlarge the number of compound peaks and thus hinder the evaluation of complex compound mixtures. In addition, crude extracts are usually a blend of various compound classes with a large number of unknown compounds. Methods used in classical chromatographic analyses like derivatisation of specific compound classes cannot be used in complex mixtures of unknown compounds as it would lead to unpredictable products. In addition, the compound concentration is highly

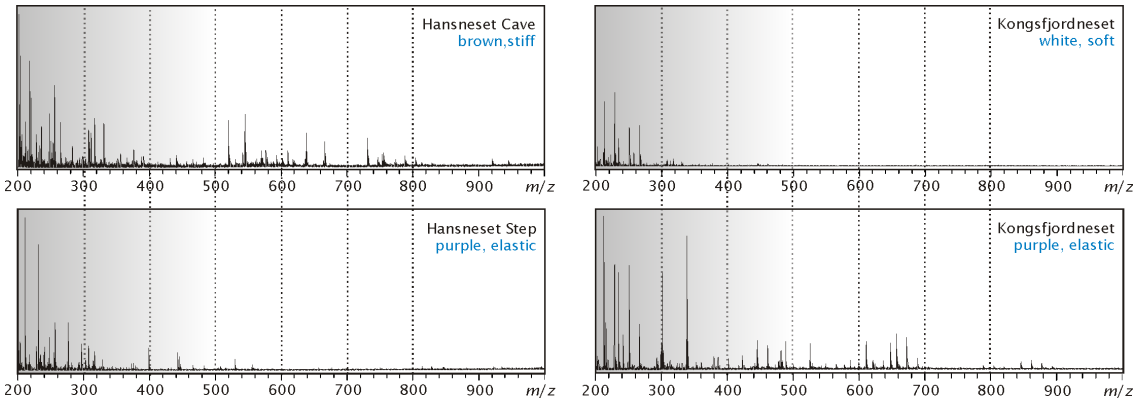

Figure 3.78 Comparison of MALDI-TOF-MS spectra obtained from analysis of the crude extract of different *Haliclona* groups obtained from different sampling sites in Spitsbergen. The area shaded in grey can show unspecific matrix peaks and should be evaluated cautiously for species specific compounds. Dotted lines are inserted for orientation.

inhomogeneous between species or even between individuals of one species. Therefore it is difficult to judge the amount of crude extract needed for each analysis. A mechanism similar to the matrix suppression effect (MSE),[159–161] where an excess of analyte is used to suppress matrix peaks, can be active in samples with one or few highly concentrated and a number of lower-concentrated metabolites. The so-called analyte suppression effect (ASE) induces suppression of lower-concentrated analytes. Since the minor metabolites often decide over a species affiliation, MALDI-MS would be unserviceable if these difficulties cannot be overcome.

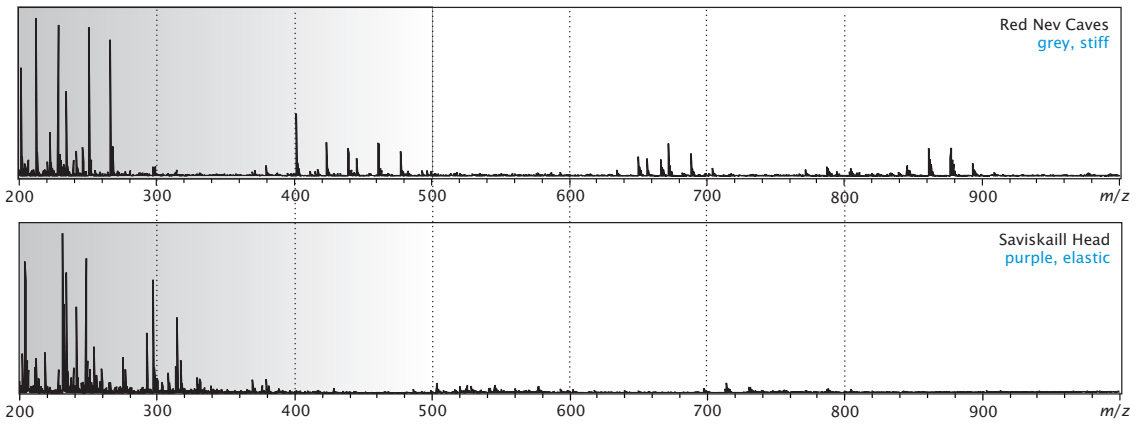

Figure 3.79 Comparison of MALDI-TOF-MS spectra obtained from analysis of the crude extract of two *Haliclona* groups from the Orkneys. The area shaded in grey can show unspecific matrix peaks and should be evaluated cautiously for species specific compounds. Dotted lines are inserted for orientation.

To address the uncertainties, a study is in progress that examines the potential of MALDI-TOF-MS to analyze small compounds directly in the crude extract of sponges (manuscript in preparation). To achieve this, thirteen species from eleven genera, all members of the class Demospongiae, are subject to a compound screening and comparison with standard LC-MS methods. The focus is laid on the possibilities of identifying known compounds with a single sample processing method that was uniformly applied to all species without species- or compound-specific method optimization, a prerequisite for a fast, universal screening and dereplication procedure. The results of this analysis are still under evaluation and therefore not described here, but despite contradicting arguments, MALDI seems a promising technique to achieve a first insight into sponge secondary metabolites. However, in species that show low general abundance in secondary metabolites like the majority of *Haliclona* specimens obtained from Spitsbergen and the Orkneys to-date, chemical methods have a poor potential in being a useful tool in taxonomy. In such cases, phylogenetic methods may be more beneficial.

3.7.3 Molecular phylogenetics

Since the genome of a species is also rather variable, conserved genome sequences must be used. Therefore, the genome of a set of *Haliclona* sponges sampled in the Kongsfjord in 2008 and 2009 is currently under investigation by a cooperation with the Bininda-Emonds working group at the University of Oldenburg. The subject of the study, as in most projects involved in the so-called "Barcoding Project", is the CO1 gene[15] on the mitochondrial DNA which has a length of 648 base pairs and is prone to very little variation (approximately 2% in organisms inside a species). This is due to the mitochondria (and thus mitochondrial DNA) being inherited only from the mother, while cell nucleus DNA in animals is inherited from both, mother and father. On the other hand, mitochondrial DNA has a relatively fast mutation rate, which results in significant variation in its DNA sequences between species (5% total or 10% of intraspecific variation[162]). This is a relevant criterion for the method to allow a statement as to whether two organisms should be grouped or belong to different species. The method can not be used to identify the species directly as

15 Mitochondrial Cytochrome *C* Oxidase subunit-1 gene.

too few sponge specific entries exist in the barcoding database. Results from this investigation are expected soon.

A different molecular biology method uses the 18S ribosomal DNA (rDNA) gene to compare the relationship status of the sample with other samples deposited in a database. This study is performed in a collaboration between the Hentschel working group in Würzburg and the Köck group in Bremerhaven, by the student Laura Gallego.

The 18S (eukaryotes) or 16S (bacteria) gene is commonly used for the purpose of species identification and database entries exist for the gene sequences of a large number of known species. Basis for the study is a set of samples obtained from the Kongsfjord and from the Orkneys in 2008. In that year, however, no *Haliclona viscosa* was sampled in the Kongsfjord which limits the obtained results to the other three species found in the Kongsfjord.

The DNA in the samples is extracted, amplified, and cloned, then extracted again and sequenced. The sequences are compared to database entries. The isolation of DNA from a sponge is unspecific, i.e. all eukaryotic DNA is extracted. Therefore, the DNA of e.g. associated polychaetes, ingested dinoflagellates and neighboring sponges is extracted and amplified as well. All clones taken together are thus expected to reflect the complete organism association inside the sample. This is confirmed by the DNA database search for the three *Haliclona* groups in the Kongsfjord that returns hits of the dinoflagellate *Gymnodinium* sp. and the ciliates *Halteria grandinella* and *Metacylis angulata* for the Spitsbergen *Haliclona* species (Table 3.3). These organisms are probably prey items of the sponges.

When focussing on the clone sequences that contain sponges as hits, the study returns three possibilities for 18S rDNA clones obtained from the purple, elastic *Haliclona* sampled at Hansneset step (Spitsbergen): *Aplysina fistularis* (93% similarity), *Mycale fibrexilis* (100% similarity) and *Haliclona* sp. OGL2003 (97% similarity); the latter returns also for the brown, stiff *Haliclona* and for the white, soft *Haliclona* but with differing similarity values. *Aplysina fistularis* can be neglected as it is a Caribbean sponge. Also *Mycale fibrexilis* can probably be neglected as it is abundant on the East coast of the USA and therefore probably a warm water organism. However, *Mycale* sponges are also present in the Kongsfjord area and can have been sampled as a neighboring organism. For *M. fibrexilis*, a barcode sequence is available; therefore, the barcode project at the University of Oldenburg may clarify these results.

Table 3.3 Results from 18S rDNA sequencing of *Haliclona* samples.

Origin	Clone	Best hit	Length	Simil.	Identity	Class
BS/HNC	1	*Gymnodinium* sp. 7-15 ITS1 clone 7-15	603 bp	87%	484/556	Dinophyceae
	2	*Gymnodinium* sp. 7-15 ITS1 clone 7-15	603 bp	86%	549/634	Dinophyceae
	5	*Haliclona* sp. OGL2003	2624 bp	97%	39/40	Demospongiae
		Amphimedon queenslandica	4101 bp	96%	155/161	Demospongiae
	8	*Halteria grandinella*	3621 bp	84%	620/734	Ciliophora
PE/HNS	1	*Metacylis angulata* clone Meta00-8	486 bp	95%	394/413	Ciliophora
	14	*Aplysina fistularis*	878 bp	93%	832/887	Demospongiae
	18	*Mycale fibrexilis*	2499 bp	100%	159/159	Demospongiae
	20	*Haliclona* sp. OGL2003	2624 bp	97%	39/40	Demospongiae
WS/KFN	1	*Haliclona* sp. OGL2003	2624 bp	99%	162/163	Demospongiae
		Haliclona amphioxa isolate BDA2	2715 bp	96%	162/168	Demospongiae
	2	*Gymnodinium aureolum* strain SWA 16	3423 bp	89%	260/292	Dinophyceae
PE/RN	1	*Hymeniacidon heliophila*	964 bp	83%	670/800	Demospongiae
		Halichondria panicea	1104 bp	98%	360/364	Demospongiae
	2	*Microciona prolifera*	2457 bp	91%	162/189	Demospongiae
PE/SH	1	*Microciona prolifera*	2457 bp	85%	162/189	Demospongiae
	2	*Hymeniacidon heliophila*	964 bp	83%	670/798	Demospongiae
		Halichondria panicea	1104 bp	99%	361/364	Demospongiae

Simil. = Similarity; bp = base pairs. Sponge groups: BS = brown, stiff;, PE = purple, elastic; WS = white, soft. Origin: HNC = Hansneset Cave; HNS = Hansneset Step; KFN = Kongsfjordneset; RN = Red Nev; SH = Saviskaill Head.

The *Haliclona* sp. OGL2003 hit is considered the closest candidate hit since it returns for all three Spitsbergen *Haliclona* groups. The original *Haliclona* sp. OGL2003 has been sampled on the coast of Massachusetts (USA),[163] i.e. an area influenced by cold Arctic Water (ArW) transported south by the East Greenland Current (EGC). However, the hit returning for all three Spitsbergen *Haliclona* groups does not necessarily indicate that all three samples are the same as the *Haliclona* sp. OGL2003, nor that all three groups belong to one species. Rather, it indicates that the three groups are closely related to *Haliclona* sp. OGL2003.

While the purple, elastic and the brown, stiff sponge have the same similarity values with *Haliclona* sp. OGL2003 (39/40 base pairs in a 2624 base pair long gene fragment, i.e. 97% similarity), the white, soft *Haliclona* has a much better fit of 162/163 base pairs (99% similarity). This suggests that the white, soft *Haliclona* is different from the other two and that possibly the other two belong in one group.

Between the *Haliclona* sponges sampled at two different sites at the Orkneys, the study returns identical results. Both specimen show similarity with *Halichondria panicea*, the bread crumb sponge (98% similarity for the Red Nev sample and 99% similarity for the Saviskaill Head sample). Both of them also show similarity with a *Microciona prolifera* sampled in Massachusetts (91% similarity of the Red Nev sample and 85% similarity for the Saviskaill Head sponge). *Microciona prolifera* (=*Clathria prolifera*), the red beard sponge, is common in the North-West Atlantic

but its morphology is so different from the sampled organisms that this hit can be neglected. However, the suggestion that the sampled sponges should be considered as a *Halichondria panicea* cannot be easily neglected. *Halichondria panicea* is a very variable sponge both in morphology and color, but it possesses an ectosome which was not found in the two samples and its spicules are larger than the ones found in the samples. However, the spicule size in *H. panicea* is very variable, between 100 and 480 µm, which would fit into the results obtained for the two specimens. Therefore, the possibility of the sponges being *Halichondria panicea* specimens cannot be completely dismissed, but the result also suggests that both sponge samples should be grouped.

3.7.4 Associated bacteria

Laura Gallego also studied the question of bacterial community composition in the *Haliclona* sponges sampled at different sampling sites and to what extend a grouping of the individuals following classical taxonomic methods is reasonable (manuscript in preparation [164]).

Sequence variations between different microbial species' DNA result in different fragmentation ("denaturation") properties of DNA molecules. According to the content and distribution of guanidine and cytosine inside the DNA fragments, the molecules will form specific bands when separated in an electrostatic field that is applied to a molecular sieve gel during denaturing gradient gel electrophoresis (DGGE). The bands can be used to visualize variations in microbial genetic diversity and provide a rough estimate of the richness and abundance of predominant microbial community members.

When looking at the DNA banding pattern of the bacterial community in the *Haliclona* sponges it is clear that the Spitsbergen sponges have a rather homogeneous bacterial community while the Orkney sponges conform to a large extend but also show additional bacteria varieties. A Quality-One (Q-One) analysis of DGGE bands obtained from amplification and separation of different DNA fragments groups the purple, elastic (Hansneset step) and the brown, stiff sponge (Hansneset cave) closely together. This is not surprising as they were sampled from geographically proximal sites. The similarity in the secondary metabolite composition of the two sponges is also observed in LC-MS analyses (Figure 3.71). The area is influenced by the same water mass, therefore advected bacteria are expected to be present

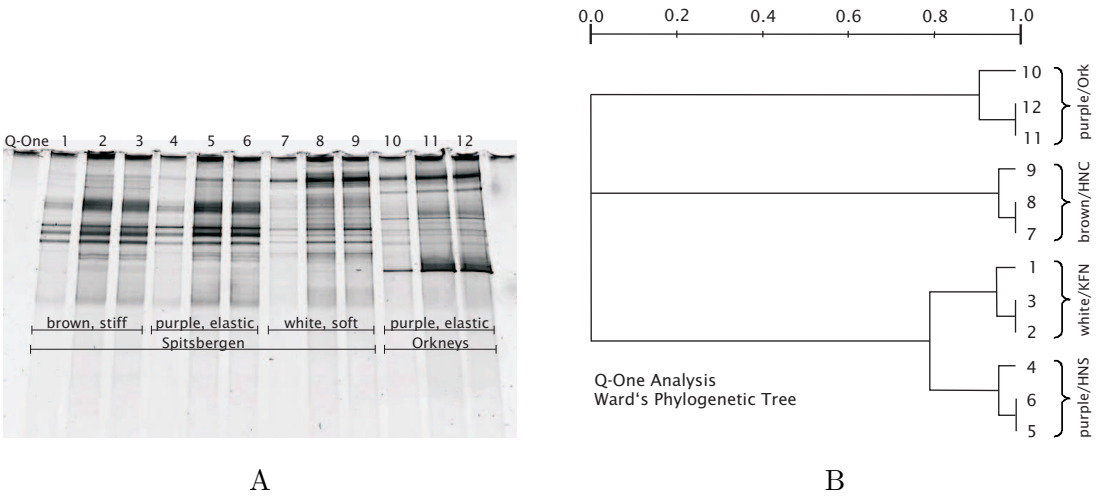

A B

Figure 3.80 DGGE gel (A) and Q-One Analysis on the distribution of the bacterial communities (B) present in different *Haliclona* sponges sampled in Spitsbergen and the Orkneys. Data shown by courtesy of L. Gallego.

in both sponges. The white, soft *Haliclona* sampled at Kongsfjordneset[16] differs from the two. Still more distant is the purple, elastic *Haliclona* sampled in the Orkneys (Figure 3.80). As the Orkneys in general are influenced by a similar water mass ("Gulf Stream") but are characterized by strongly diverging environmental conditions otherwise (especially temperature), the separation of Orkney samples from Spitsbergen samples fits in the picture.

A comparison between the purple, elastic *Haliclona* at Hansneset, Kongsfjordneset and the Orkneys with a white, soft *Haliclona* from Kongsfjordneset shows that both the white and the purple sponge at Kongsfjordneset contain a bacteria composition that is more similar to the Orkneys than to Hansneset (Figure 3.81). The secondary metabolite similarity between the purple, elastic *Haliclona* at Kongsfjordneset and the white, soft *Haliclona* from the same area is also found in LC-MS experiments (Figure 3.71). Although the secondary metabolites are different in intensity, the compound pattern between the two sponges is similar. This acknowledges the importance of advection processes and uptake by filtration in contrast to resident and inherited bacteria. The Kongsfjordneset and Orkney environment are similar in being oceanic environments while the Hansneset area is a coastal environment influenced by high sediment loads. The *Haliclona* samples from Red Nev (Orkneys)

16 In 2008, no white, soft sponges were found in Hansneset.

also group closely together, but away from the oceanic Kongsfjordneset (Spitsbergen) and Saviskaill Head (Orkneys) as well as the coastal Spitsbergen samples. This suggests an adaption of the bacterial community to the cave habitat. In general, the two Red Nev samples show very few bands in the DGGE gel which indicates little diversity in the bacterial community (Figure 3.81)

Another question addressed by the analysis is whether it is possible to group the sampled organisms at a given sampling site by morphological characters and color. The DGGE results show very similar banding patterns for different individuals of a sponge group sampled at one site and thus supports the approach to group the individuals (Figure 3.82 and 3.83).

Sequencing of the bacterial DNA yielded that the purple, elastic *Haliclona* from the Orkneys contains β- and γ-Proteobacteria and Bacteria while the purple, elastic *Haliclona* from Hansneset is similar but does not contain the β-Proteobacteria. In the Hansneset specimen, four out of ten examined clones identify as Arctic surface sediment associated clones and one as a surface seawater associated clone. The other five are uncultured bacteria clones. The association with sediment bacteria fits well into the general discription of the Hansneset environment which is influenced by turbid waters that result from river runoff and melting glacial ice.

Five out of ten clones obtained from the Orkney sample associated bacteria identify as *Haliclona simulans* associated clones, two are a "marine sponge associated

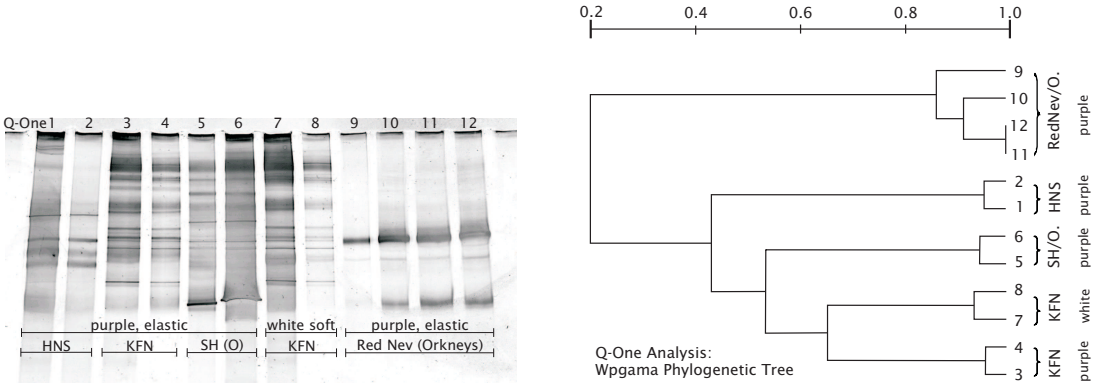

A B

Figure 3.81 DGGE gel (A) and Q-One Analysis on the distribution of the bacterial communities (B) present in different *Haliclona* sponges sampled in Spitsbergen (HNS = Hansneset step, KFN = Kongsfjordneset) and the Orkneys (SH/O =Saviskaill Head, Orkneys). Data shown by courtesy of L. Gallego.

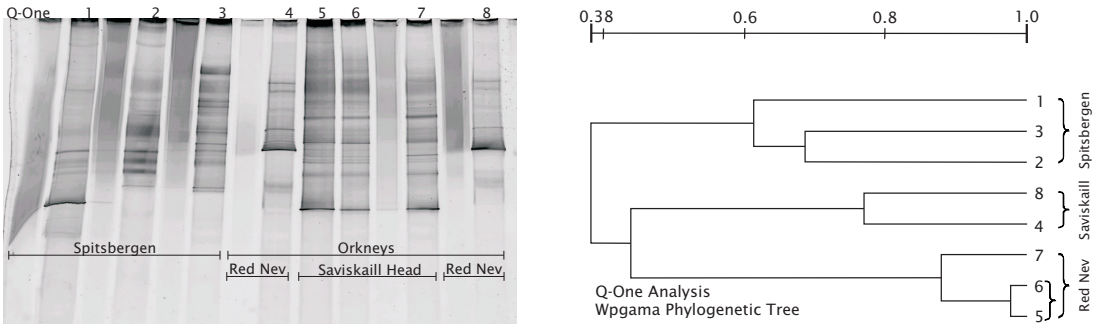

A B

Figure 3.82 DGGE gel (A) and Q-One Analysis on the distribution of the bacterial community (B) present in several organisms of the purple, elastic *Haliclona* sampled in Spitsbergen or the Orkneys (Saviskaill Head vs. Red Nev). Data shown by courtesy of L. Gallego.

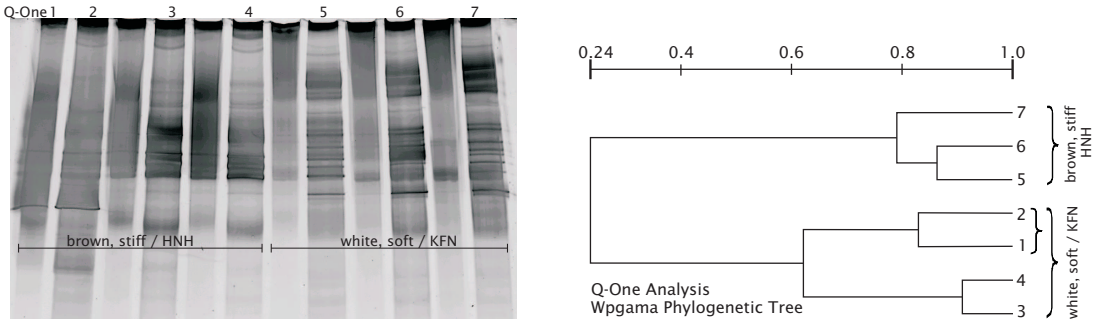

A B

Figure 3.83 DGGE gel (A) and Q-One Analysis on distribution of the bacterial community (B) present in several organisms of the white soft *Haliclona* sampled at Kongsfjordneset (KFN) and the brown, stiff *Haliclona* sampled in the cave at Hansneset (HNC). The study was performed for the chemical similarity of the two sponge groups, disregarding the color. Data shown by courtesy of L. Gallego.

Spongibacter nickelotolerans"; another two are an *Emiliania huxleyi* chloroplast strain and therefore probably prey-derived and the last two are an Arctic surface sediment associated clone and an uncultured bacterium.

The association of the purple, elastic *Haliclona* from the Orkneys with *Haliclona simulans* associated clones suggests that the sampled sponge is a *H. simulans*. *Haliclona simulans* does indeed show very variable growth forms and can grow in thin cushions but is usually an erect growing, branching sponge. A picture in the Encyclopedia of Marine Life[165] shows a purple cushion-like sponge that looks similar to the sampled sponges. However, the taxonomic sponge description does not fit,

especially as the sponge is described as hard and brittle. Thus, the *H. simulans* associated clone may not be confined to *H. simulans* but also be present in other sponges.

The brown, stiff *Haliclona* found in Hansneset cave associates with Bacteria and α- and γ-Proteobacteria. Two out of nine are Arctic surface sediment associated clones, four are uncultured bacteria, one is an *Axinella corrugata* associated α-Proteobacterium, one is a gill symbiont (γ-Proteobacterium) of the vent mussel *Bathymodiolus puteoserpentis* that lives around hydrothermal vents in the Atlantic ocean and one is a Lake Mackenzie (Texas) water associated clone.

The white, soft *Haliclona* from Kongsfjordneset also associates with the Lake Mackenzie clone as well as clones found in Arctic, Antarctic and Spitsbergen seawater. Two are uncultured bacteria and one is a *Tethya aurantium* associated clone. The absence of sediment associated clones in this sponge confirms that the habitat is much more influenced by oceanic water than the coastal site Hansneset Step.

Conclusion

The differences in bacterial communities between purple, elastic *Haliclonas* sampled at different sites in the same fjord shows that bacterial communities should carefully be consulted for taxonomic identification. As in the example of the *Haliclona simulans* associated clone, the possibility of the same bacteria being present in related sponge species should always be considered. Several bacteria species seem to be ubiquitously present, even if they are mainly found in a specific sample; this is the case in the gill symbiont of a hydrothermal vent mussel which lives in a significantly different environment than the sampled sponge; another example is the Lake Mackenzie (Texas) water clone that usually lives in fresh water in a warm environment but is found in a marine Arctic sponge. However, the finding of the bacteria's DNA inside the sponge does not allow inference about the viability of the bacterium.

The study of the direct phylogenetic relationships of the sponge samples in the Kongsfjord and from around the Orkneys suggests that two hitherto separated groups should be united to form one group; the purple, elastic sponge should be joined with the brown stiff *Haliclona* and the Saviskaill Head sample should be united with the Red Nev cave sample. The latter is also proposed by the results

of classical taxonomic identification. The identity of the sponges is, however, still unknown.

4
Stylissa caribica

Stylissa caribica is a sponge that belongs to the order Halichondrida, family Dictyonellidae, and was first described in 1998. It is the only *Stylissa* species known from the Caribbean,[1] while another three species, *Stylissa massa*, *S. flabelliformis*, and *S. variabilis*, share a habitat in the Indo-west Pacific region. A fourth species known as *Acanthella* or *Axinella carteri*, also occurs in the Pacific and was re-classified to the genus *Stylissa*.[78] *Stylissa caribica* is subject to natural products research since 2001 and proves to be a rich source of pyrrole-imidazole alkaloids,[167,168] which are currently the object of a different PhD thesis. In addition to various pyrrole-imidazole alkaloids, Achim Grube isolated four compounds from a different compound class during the course of his study of *S. caribica*.[168] They are cyclic peptides and were conjointly identified.[169]

Stylissa caribica. Picture taken by G. Schmidt

Cyclic peptides are reported regularly from different bacteria, funghi, plants and animals. The most well-known is probably cyclosporine A (**84**), an undecapeptide produced by the fungus *Trichoderma polysporum*.[2] In general, cyclic peptides differ

1 *S. caribica* was claimed to be the same species as *Teichaxinella morchella* Wiedenmayer, 1977 [166] which was recently reclassified to *Axinella corrugata* but confirmation/rejection by taxonomists is missing.[78]

2 The fungus was reclassified to *Tolypocladium inflatum*. Later, several other fungi species were also found to produce cyclosporine A.

widely in peptide chain length and amino acid composition but common to most of them is their bioactive potential that would make them an interesting object for pharmaceutical use.

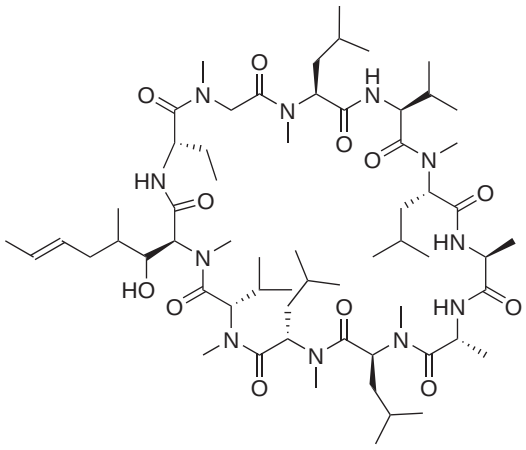

Cyclosporine A (**84**)

Cyclic peptides are characterized by their exceptional stability compared to linear peptides of the same sequence and chain length. They are much more stable towards heating and extreme pH and without a beginning or an end they are not targeted by proteolytic enzymes. The ends of linear peptides are often flexible and ill-defined, in contrast to their highly structured interior. This flexibility is bad from an entropic perspective when proteins bind to their molecular receptors, leading to reduced binding affinity and biological activity.[170] The resistance to protease digestion and improved thermodynamic stability of cyclic peptides can improve the biological activity of a peptide *in vivo*.[171] This is exemplified by the loss of hemolytic activity in the linear analogue of the cyclic peptide kalata B1.[172,173]

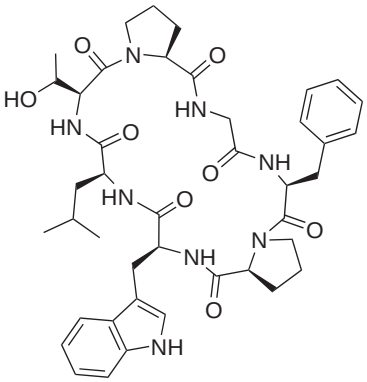

Phakellistatin 13 (**85**)

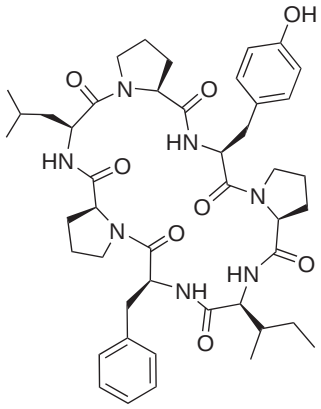

Stylisin 1 (**86**)

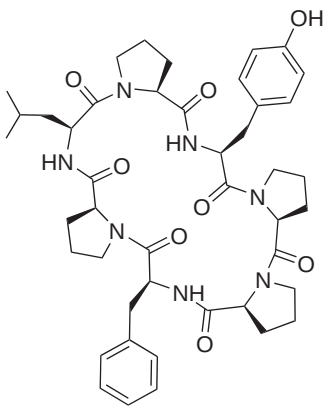

Stylisin 2 (**87**)

Cyclic peptides are not uncommon in sponges. Table 4.1 represents a selection of heptapeptides isolated from Halichondrida sponges. From *Stylissa caribica*, nine heptapeptides were reported so far, phakellistatin 13 (**85**), stylisins 1 (**86**) and 2 (**87**),[196] and the stylissamides A–F (**88**–**93**)[169,197], while there are no reports of

Table 4.1 Cyclic heptapeptides isolated from different sponges of the order Haplosclerida, class Demospongiae.

Compound name[a]	Sequence (*cyclo*-)[b]	isolated from[c]	Reference
Axinastatin 1	Pro-Phe-Val-Val-Pro-Val-Asn	*Axinella* sp.	[174,175]
Axinastatin 2	Pro-Phe-Val-Leu-Pro-Val-Asn	*Axinella* sp.	[176,177]
Axinastatin 3	Pro-Phe-Ile-Leu-Pro-Val-Asn	*Axinella* sp.	[176,177]
Axinastatin 4	Pro-Leu-Trp-Val-Pro-Leu-Thr	*Axinella carteri*	[177]
Axinellin A	Pro-Phe-Thr-Ile-Phe-Pro-Asn	*Axinella carteri*	[178]
Euryjanicin A	Pro-Ile-Ser-Phe-Val-Pro-Trp	*Prosuberites laughlini*	[179]
Euryjanicin B	Pro-Phe-Val-Pro-Pro-Ala-Thr	*Prosuberites laughlini*	[180]
Euryjanicin C	Pro-Ile-Ser-Ile-Pro-Leu-Phe	*Prosuberites laughlini*	[180]
Euryjanicin D	Pro-Ile-Phe-Ser-Pro-Ile-Phe	*Prosuberites laughlini*	[180]
Hymenamide A	Pro-Pro-Val-Pro-Phe-Trp-Arg	*Hymeniacidon* sp.	[181]
Hymenamide B	Pro-Pro-Asn-Phe-Val-Glu-Phe	*Hymeniacidon* sp.	[181]
Hymenamide C	Pro-Phe-Gly-Pro-Glu-Leu-Trp	*Axinella carteri*	[182]
Hymenamide D	Pro-Tyr-Asp-Pro-Leu-Ala-Ile	*Hymeniacidon* sp.	[183]
Hymenamide E	Pro-Thr-Thr-Pro-Tyr-Phe-Phe	*Hymeniacidon* sp.	[183]
Hymenamide F	Pro-Pro-Ala-Val-Met-Leu-Arg	*Hymeniacidon* sp.	[184]
Malaysiatin	Pro-Pro-Phe-Val-Val-Val-Asn	*Pseudoaxinyssa* sp.	[185]
Phakellistatin 1	cPro-Ile-cPro-Tyr-cPro-Phe-Ile	*Phakellia costata*	[186,187]
Phakellistatin 2	cPro-Tyr-cPro-Phe-cPro-Ile-Ile	*Stylotella aurantium* *Phakellia carteri* *Stylotella aurantium*	[175,188–190]
Phakellistatin 4	Pro-Thr-Pro-Phe-Ile-Phe-Ser	*Phakellia costata*	[188]
Phakellistatin 5	Pro-Phe-Asn-Ala-Met-Ala-Ile	*Phakellia costata*	[191,192]
Phakellistatin 6	Pro-Ile-Pro-Phe-Pro-Trp-Leu	*Phakellia costata*	[193]
Phakellistatin 13 (**85**)	Pro-Gly-Phe-Pro-Trp-Leu-Thr	*Phakellia fusca* *Stylissa caribica*	[194]
Pseudoaxinellin 1	Pro-Val-Asn-Pro-Phe-Val-Val	*Pseudoaxinella massa*	[195]
Stylisin 1 (**86**)	Pro-Leu-Pro-Tyr-Pro-Ile-Phe	*Stylissa caribica*	[196]
Stylisin 2 (**87**)	Pro-Ile-Pro-Tyr-Pro-Pro-Phe	*Stylissa caribica*	[196]
Stylissamide A (**88**)	tPro-Tyr-Lys-tPro-cPro-Val-Tyr	*Stylissa caribica*	[169]
Stylissamide B (**89**)	cPro-Phe-cPro-tPro-cPro-Ile-Tyr	*Stylissa caribica*	[169]
Stylissamide C (**90**)	cPro-Tyr-cPro-Phe-cPro-Phe-Ile	*Stylissa caribica*	[169]
Stylissamide D (**91**)	cPro-Tyr-cPro-Leu-cPro-Phe-Ile	*Stylissa caribica*	[169]
Stylissamide E (**92**)	cPro-Tyr-tPro-Ala-Ile-Gln-Ile	*Stylissa caribica*	[197]
Stylissamide F (**93**)	tPro-cPro-Phe-Asp-tPro-Arg-Phe	*Stylissa caribica*	[197]
Stylostatin 1	Pro-Phe-Asn-Ser-Leu-Ala-Ile	*Stylotella aurantium*	[198]
Stylopeptide 1	Pro-Ile-Pro-Leu-Ile-Phe-Ser	*Stylotella aurantium*	[199]
Wainunuamide	tPro-His-tPro-cPro-Gly-Leu-Phe	*Stylotella aurantium*	[200]

[a] Only heptapeptides are mentioned that contain proteinogenic amino acids.
[b] cPro = *cis*-proline, tPro = *trans*-proline, Pro = proline with undetermined configuration.
[c] Species names are given as mentioned in the original publication and may have change since.

cyclic peptides from other *Stylissa* species. However, if the taxonomic reclassification of *Axinella carteri* to the genus *Stylissa* proves to be valid, then three (possibly six) heptapeptides must be considered present in *Stylissa* from the Pacific ocean: axinastatin 4, axinellin A and hymenamide C (as well as axinastatins 1-3 if *Axinella* sp. was also a *Stylissa* sp.).

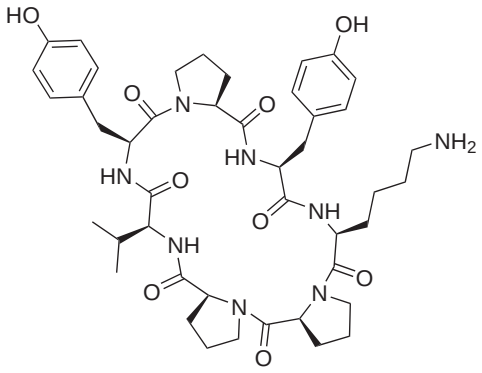

Stylissamide A (**88**)

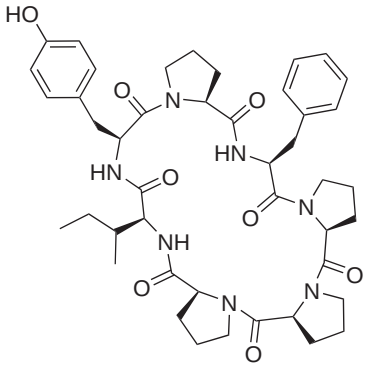

B (**89**)

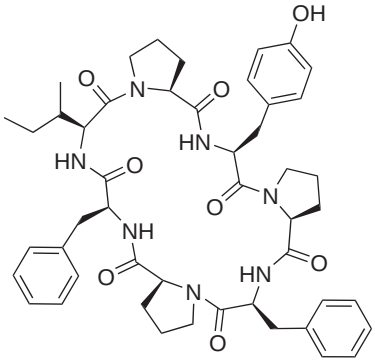

C (**90**)

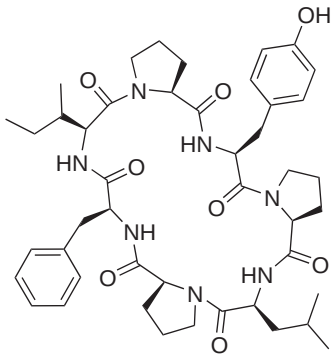

D (**91**)

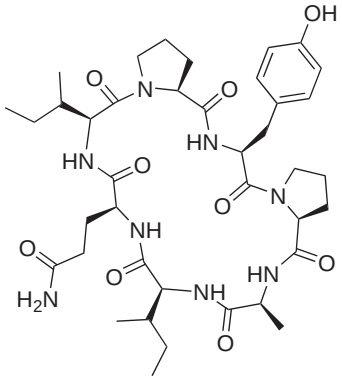

E (**92**)

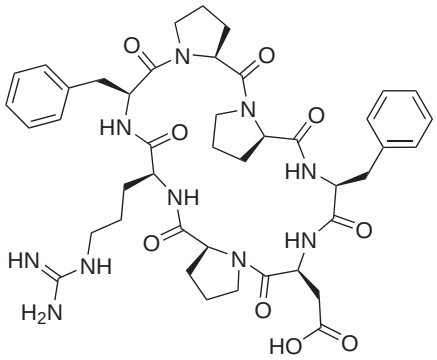

F (**93**)

The most intriguing feature in these cyclic peptides is that they are very rich in proline, taking into account the length of the peptide chain. Axinastatin 4, axinellin A, hymenamide C, phakellistatin 13 (**85**) and stylissamide E (**92**) contain two, stylisin 1 (**86**) and stylissamide A (**88**), C (**90**), D (**91**) and F (**93**) three proline residues. In stylisin 2 (**87**) and stylissamide B (**89**) four out of the total of seven amino acids are prolines.

This makes the sequence assignment by mass spectrometric methods difficult since proline-containing peptides preferentially fragment at a proline residue.[201] In the case of stylissamide B (**89**), this results in four fragmentation pathways with overlapping fragment masses. An additional challenge in mass spectrometric experiments exhibited the simultaneous presence of isomeric amino acids like leucin and isoleucin (both $m/z = 113.0841$) in stylissamide D (**91**) as well as the coexistence of tripeptide fragments of similar fragment mass in stylissamide C (**90**) and D (**91**) (see publication 1).

Similarly, the dominant presence of one amino acid hampers evaluation of 2D NMR experiments due to the resulting overlap in signals, especially in the $H\alpha_{(i)}/CO_{(i-1)}$ and $NH_{(i)}/CO_{(i-1)}$ regions of the $^{1}H,^{13}C$-HMBC spectrum used for assigning the peptide sequence.

A combination of both methods, mass spectrometry with exact mass measurements in the fragmentation mode and NMR spectroscopy with selective experiments, finally led to the sequence assignment for all stylissamides. Both, the evaluation of stylissamide mass spectra derived from different ionization and fragmentation methods as well as extensive 2D NMR experiments are described in publication 1 (page 137).

5
Material and Methods

Sponge material

Haliclona spp.

The sponges were collected by scuba divers in a depth range of 3-30 m in the Kongsfjord, Spitsbergen and around the Orkneys Islands, Great Britain. Sponges sampled in the three areas before the year 2007 were collected by Michael Assmann and other members of the AWI Scientific Diving Team.

The Orkney samples in 2007 were collected by G. Schmidt from different locations around the islands whereas the samples in June 2008 and July 2009 were obtained from the same diving locations by S. Fuhrmann, R. Lehmann and S. Bleck (AWI Diving Team). In the Kongsfjord, sponges were collected by G. Schmidt in July 2008 and June/July 2009.

Sponges were cut off from the hard substrate and collected into diver's mesh bags. On board the diving boat, they were removed from the bag and maintained in containers filled with ambient seawater. This was done to minimize stress or damage to the animal by the net from beating waves during the transport back to land or the research vessel.

In the laboratory, a small piece of each individual was conserved in 90 % ethanol and used for taxonomic identification, a second piece was removed for bacteria isolation and stored at 4 °C in ambient seawater until further use, and the remaining sponge material was individually packed into polypropylene zipper bags and frozen at –20 °C. Later, this frozen sponge material was freeze-dried and again stored at –20 °C.

Stylissa caribica

Stylissa caribica was collected in Bahamian waters in a depth range of 10-30 m in 2008 by Gesine Schmidt and before 2008 by Michael Assmann and other members of the University of North Carolina Wilmington scientific diving team. On board, the sponges were identified taxonomically by Prof. Sven Zea, then frozen at –20 °C. Transport to Germany was performed on dry ice; subsequently the sponges were freeze-dried and stored at –20 °C.

Taxonomic Identification

Taxonomic identification was carried out on a Zeiss Axioskop 40 equipped with a 10×/0.25 and a 40×/0.65 Ph2 Achroplan achromatic system. A Neubauer Improved Zählkammer[1] with 1 mm edge length in the major square, 0.2 mm edge length in the minor square and 0.4 mm edge length in the smallest square was used for length measurement. A digital camera with 3.5 × internal zoom was mounted on the system and pictures were taken of every specimen, with special focus on the choanosome arrangement and the spicule size. For spicule size determination, 10 spicules of every specimen were measured by applying the Zählkammer measure to the spicule photo.

Separation of Bacteria and Sponge Cells

The cell subdivision and extraction procedure followed a method described by Laroche et al. (2007).[202] Briefly, approximately 2 cm^3 of a fresh sponge individual were pestled, the water-cell-suspension was transferred into a graduated cylinder and filled to 4 mL with salt water (3.4 % NaCl). This solution which contained compartmentalized or small aggregates of sponge- and bacteria cells was poured over a 40 µm sieve into a 15 mL vial from which it was equally distributed into four 2 mL vials and labelled SC (sponge cells). The SC-vials were then centrifuged at 1 500 rpm and 4 °C for 5 minutes. The supernatant of each of the four vials was transferred to four 1.5 mL vials labelled BC (bacteria cells). The 1.5 mL BC-vials were centrifuged at 13 000 rpm and 4 °C for 25 min. The supernatants were merged in a storage vial and labelled SN (supernatant).

1 www.zaehlkammer.de/deutsch/neubauer.improved.html

The procedure was repeated starting with addition of 1 mL of salt water to each of the SC-vials. The quality of the cell separation was inspected by observing the cell size in light microscopy under oil: sponge cells 10-40 µm, bacteria cells 0.2-5 µm. Subsequently, all samples were frozen promptly in a steel cooling block at –80 °C and shipped to Bremerhaven in a liquid nitrogen saturated dry shipper at a temperature lower than –80 °C.

Sponge Tissue Extraction

Crude extracts were prepared by exhaustive extraction of one volume of freeze-dried, homogenized sponge with the ten-fold volume of methanol : dichloromethane (MeOH : DCM 1 : 1). Extracts were filtered (Schleicher & Schüll black ribbon paper, Nr. 589[1]), then concentrated by rotaevaporation. For TLC and HPLC analyses, the crude extract was redissolved in methanol.

Bacteria/Sponge Cell Extraction

The bacteria and sponge cell samples were thawed by adding 1 mL methanol to each vial. The cell pellet was suspended in a vortexer, treated with ultrasound for 15 min, then centrifuged. The sponge cell extract was filtered (Ederol, Nr. 53) into HPLC vials whereas the bacteria cell extract was transferred without filtering. Of each sample, 20 µL of the dissolved extract were injected during HPLC instead of the 5 µL used for crude extracts. This was done to account for the lower crude extract concentration in the cell isolates. Each sample was subjected to the same HPLC method as the sponge crude extracts to allow comparability.

Thin Layer Chromatography (TLC)

Glass plates precoated with a Merck RP-18 F_{254S} stationary phase were used for TLC. The mobile phase consisted of butanol saturated with acidic water. A mixture of pure, synthetic haliclamines C and D (R_f ~0.8) and cyclostellettamines C, N, L, and Q (R_f ~0.4) was used as a control, applied onto each TLC plate and run with the crude extracts. Dragendorff's reagent for staining alkaloids as well as vanillin reagent and sulphuric acid (~5 %) for a broader compound spectrum served as dye. The plates were heated, then photographed immediately.

Mobile phase — $BuOH : CH_3COOH$ (glacial) : H_2O (4 : 1 : 5)

Dragendorff's spray reagent — prefabricated, Merck 1.02035.0100

Vanillin spray reagent — 6 g vanillin in 250 mL EtOH and 2.5 mL H_2SO_4 (95-97 %)

Sulphuric acid spray solution — 10 mL H_2SO_4 (95-97 %) in 190 mL H_2O

High Performance Liquid Chromatography (HPLC)

High performance liquid chromatography (HPLC) used two different systems; an analytical system and a preparative system. Both were fitted with a quarternary pump to allow ternary or quarternary gradients and a diode array detector (DAD) to record UV spectra. Analytical HPLC used an Agilent 1100 system equipped with a Waters XTerra MS RP_{18} column (3.0×150 mm, 3.5 µm) and a tempered column compartment. The preparative system consisted of a Jasco 1500 series HPLC equipped with a Prontosil Eurobond RP_{18} column (20×250 mm, 5 mm), a tempered column compartment and two simultaneously operating detector types, a DAD and an evaporative light scattering detector (ELSD).

HPLC of *Haliclona viscosa* extracts

Analytical HPLC was run with a linear ACN/HCOOH (0.1 % in H_2O) gradient at 35 °C and a flow rate of 0.4 mL min^{-1}; 0 min: 20 % ACN/80 % HCOOH; 25 min: 55 % ACN/45 % HCOOH; 27 min: 100 % ACN.

During preparative HPLC, an ACN/H_2O (both 0.1 % TFA) gradient at 40 °C and a flow rate of 8 ml min^{-1} was used; 0-5 min: 30 % ACN/70 % H_2O isocratic; 35-40 min: 60 % ACN/40 % H_2O isocratic; 50 min: 100 % ACN.

HPLC of *Stylissa caribica* extracts

During analytical HPLC, the instrument supplied an ACN/HCOOH (0.1 % in H_2O) gradient at 25 °C with a flow rate of 0.4 mL min^{-1}; 0 min: 10 % ACN/90 % HCOOH; 30 min: 60 % ACN/40 % HCOOH.

High Resolution Mass Spectrometry (HRMS)

Accurate mass spectra were acquired using a Bruker microTOF$_{LC}$ mass spectrometer. The instrument was equipped with an ESI source which operated in positive mode and used the following conditions: dry gas flow 5 L min^{-1}, dry gas temperature 180 °C, nebulizer gas pressure 0.4 bar, capillary voltage 4500 V (7 nA). The capillary exit was set to 100 V and the skimmer to 50 V. For fragmentation experiments, the voltage of the capillary exit voltage was raised to 150-200 V while the skimmer voltage remained the same. The instruments was externally calibrated prior to every experiment using sodium formiate clusters of the following reference masses: 226.9515, 294.9389, 362.9263, 430.9138, 498.9012, 566.8886, 634.8760, 702.8635 and 770.8509. Calibration resulted in the standard deviation of the calibration curve (quadratic calibration) being below 5 ppm.

For experiments that used liquid chromatography coupled to mass spectrometry (LCMS), the gas flow into the instrument was increased to reach 4 bar nebulizer gas pressure and 9 L min^{-1} dry gas flow. The instrument was externally calibrated prior to every LCMS experiment, with the exception of over-night recordings.

Matrix-Assisted Laser Desorption/Ionisation Mass Spectrometry (MALDI-MS)

All MALDI-MS measurements were acquired at the GKSS Forschungszentrum Geesthacht, Germany, using a Bruker ultraflex II TOF/TOF mass spectrometer. For MALDI-MS measurements, approximately 10 mg of freeze-dried and homogenised sponge were weighed into a 1.5 mL vial. Directly before the measurement, 100 µL methanol (MeOH) were added to the vial, the mixture was treated with ultrasound for 10 min and then centrifuged. In a vial cap, 0.5 µL of the supernatant were mixed with 0.5 µL of matrix solution and of this mix, 0.5 µL were pipetted onto an Anchorchip™ target plate spot. Pure matrix solution pipetted onto a spot served as a blank. All solutions were left to dry, then checked for adequate crystallisation and, where necessary, re-crystallised.

After the drying was complete, the target plate was inserted into the machine, the machine evacuated and the samples measured with adaptive laser power ("fuzzy control") in positive mode. Peaks present in the blanks were regarded as background in the sample measurements.

Matrix solution — $5\,\mathrm{mg}$ HCCA in $1\,\mathrm{mL}$ ACN : $0.01\,\%$ TFA $(1:1)$

Re-crystallisation solution — EtOH : acetone : $0.01\,\%$ TFA $(6:3:1)$

6
Publications

Articles

1. G. Schmidt, A. Grube, M. Köck. Stylissamides A-D — New Proline-Containing Cyclic Heptapeptides from the Marine Sponge *Stylissa caribica*. *Eur. J. Org. Chem.*, **2007**, 4103-4110. DOI: 10.1002/ejoc.200700013. 137

2. G. Schmidt, C. Timm, M. Köck. New Haliclamines E and F from the Arctic Sponge *Haliclona viscosa*. *Org. Biomol. Chem.* **2009**, *7* (15), 3061-3064. DOI: 10.1039/B904157E. 161

Poster Presentations

1. A. Grube, G. Schmidt, M. Köck. New Cyclic Heptapeptides and Pyrrole-Imidazole Alkaloids from the Caribbean Sponge *Stylissa caribica*. 12^{th} International Symposium on Marine Natural Products, Queenstown, New Zealand (2007). 171

2. G. Schmidt, A. Grube, S. Frickenhaus, M. Köck. Conformational Studies on Stylissamides, Cyclic Heptapeptides from *Stylissa caribica*. 5^{th} European Conference on Marine Natural Products, Ischia, Naples, Italy (2007). ... 173

3. G. Schmidt, C. Cychon, M. Köck. Secondary Metabolites in Marine Sponges; Qualitative and Quantitative Variation over Time. AWIPEV-Workshop Bremen, Germany (2008). 175

DOI: 10.1002/ejoc.200700013

Stylissamides A–D – New Proline-Containing Cyclic Heptapeptides from the Marine Sponge *Stylissa caribica*

Gesine Schmidt,[a] Achim Grube,[a] and Matthias Köck*[a]

Keywords: Marine natural products / Mass spectrometry / NMR spectroscopy / Peptides

Four new cyclic heptapeptides, stylissamides A–D (**1**–**4**), were isolated from the Caribbean sponge *Stylissa caribica*. The structures of these metabolites were elucidated by NMR and MS/MS methods. The peptides contain three and, in one case, four proline residues. The sequence assignment of **1**–**4** by NMR was supported by fragmentations in HR-MS/MS measurements. The absolute configuration of all amino acid residues was assigned as L using Marfey's method and the OPA method.

Introduction

Sponges of the order Halichondrida are a rich source of non-ribosomal cyclic peptides containing seven to ten amino acids.[1] Sponges of the genus *Phakellia* reveal the substance class of phakellistatins whereas sponges of the genus *Hymeniacidon* contain the hymenamides. The phakellistatins especially, such as phakellistatin 2 (**5**),[2] show cytotoxic effects against a variety of tumour cell lines.[3] Very recently, two cyclic heptapeptides, stylisin 1 (**6**) and 2 (**7**), were isolated from the Jamaican sponge *Stylissa caribica* (see Scheme 1). In contrast to other cyclic peptides they are inactive in antimicrobial, anti-malarial, anti-cancer, anti-HIV-1, anti-Mtb, and anti-inflammatory assays.[4] The Caribbean sponge *Stylissa caribica* (order Halichondrida) was found to be a rich source of pyrrole-imidazole alkaloids.[5] Using HPLC-HRMS screening of the crude extract several new metabolites were isolated: 4-bromopyrrole-2-carboxy-N(ε)-lysine,[6] 4-bromopyrrole-2-carboxyarginine,[6] oxocyclostylidol,[7] and stylissadines A and B.[8] In the course of this investigation a Sephadex LH-20 fraction of the *n*-butanol phase was analyzed. This fraction contained four non-brominated compounds with molecular masses between *m*/*z* 800 and 900. A comparison of the accurate molecular masses with the literature (MarinLIT®) revealed four metabolites with a previously unobserved mass which were separated by preparative HPLC. Herein, we report the structure elucidation of these new compounds by spectroscopic methods (NMR, MS, and MS^n).

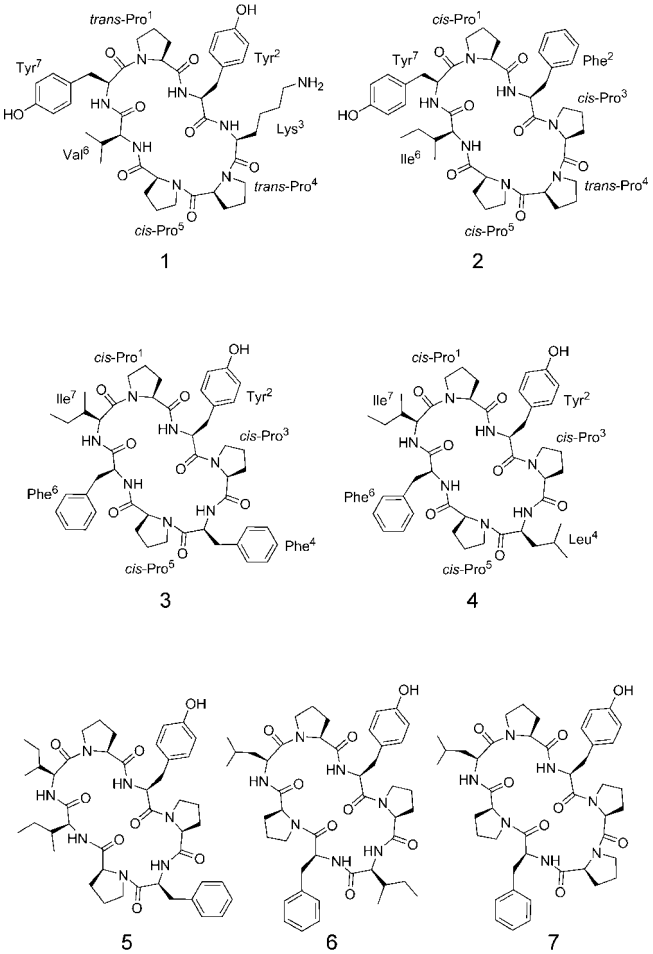

Scheme 1. Structural formulae of stylissamides A–D (**1**–**4**), phakellistatin 2 (**5**), stylisin 1 (**6**), and stylisin 2 (**7**).

[a] Alfred-Wegener-Institut für Polar- und Meeresforschung in der Helmholtz-Gemeinschaft,
Am Handelshafen 12, 27570 Bremerhaven, Germany
Fax: +49-471-4831-1425
E-mail: mkoeck@awi.de

Supporting information for this article is available on the WWW under http://www.eurjoc.org or from the author.

Results and Discussion

In our continuous search for new bioactive secondary metabolites of marine sponges from tropical waters, *Stylissa caribica* was collected by SCUBA at Little San Salvador in the Bahamas (23 m depth, July 2000). The freeze-dried sponge tissue was extracted with a 1:1 mixture of MeOH/CH_2Cl_2 and the crude extract was partitioned by liquid/liquid extraction between *n*-hexane, *n*BuOH and H_2O.

The resulting *n*BuOH phase was purified by Sephadex LH-20 chromatography. Final purification of the four metabolites was achieved by preparative RP_{18} HPLC. The fact that the metabolites were not halogenated, the characteristic 1D NMR spectra and the occurrence of cyclic peptides in other sponges of the order Halichondrida suggested the compounds were peptides. The four compounds were elucidated by 2D NMR and MS methods. The NMR spectroscopic data are summarized in Tables 1, 3, 5 and 6 respectively.

For each of the four compounds **1**–**4** (see Scheme 1) seven carbonyl carbons were observed in the ^{13}C NMR spectrum. The ^1H NMR spectrum showed four amide protons for **1**, **3**, and **4** and three amide protons for **2**. Together with the results of the HPLC analysis of the hydrolysed metabolites (Marfey's method) which showed that proline was a common amino acid in all four compounds, these results indicated the assignment to the structural class of heptapeptides. Due to the cyclic peptides found in other sponges of the order Halichondrida the degrees of unsaturation for the molecular formulae of **1**–**4** (HR-MS) were compared to the sum of degrees of unsaturation in the amino acids contained in each peptide. The molecular formula of **1** resulted in 19 degrees while the amino acids accounted for 18 degrees of unsaturation, indicating the cyclic nature of this compound. The degrees of unsaturation were compared in the same way for compounds **2** (20 vs. 19), **3** (23 vs. 22) and **4** (19 vs. 18), and suggested a cyclic structure for these compounds as well.

The molecular weight of **1** (*m/z* 845.4555 $[M + H]^+$) was obtained from the ESI mass spectrum (HR-ESIMS) and indicated the molecular formula $C_{44}H_{61}N_8O_9$. The ^1H NMR spectrum of **1** displayed four amide proton signals at 7.67, 7.62, 7.33 and 7.24 ppm in addition to seven carbonyl signals at 171.5, 171.4, 2 × 170.5, 170.0, 169.1 and 167.9 ppm in the ^{13}C NMR spectrum (see Table 1). All amino acid residues were assigned by 2D NMR techniques as 3 × Pro, Val, Lys, and 2 × Tyr, which was in accordance with the carbonyl and amide proton signals and defined the molecule as a heptapeptide. The amino acid sequence was established by a combination of classical and semi-selective $^1H,^{13}C$-HMBC experiments between the NH, Hα, and in the case of proline, Hδ of one amino acid and the carbonyl carbon of the preceding amino acid. The correlations Pro^1-Hα/Tyr^7-CO and Pro^1-Hδ/Tyr^7-CO proved the fragment Tyr^7-Pro^1. The correlations Lys^3-Hα/Tyr^2-CO, Pro^4-Hα/Lys^3-CO, Pro^5-Hα/Pro^4-CO, Val^6-Hα/Pro^5-CO and Tyr^7-Hα/Val^6-CO lengthened this fragment to give the final sequence Tyr^2-Lys^3-Pro^4-Pro^5-Val^6-Tyr^7-Pro^1. In addition to the $H\alpha_{(i)}/CO_{(i-1)}$ correlations the amide $NH_{(i)}/CO_{(i-1)}$ correlations were observed for Lys^3-NH/Tyr^2-CO, Val^6-NH/Pro^5-CO and Tyr^7-NH/Val^6-CO. The ring closure in stylissamide A (**1**) was given by another $^1H,^{13}C$-HMBC correlation between Tyr^2-NH and Pro^1-CO and two NOE correlations between Tyr^2-NH and both, Pro^1-Hα and Pro^1-Hγ.

Table 1. ^1H, ^{13}C and ^{15}N NMR chemical shifts of stylissamide A (**1**) in $[D_6]$DMSO.[a]

Entry	Residue	Position	δ_C/δ_N	δ_H, mult. (*J* /Hz)
1	Pro^1	N	135	–
2		CO	171.4	–
3		α	62.6	3.97, dd (7.3, 9.0)
4		β, β′	28.3	2.02, m; 1.60, m
5		γ, γ′	24.8	2.02, m
6		δ, δ′	46.7	3.74, m
7	Tyr^2	NH	108	7.67, d (8.1)
8		CO	170.5	–
9		α	54.2	4.32, m
10		β, β′	34.2	3.17, dd (3.1, 14.0); 2.89, dd (11.8, 14.0)
11		1	128.2	–
12		2, 6	129.2	7.00, d (7.6)
13		3, 5	114.6	6.65, d (7.6)
14		4	155.6	–
15		OH	–	9.18, s
16	Lys^3	NH	115	7.33, d (7.0)
17		CO	167.9	–
18		α	50.4	4.40, d (8.4)
19		β, β′	30.5	1.82, m; 1.50, m
20		γ, γ′	22.0	1.32, m; 1.31, m
21		δ, δ′	26.4	1.57, m
22		ε, ε′	38.3	2.76, dd (7.0, 14.3)
23		NH_2	34	7.76, s
24	Pro^4	N	139	–
25		CO	170.0	–
26		α	58.6	4.30, m
27		β, β′	27.7	2.17, m; 1.74, m
28		γ, γ′	24.2	1.91, m, 1.85, m
29		δ, δ′	46.6	3.44, m; 3.34, m
30	Pro^5	N	126	–
31		CO	170.5	–
32		α	60.0	4.42, d (8.4)
33		β, β′	30.9	2.17, m; 2.07, m
34		γ, γ′	21.5	1.85, m; 1.51, m
35		δ, δ′	46.1	3.42, m
36	Val^6	NH	117	7.62, d (8.4)
37		CO	169.1	–
38		α	61.3	3.67, t (8.4)
39		β	29.5	1.77, m
40		γ	18.9	0.77, d (6.7)
41		γ′	18.9	0.45, d (6.7)
42	Tyr^7	NH	112.7	7.24, d (8.7)
43		CO	171.5	–
44		α	51.3	4.90, dt (3.4, 9.8)
45		β, β′	37.0	3.28, m; 2.39, dd (10.7, 14.0)
46		1	126.4	–
47		2, 6	129.9	7.07, d (7.6)
48		3, 5	114.8	6.67, d (7.6)
49		4	155.8	–
50		OH	–	9.23, s

[a] ^1H and ^{13}C chemical shifts were referenced to the $[D_6]$DMSO signal (2.50 ppm and 39.5 ppm, respectively). ^{15}N NMR spectra were not calibrated with an external standard. Therefore, the ^{15}N NMR shifts are given without decimals. The δ value has an accuracy of about 1 ppm in reference to NH_3 (δ = 0 ppm).

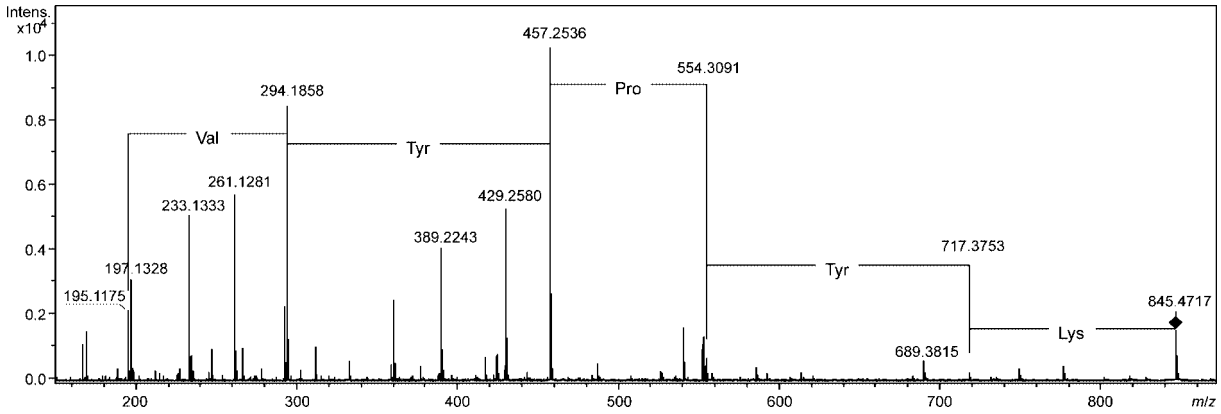

Figure 1. HR-MS/MS spectrum of stylissamide A (**1**). The precursor ion is indicated by the filled square. Only the main fragmentation pathway is indicated. Masses associated with this fragmentation pathway and the corresponding observed masses derived from CO loss (28 amu) are given.

The sequence was supported by other NOE correlations between $NH_{(i)}$ and $H\alpha_{(i-1)}$ and in the case of proline $H\delta_{(i)}$ and $H\alpha_{(i-1)}$ (see Figure 3 and Supporting Information).

The sequence of stylissamide A (**1**) was further supported by the fragmentation pattern obtained through HR-MS/MS and MS^n measurements. Although, the cyclic structure of the peptides **1**–**4** does not provide a definite position for ring-opening reactions the protonated amide nitrogen may be favoured in such reactions.[9] Mass spectrometric studies on cyclic and linear peptides containing proline residues showed a preferential protonation of the proline nitrogen due to a high proton affinity.[10] For stylissamide A (**1**) there are three proline residues which are preferred for ring-opening reactions. The occurrence of at least three proline residues in the stylissamides and the resulting possibilities for protonation and subsequent ring opening prevent the sequencing only by CID-MS^n experiments. However, the combined application of HR-MS/MS and MS^n experiments allows for sequencing the peptide fragments.[11]

For stylissamide A (**1**) the combination of these techniques (see Supporting Information) confirmed the sequence assignments by NMR spectroscopy. After ring opening at the Lys-Pro amide bond successive losses of Lys, Tyr, Pro, Tyr and Val gave the corresponding acylium ions (b_n fragments) at *m*/*z* 717.3753, 554.3091, 457.2536, 294.1858 and 195.1175 (see Figure 1, Table 2). Other fragments from ring openings at the Tyr-Pro and Pro-Pro amide bonds are found as well and confirmed the results mentioned before. The main peak at *m*/*z* 457.2536 was determined to be the Pro-Pro-Val-Tyr and Pro-Val-Tyr-Pro fragments.

The *cis*/*trans* configuration of the peptide bond preceding the proline residues was determined on the basis of the Cβ and Cγ shift difference ($\Delta\delta_{\beta\gamma}$)[12] and upon the presence of an NOE correlation between the proline Hα and the Hα of the preceding amino acid, which is present in a *cis* configuration but absent in *trans*-proline.[13] The $\Delta\delta_{\beta\gamma}$ of Pro^1 and Pro^4 were both 3.5 ppm and that of Pro^5 was 9.5 ppm. This indicated a *trans* configuration for Pro^1 and Pro^4 and a *cis* configuration for Pro^5. The NOE correlation Pro^4-Hα/Pro^5-Hα was observed while the correlations Tyr^7-Hα/Pro^1-Hα and Lys^3-Hα/Pro^4-Hα were not present. Thus, the amino acid sequence of **1** was established as cyclo-(*trans*-Pro^1-Tyr^2-Lys^3-*trans*-Pro^4-*cis*-Pro^5-Val^6-Tyr^7).

Table 2. Fragments observed in HR-MS/MS and MS^n experiments of stylissamide A (**1**).

m/*z*	Fragment formula	Error [ppm]	Sequence	MS^3 loss
195.1175	$C_{10}H_{15}N_2O_2$	24.2	Pro-Pro	–
197.1328	$C_{10}H_{17}N_2O_2$	22.2	Pro-Val	–
261.1281	$C_{14}H_{17}N_2O_3$	18.1	Pro-Tyr	–
294.1858	$C_{15}H_{24}N_3O_3$	15.5	Pro-Pro-Val	Pro, Val
389.2243	$C_{20}H_{29}N_4O_4$	15.3	Pro-Tyr-Lys	Lys
457.2536	$C_{24}H_{33}N_4O_5$	19.8	Pro-Pro-Val-Tyr Pro-Val-Tyr-Pro	Pro, Tyr
554.3091	$C_{29}H_{40}N_5O_6$	21.2	Pro-Pro-Val-Tyr-Pro	–[a]
717.3753	$C_{38}H_{49}N_6O_8$	20.5	Pro-Pro-Val-Tyr-Pro-Tyr	Pro, Tyr

[a] Due to the low intensity of this fragment it was not possible to perform MS^3 measurements.

The molecular weight of **2** (*m*/*z* 812.4311 $[M + H]^+$) as determined by HR-ESIMS indicated the molecular formula $C_{44}H_{58}N_7O_8$. The ^1H NMR spectrum of **2** showed three amide proton signals at 8.65, 8.24 and 6.45 ppm while the ^{13}C NMR spectrum showed four carbonyl carbons at 171.2, 170.2, 168.5, 167.6 ppm and three carbonyl carbon signals at approximately 169.8 ppm, which could be differentiated into two signals at 169.75 ppm and one at 169.81 ppm (see Table 3). All amino acid residues were assigned by 2D NMR techniques as 4 × Pro, Ile, Phe and Tyr which defined the heptapeptide structure. Sequence assignments by $^1H,^{13}C$-HMBC experiments were difficult due to the overlap of the carbonyl carbon chemical shifts of two prolines (Pro^1 and Pro^4) and isoleucine. A semi-selective $^1H,^{13}C$-HMBC experiment allowed us to assign the three carbonyl C atoms at 169.8 ppm to two prolines (169.75 ppm) and isoleucine (169.81 ppm). The fragment Pro^5-Ile^6 was assigned from the correlations Ile^6-NH/Pro^5-CO and Ile^6-Hα/Pro^5-CO as well as a weak correlation Ile^6-Hγ/Pro^5-CO and the NOE correlation Ile^6-NH/Pro^5-Hα. The fragments Ile^6-Tyr^7 and Tyr^7-Pro^1 were proven by the correlations Tyr^7-

NH/Ile^6-CO, Tyr^7-Hα/Ile^6-CO, Pro^1-Hα/Tyr^7-CO, Pro^1-Hδ/Tyr^7-CO and the NOE correlations Tyr^7-NH/Ile^6-Hα and Pro^1-Hα/Tyr^7-Hα, thereby establishing the partial sequence Pro^5-Ile^6-Tyr^7-Pro^1. Another fragment Pro^3-Pro^4 was given by the correlation Pro^4-Hα/Pro^3-CO. Pro^1 and Pro^4 showed the same carbonyl carbon shift at δ 169.75 ppm. Associated with this shift were the correlations Phe^2-NH/169.75 ppm, Phe^2-Hα/169.75 ppm, Pro^5-Hα/169.75 ppm and Pro^5-Hδ/169.75 ppm which suggested the fragments Pro^1-Tyr^2 or Pro^4-Tyr^2 and Pro^1-Pro^5 or Pro^4-Pro^5, respectively. Taking into account the partial sequence Pro^5-Ile^6-Tyr^7-Pro^1 a segment Pro^1-Pro^5 was ruled out, therefore establishing the segment Pro^4-Pro^5 and consequently Pro^1-Phe^2. Both segments were supported by the NOE correlations Pro^4-Hα/Pro^5-Hα and Pro^1-Hδ/Phe^2-NH. This defined the final sequence as Pro^3-Pro^4-Pro^5-Ile^6-Tyr^7-Pro^1-Phe^2. The ring closure was given by the two NOE correlations Phe^2-Hα/Pro^3-Hα and Phe^2-Hβ/Pro^3-Hα as well as the two weak HMBC correlations Pro^3-Hα/Phe^2-CO and Pro^3-Hδ/Phe^2-CO. The configuration of the peptide bonds preceding the proline residues was determined to be *cis* for Pro^1, Pro^3, and Pro^5 and *trans* for Pro^4 by the $\Delta\delta_{\beta\gamma}$ values (9.4, 8.3, and 8.6 ppm for Pro^1, Pro^3, and Pro^5, respectively, and 2.6 ppm for Pro^4). The NOE correlations Tyr^7-Hα/Pro^1-Hα, Phe^2-Hα/Pro^3-Hα and Pro^4-Hα/Pro^5-Hα were observed whereas Pro^3-Hα/Pro^4-Hα was not present. This confirmed the configurational assignment. The sequence of **2** was thus established as cyclo-(*cis*-Pro^1-Phe^2-*cis*-Pro^3-*trans*-Pro^4-*cis*-Pro^5-Ile^6-Tyr^7) and confirmed on the basis of MS^n data (see Figure 3 and Supporting Information). The fragment *m*/*z* 308.1979, assigned as Pro-Pro-Ile, lost Ile and Pro under MS^3 conditions. The main fragment at *m*/*z* 405.2511 lost Pro to yield the mass *m*/*z* 308.1979 and Ile to give the mass *m*/*z* 292.2 (Pro-Pro-Pro) under MS^3 conditions. The fragment at *m*/*z* 568.3178 lost Tyr to give the mass *m*/*z* 405.2511 and lost also Pro to give the fragment at *m*/*z* 471.2632 (see Figure 2, Table 4). This fragmentation pathway is only possible for the sequence Pro-Pro-Pro-Ile-Tyr which is in accordance with the NMR spectroscopic data.

The molecular weight of **3** (*m*/*z* 862.4490 [M + H]$^+$, HR-ESIMS) indicated the molecular formula $C_{48}H_{60}N_7O_8$. The ^{1}H NMR spectrum of **3** showed four amide proton signals at 8.96, 8.89, 8.16 and 6.62 ppm while the ^{13}C NMR spectrum displayed five carbonyls at 171.7, 171.5, 169.8, 169.0, 168.3 ppm and two carbonyl carbon signals at approximately 169.6 ppm, which could be differentiated into 169.66 ppm and 169.64 ppm (see Table 5). The amino acid residues were identified by 2D NMR as 3 × Pro, Ile, 2 × Phe and Tyr, which indicated a heptapeptide. Due to the overlapping carbonyl carbon signals a semi-selective ^{1}H,^{13}C-HMBC experiment was needed for the sequence assignment. The correlation Tyr^2-Hα/Pro^1-CO defined the segment Pro^1-Tyr^2. Pro^1-Hα and Pro^1-Hδ displayed correlations to Ile^7-CO. Along with the correlations Ile^7-Hα/Phe^6-CO, Phe^6-NH/Pro^5-CO, Pro^5-Hα/Phe^4-CO and Phe^4-Hα/Pro^3-CO the final sequence Pro^3-Phe^4-Pro^5-Phe^6-Ile^7-Pro^1-Tyr^2 was established. Additional ^{1}H,^{13}C-HMBC correlations between the amide proton and the carbonyl carbon of the preceding amino acid existed for Tyr^2-NH/Pro^1-CO, Pro^4-NH/Pro^3-CO and Ile^7-NH/Phe^6-CO. A weak correlation existed between Pro^3-Hδ and Tyr^2-CO which indicated the ring closure. This weak correlation was supported by an NOE correlation between Pro^3-Hα and Tyr^2-Hβ. The $\Delta\delta_{\beta\gamma}$ values clearly indicated a *cis* configuration for all pep-

Table 3. ^{1}H, ^{13}C and ^{15}N NMR chemical shifts of stylissamide B (**2**) in [D$_6$]DMSO.[a]

Entry	Residue	Position	δ_C/δ_N	δ_H, mult. (*J* /Hz)
1	Pro^1	N	131	–
2		CO	169.75[b]	–
3		α	60.5	3.49, d (8.5)
4		β, β′	30.4	1.68, m; 1.53, m
5		γ, γ′	21.0	1.38, m; 1.29, m
6		δ, δ′	45.4	3.22, m; 3.10, m
7	Phe^2	NH	114	6.45, d (3.9)
8		CO	167.6	–
9		α	52.1	4.14, m
10		β, β′	35.8	3.12, m
11		1	135.9	–
12		2, 6	127.6	7.22, m
13		3, 5	129.3	6.95, d (6.4)
14		4	126.3	7.19, m
15	Pro^3	N	130	–
16		CO	168.5	–
17		α	56.1	4.45, m
18		β, β′	29.1	2.03, m; 1.81, m
19		γ, γ′	20.8	1.79, m
20		δ, δ′	46.4	3.41, m; 3.31, m
21	Pro^4	N	133	–
22		CO	169.75[b]	–
23		α	58.3	4.30, t (7.8)
24		β, β′	27.5	2.28, m; 1.66, m
25		γ, γ′	24.9	2.06, m; 1.91, m
26		δ, δ′	46.7	3.65, m; 3.42, m
27	Pro^5	N	128	–
28		CO	170.2	–
29		α	60.3	4.41, t (8.1)
30		β, β′	30.2	2.33, dd (6.4, 11.6); 1.90, m
31		γ, γ′	21.6	1.82, m; 1.46, m
32		δ, δ′	45.6	3.39, m; 3.21, m
33	Ile^6	NH	122	8.65, d (9.2)
34		CO	169.81[b]	–
35		α	56.8	4.01, m
36		β	34.8	1.83, m
37		β-Me	15.3	0.68, d (7.1)
38		γ, γ′	24.6	1.23, m; 1.04, m
39		δ	10.6	0.72, t (7.4)
40	Tyr^7	NH	122	8.24, d (8.5)
41		CO	171.2	–
42		α	50.9	4.43, m
43		β, β′	37.2	2.78, dd (10.6, 13.0); 2.61, dd (6.7, 13.0)
44		1	126.2	–
45		2, 6	129.8	6.96, d (7.4)
46		3, 5	114.7	6.67, d (7.8)
47		4	155.9	–
48		OH	–	9.28, s

[a] ^{1}H and ^{13}C chemical shifts are referenced to the [D$_6$]DMSO signal (2.50 ppm and 39.5 ppm, respectively). ^{15}N NMR spectra were not calibrated with an external standard. Therefore, the ^{15}N NMR shifts are given without decimals. The δ value has an accuracy of about 1 ppm in reference to NH_3 (δ = 0 ppm). [b] ^{13}C NMR shifts of carbonyl carbons are given with two decimals if one decimal did not allow for differentiation of two or three different carbonyl carbons.

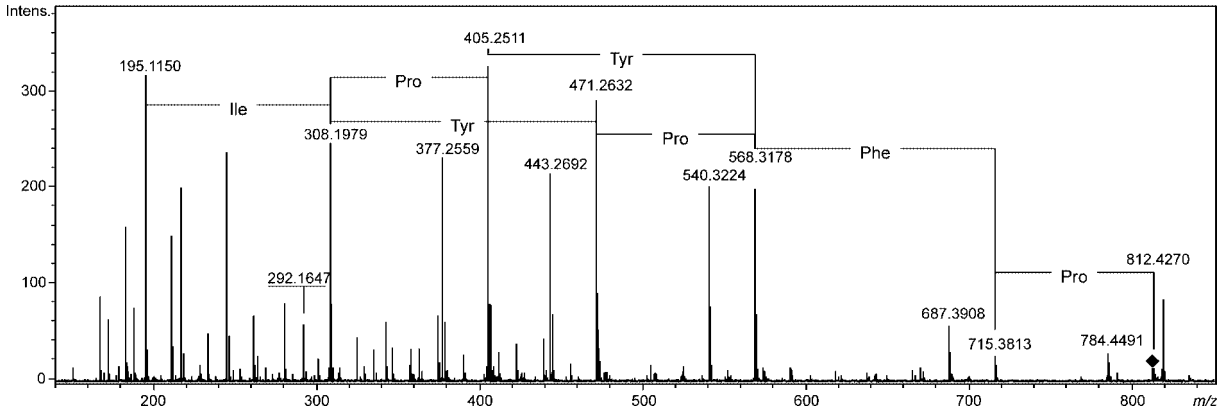

Figure 2. HR-MS/MS spectrum of stylissamide B (**2**). The precursor ion is indicated by the filled square. Only the main fragmentation pathway is indicated. Masses associated with this fragmentation pathway and the corresponding observed masses derived from CO loss (28 amu) are given.

tide bonds preceding the proline residues in **3**, with $\Delta\delta_{\beta\gamma}$ values of 9.6, 9.5 and 9.3 ppm for Pro[1], Pro[3], and Pro[5], respectively. The corresponding NOE correlations between the proline Hα and the Hα of the preceding amino acid were present for Pro[3] and Pro[5], but not for Pro[1] due to overlapping signals. The sequence of **3** was therefore established as cyclo-(*cis*-Pro[1]-Tyr[2]-*cis*-Pro[3]-Phe[4]-*cis*-Pro[5]-Phe[6]-Ile[7]) as shown in Figure 3.

Table 4. Fragments observed in HR-MS/MS and MS^n experiments on stylissamide B (**2**).

m/z	Fragment formula	Error [ppm]	Sequence	MS^3 loss
195.1150	$C_{10}H_{15}N_2O_2$	11.4	Pro-Pro	–
292.1647	$C_{15}H_{22}N_3O_3$	2.8	Pro-Pro-Pro	–[a]
308.1979	$C_{16}H_{26}N_3O_3$	3.3	Pro-Pro-Ile	Pro, Ile
405.2511	$C_{21}H_{33}N_4O_4$	3.6	Pro-Pro-Pro-Ile	Pro, Ile
471.2632	$C_{25}H_{35}N_4O_5$	6.5	Pro-Pro-Ile-Tyr	Tyr, Ile
568.3178	$C_{20}H_{29}N_4O_4$	8.4	Pro-Pro-Pro-Ile-Tyr	Tyr, Pro

[a] Due to the low intensity of this fragment it was not possible to perform MS^3 measurements.

The molecular weight of **4** (*m/z* 828.4657 $[M + H]^+$, HR-ESIMS) indicated the molecular formula $C_{45}H_{62}N_7O_8$. The ^1H and ^{13}C NMR spectra of **4** showed four amide signals at 8.81, 8.70, 8.10 and 6.57 ppm and seven carbonyls at 171.6, 171.2, 170.7, 170.5, 169.5, 169.4 and 168.2 ppm, respectively (see Table 6). The amino acid residues were determined as 3 × Pro, Leu, Ile, Phe and Tyr. The HMBC correlations between Ile[7]-Hα/Phe[6]-CO, Phe[6]-Hα/Pro[5]-CO and Pro[5]-Hα/Leu[4]-CO determined a segment Leu[4]-Pro[5]-Phe[6]-Ile[7]. Leu-Hα and Tyr-Hα showed the same ^1H chemical shift, and both correlated to Pro[1]-CO and Pro[3]-CO which made it difficult to assign a partial sequence Pro[1]-Leu rather than Pro[3]-Leu or Pro[1]-Tyr rather than Pro[3]-Tyr from the Hα-correlations. However, a clear $NH_{(i)}/CO_{(i-1)}$ HMBC correlation established Pro[3]-Leu[4] and consequently Pro[1]-Tyr[2], which defined two segments Pro[3]-Leu[4]-Pro[5]-Phe[6]-Ile[7] and Pro[1]-Tyr[2]. A weak correlation between Pro[3]-Hδ and Tyr[2]-CO connected both segments. Another weak correlation Pro[1]-Hα/Ile[7]-CO indicated the ring closure. NOE correlations supported the sequence; the correlations Ile[7]-CH_3/Pro[1]-Hα and Phe[6]-Hα/Ile[7]-NH proved the sequence Phe[6]-Ile[7]-Pro[1] and the second segment Tyr[2]-Pro[3]-Leu[4]-Pro[5] was given by the correlations Leu[4]-Hβ′/Pro[5]-Hα, Pro[3]-Hα/Leu[4]-NH and Tyr[2]-Hβ′/Pro[3]-Hα. The $\Delta\delta_{\beta\gamma}$ values (9.7, 8.7 and 10.0 ppm for Pro[1], Pro[3], and Pro[5], respectively) clearly indicated a *cis* configuration for all peptide bonds preceding the proline residues in **4**. The corresponding NOE correlations between the proline Hα and the Hα of the preceding amino acid were present only for Pro[5], but were, if present, overlapped for Pro[1] and Pro[3]. The amino acid sequence of **7** was established as cyclo-(*cis*-Pro[1]-Tyr[2]-*cis*-Pro[3]-Lys[4]-*cis*-Pro[5]-Phe[6]-Ile[7]).

The MS^n analysis of stylissamides C (**3**) and D (**4**) was complicated by the occurrence of the tripeptide fragments Pro-Tyr-Pro and Pro-Phe-Ile (see Figure 4). Both fragments have a similar molecular mass of *m/z* 358.1761 and *m/z* 358.2125, calculated for Pro-Tyr-Pro and Pro-Phe-Ile, respectively, which prevent a differentiation of these fragments under standard MS^n conditions. However, the sequences of **3** and **4** could be followed by the HR-MS/MS spectra of each compound. Both peptides successively lost Ile, Phe and Pro to give the fragments at *m/z* 505.2484 (**3**) and *m/z* 471.2645 (**4**). Starting from these fragments stylissamide C (**3**) lost Phe whereas stylissamide D (**4**) lost Leu to give the fragment at *m/z* 358.20. An identical fragmentation pattern for both molecules starting from this fragment indicated the tripeptide sequence Pro-Tyr-Pro. These results confirmed the different composition of **3** and **4** in only one amino acid.

The absolute configuration of the amino acid residues of stylissamide A-D (**1**–**4**) was determined by Marfey's method[14] and the OPA method[15] after hydrolysis of **1**–**4**. All amino acids were found to possess L-configurations.

Conclusions

The isolated stylissamides A-D (**1**–**4**) extend the variety of cyclic and proline-rich peptides from marine sponges. In addition to the stylisins 1 (**6**) and 2 (**7**)[4] these metabolites are the first examples of cyclic peptides from the sponge

Table 5. ^{1}H, ^{13}C and ^{15}N NMR chemical shifts of stylissamide C (**3**) in [D_6]DMSO.[a]

Entry	Residue	Position	δ_C/δ_N	δ_H, mult. (J /Hz)
1	Pro[1]	N	120	–
2		CO	169.8	–
3		α	61.0	4.36, m
4		β, β′	30.9	2.22, m; 2.04, m
5		γ, γ′	21.3	1.78, m; 1.45, m
6		δ, δ′	45.7	3.38, m
7	Tyr[2]	NH	113	6.62, d
8		CO	168.3	–
9		α	52.0	4.33, m
10		β, β′	34.5	3.22, dd (6.1, 13.8); 2.92, m
11		1	125.3	–
12		2, 6	130.3	6.73, d (8.5)
13		3, 5	114.5	6.62, d
14		4	155.9	–
15		OH	–	9.21, s
16	Pro[3]	N	129	–
17		CO	171.5	–
18		α	57.3	4.60, d (8.1)
19		β, β′	30.5	2.17, m; 2.01, m
20		γ, γ′	21.0	2.00, m; 1.89, m
21		δ, δ′	46.5	3.57, m; 3.32, m
22	Phe[4]	NH	124	8.96, d (1.6)
23		CO	169.0	–
24		α	53.3	4.32, m
25		β, β′	35.8	3.10, m; 2.93, m
26		1	135.6	–
27		2, 6	128.9	7.25, m
28		3, 5	128.4	7.32, t (7.3)
29		4	126.7	7.25, t (7.3)
30	Pro[5]	N	132	–
31		CO	169.64[b]	–
32		α	59.6	3.03, d (7.9)
33		β, β′	29.8	1.61, m; 0.84, m
34		γ, γ′	20.5	1.32, m; 0.47, m
35		δ, δ′	45.5	3.09, m; 2.89, m
36	Phe[6]	NH	122	8.89, d (8.5)
37		CO	169.66[b]	–
38		α	54.1	4.22, m
39		β, β′	35.5	2.76, dd (3.5, 13.3); 2.68, t (12.9)
40		1	138.9	–
41		2, 6	128.6	7.23, m
42		3, 5	127.3	7.21, t (7.4)
43		4	125.4	7.12, t (7.4)
44	Ile[7]	NH	115	8.16, d (9.4)
45		CO	171.7	–
46		α	53.0	4.32, m
47		β	37.3	1.64, m
48		β-Me	14.5	0.79, d (6.9)
49		γ, γ′	23.8	1.49, m; 1.02, m
50		δ	10.5	0.80, t (7.1)

[a] ^{1}H and ^{13}C chemical shifts are referenced to the [D_6]DMSO signal (2.50 ppm and 39.5 ppm, respectively). ^{15}N NMR spectra were not calibrated with an external standard. Therefore, the ^{15}N NMR shifts are given without decimals. The δ value has an accuracy of about 1 ppm in reference to NH_3 (δ = 0 ppm). [b] ^{13}C NMR shifts of carbonyl carbons are given with two decimals if one decimal did not allow for differentiation of two or three different carbonyl carbons.

Stylissa caribica. In fact, stylissamide B (**2**) is the first cyclic heptapeptide from marine sponges of the order Halichondrida that includes the tripeptide fragment Pro-Pro-Pro.

The sequences of stylissamides C (**3**) and D (**4**) differ by only one amino acid. Phenylalanine in stylissamide C (**3**) is replaced by leucine in stylissamide D (**7**). In addition, **3** differs by only one amino acid from phakellistatin 2 (**5**), isolated from the marine sponge *Phakellia carteri*.[2] Here, the fragment Phe-Ile in **3** is replaced by Ile-Ile in **5**. The sequence of stylissamide D (**4**) shows a striking resemblance to that of stylisin 1 (**6**) in that it is inverse to the sequence of **6**.

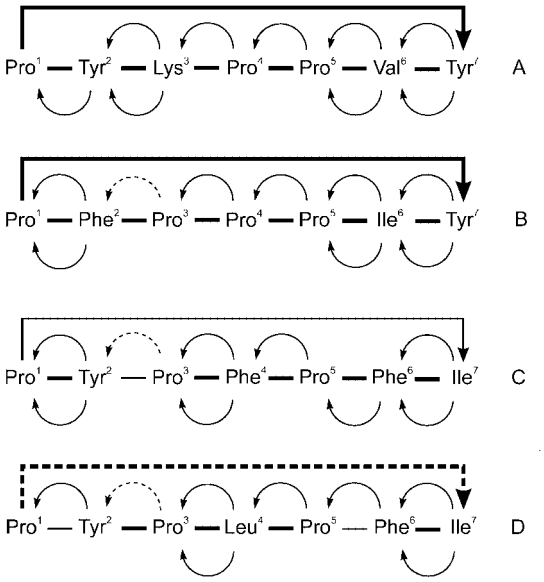

Figure 3. Sequential $^{1}H,^{13}C$-HMBC and $^{1}H,^{1}H$-NOE correlations in stylissamides A–D (**1**–**4**). Solid arrows above the sequence indicate $H\alpha_{(i)}/CO_{(i-1)}$ HMBC correlations, and dashed arrows show $H\delta_{(i)}/CO_{(i-1)}$ HMBC correlations. Arrows below indicate $NH_{(i)}/CO_{(i-1)}$ HMBC correlations. Standard bonds indicate that no NOE correlation was observed. Bold bonds indicate $NH_{(i)}/H\alpha_{(i-1)}$ and $H\delta_{(i)}/H\alpha_{(i-1)}$ NOE correlations between adjacent amino acids.

In contrast to members of the phakellistatin or hymenamide group no antimicrobial or cytotoxic effect was found for stylissamide A (**1**). The biological activities of the remaining metabolites are under investigation.

Experimental Section

General: ^{1}H, ^{13}C and ^{15}N NMR spectra were recorded with Bruker Avance 400 and 600 NMR spectrometers. All experiments were measured at 298 K or 300 K. The DQF-$^{1}H,^{1}H$-COSY, $^{1}H,^{13}C$-HSQC, $^{1}H,^{13}C$-HMBC, $^{1}H,^{15}N$-HSQC, $^{1}H,^{15}N$-HMBC, and $^{1}H,^{1}H$-NOESY experiments were carried out using standard parameters. The mixing time for NOESY spectra was 200 ms, and the delay for HMBC measurements was 80 ms. HPLC-MS analyses were performed with an Agilent 1100 HPLC system and a Bruker Daltonics microTOF$_{LC}$ mass spectrometer. Separation was achieved by a Waters XTerra RP_{18} column (3.0 × 150 mm, 3.5 μm) applying a MeCN/H_2O/HCOOH gradient [0 min: 10% MeCN/90% HCOOH (0.01%); 30 min: 60% MeCN/40% HCOOH (0.01%) with a flow rate of 0.4 mL/min]. UV spectra were recorded during HPLC analysis with a DAD (Agilent). Accurate mass spectra were acquired using a Bruker microTOF$_{LC}$ mass spectrometer. Accurate MS/MS spectra were acquired using a Bruker microTOF$_{Q}$. Mass calibration was performed using sodium formiate cluster. MS^3 spectra were acquired using a Bruker Esquire 3000plus ion trap. All mass spectrometers were equipped with an ESI-source.

Table 6. ^{1}H, ^{13}C and ^{15}N NMR chemical shifts of stylissamide D (**4**) in [D_6]DMSO.[a]

Entry	Residue	Position	δ_C/δ_N	δ_H, mult. (J /Hz)
1	Pro[1]	N	131	–
2		CO	169.4	–
3		α	60.9	4.31, m
4		β, β′	31.0	2.20, m; 2.00, m
5		γ, γ′	21.3	1.77, m; 1.48, m
6		δ, δ′	45.7	3.37, m
7	Tyr[2]	NH	112	6.57, d (3.9)
8		CO	168.2	–
9		α	51.7	4.41, m
10		β, β′	34.8	3.17, m; 2.91, dd (2.6, 14.3)
11		1	125.3	–
12		2, 6	130.2	6.72, d (7.8)
13		3, 5	114.6	6.61, d (7.5)
14		4	155.7	–
15		OH	–	9.17, s
16	Pro[3]	N	130	–
17		CO	171.6	–
18		α	57.4	4.58, d (7.5)
19		β, β′	30.1	2.11, m; 1.95, m
20		γ, γ′	21.4	2.05, m; 1.86, m
21		δ, δ′	46.6	3.54, m; 3.29, m
22	Leu[4]	NH	125	8.70, m
23		CO	170.5	–
24		α	51.1	4.42, m
25		β, β′	37.9	1.53, t (11.7); 1.28, t (11.7)
26		γ	23.9	1.87, m
27		δ	23.2	0.94, d (6.4)
28		δ′	20.3	0.86, d (6.4)
29	Pro[5]	N	127	–
30		CO	170.7	–
31		α	59.9	4.02, d (8.1)
32		β, β′	31.0	1.99, m; 1.90, m
33		γ, γ′	21.0	1.54, m; 0.82, m
34		δ, δ′	46.1	3.23, m; 3.06, t (9.8)
35	Phe[6]	NH	122	8.81, d (8.4)
36		CO	169.5	–
37		α	54.6	4.25, m
38		β, β′	35.2	2.74, m
39		1	139.2	–
40		2, 6	128.8	7.31, d (7.5)
41		3, 5	127.6	7.24, t (7.5)
42		4	125.7	7.14, t (7.5)
43	Ile[7]	NH	115	8.10, d (9.5)
44		CO	171.2	–
45		α	52.6	4.33, m
46		β	36.9	1.66, m
47		β-Me	14.4	0.77, d (7.4)
48		γ, γ′	23.5	1.45, m; 1.10, m
49		δ	10.1	0.76, t (7.4)

[a] ^{1}H and ^{13}C chemical shifts are referenced to the [D_6]DMSO signal (2.50 ppm and 39.5 ppm, respectively). ^{15}N NMR spectra were not calibrated with an external standard. Therefore, the ^{15}N NMR shifts are given without decimals. The δ value has an accuracy of about 1 ppm in reference to NH_3 (δ = 0 ppm).

Extraction and Isolation: The sponge *Stylissa caribica* was collected by SCUBA at Little San Salvador in the Bahamas (23 m depth, July 2000). The samples were immediately frozen after collection and kept at –20 °C until extraction. The freeze dried sponge samples of *Stylissa caribica* (94.7 g) were crushed with a mill and extracted exhaustively at room temp. with a 1:1 mixture of CH_2Cl_2/MeOH. The orange-colored crude extract of *Stylissa caribica* was partitioned between *n*-hexane (4 × 400 mL) and MeOH (300 mL). The MeOH extract was then partitioned between *n*-BuOH (3 × 500 mL) and H_2O (300 mL). The resulting *n*-BuOH (15.9 g) phase from the solvent-partitioning scheme was purified by gel chromatography on Sephadex LH-20 (Pharmacia) using MeOH as the mobile phase. The final purification of the isolated compounds was achieved by preparative RP_{18} HPLC on a Kromasil RP_{18} column (16 × 250 mm, 10 μm) applying a MeCN/TFA (0.1% in water) gradient to afford **1** (35.3 mg, 0.037% of dry weight), **2** (8.7 mg, 0.009% of dry weight), **3** (12.5 mg, 0.013% of dry weight), and **4** (5.1 mg, 0.005% of dry weight).

Stylissamide A (1): was obtained as a light yellow powder. UV (DAD): λ_{max} = 224, 275 nm. $[a]_D^{20}$ = 86.8 (*c* = 0.46, MeOH); HPLC/HR(+)ESI-MS: R_t = 11.0 min, *m/z* 845.4555 $[M + H]^+$ (calcd. for $C_{44}H_{61}N_8O_9$ 845.4556), Δ*m* = 0.1 ppm.

Stylissamide B (2): was obtained as a light yellow powder. UV (DAD): λ_{max} = 275 nm; HPLC/HR(+)ESI-MS: R_t = 21.6 min, *m/z* 812.4311 $[M + H]^+$ (calcd. for $C_{44}H_{58}N_7O_8$ 812.4341), Δ*m* = 3.7 ppm.

Stylissamide C (3): was obtained as a light yellow powder. UV (DAD): λ_{max} = 232, 275 nm; HPLC/HR(+)ESI-MS: R_t = 25.2 min, *m/z* 862.4490 $[M + H]^+$ (calcd. for $C_{48}H_{60}N_7O_8$ 862.4498), Δ*m* = 0.9 ppm.

Stylissamide D (4): was obtained as a light yellow powder. UV (DAD): λ_{max} = 229, 275 nm; HPLC/HR(+)ESI-MS: R_t = 24.3 min, *m/z* 828.4657 $[M + H]^+$ (calcd. for $C_{45}H_{62}N_7O_8$ 828.4654), Δ*m* = 0.3 ppm.

Determination of the Absolute Configuration of Proline by Marfey's Method: The analysis was performed using a modified Marfey's method.[14] Stylissamides A–D (**1**–**4**, 700 μg each) were placed in 1 mL conical vials containing HCl (16%, 0.5 mL), and the sealed vials were heated at 100 °C for 12 h. After evaporation of the solvent under N_2, H_2O (100 μL) was added. A 40 μL aliquot of this solution was used for the OPA method. To the remaining hydrolysis solution (60 μL), $NaHCO_3$ (0.1 M, 100 μL) and 1-fluoro-2,4-dinitrophenyl-5-L-alanine amide (L-FDAA, 0.1%, 50 μL) in acetone were added, and the sealed vials were heated at 80 °C for 5 min. To the reaction mixture were added HCl (0.2 M, 50 μL) and 50% aqueous MeCN (containing 0.1% formic acid, 90 μL). The mixture was subjected to HPLC analysis [Waters XTerra RP_{18} column (3.0 × 150 mm, 3.5 μm); MeCN/H_2O/HCOOH gradient: 0 min: 30% MeCN/70% HCOOH (0.01%); 30 min: 60% MeCN/40% HCOOH (0.01%) with a flow rate of 0.4 mL/min]. UV detection was performed at a wavelength of 340 nm.

Determination of the Absolute Configuration of Amino Acids by the OPA Method: The analysis was performed using a modification of a previously described method.[15] A 40 μL aliquot of the hydrolysis solution was used for the OPA method. In an HPLC vial, 80 μL of *o*-phthaldialdehyde (OPA) solution and 80 μL of *N*-isobutyryl-cysteine (0.1%) were added to this solution, and after a reaction time of 2 min 20 μL of the reaction mixture were subjected to HPLC analysis [Phenomenex Hyperclone BDS C18 column (4.0 × 250 mm, 5 μm); MeOH/NaOAc gradient: solution A: 125 mM NaOAc in water and 20 mL MeOH, adjusted to pH 6.8 using diluted HOAc; solution B: MeOH].

Supporting Information (see also the footnote on the first page of this article): MS and 1D ^{1}H NMR spectra of compounds **1**–**4**, MS^n spectra of compounds **1** and **2**, $^{1}H,^{1}H$-COSY-, $^{1}H,^{1}H$-NOESY-, $^{1}H,^{13}C$-HMBC and semi-selective $^{1}H,^{13}C$-HMBC data for compounds **1**–**4**, assigned $^{1}H,^{13}C$-HMBC and $^{1}H,^{1}H$-NOESY spectra for compound **2**, $\Delta\delta_{\beta\gamma}$ values and NOE correlations used for the *cis*/*trans* configuration assignments for compounds **1**–**4**.

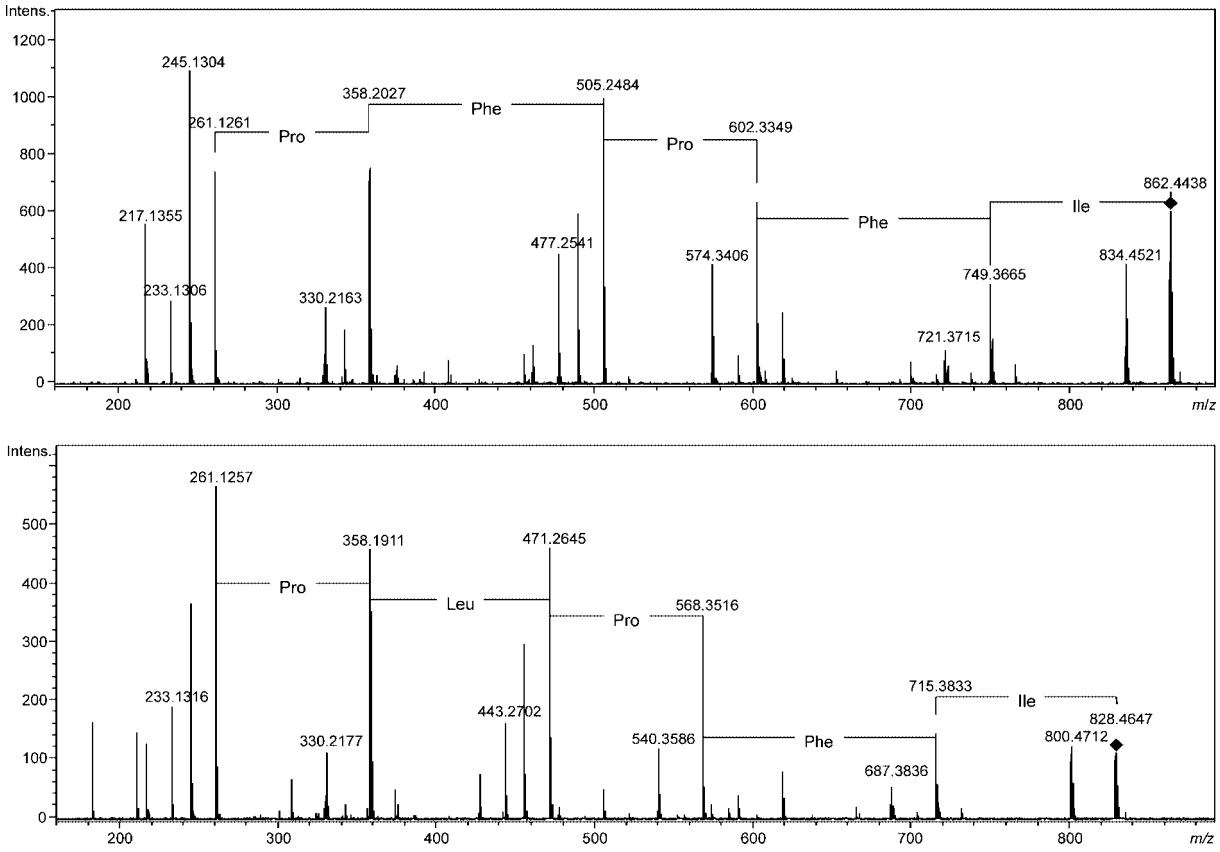

Figure 4. HR-MS/MS spectra of stylissamide C (**3**, above) and stylissamide D (**4**). The precursor ions are indicated by the filled squares. Only the main fragmentation pathways are given. Masses associated with this fragmentation pathway and the corresponding observed masses derived from CO loss (28 amu) are given.

Acknowledgments

Sponge collection was carried out by Dr. Michael Assmann during a scientific expedition to the Bahamas in 2000. During this time the project was sponsored by the Deutsche Forschungsgemeinschaft (DFG) (Ko1314/3-1 to 3-4). We would like to acknowledge the support of Prof. Dr. Joseph R. Pawlik (University of North Carolina, Wilmington, USA) who gave members of the Köck research group the opportunity to participate in scientific sojourns to the Bahamas. We further thank Ellen Lichte for performing preparative HPLC analysis, Kai-Uwe Ludwichowski for amino acid analysis and Dr. Andreas Jakob (Bruker Daltonics, Bremen, Germany) for performing QTOF measurements.

[1] S. Matsunaga, N. Fusetani, *Curr. Org. Chem.* **2003**, *7*, 945–966.
[2] G. R. Pettit, R. Tan, M. D. Williams, L. P. Tackett, J. M. Schmidt, *Bioorg. Med. Chem. Lett.* **1993**, *3*, 2869–2874.
[3] a) G. R. Pettit, Z. Cichacz, J. Barkoczy, A.-C. Dorsaz, D. L. Herald, M. D. Williams, D. L. Doubek, J. M. Schmidt, L. P. Tackett, D. C. Brune, R. L. Cerny, J. N. A. Hooper, G. J. Bakus, *J. Nat. Prod.* **1993**, *56*, 260–267; b) W.-L. Li, Y.-H. Yi, H.-M. Wu, Q.-Z. Xu, H.-F. Tang, D.-Z. Zhou, H.-W. Lin, Z.-H. Wang, *J. Nat. Prod.* **2003**, *66*, 146–148; c) G. R. Pettit, R. Tan, *J. Nat. Prod.* **2005**, *68*, 60–63.
[4] R. Mohammed, J. Peng, M. Kelly, M. T. Hamann, *J. Nat. Prod.* **2006**, *69*, 1739–1744.
[5] M. Assmann, R. W. M. van Soest, M. Köck, *J. Nat. Prod.* **2001**, *64*, 1345–1347.
[6] A. Grube, E. Lichte, M. Köck, *J. Nat. Prod.* **2006**, *69*, 125–127.
[7] A. Grube, M. Köck, *J. Nat. Prod.* **2006**, *69*, 1212–1214.
[8] A. Grube, M. Köck, *Org. Lett.* **2006**, *8*, 4675–4678.
[9] a) K. B. Tomer, F. W. Crow, M. L. Gross, K. D. Kopple, *Anal. Chem.* **1984**, *56*, 880–886; b) R. N. Grewal, H. E. Aribi, A. G. Harrison, K. W. M. Siu, A. C. Hopkinson, *J. Phys. Chem. B* **2004**, *108*, 4899–4908.
[10] B. L. Schwartz, M. M. Bursey, *Biol. Mass Spectrom.* **1992**, *21*, 92–96.
[11] K. Eckart, *Mass Spectrom. Rev.* **1994**, *13*, 23–55.
[12] I. Z. Siemion, T. Wieland, K.-H. Pook, *Angew. Chem. Int. Ed. Engl.* **1975**, *14*, 702–703.
[13] K. Wüthrich, M. Billeter, W. Braun, *J. Mol. Biol.* **1984**, *180*, 715–740.
[14] P. Marfey, *Carlsberg Res. Commun.* **1984**, *49*, 591–596.
[15] H. P. Fitznar, J. M. Lobbes, G. Kattner, *J. Chromatogr. A* **1999**, *832*, 123–132.

Received: January 8, 2007
Published Online: July 16, 2007

6.1.1 Supporting Information

Stylissamides A-D — New Proline-Containing Cyclic Heptapeptides from the Marine Sponge *Stylissa caribica*

Gesine Schmidt[1], Achim Grube[1], and Matthias Köck[1]*

[1]Alfred-Wegener-Institut für Polar- und Meeresforschung in der Helmholtz-Gemeinschaft, Am Handelshafen 12, D-27570 Bremerhaven, Germany

*To whom correspondence should be addressed. mkoeck@awi.de

Stylissamide A

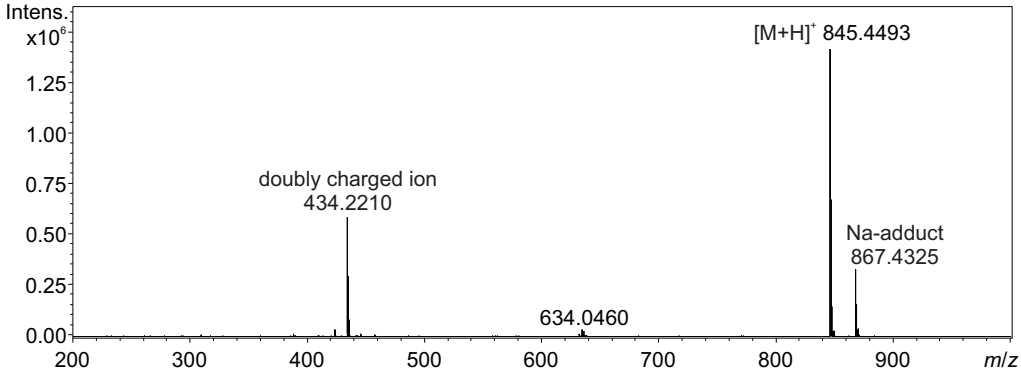

Figure 6.1 MS spectrum of stylissamide A (**1**).

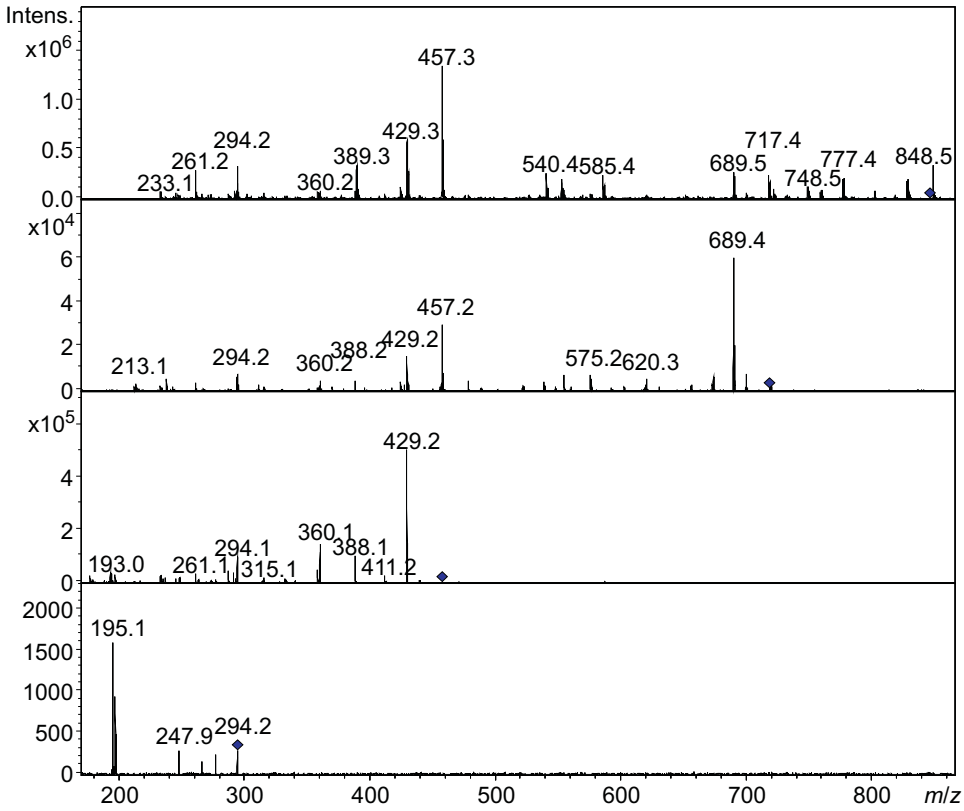

Figure 6.2 Sections of MS^n spectra of stylissamide A (**1**). Precursor ions are marked with filled squares. The ion at m/z 845.7 lost Lys to give the fragment at m/z 717.4. The fragment at m/z 717.4 lost Tyr to give the fragment at m/z 554.4 (Pro-Pro-Val-Tyr-Pro). By the loss of Pro from m/z 554.4 the fragment at m/z 457.2 (Pro-Pro-Val-Tyr) occurred. Due to the low intensity of the fragment at m/z 554.4 it was not possible to perform MS^3 experiments on this ion. Finally the loss of Tyr (m/z 294.2) and Val (m/z 195.1) defined the fragment at m/z 195.1 as Pro-Pro.

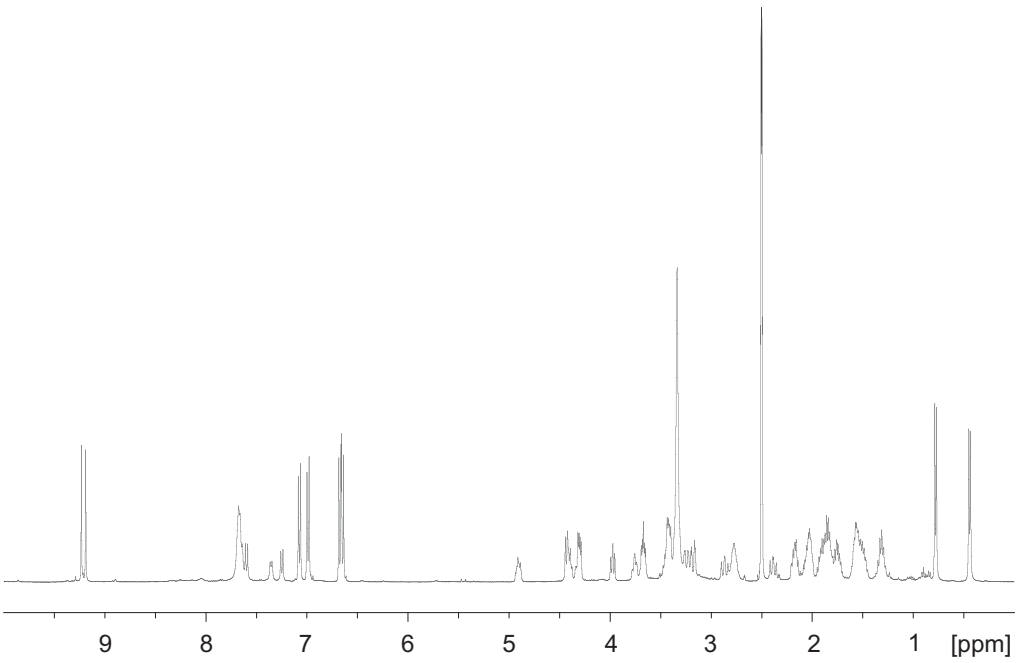

Figure 6.3 1D ^{1}H-NMR spectrum of stylissamide A (**1**) in DMSO-d_6.

Table 6.1 ^{1}H,^{1}H-COSY, sequential ^{1}H,^{1}H-NOESY and ^{1}H,^{13}C-HMBC correlations of stylissamide A (**1**)

	Pos	δC/δN	δH	COSY (H–H)	seq. NOESY (H–H)	HMBC (H–C)
Pro[1]	N	135	-			
	CO	171.4	-			
	α	62.6	3.97	1-β,β'	2-NH, 3-NH	1-CO, 7-CO, 1-α, 1-β
	β	28.3	2.02[a]	1-α, 1-β', 1-γ,γ'^{a}		
	β'	28.3	1.60	1-α, 1-β^{a}, 1-γ,γ'^{a}		
	γ, γ'	24.8	2.02[a]	1-β,β', 1-δ,δ'	2-NH	
	δ, δ'	46.7	3.74	1-γ,γ'	7-α, 7-β, 7-2/6	
Tyr[2]	NH	108	7.67	2-α	1-α, 1-γ,γ', 3-NH, 3-δ,δ'	1-CO, 2-β
	CO	170.5	-			
	α	54.2	4.32	2-NH, 2-β,β'	3-NH	2-1
	β	34.2	3.17	2-α, 2-β'		2-CO, 2-α, 2-2/6
	β'	34.2	2.89	2-α, 2-β		2-2/6
	1	128.2	-			
	2,6	129.2	7.00	2-3/5		2-β, 2-2/6, 2-3/5, 2-4
	3,5	114.6	6.65	2-2/6		2-1, 2-3/5, 2-4
	4	155.6	-			
	OH	-	9.18			2-2/6, 2-3/5, 2-4
Lys[3]	NH	115	7.33	3-α	1-α , 2-NH, 2-α, 4-α	2-CO, 3-CO
	CO	167.9	-			
	α	50.4	4.40	3-NH, 3-β,β'^{a}	4-α	2-CO, 3-CO, 3-α
	β	30.5	1.82	3-α, 3-β'^{a}, 3-γ,γ'^{a}		3-CO, 3-α, 3-β
	β'	30.5	1.50[a]	3-α, 3-β, 3-γ,γ'^{a}		3-CO, 3-α
	γ	22	1.32[a]	3-β,β'^{a}, 3-γ'^{a}, 3-δ,δ'		3-α, 3-β, 3-e
	γ'	22	1.31[a]	3-β,β'^{a}, 3-γ^{a}, 3-δ,δ'		
	δ, δ'	26.4	1.57	3-γ,γ'^{a}, 3-ε,ε'	2-NH, 4-δ,δ'	3β, 3ε
	ε, ε'	38.3	2.76	3-δ,δ', 3-NH2		
	NH2	34	7.76	3-ε,ε'		

continued on next page

continued from previous page

	Pos	δC/δN	δH	COSY (H–H)	seq. NOESY (H–H)	HMBC (H–C)
Pro^4	N	139	-			
	CO	170	-			
	α	58.6	4.30	4-β,β'	3-NH, 5-α	3-CO, 4-CO, 4-α, 4-β, 4-γ, 4-δ
	β	27.7	2.17	4-α, 4-β', 4-γ'		4-CO, 4-α, 4-β, 4-γ, 4-δ
	β'	27.7	1.74	4-α, 4-β	5-α	4-CO, 4-γ, 4-δ
	γ	24.2	1.91	4-γ' 4-δ,δ'		4-α, 4-β, 4-δ
	γ'	24.2	1.85	4-β, 4-γ, 4-δ,δ'		4-α, 4-β, 4-δ
	δ	46.6	3.44	4-γ,γ', 4-δ'	3-NH, 3-α, 3-δ,δ'	4-CO, 4-α, 4-β, 4-γ
	δ'	46.6	3.34	4-γ,γ', 4-δ	3-NH, 3-α, 3-δ,δ'	4-α, 4-β, 4-γ
Pro^5	N	126	-			
	CO	170.5	-			
	α	60	4.42	5-β,β'	4-α, 4-β', 6-NH	4-CO, 5-CO, 5-α, 5-β, 5-γ, 5-δ
	β	30.9	2.17	5-α, 5-β', 5-γ		5-γ, 5-δ
	β'	30.9	2.07	5-α, 5-β, 5-γ'^a		5-CO, 5-α, 5-β, 5-γ
	γ	21.5	1.85	5-β, 5-δ,δ'		5-α, 5-β
	γ'	21.5	1.51^a	5-β', 5-δ,δ'	6-NH	
	δ, δ'	46.1	3.42	5-γ,γ'^a	4-α, 4-β, 6-NH	5-β, 5-γ
Val^6	NH	117	7.62	6-α	5-α, 5-γ', 5-δ,δ', 7-NH	5-CO, 6-α, 6-β
	CO	169.1	-			
	α	61.3	3.67	6-NH, 6-β	7-NH, 7-α, 7-β, 7-2/6	5-CO, 6-CO, 6-α, 6-β, 6-γ
	β	29.5	1.77	6-α, 6-γ,γ'	7-NH	6-CO, 6-α, 6-β, 6-γ
	γ	18.9	0.77	6-β	7-NH	6-α, 6-β, 6-γ
	γ'	18.9	0.45	6-β	7-NH	6-α, 6-β, 6-γ
Tyr^7	NH	112.7	7.24	7-α	6-NH, 6-α, 6-β, 6-γ,γ'	6-CO, 7-CO, 7-α
	CO	171.5	-			
	α	51.3	4.90	7-NH, 7-β,β'	1-δ,δ', 6-α	6-CO, 7-CO, 7-β, 7-1
	β	37	3.28	7-α, 7-β'	1-δ,δ', 6-α	7-1, 7-2/6
	β'	37	2.39	7-α, 7-β		7-CO, 7-α, 7-1, 7-2/6
	1	126.4	-			
	2,6	129.9	7.07	7-3/5	1-δ,δ', 6-α	7β, 7-2/6, 7-3/5, 7-4
	3,5	114.8	6.67	7-2/6		7-1, 7-3/5, 7-4
	4	155.8	-			
	OH	-	9.23			7-2/6, 7-3/5, 7-4

^{a} Signals are overlapped. Spins were established through ^{1}H,^{13}C- and ^{1}H,^{15}N-HSQC-TOCSY experiments.

Stylissamide B

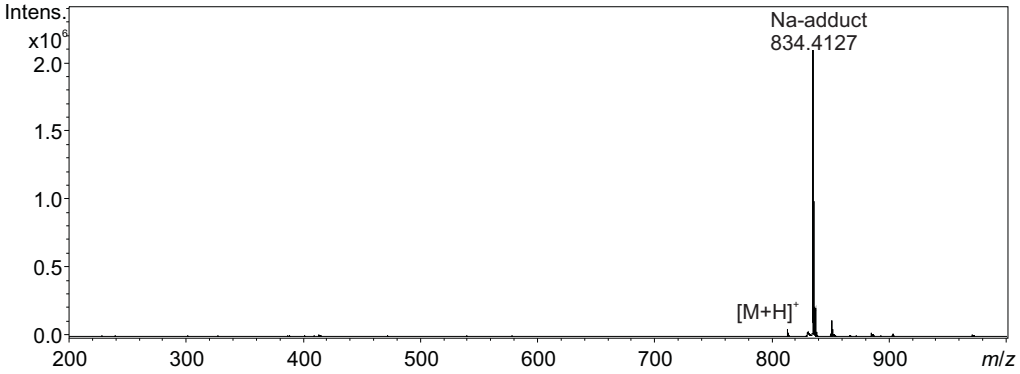

Figure 6.4 MS spectrum of stylissamide B (**2**).

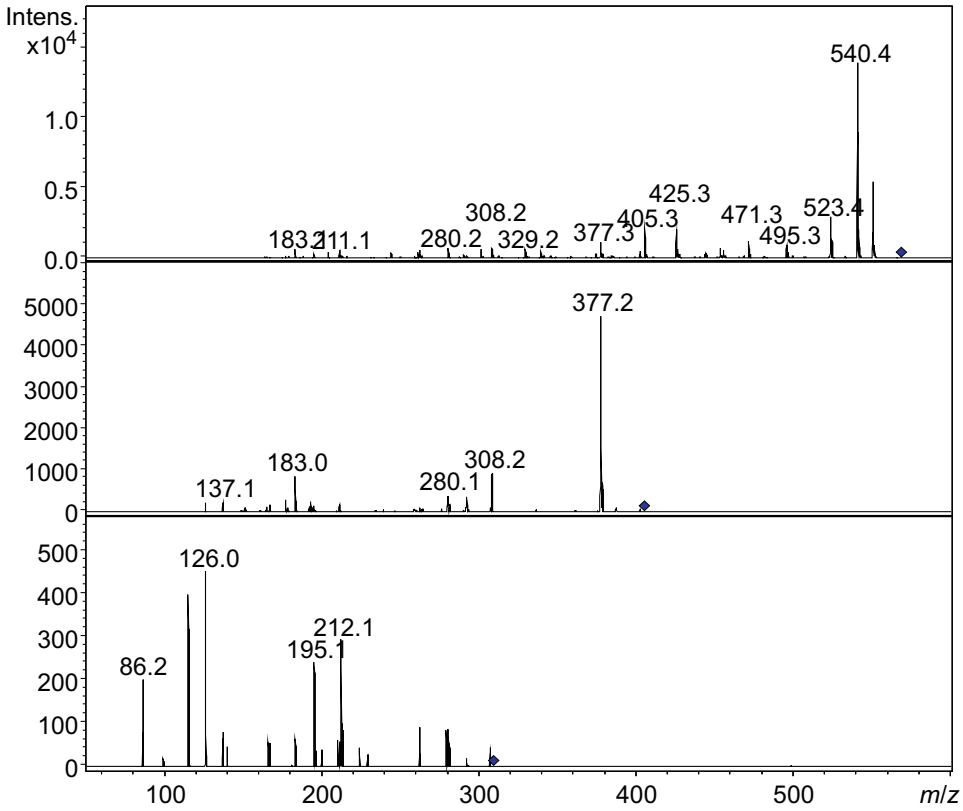

Figure 6.5 Sections of MS^n spectra of stylissamide B (**2**). Precursor ions are marked with filled squares. The fragment at m/z 568.0 lost Tyr to give the fragment at m/z 405.3 (Pro-Pro-Ile-Pro). By the loss of Pro from m/z 405.3 the fragment at m/z 308.2 occurred. Finally the loss of Ile (m/z 195.1) and Pro (m/z 212.1) defined the fragment at m/z 308.2 as Pro-Pro-Ile. Additionally at m/z 86.2 the immonium fragment of Ile and at m/z 126.0 the 1-Oxo-5,6,7,7a-tetrahydro-1H-pyrrolo[1,2-c]oxazol-4-ylium fragment of Pro-Pro[1] occurred.

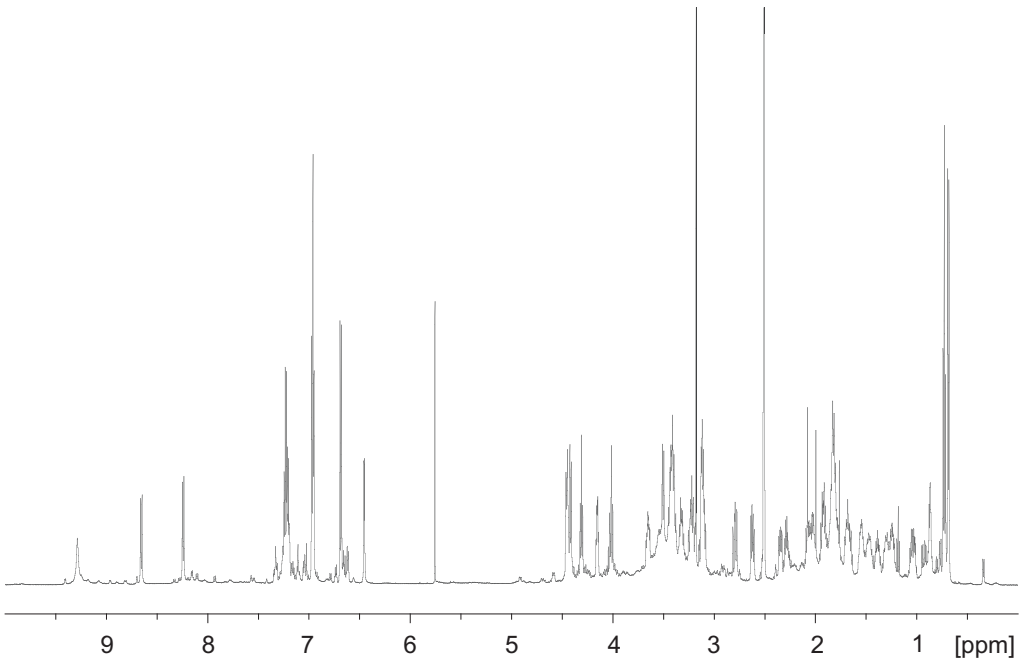

Figure 6.6 1D ^{1}H-NMR spectrum of stylissamide B (**2**) in DMSO-d_6.

Table 6.2 ^{1}H,^{1}H-COSY, sequential ^{1}H,^{1}H-NOESY and ^{1}H,^{13}C-HMBC correlations of stylissamide B (**2**)

	Pos	δC/δN	δH	COSY (H–H)	seq. NOESY (H–H)	HMBC (H–C)
Pro^{1}	N	131.0	-			
	CO	169.75^{c}	-			
	α	60.5	3.49	1-β	7-α	1-CO/4-CO^{c}, 7-CO, 1-β, 1-γ, 1-γ
	β	30.4	1.68	1-α, 1-γ,γ'		1-γ, 1-γ
	β'	30.4	1.53	1-γ,γ'		1-α
	γ	21.0	1.38	1-β,β', 1-γ', 1-γ,γ'		1-CO/4-CO, 1-α, 1-γ
	γ'	21.0	1.29	1-β,β', 1-γ, 1-γ,γ'		
	γ	45.4	3.22	1-γ,γ', 1-γ'	2-NH, 6-NH	1-α, 1-β, 1-γ
	γ'	45.4	3.10	1-γ,γ', 1-γ	2-NH, 6-NH	7-CO, 1-α, 1-β, 1-γ
Phe^{2}	NH	114.0	6.45	2-α	1-γ,γ'	1-CO/4-CO^{c}, 2-CO, 2-α, 2-β
	CO	167.6	-			
	α	52.1	4.14	2-NH, 2-β,β'	3-α	1-CO/4-CO^{c}, 2-CO, 2-β, 2-1
	β, β'	35.8	3.12	2-α	3-α	2-CO, 2-α
	1	135.9	-			
	2/6	127.6	7.22	2-3/5		2-β, 2-1, 2-2/6, 2-3/5, 2-4
	3/5	129.3	6.95	2-2/6		2-α, 2-β, 2-2/6, 2-3/5, 2-4
	4	126.3	7.19			2-1, 2-2/6, 2-3/5
Pro^{3}	N	130.0	-			
	CO	168.5	-			
	α	56.1	4.45	3-β	2-α, 2-β,β', 4-γ,γ'	2-CO, 3-β, 3-γ, 3-γ
	β	29.1	2.03	3-α, 3-β', 3-γ,γ'		3-CO, 3-α, 3-γ, 3-γ
	β'	29.1	1.81	3-β		3-CO, 3-α, 3-γ, 3-γ
	γ, γ'	20.8	1.79	3-β, 3-γ,γ'		3-α, 3-β, 3-γ
	γ	46.4	3.41	3-γ,γ', 3-γ'		3-α, 3-β, 3-γ
	γ'	46.4	3.31	3-γ,γ', 3-γ		2-CO, 3-α, 3-β, 3-γ
Pro^{4}	N	133.0	-			
	CO	169.75^{c}	-			

continued on next page

continued from previous page

	Pos	δC/δN	δH	COSY (H–H)	seq. NOESY (H–H)	HMBC (H–C)
	α	58.3	4.30	4-β,β'	5-α, 6-NH	1-CO/4-CO[c], 3-CO, 4-β, 4-γ, 4-γ
	β	27.5	2.28	4-α, 4-β', 4-γ,γ'		1-CO/4-CO[c], 4-α, 4-γ, 4-γ
	β'	27.5	1.66	4-α, 4-β, 4-γ,γ'		1-CO/4-CO[c], 4-α, 4-γ, 4-γ
	γ	24.9	2.06	4-β,β', 4-γ', 4-γ,γ'		4-α, 4-β, 4-γ
	γ'	24.9	1.91	4-β,β', 4-γ, 4-γ,γ'		4-α, 4-β, 4-γ
	γ	46.7	3.65	4-γ,γ', 4-γ'	3-α	4-α, 4-β, 4-γ
	γ'	46.7	3.42	4-γ,γ', 4-γ	3-α	4-α, 4-β, 4-γ
Pro[5]	N	128.0	-			
	CO	170.2	-			
	α	60.3	4.41	5-β'	4-α, 6-NH	1-CO/4-CO[c], 5-CO, 5-β, 5-γ, 5-γ
	β	30.2	2.33	5-β', 5-γ'		5-CO, 5-α, 5-γ, 5-γ
	β'	30.2	1.90	5-α, 5-β, 5-γ'		5-CO, 5-α, 5-γ, 5-γ
	γ	21.6	1.82	5-γ', 5-γ,γ'		5-α, 5-β
	γ'	21.6	1.46	5-β,β', 5-γ, 5-γ,γ'		5-β, 5-γ
	γ	45.6	3.39	5-γ,γ', 5-γ'		5-α, 5-β, 5-γ
	γ'	45.6	3.21	5-γ,γ', 5-γ	6-NH	1-CO/4-CO[c], 5-α, 5-β, 5-γ
Ile[6]	NH	122.0	8.65	6-α	4-α, 5-α, 5-γ,γ', 7-NH	5-CO, 6-α, 6-β
	CO	169.8	-			
	α	56.8	4.01	6-NH, 6-β	7-NH	5-CO, 6-CO, 6-β, 6-β-Me, 6-γ
	β	34.8	1.83	6-α, 6-β-Me, 6-γ'	7-NH	6-α, 6-β-Me, 6-γ, 6-γ
	β-Me	15.3	0.68	6-β		6-α, 6-β, 6-γ
	γ	24.6	1.23	6-γ', 6-γ		6-α, 6-β, 6-β-Me, 6-γ
	γ'	24.6	1.04	6-β, 6-γ, 6-γ		6-α, 6-β, 6-β-Me, 6-γ
	γ	10.6	0.72	6-γ,γ'	7-NH	6-β, 6-γ
Tyr[7]	NH	122.0	8.24	7-α	6-NH, 6-α, 6-β, 6-γ	6-CO, 7-α, 7-β
	CO	171.2	-			
	α	50.9	4.43	7-NH, 7-β,β'	1-α	6-CO, 7-CO, 7-β, 7-1
	β	37.2	2.78	7-α, 7-β'		7-CO, 7-α, 7-1, 7-2/6
	β'	37.2	2.61	7-α, 7-β		7-CO, 7-α, 7-1, 7-2/6
	1	126.2	-			
	2/6	129.8	6.96	7-3/5		7-α, 7-β, 7-2/6, 7-3/5, 7-4
	3/5	114.7	6.67	7-2/6		7-β, 7-1, 7-2/6, 7-3/5, 7-4
	4	155.9	-			
	OH	-	9.28			

[a] Signals are overlapped. Spin systems were established with the aid of $^{1}H,^{13}C$- and $^{1}H,^{15}N$-HSQC-TOCSY experiments.
[b] Intra-residual protons are overlapped.
[c] Carbonyl are overlapped.

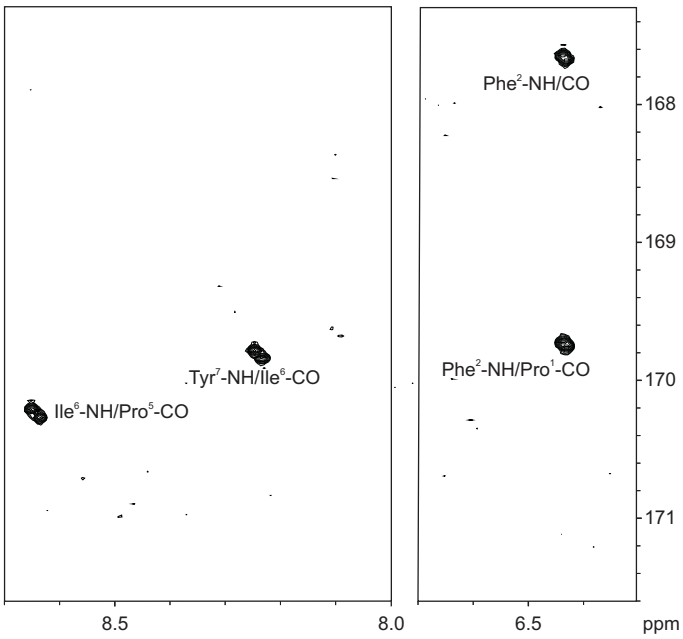

Figure 6.7 Section 1 (amide proton area) of the semi-selective ^{1}H,^{13}C-HMBC spectrum of stylissamide B (**2**) in DMSO-d_6.

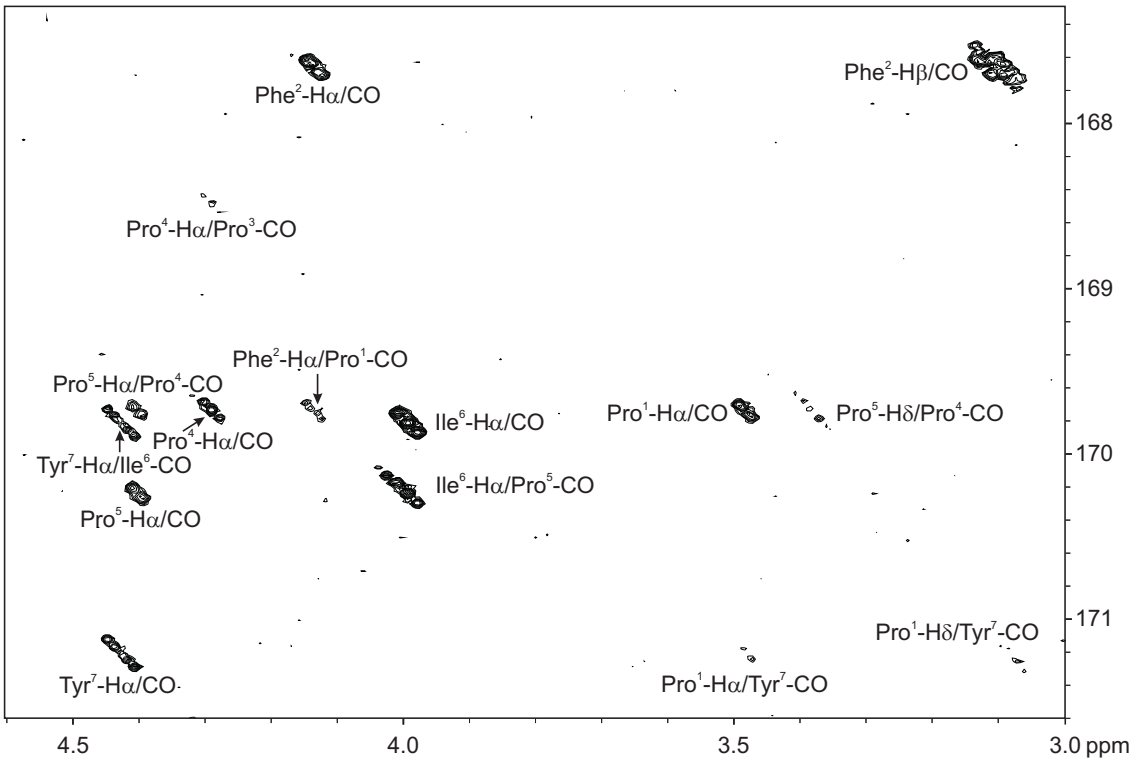

Figure 6.8 Section 2 (α- and δ-proton area) of the semi-selective ^{1}H,^{13}C-HMBC spectrum of stylissamide B (**2**) in DMSO-d_6.

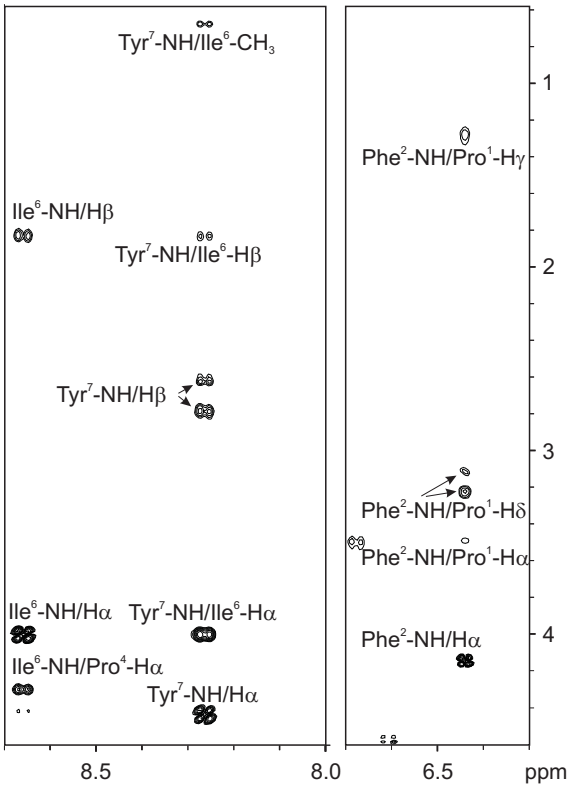

Figure 6.9 Section 1 (amide proton area) of the ^{1}H,^{1}H-NOESY spectrum of stylissamide B (**2**) in DMSO-d_6.

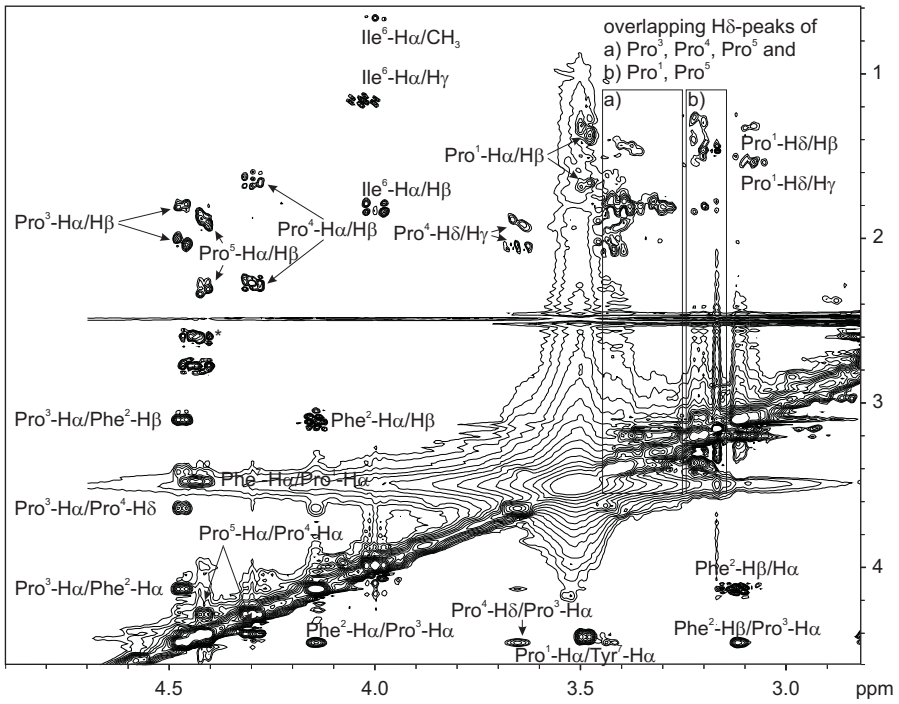

Figure 6.10 Section 2 (α- and δ-proton area) of the ^{1}H,^{1}H-NOESY spectrum of stylissamide B (**2**) in DMSO-d_6.

Stylissamide C

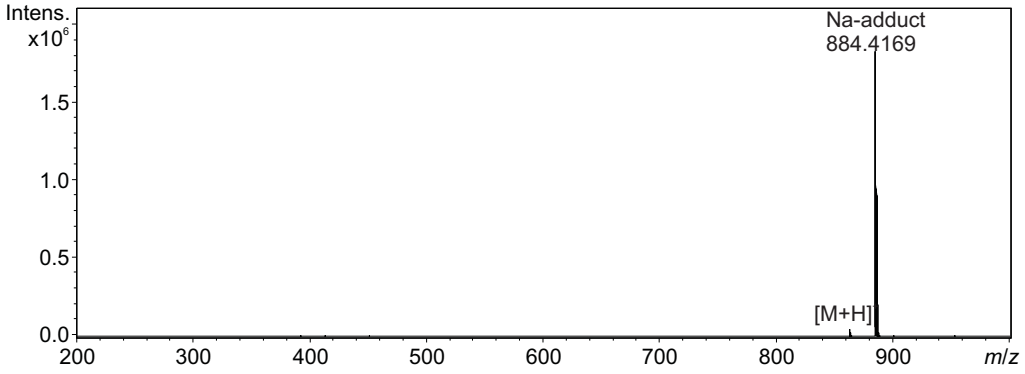

Figure 6.11 MS spectrum of stylissamide C (**3**).

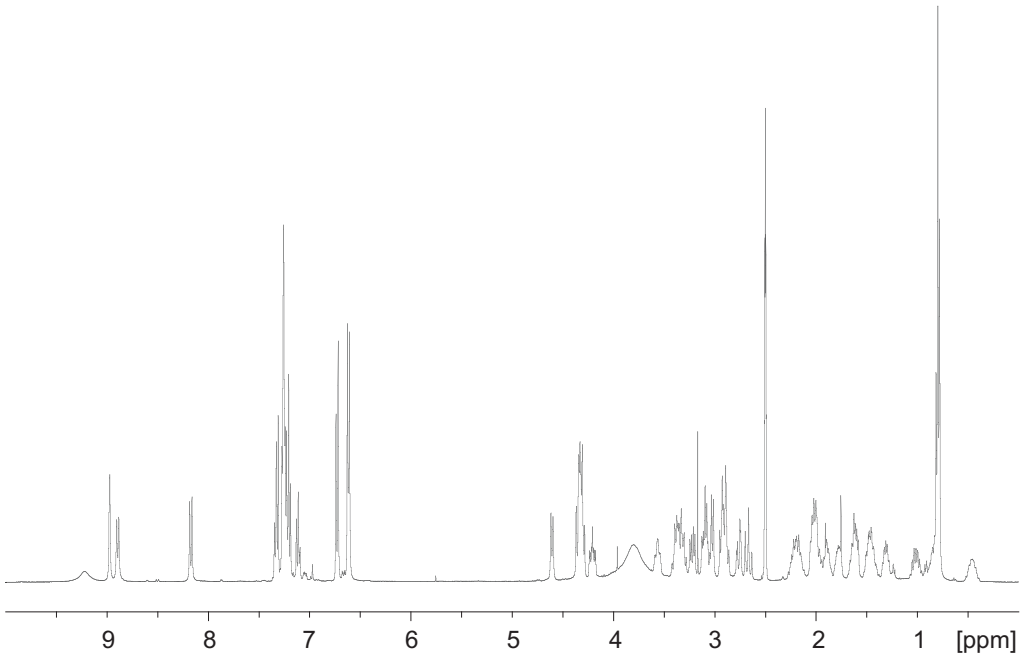

Figure 6.12 1D ^{1}H-NMR spectrum of stylissamide C (**3**) in DMSO-d_6.

Table 6.3 ^{1}H,^{1}H-COSY, sequential ^{1}H,^{1}H-NOESY and ^{1}H,^{13}C-HMBC correlations of stylissamide C (**3**).

	Pos	δC/δN	δH	COSY (H–H)	seq. NOESY (H–H)	HMBC (H–C)
Pro^{1}	N	120.0	-			
	CO	169.8	-			
	α	61.0	4.36	1-β,β'	7-δ, 7-β	7-CO, 1-CO, 1-β, 1-γ, 1-δ
	β	30.9	2.22	1-α, 1-β', 1-γ,γ'		1-CO, 1-α
	β'	30.9	2.04	1-α, 1-β, 1-γ,γ'		1-CO, 1-δ
	γ	21.3	1.78	1-β,β', 1-γ', 1-δ,δ'		
	γ'	21.3	1.45	1-β,β', 1-γ', 1-δ,δ'	2-NH	

continued on next page

continued from previous page

	Pos	δC/δN	δH	COSY (H–H)	seq. NOESY (H–H)	HMBC (H–C)
	δ, δ'	45.7	3.38	1-γ,γ'	2-NH	7-CO, 1-α, 1-β, 1-γ
Tyr[2]	NH	113.0	6.62[a,b]	2-α	1-δ,δ', 1-γ'	[b] 1-CO, 2-CO, 2-α, 2-1, 2-2/6, 2-3/5, 2-4
	CO	168.3	-			
	α	52.0	4.33	2-NH[a], 2-β,β'		1-CO, 2-CO, 1-1, 1β
	β	34.5	3.22	2-α, 2-β'	3-α	2-CO, 2-α, 2-1, 2-2/6
	β'	34.5	2.92	2-α, 2-β		2-CO, 2-α, 2-1, 2-2/6
	1	125.3	-			
	2/6	130.3	6.73	2-3/5[a]		2-α, 2-β, 2-2/6, 2-3/5, 2-4
	3/5	114.5	6.62[a,b]	2-2/6		[b] 1-CO, 2-CO, 2-α, 2-1, 2-2/6, 2-3/5, 2-4
	4	155.9	-			
	OH	-	9.21			
Pro[3]	N	129.0	-			
	CO	171.5	-			
	α	57.3	4.60	3-β,β'[a],	4-NH, 4-α, 4-β', 2-β	3-CO, 3-β, 3-γ, 3-δ
	β	30.5	2.17	3-α, 3-β'[a], 3-γ[a],γ'		3-CO
	β'	30.5	2.01[a,b]	3-β, 3-γ'		[b] 3-CO, 3-δ
	γ	21.0	2.00[a,b]	3-γ', 3-β, 3-δ,δ'		[b] 3-CO, 3-δ
	γ'	21.0	1.89	3-β,β'[a], 3-γ, 3-δ,δ'		3-α
	δ	46.5	3.57	3-γ[a],γ', 3-δ'		2-CO, 3-β, 3-γ
	δ'	46.5	3.32	3-γ[a],γ', 3-δ		3-α, 3-β, 3-γ
Phe[4]	NH	124.0	8.96	4-α[a]	3-α	3-CO, 4-CO, 4-α, 4-β
	CO	169.0	-			
	α	53.3	4.32[a]	4-β,β'	3-α, 5-α	3-CO
	β	35.8	3.10	4-α[a], 4-β'		4-CO, 4-α, 4-1, 4-2/6
	β'	35.8	2.93	4-α[a], 4-β	3-α	4-CO, 4-α, 4-1, 4-2/6
	1	135.6	-			
	2/6	128.9	7.25[a,b]	04.03.05		[b] 4-β, 4-1
	3/5	128.4	7.32	4-2/6[a], 4-4[a]		4-1, 4-2/6, 4-3,5
	4	126.7	7.25[a,b]			[b] 4-β, 4-1
Pro[5]	N	132.0	-			
	CO	169.6	-			
	α	59.6	3.03	5-β,β'	4-α, 6-NH	4-CO, 5-CO, 5-β, 5-γ
	β	29.8	1.61	5-α, 5-β', 5-γ'		5-CO, 5-γ, 5-δ
	β'	29.8	0.84	5-α, 5-β, 5-γ,γ'		5-CO, 5-α, 5-γ
	γ	20.5	1.32	5-β', 5-γ', 5-δ,δ'		5-α, 5-β
	γ'	20.5	0.47	5-β,β', 5-γ, 5-δ,δ'		
	δ	45.5	3.09	5-γ,γ', 5-δ'	4-β'	5-γ
	δ'	45.5	2.89	5-γ,γ', 5-δ	4-β', 6-NH	5-β, 5-γ
Phe[6]	NH	122.0	8.89	6-α	5-α, 5-δ'	5-CO, 6-β
	CO	169.7	-			
	α	54.1	4.22	6-NH, 6-β,β'	7-NH	6-CO, 6-β, 6-1
	β	35.5	2.76	6-α, 6-β'	7-α	6-CO, 6-1, 6-2/6
	β'	35.5	2.68	6-α, 6-β		6-CO, 6-1, 6-2/6
	1	138.9	-			
	2/6	128.6	7.23	06.03.05		6-1, 6-2/6, 6-4
	3/5	127.3	7.21	6-2/6, 6-4		6-1, 6-3/5
	4	125.4	7.12	06.03.05		6-1, 6-2/6, 6-4
Ile[7]	NH	115.0	8.16	7-α[a]		6-CO, 7-α
	CO	171.7	-			
	α	53.0	4.32[a]	7-NH, 7-β	6-α, 6-β	6-CO, 7-CO, 7-β, 7-β-Me, 7-γ
	β	37.3	1.64	7-β-Me, 7-γ,γ'		7-α, 7-β-Me, 7-γ, 7-δ
	β-Me	14.5	0.79	7-β		7-α, 7-β, 7-γ
	γ	23.8	1.49	7-β, 7-γ', 7-δ		7-α, 7-β, 7-β-Me, 7-δ
	γ'	23.8	1.02	7-β, 7-γ, 7-δ		7-α, 7-β, 7-β-Me, 7-δ
	δ	10.5	0.80	7-γ,γ'		7-γ

[a] Signals are overlapped. Spin systems were established with the aid of $^{1}H,^{13}C$- and $^{1}H,^{15}N$-HSQC-TOCSY experiments.
[b] Intra-residual protons are overlapped.

Stylissamide D

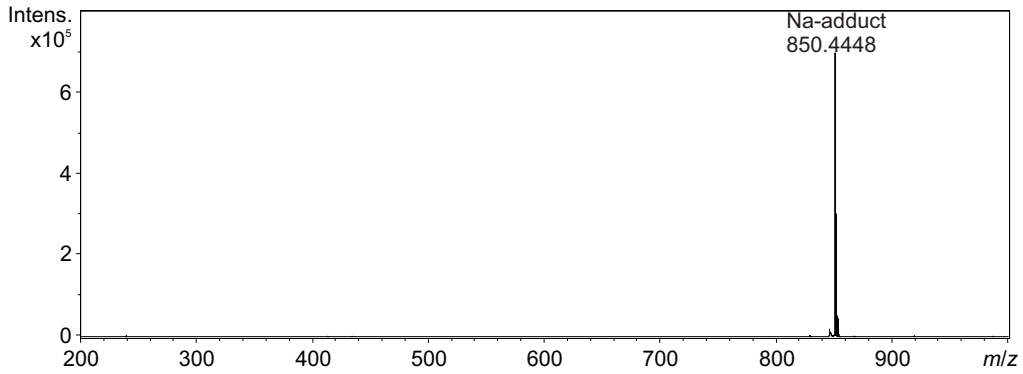

Figure 6.13 MS spectrum of stylissamide D (**4**).

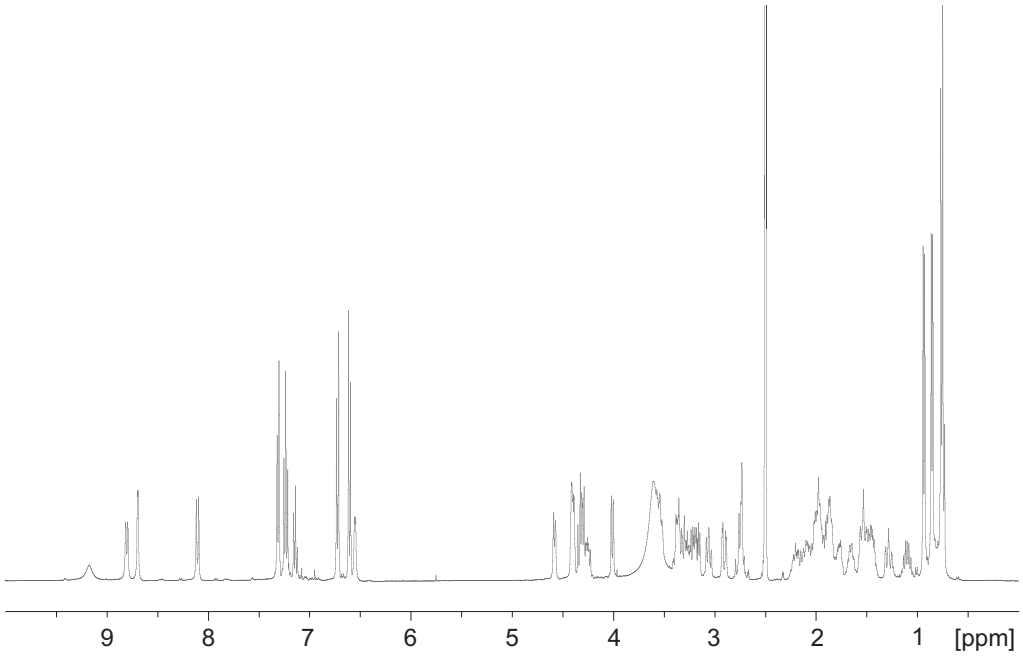

Figure 6.14 1D ^{1}H-NMR spectrum of stylissamide D (**4**) in DMSO-d_6.

Table 6.4 ^{1}H,^{1}H-COSY, sequential ^{1}H,^{1}H-NOESY and ^{1}H,^{13}C-HMBC correlations of stylissamide D (**4**)

	Pos	δC/δN	δH	COSY (H–H)	seq. NOESY (H–H)	HMBC (H–C)
Pro^{1}	N	131.0	-			
	CO	169.4	-			
	α	60.9	4.31	1-β,β'	7-δ	1-CO, 7-CO (weak), 1-β, 1-γ, 1-δ
	β	31.0	2.20	1-α, 1-β', 1-γ'		1-CO, 1-α
	β'	31.0	2.00	1-α, 1-β, 1-γ'		1-CO
	γ	21.3	1.77	1-γ', 1-δ,δ'		
	γ'	21.3	1.48	1-β,β', 1-γ, 1-δ,δ'		

continued on next page

continued from previous page

	Pos	δC/δN	δH	COSY (H–H)	seq. NOESY (H–H)	HMBC (H–C)
	δ, δ'	45.7	3.37	1-γ,γ'		1-β, 1-γ
Tyr[2]	NH	112.0	6.57	2-α[a]		
	CO	168.2	-			
	α	51.7	4.41[a,c]	2-NH, 2-β,β'		[c] 1-CO, 2-CO, 3-CO, 4-CO, 2-β, 2-1
	β	34.8	3.17	2-α[a], 2-β'		2-CO, 2-α, 2-1, 2-2/6
	β'	34.8	2.91	2-α[a], 2-β	3-α	2-CO, 2-1, 2-2/6
	1	125.3	-			
	2/6	130.2	6.72	2-3/5		2-β, 2-2/6, 2-4
	3/5	114.6	6.61	2-2/6		2-1, 2-3/5, 2-4
	4	155.7	-			
	OH	-	9.17			
Pro[3]	N	130.0	-			
	CO	171.6	-			
	α	57.4	4.58	3-β,β'	2-β', 4-NH	2-CO (weak), 3-β, 3-γ, 3-δ
	β	30.1	2.11	3-α, 3-β', 3-γ,γ'		
	β'	30.1	1.95	3-α, 3-β, 3-γ'		
	γ	21.4	2.05	3-β, 3-γ', 3-δ,δ'		
	γ'	21.4	1.86	3-β,β', 3-γ, 3-δ,δ'		
	δ	46.6	3.54	3-γ,γ', 3-δ'		
	δ'	46.6	3.29	3-γ,γ', 3-δ		
Leu[4]	NH	125.0	8.70	4-α[a]	3-α	3-CO, 4-CO
	CO	170.5	-			
	α	51.1	4.42[a,c]	4-NH, 4-β,β'	5-α	[c] 1-CO, 2-CO, 3-CO, 4-CO
	β	37.9	1.53	4-α[a], 4-β', 4-γ		
	β'	37.9	1.28	4-α[a], 4-β, 4-γ	5-α	
	γ	23.9	1.87	4-β,β', 4-δ,δ'		
	δ	23.2	0.94	4-γ		4-β, 4-γ, 4-δ'
	δ'	20.3	0.86	4-γ		4-β, 4-δ
Pro[5]	N	127.0	-			
	CO	170.7	-			
	α	59.9	4.02	5-β,β'	4-α, 4-β'	4-CO, 5-CO, 5-β, 5-γ, 5-δ
	β	31.0	1.99	5-α, 5-β', 5-γ,γ'		5-CO, 5-δ
	β'	31.0	1.90	5-α, 5-β, 5-γ,γ'		5-CO, 5-α
	γ	21.0	1.54	5-β,β', 5-γ'		5-α
	γ'	21.0	0.82	5-β,β', 5-γ, 5-δ,δ'		
	δ	46.1	3.23	5-γ', 5-δ'		5-γ
	δ'	46.1	3.06	5-γ', 5-δ		5-β
Phe[6]	NH	122.0	8.81	6-α		
	CO	169.5	-			
	α	54.6	4.25	6-NH, 6-β,β'	7-NH	5-CO, 6-CO, 6-β, 6-1
	β, β'	35.2	2.74	6-α		6-CO, 6-α, 6-1, 6-2/6
	1	139.2	-			
	2/6	128.8	7.31	6-3/5		6-β, 6-2/6, 6-4
	3/5	127.6	7.24	6-2/6, 6-4		6-1, 6-3/5
	4	125.7	7.14	6-3/5		6-1, 6-2/6
Ile[7]	NH	115.0	8.10	7-α	6-α	6-CO
	CO	171.2	-			
	α	52.6	4.33	7-NH, 7-β		6-CO, 7-CO, 7-β, 7-β-Me, 7-γ
	β	36.9	1.66	7-α, 7-β-Me[a], 7-γ'		
	β-Me	14.4	0.77[a,b]	7-β		
	γ	23.5	1.45	7-γ', 7-δ[a]		7-β
	γ'	23.5	1.10	7-β, 7-γ, 7-δ[a]		7-α, 7-β, 7-β-Me, 7-δ
	δ	10.1	0.76[a,b]	7-γ,γ'		7-γ

[a] Signals are overlapped. Spin systems were established with the aid of $^{1}H,^{13}C$- and $^{1}H,^{15}N$-HSQC-TOCSY experiments.
[b] Intra-residual protons are overlapped.
[c] Carbonyls are overlapped.

Table 6.5 Differential ^{13}C values and NOESY correlations necessary to determine the configuration of proline residues in the stylissamides A-D (**1**-**4**).

		$\Delta\delta_{\beta\gamma}$ (ppm)	$H\alpha_{(i)}$-$H\alpha_{(i-1)}$ NOE correlation	configuration
Stylissamide A (**1**)	Pro^1	3.5	invisible	*trans*
	Pro^4	3.5	invisible	*trans*
	Pro^5	9.4	visible	*cis*
Stylissamide B (**2**)	Pro^1	9.4	visible	*cis*
	Pro^3	8.3	visible	*cis*
	Pro^4	2.6	invisible	*trans*
	Pro^5	8.6	visible	*cis*
Stylissamide C (**3**)	Pro^1	9.6	overlapped if present	*cis*
	Pro^3	9.5	visible	*cis*
	Pro^5	9.3	visible	*cis*
Stylissamide D (**4**)	Pro^1	9.7	overlapped if present	*cis*
	Pro^3	8.7	overlapped if present	*cis*
	Pro^5	10	visible	*cis*

New haliclamines E and F from the Arctic sponge *Haliclona viscosa*†

Gesine Schmidt, Christoph Timm and Matthias Köck*

Received 27th February 2009, Accepted 13th May 2009
First published as an Advance Article on the web 18th June 2009
DOI: 10.1039/b904157e

The Arctic sponge *Haliclona viscosa* is a rich source of 3-alkyl pyridinium alkaloids. Herein, we report the identification of two new haliclamines from the crude extract of this sponge. Due to the lack of sponge material, identification relied on HR-LCMS measurements and comparison with synthetic compounds.

Introduction

The sponge genus *Haliclona* comprises more than 400 species with a worldwide distribution and is a rich source of alkaloids, many of them with cytotoxic properties. Examples include the manzamines,[1] papuamines,[2] haliclonadiamines,[3] haliclamines,[4] halicyclamines,[5] and haliclonacyclamines.[6] The species *Haliclona viscosa* contains several types of 3-alkyl pyridinium alkaloids (3-APA) such as viscosaline,[7] the trimeric viscosamine,[8] the dimeric cyclostellettamines and haliclamines[9] and the first cyclic monomer of the 3-APA motif.[10] In our continuous search for bioactive compounds, we investigated the crude extract of a *H. viscosa* specimen collected in 2003. It contained two new 3-alkyl tetrahydropyridinium compounds, haliclamines E (**1**) and F (**2**), in addition to the main metabolites, haliclamines C (**3**) and D (**4**) (Scheme 1). Herein, we report the identification of the new compounds from the crude extract.

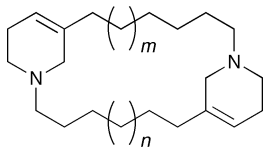

Haliclamines (**1**-**4**)

1/N: $m = 4$, $n = 5$
2/R: $m = 6$, $n = 6$
3/O: $m = 4$, $n = 6$
4/Q: $m = 5$, $n = 6$

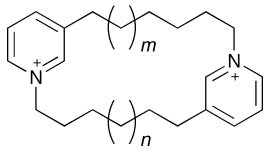

Cyclostellettamines (N-Q)

Scheme 1 Structural formulae of haliclamines E (**1**), F (**2**), C (**3**) and D (**4**), and cyclostellettamines N, R, O and Q.

Alfred-Wegener-Institut für Polar- und Meeresforschung, Am Handelshafen 12, 27570, Bremerhaven, Germany. E-mail: mkoeck@awi.de; Fax: +49 (0) 471 4831 1425; Tel: +49 (0) 471 4831 1498

† Electronic supplementary information (ESI) available: MS spectra of the natural and the synthetic haliclamines; NMR spectra and shifts of the synthetic haliclamines; synthetic pathway of compounds **1**–**4**. See DOI: 10.1039/b904157e

Results and discussion

A freeze-dried specimen of *Haliclona viscosa*, collected off Blomstrandhalvøya in Kongsfjorden, Svalbard, by SCUBA diving in 2003 was exhaustively extracted with a 1:1 mixture of methanol/dichloromethane. The crude extract was subjected to an LCMS analysis. In addition to the main metabolites haliclamines C (**3**) and D (**4**),[9] it contained several unknown compounds. Since the sponge material was sparse and only a small amount of crude extract was available, further isolation of these compounds, followed by NMR spectroscopy, was not possible. However, the combined application of HPLC and HRMS indicated that two of the secondary metabolites were related to the haliclamines and the cyclostellettamines.

The high-resolution mass spectrum for compound **1** at a retention time (t_R, Fig. 1) of 27.2 min, obtained from ESI ionization, suggested the molecular formula $C_{29}H_{52}N_2$ (*m/z* 429.4217 $[M + H]^+$). The molecular weight was 14 mass units less than that of haliclamine C (**3**, *m/z* 443.4320 $[M + H]^+$; $t_R = 28.7$ min), indicating that one alkyl chain of compound **1** was by one methylene group shorter than haliclamine C (**3**). The atmospheric pressure ionization-collision induced dissociation-MS/MS (API-CID-MS/MS) spectrum of haliclamine C (**3**) showed two fragment peaks of *m/z* 208.210 and *m/z* 236.240, which correspond to a tetrahydropyridinium (THP) moiety connected to an alkyl chain of

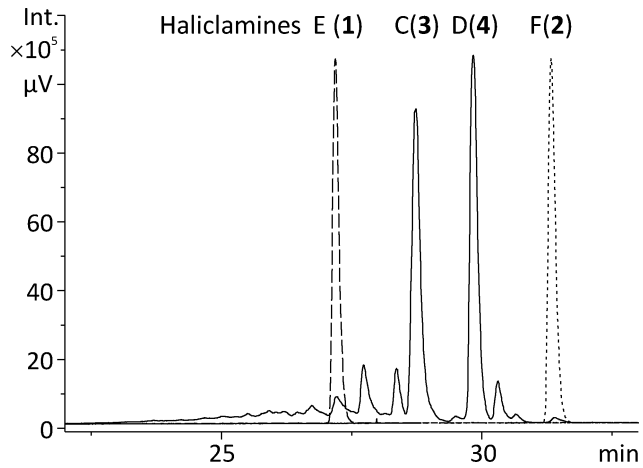

Fig. 1 Comparison of retention times of synthetic haliclamines E (**1**, dashed line) and F (**2**, dotted line) with the crude extract of *Haliclona viscosa* (continuous line).

Table 1 Comparison of mass spectrometric data of the naturally occurring and the synthetic haliclamine E (**1**). Masses were acquired with a Bruker micrOTOF mass spectrometer equipped with an ESI source

Ion[a]	Natural compound **1**	Synthetic compound **1**
$[M + H]^+$	$m/z = 429.4235$, $\Delta m = 7.5$ ppm	$m/z = 429.4217$, $\Delta m = 3.3$ ppm
$[M + 2H]^{2+}$	n.a.	$m/z = 215.2160$, $\Delta m = 10.1$ ppm
TFA salt $[M + H]^+$	n.a.	$m/z = 543.4123$, $\Delta m = 1.7$ ppm
fragment C_n	$m/z = 208.2118$, $\Delta m = 27.9$ ppm	$m/z = 208.2071$, $\Delta m = 5.5$ ppm
fragment C_m	$m/z = 222.2261$, $\Delta m = 20.1$ ppm	$m/z = 222.2220$, $\Delta m = 1.8$ ppm

[a] The doubly charged molecular ion originates from an experiment with a low voltage difference between capillary exit and skimmer. The singly charged fragments C_n/C_m consists of a tetrahydropyridinium moiety and a side chain of nine/ten methylene groups.

9 and 11 carbons, respectively.[9] The mass spectrum of compound **1** showed two similar fragments at *m/z* 208.2118 and *m/z* 222.2261, which suggested that **1** contains side chains of 9 and 10 methylene groups in addition to the two THP moieties. To add structural proof to this suggestion, the proposed compound **1** was synthesized by reduction of the corresponding cyclostellettamine.[11] The cyclostellettamine was prepared following a method described by Baldwin *et al.*[11] Subsequently, chromatographic and mass spectrometric data of the synthetic product were compared to those of the natural compound **1**.

The synthetic and the natural compound **1** eluted at the same retention time (Fig. 1). Both the molecular weight and the fragments of the synthetic product agreed with the natural compound. The synthetic product **1** showed a molecular mass of *m/z* 429.4217 ($[M + H]^+$), a doubly charged molecular ion at *m/z* 215.2160 and a peak at *m/z* 543.4123 resulting from salt formation with the TFA anion introduced during chromatographic purification (Fig. 2, Table 1). The mass spectrum of the synthetic compound also contained two peaks of lower intensity at *m/z* 208.2071 and *m/z* 222.2220 which correspond to the two fragments expected from THP moieties with C_9 and C_{10} alkyl chains each. Under API-CID-MS/MS (Skimmer-CID) conditions, these fragments became more pronounced whereas the doubly charged molecular ion and the TFA salt ion were eliminated (see Supporting Information for details†).

Compound **2** (*m/z* 471.4664 $[M + H]^+$; $t_R = 31.3$ min) was 14 mass units larger than haliclamine D (**4**, *m/z* 457.4470 $[M + H]^+$; $t_R = 29.8$ min) and suggested the molecular formula $C_{32}H_{58}N_2$. As haliclamine D (**4**) includes two chains of 10 and 11 methylene groups, respectively,[9] compound **2** was likely to contain chains of either 10 and 12 or chains of equal length of 11 methylene groups. Since the spectrum of the natural compound **2** also comprised a singly charged fragment at *m/z* 236.2422 it was concluded that the alkyl chains contained 11 methylene groups, and hence this compound was synthesized and compared. The synthetic product eluted at the same retention time (Fig. 1) and showed a similar mass spectrum as the natural compound **2** (Fig. 3, Table 2). It showed a molecular mass of *m/z* 471.4664 ($[M + H]^+$), a doubly charged molecular ion at *m/z* 236.2364 and a TFA adduct at *m/z* 585.4567. An API-CID-MS/MS experiment eliminated the TFA salt ion

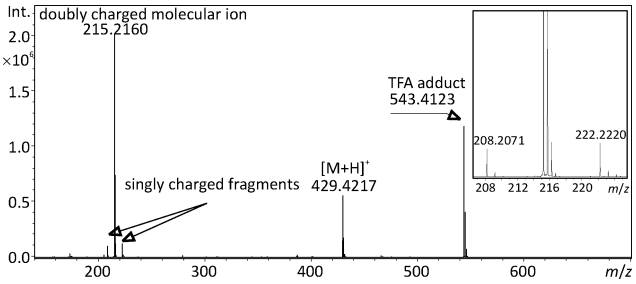

Fig. 2 ESI-TOF-MS spectrum of synthetic haliclamine E (**1**). The section shows a detail of the doubly charged molecular ion and the two singly charged fragments.

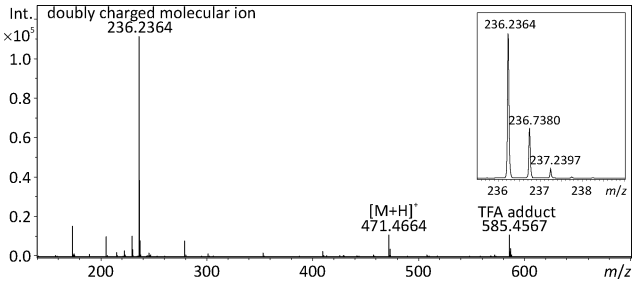

Fig. 3 TOF-MS spectrum of synthetic haliclamine F (**2**) under standard ESI conditions. The section shows a detail of the doubly charged molecular ion.

Table 2 Comparison of mass spectrometric data of the naturally occurring and the synthetic haliclamine F (**2**). Masses were acquired with a Bruker micrOTOF mass spectrometer equipped with an ESI source

Ion[a]	Natural compound **2**	Synthetic compound **2**
$[M + H]^+$	$m/z = 471.4710$, $\Delta m = 7.9$ ppm	$m/z = 471.4664$, $\Delta m = 1.8$ ppm
$[M + 2H]^{2+}$	n.a.	$m/z = 236.2364$, $\Delta m = 3.9$ ppm
TFA salt $[M + H]^+$	n.a.	$m/z = 585.4567$, $\Delta m = 5.8$ ppm
fragment $C_n = C_m$	$m/z = 236.2422$, $\Delta m = 21.0$ ppm	$m/z = 236.2355$, $\Delta m = 7.5$ ppm

[a] The doubly charged molecular ion originates from an experiment with low voltage difference between capillary exit and skimmer. The singly charged fragments C_n and C_m consist of a tetrahydropyridinium moiety and a side chain of 11 methylene groups, each.

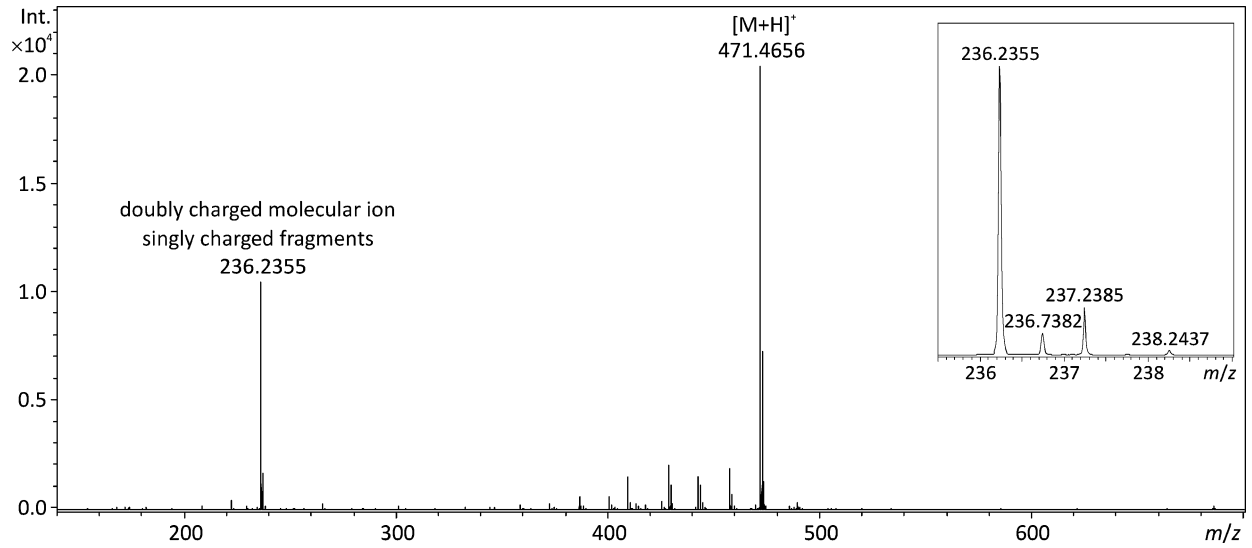

Fig. 4 ESI-TOF-MS spectrum of the synthetic haliclamine F (**2**) resulting from an API-CID-MS/MS experiment. The section shows a detail of the doubly charged molecular ion which is superimposed by the singly charged fragment.

and resulted in a peak at *m/z* 236.2355 that contained the isotopic pattern of the doubly charged molecular ion superimposed by the singly charged fragment (THP + C_{11} alkyl chain, Fig. 4).

Conclusions

Our investigations proved again that *Haliclona* sponges from Arctic waters are a rich source of interesting secondary metabolites. The two new members of the haliclamine family, the haliclamines E (**1**) and F (**2**), were directly identified from a sponge crude extract using a HR-LCMS method. In this context the identification was supported by the known biosynthetic origin of the 3-alkyl pyridinium alkaloids which are a common theme in sponges of the order Haplosclerida. Furthermore, a direct comparison was possible because the compounds were available through synthesis.

Experimental

Animal material

A specimen of *Haliclona viscosa* was collected off Blomstrandhalvøya by SCUBA diving in Kongsfjorden, Svalbard in June 2003. A voucher specimen is deposited at the Zoölogisch Museum, Amsterdam, The Netherlands (voucher reference MAK301, no ZMA registration number available yet). Samples of *H. viscosa* were divided into portions, immediately frozen after collection and kept at –20 °C until extraction.

Extraction and analysis of the natural compounds

Freeze-dried sponge tissue (4.18 g) was exhaustively extracted at room temperature with a 1:1 mixture of methanol and dichloromethane (4 × 80 mL). The resulting crude extract (1.22 g, 29.2%) was investigated by HR-LCMS on an Agilent 1100 series instrument coupled to a micrOTOF$_{LC}$ mass spectrometer (Bruker Daltonics). The HPLC was equipped with a Waters XTerra MS C_{18} column (3 × 150 mm, 3.5 µm, 30 °C) and a MeCN/H_2O (5 mM NH_4OAc) gradient (30% MeCN/70% H_2O to 50% MeCN/50% H_2O in 30 min) at a flow rate of 0.4 mL min^{-1} was applied. UV spectra were recorded with a DAD at 260 nm. The mass spectrometer was equipped with an ESI source (capillary exit 100 V, skimmer 50 V).

Synthesis, purification and analysis of the synthetic compounds

All solvents were purified by distillation, with the exception of THF which was distilled from sodium/benzophenone under argon. A solution of the respective cyclostellettamine (0.13 mmol, cyclostellettamine N or R, Scheme 1) in 10 mL CH_2Cl_2/MeOH (1:1) was cooled to –40 °C and $NaBH_4$ (0.10 g, 2.63 mmol) was added. After stirring for two hours in the cold, the mixture was allowed to warm up to room temperature, 5 mL of 2 M NaOH solution were added and it was stirred for an additional 15 minutes. It was then poured onto 15 mL water and extracted with CH_2Cl_2 (3 × 10 mL). Drying of the combined organic extracts over $MgSO_4$ and removal of the solvent yielded the crude product (47 mg of **1**, 29 mg of **2**). The crude product was purified *via* preparative HPLC and yielded 32 mg (32%) of haliclamine E (**1**) and 20 mg (20%) of haliclamine F (**2**) as TFA salts.

Purification of the synthetic compounds was performed on a Jasco 1500 series HPLC system. It was equipped with a Prontosil Eurobond RP_{18} column (20 × 250 mm, 5 µm, 40 °C) applying a MeCN (0.1%TFA)/H_2O (0.1% TFA) gradient (30% MeCN/70% H_2O isocratic for 5 min; to 60% MeCN/40% H_2O in 30 min; isocratic for 5 minutes; to 100% MeCN in 10 min) with a flow rate of 8 mL min^{-1}. Analytical HPLC used a Kromasil RP_{18} column (4.6 × 250 mm, 5 µm, 40 °C), as before with a MeCN (0.1%TFA)/H_2O (0.1% TFA) gradient (from 100% H_2O to 80% MeCN/20% H_2O in 40 min; to 100% MeCN in 5 min) at a flow rate of 1 mL min^{-1}. UV spectra were recorded during HPLC analyses with a DAD (Jasco).

ESI mass spectra of the synthetic compounds were acquired using the micrOTOF$_{LC}$ mass spectrometer (Bruker Daltonics) in

direct injection mode and the same voltages as described for the natural compounds. For API-CID-fragmentation, the voltage of the capillary exit was raised to 180 V while the voltage of the skimmer 1 remained at 50 V. The MS system was externally calibrated in positive mode using sodium formiate cluster prior to every analysis.

Column chromatography was performed on silica gel 60 (Merck, particle size 0.04–0.063 mm). Aluminium plates precoated with Merck silica 60 were used for TLC. Compounds were visualized by UV irradiation (254 nm) or dyeing with $KMnO_4$ solution (1 g $KMnO_4$, 6.6 g K_2CO_3, 2 mL 5% NaOH solution in 100 mL H_2O). NMR spectra were recorded with a Bruker AM 300 (300 MHz) spectrometer. All experiments were performed at 300 K. Chemical shifts are quoted in ppm and are referenced to the appropriate solvent signal. FT-IR spectra were recorded on a Perkin-Elmer 1600 series spectrometer. Absorption maxima are reported in wave numbers and the following abbreviations are used: s strong, m medium, w weak.

Haliclamine E (1). White amorphous powder. TLC R_f: 0.43 (9:1 CH_2Cl_2/MeOH ($KMnO_4$)). IR (KBr, cm^{-1}): ν = 2932 m, 2860 m, 2623 w, 1685 s, 1465 w, 1406 w, 1198 s, 1162 s, 1133 s, 828 m, 797 m, 719 m. The compound does not show UV absorption. HRMS ((+)-ESI): m/z = 429.4217 (calcd. 429.4203 for $C_{29}H_{53}N_2^+$ $[M + H]^+$); m/z = 215.2160 (calcd. 215.2138 for $C_{29}H_{54}N_2^{2+}$ $[M + H]^{2+}$); m/z = 543.4123 (calcd. 543.4127 for $C_{29}H_{54}N_2^{2+} \times C_2F_3O_2^-$ $[M + H]^+$).

Haliclamine F (2). White amorphous powder. TLC R_f: 0.43 (9:1 CH_2Cl_2/MeOH ($KMnO_4$)). IR (KBr, cm^{-1}): ν = 2928 s, 2856 m, 1675 s, 1465 w, 1412 w, 1197 s, 1170 s, 1132 s, 828 w, 798 w, 720 m. The compound does not show UV absorption. HRMS ((+)-ESI): m/z = 471.4664 (calcd. 471.4673 for $C_{32}H_{59}N_2$); m/z = 236.2364 (calcd. 236.2373 for $C_{32}H_{60}N_2^{2+}$ $[M + H]^{2+}$); m/z = 585.4567 (calcd. 585.4601 for $C_{32}H_{59}N_2^{2+} \times C_2F_3O_2^-$ $[M + H]^+$).

Acknowledgements

Sponge collection was performed by the AWI scientific diving team during the annual summer expedition 2003 at the AWIPEV Arctic Research Base, Ny-Ålesund, Svalbard. Sponge identification was kindly conducted by Wallie H. de Weerdt and Dr. Rob W. M. van Soest (Institute for Biodiversity and Ecosystem Dynamics (Zoological Museum), University of Amsterdam, The Netherlands). We would like to thank Prof. Michael Göbel (Universität Frankfurt/Main, Germany) for his support of this project, especially for providing the laboratory space, and Dr. Achim Grube (now Boehringer Ingelheim, Biberach, Germany) for discussions on the MS spectra.

Notes and references

1 R. Sakai, T. Higa, C. W. Jefford and G. Bernardinelli, *J. Am. Chem. Soc.*, 1986, **108**, 6404–6405; R. Sakai, S. Kohmoto, T. Higa, C. W. Jefford and G. Bernardinelli, *Tetrahedron Lett.*, 1987, **28**, 5493–5496.
2 B. J. Baker, P. J. Scheuer and J. N. Shoolery, *J. Am. Chem. Soc.*, 1988, **110**, 965–966.
3 E. Fahy, T. F. Molinski, M. K. Harper, B. W. Sullivan, D. J. Faulkner, L. Parkanyi and J. Clardy, *Tetrahedron Lett.*, 1988, **29**, 3427–3428.
4 N. Fusetani, K. Yasumuro and S. Matsunaga, *Tetrahedron Lett.*, 1989, **30**, 6891–6894.
5 M. Jaspars, V. Pasupathy and P. Crews, *J. Org. Chem.*, 1994, **59**, 3253–3255.
6 R. D. Charan, M. J. Garson, I. M. Brereton, A. C. Willis and J. N. A. Hooper, *Tetrahedron*, 1996, **52**, 9111–9120; R. J. Clark, K. L. Field, R. D. Charan, M. J. Garson, I. M. Brereton and A. C. Willis, *Tetrahedron*, 1998, **54**, 8811–8826.
7 C. A. Volk and M. Köck, *Org. Biomol. Chem.*, 2004, **2**, 1827–1830.
8 C. A. Volk and M. Köck, *Org. Lett.*, 2003, **5**, 3567–3569.
9 C. A. Volk, H. Lippert, E. Lichte and M. Köck, *Eur. J. Org. Chem.*, 2004, 3154–3158.
10 C. Timm, C. Volk, F. Sasse and M. Köck, *Org. Biomol. Chem.*, 2008, **6**, 4036–4040.
11 J. E. Baldwin, D. A. James and V. Lee, *Tetrahedron Lett.*, 2000, **41**, 733–736.

6.2.1 Supporting Information

New Haliclamines E and F from the Arctic Sponge *Haliclona viscosa*

Gesine Schmidt, Christoph Timm, and Matthias Köck*

*To whom correspondence should be addressed. mkoeck@awi.de

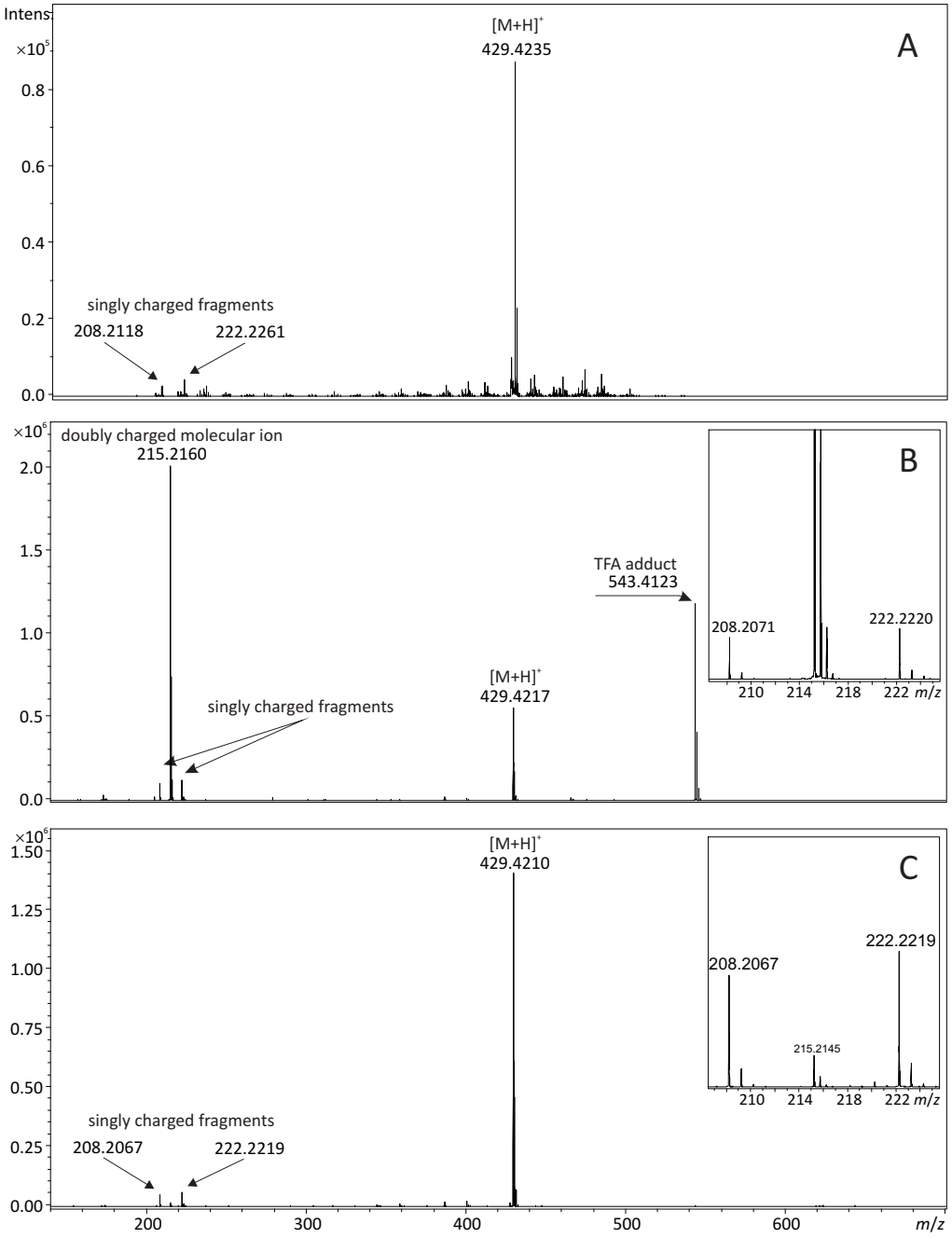

Figure 6.15 Comparison of mass spectra of the natural and the synthetic compound **1**. – (A). Mass trace obtained from an LCMS experiment of the crude extract of *Haliclona viscosa*. – (B). Synthetic compound under standard ESI conditions. – (C). Synthetic compound under API-CID-MS/MS conditions. The sections show details of the doubly charged molecular ion and the singly charged fragments.

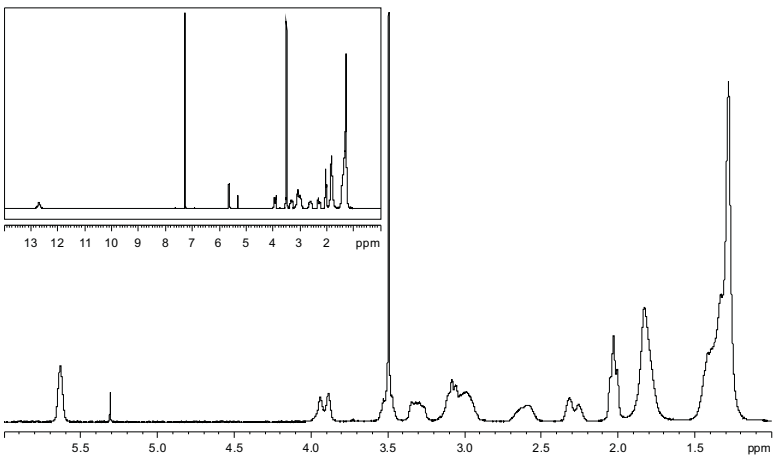

Figure 6.16 Details and full scan (box) of a 1D ^{1}H-NMR spectrum (300 MHz, $CDCl_3$) of the synthetic haliclamine E (**1**).

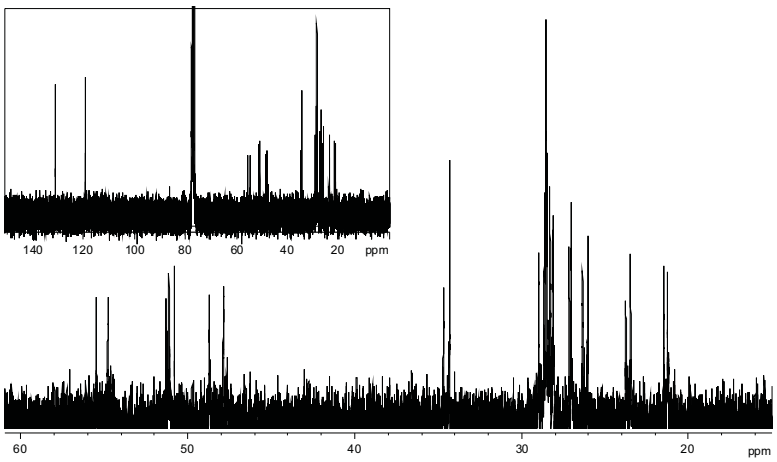

Figure 6.17 Details and full scan (box) of a 1D ^{13}C-NMR spectrum (75 MHz, $CDCl_3$) of the synthetic haliclamine E (**1**).

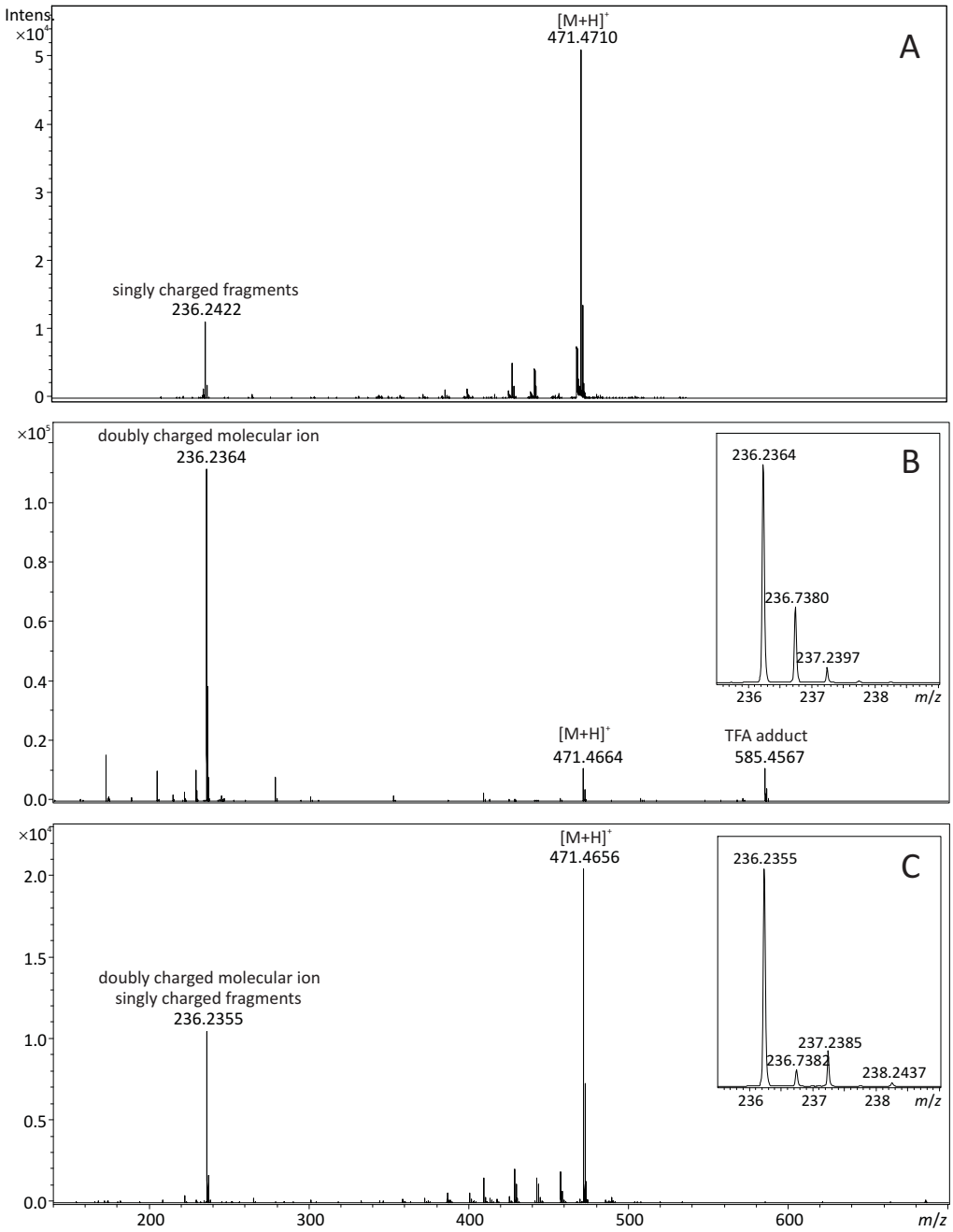

Figure 6.18 Comparison of mass spectra of the natural and the synthetic compound **2**. – (A). Mass trace obtained from an LCMS experiment of the crude extract of *Haliclona viscosa*. – (B). Synthetic compound under standard ESI conditions. The section shows a detail of the doubly charged molecular ion. – (C). Synthetic compound under API-CID-MS/MS conditions. The section shows a detail of the doubly charged molecular ion superimposed by the singly charged fragment.

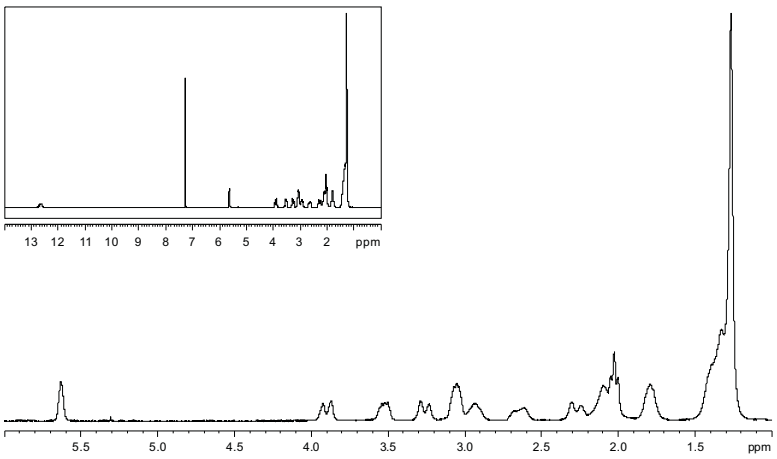

Figure 6.19 Details and full scan (box) of a 1D ^{1}H-NMR spectrum (300 MHz, $CDCl_3$) of the synthetic haliclamine F (**2**).

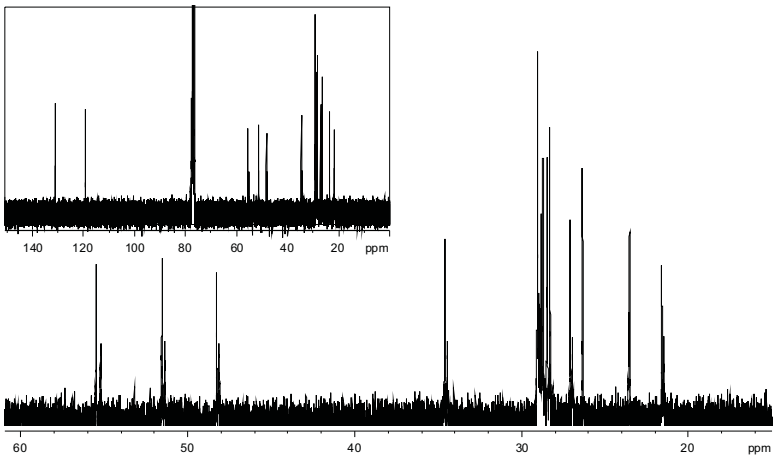

Figure 6.20 Details and full scan (box) of a 1D ^{13}C-NMR spectrum (75 MHz, $CDCl_3$) of the synthetic haliclamine F (**2**).

Table 6.6 ^{1}H- and ^{13}C-NMR data of Haliclamines E (**1**) and F (**2**) in $CDCl_3$. The compounds in the solution were present as TFA salts.

Haliclamine E (1)			Haliclamine F (2)		
pos.	δH	δC	pos.	δH	δC
NH, NH'	12.62 (br. s, 2 H)		NH, NH'	12.62 (s, 2 H)	
2	3.90 (d, 2 H, 15.7 Hz)	51.1	2	3.89 (d, 2 H, 15.8 Hz)	51.5
2'	3.21-3.37 (m, 2 H)	50.8	2'	3.25 (d, 2 H, 16.0 Hz)	51.4
3, 3'		131,1	3, 3'		131.1
4, 4'	5.62 (s, 2 H)	119.1	4, 4'	5.62 (s, 2 H)	119.1
5	2.51-2.69 (m, 2 H)	21.5	5	2.55-2.72 (m, 2 H)	21.6
5'	2.27 (d, 2 H, 17.3 Hz)	21.8	5'	2.26 (d, 2 H, 18.5 Hz)	21.5
6	3.34-3.55 (m, 2 H)	48.7	6	3.46-3.58 (m, 2 H)	48.3
6'	2.87-3.16 (m, 6 H)[a]	47.9	6'	2.85-3.11 (m, 6 H)[b]	48.1
7, 7'	2.20 (t, 4 H, 6.6 Hz)	34.3, 34.7	7, 7'	2.01 (t, 4 H, 7.1 Hz)	34.4, 34.6
8-13, 8'-14'	1.18-1.49 (m, 26 H)	26.0, 26.4, 27.0, 27.1, 27.2, 28.0–28.7, 29.0	8-15, 8'-15'	1.18-1.49 (m, 32 H)	26.4, 27.0, 27.1, 28.3–29.0
14, 15'	1.72-1.89 (4 H, m)	23.5, 23.8	16, 16'	1.70-1.85 (m, 4 H)	23.5
15, 16'	2.87-3.16 (m, 6 H)[a]	54.8, 55.5	17, 17'	2.85-3.11 (m, 6 H)[b]	55.2, 55.5

[a] Assignments are interchangeable. [b] Assignments are interchangeable.

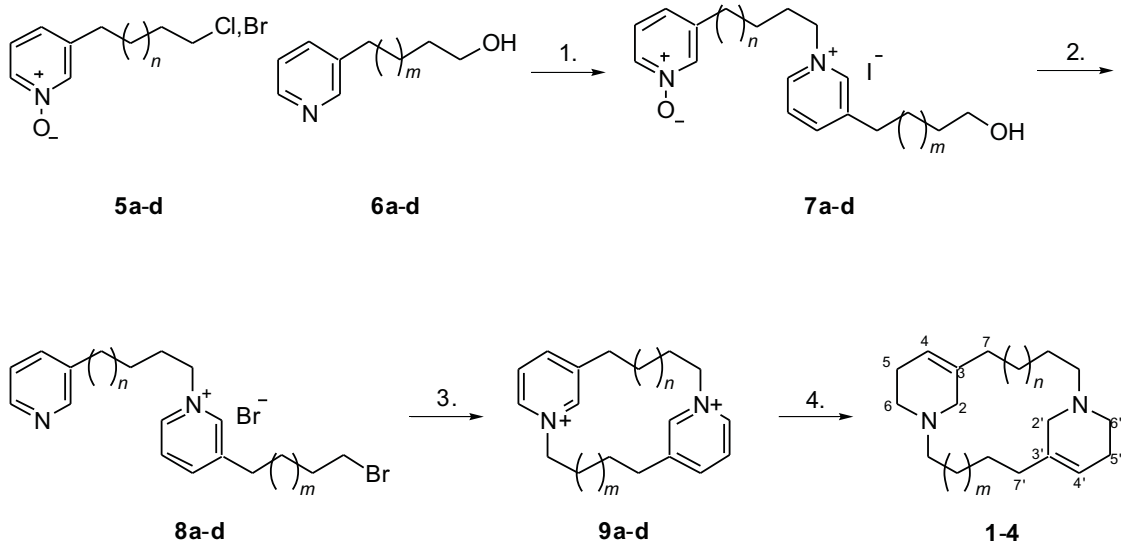

a = **1**: *n* = 6, *m* = 7; **b** = **2**: *n* = 8, *m* = 8; **c** = **3**: *n* = 6, *m* = 8; **d** = **4**: *n* = 7, *m* = 8

Figure 6.21 Synthetic pathway of haliclamines E (**1**), F (**2**), C (**3**) and D (**4**). – 1. Synthesis of *N*-oxide dimers. – 2./3. Synthesis of cyclostellettamines. – 4. Synthesis of haliclamines (refer to paragraphs in the text).

New Cyclic Heptapeptides and Pyrrole-Imidazole Alkaloids from the Caribbean Sponge *Stylissa caribica*

Gesine Schmidt, Achim Grube, and Matthias Köck

Alfred-Wegener-Institut für Polar- und Meeresforschung in der Helmholtz-Gemeinschaft, Am Handelshafen 12, D-27570 Bremerhaven, Germany

The marine sponge *Stylissa caribica* investigated by a MS-guided fractionation revealed several new secondary metabolites. The crude extract was analysed by HPLC-HRMS and the masses of the detected compounds were compared to literature (MarinLit®). This approach allowed the isolation of four new cyclic heptapeptides.

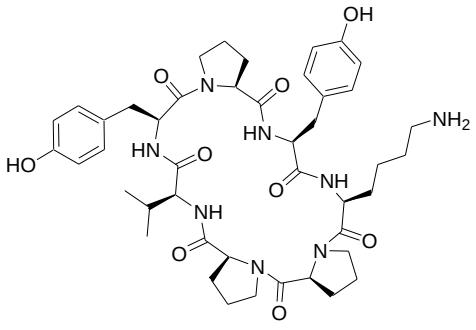

Stylissamide A

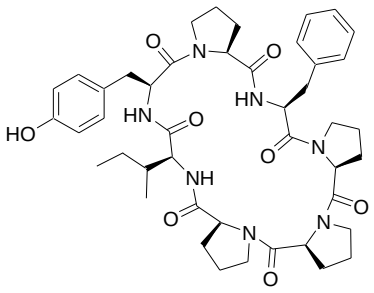

Stylissamide B

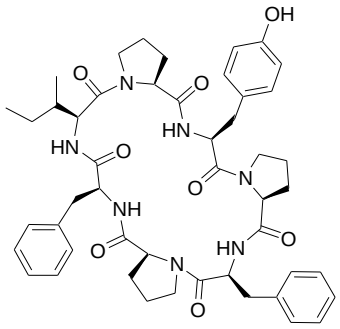

Stylissamide C

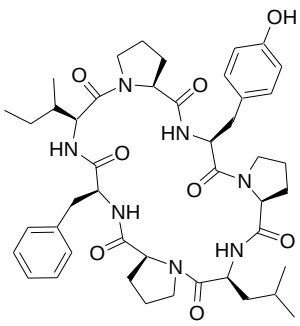

Stylissamide D

The heptapeptides stylissamides A to D are related to the phakellistatins, the hymenamides, and the stylisins.[1] The structures were elucidated using HMBC and NOESY correlations as well as MS^n results.[2] In addition to the cyclic heptapeptides, six new pyrrole-imidazole alkaloids, 4-bromopyrrole-2-carboxy-*N*(ε)-lysine[3], 4-bromopyrrole-2-carboxyarginine[3], oxocyclostylidol[4], tetrabromostyloguanidine,[5] and the first tetrameric derivatives stylissadines A and B[6] were recently isolated from this sponge. Thus, the sponge *Stylissa caribica* was shown to be a rich source of new secondary metabolites of two different structure classes.

1. a) S. Matsunaga, N. Fusetani, *Curr. Org. Chem.* **2003**, *7*, 945-966; b) R. Mohammed, J. Peng, M. Kelly, M. T. Hamann, *J. Nat. Prod.* **2006**, *69*, 1739-1744.
2. G. Schmidt, A. Grube, M. Köck, *Eur. J. Org. Chem.* **2007**, submitted.
3. A. Grube, E. Lichte, M. Köck, *J. Nat. Prod.* **2006**, *69*, 125-127.
4. A. Grube, M. Köck, *J. Nat. Prod.* **2006**, *69*, 1212-1214.
5. A. Grube, M. Köck, *Angew. Chem. Int. Ed*. **2007**, in press.
6. A. Grube, M. Köck, *Org. Lett.* **2006**, *8*, 4675-4678.

Conformational Studies on Stylissamides, Cyclic Heptapeptides from *Stylissa caribica*

Gesine Schmidt, Achim Grube, and Matthias Köck

Alfred-Wegener-Institut für Polar- und Meeresforschung in der Helmholtz-Gemeinschaft,
Am Handelshafen 12, D-27570 Bremerhaven, Germany
E-mail: mkoeck@awi.de

The marine sponge *Stylissa caribica* investigated by a MS-guided fractionation revealed several new secondary metabolites. In addition to six new pyrrole-imidazole alkaloids[1] (including the first tetrameric derivatives stylissadines A and B)[2], four cyclic heptapeptides stylissamide A to D were isolated from this sponge.[3]

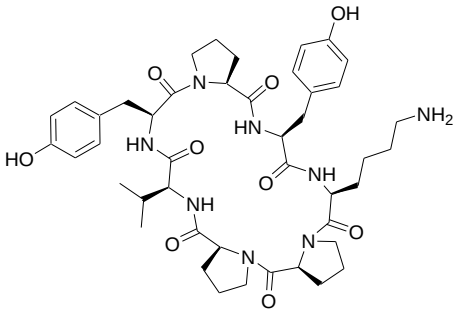

Stylissamide A

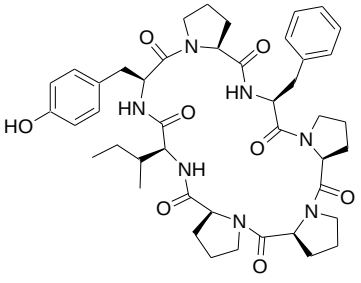

Stylissamide B

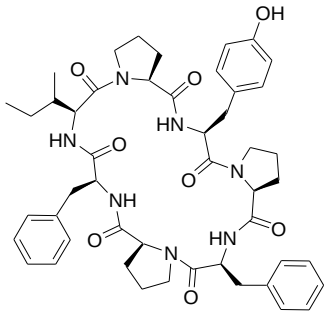

Stylissamide C

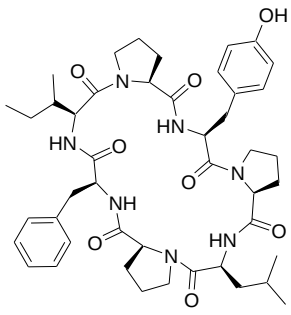

Stylissamide D

The structures of the stylissamides were elucidated using HMBC and NOESY correlations as well as MS^n results. The stylissamides A to D are related to the phakellistatins, the hymenamides, and the stylisins.[4] NOESY experiments with mixing times of 100, 150, and 200 ms formed the basis of studies on the conformation of the stylissamides. The NOE-derived interproton distances served as distance restraints in computation analyses to investigate the tertiary structure of the molecules.

References

1. a) A. Grube, E. Lichte, M. Köck, *J. Nat. Prod.*, **2006**, *69*, 125-127; b) A. Grube, M. Köck, *J. Nat. Prod.*, **2006**, *69*, 1212-1214; c) A. Grube, M. Köck, *Angew. Chem. Int. Ed.*, **2007**, *46*, 2320-2324.
2. A. Grube, M. Köck, *Org. Lett.*, **2006**, *8*, 4675-4678.
3. G. Schmidt, A. Grube, M. Köck, *Eur. J. Org. Chem.*, **2007**, in press.
4. a) S. Matsunaga, N. Fusetani, *Curr. Org. Chem.*, **2003**, *7*, 945-966; b) R. Mohammed, J. Peng, M. Kelly, M. T. Hamann, *J. Nat. Prod.*, **2006**, *69*, 1739-1744.

Secondary Metabolites in Marine Sponges – Qualitative and Quantitative Variation over Time

Gesine Schmidt, Christine Cychon and Matthias Köck

Alfred-Wegener-Institute for Polar and Marine Research,
Am Handelshafen 12, 27570 Bremerhaven, Germany
Email: matthias.koeck@awi.de

In previous years, the composition and quantity of *Haliclona viscosa* metabolites changed with habitat and year, while a sympatric species, *Haliclona rosea*, did not show this variation (unpubl. data). This raises the question whether the variation in *H. viscosa* is due to an ability to adapt to varying environmental conditions (e.g. light, water temperature, different colonizing bacteria) or due to increased environmental pressure in some years that lowers the compound productivity of the sponge.

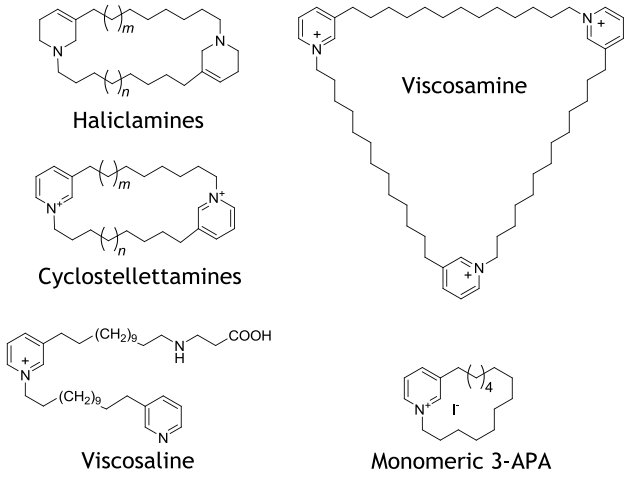

The present study addresses the magnitude and quality of the metabolite variation in *H. viscosa* and *H. rosea* both between the polar habitat Spitsbergen and the temperate British Isles, and within each of the two habitats. To examine this, sponges are collected in three subsequent years by scuba diving at different sites and depth in Kongsfjorden, Spitsbergen and around the British Isles at times when metabolite production is highest.

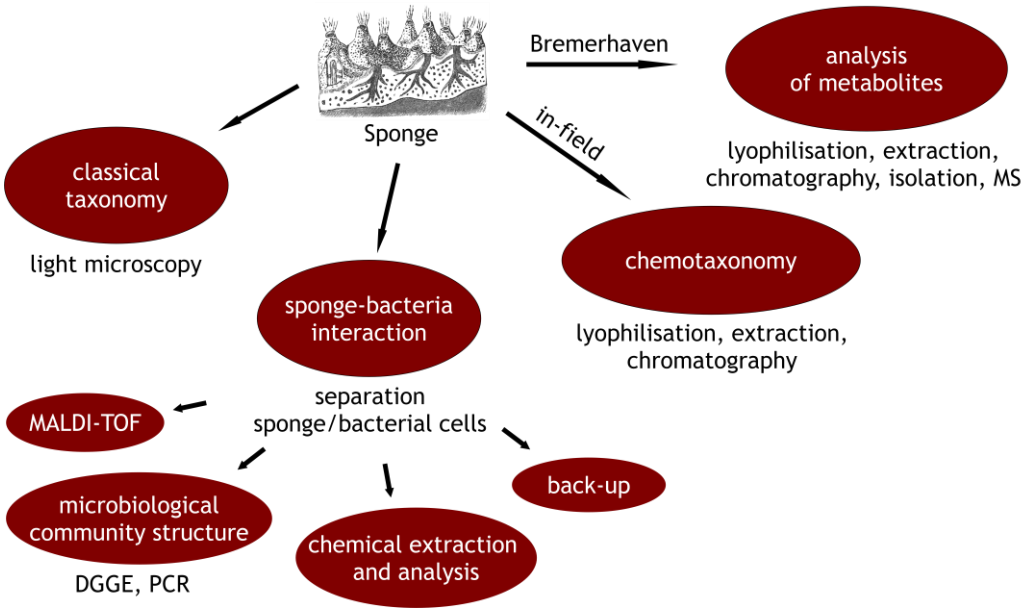

Study of the MS Fragmentation of the Haliclamines

Gesine Schmidt and Matthias Köck

Alfred-Wegener-Institut für Polar- und Meeresforschung in der Helmholtz-Gemeinschaft, Am Handelshafen 12, D-27570 Bremerhaven, Germany

E-mail: mkoeck@awi.de

Two new 3-alkyl-pyridinium alkaloids, haliclamines E and F, were identified in the crude extract of the Arctic sponge *Haliclona viscosa* using LC-MS methods. Due to the scarcity of sponge material available, the compounds were not isolated and the structure elucidation relied on the chromatographic comparison with synthetic compounds.[1]

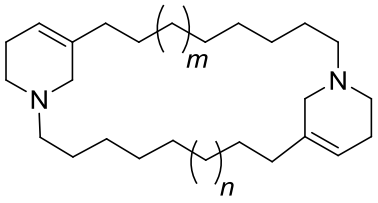

Haliclamine E: m = 2, n = 3
Haliclamine F: m = n = 4

The MS fragmentation pattern of the haliclamines in general was examined on the basis of the synthetic compounds. Naturally occurring as well as to-date unreported haliclamines of (a) equal alkyl chain length and (b) chain length differences of one, two or three methylene groups were subject to extensive ion trap- and API-CID-MS/MS examinations.

The MS fragmentation of these compounds is similar to the cyclostellettamines[2] but strongly influenced by the tetrahydropyridine moiety and the ionization method applied in mass spectrometric analyses.[3]

References

1. G. Schmidt, C. Timm, M. Köck, *Org. Biomol. Chem.* **2009**, *accepted for publication*.
2. A. Grube, C. Timm, M. Köck, *Eur. J. Org. Chem.* **2006**, 1285-1295.
3. G. Schmidt, C. Timm, E. Lichte, M. Köck, **2009**, *in preparation.*

MALDI-TOF-MS, a suitable method for metabolite screening?

Christine Cychon, Gesine Schmidt, and Matthias Köck

Alfred-Wegener-Institut für Polar- und Meeresforschung in der Helmholtz-Gemeinschaft, Am Handelshafen 12, D-27570 Bremerhaven, Germany

E-mail: mkoeck@awi.de

Next to standard LC-MS applications, MALDI[1]-TOF mass spectrometry is a powerful method to analyze and characterize macromolecules like proteins[2], carbohydrates[3], oligonucleotides[4] and synthetic polymers[5]. Research on small molecules did not, for traditional and technical reasons, focus on MALDI, but applications in the investigation of bacteria regarding their chemotaxonomy[6] and secondary metabolism[7] are becoming more frequent. During our search for new natural products, we are applying MALDI-TOF-MS for a direct screening of secondary metabolites in sponge tissue.[8] Due to the simple sample preparation, this method allows a broad insight into the compound spectrum at an early stage of investigation. Besides this, challenging questions regarding the qualitative and quantitative sample preparation, compound distribution and stability, etc. have emerged. Here, we want to discuss our experiences with this procedure using the sponge *Stylissa caribica* as an example. What are the possibilities and perspectives of MALDI-TOF-MS and where are the limits in natural products research?

Notes and References

1. Matrix assisted laser desorption/ionization
2. Chaurand, D. Cornett, R. M. Caprioli, *J. Proteome Res.* **2006**, *5*, 2889-2900.
3. D. Harvey, *Mass. Spectom. Rev.* **2006**, *25*, 595-662.
4. E. Nordhoff, M. Schürenberg, G. Thiele, C. Lübbert, K. Kloeppel, D. Theiss, H. Lehrach, J. Gobom, *Int. J. Mass. Spectrom.* **2003**, *226*, 163-180.
5. G. Montaudo, F. Samperi, M. Montaudo, *Prog. Polym. Sci.* **2006**, *31*, 277-357.
6. D. Dickinson, M. La Duc, M. Satomi, J. Winefordner, D. Powell, K. Venkateswaran, *J. Microbiol. Meth.* **2004**, *58*, 1-12.
7. M. Erhard, H. Von Doehren, P. Jungblut, *Nature Biotech.* **1997**, *15*, 906-909.
8. A. Grube, T. Maier, M. Kostrzewa, M. Köck, *Z. Naturf.* **2007**, *62*, 600-604.

7
Manuscripts

The following manuscripts are prepared to be submitted and form part of this thesis:

Articles

1. G. Schmidt, C. Timm, A. Grube, E. Lichte, M. Köck. Systematic investigation of the MS-Fragmentation of Haliclamines. **Submitted**. 183

2. G. Schmidt, C. Timm, M. Köck. Haliclocyclin C, a new monomeric 3-alkyl pyridinium alkaloid from the Arctic marine sponge *Haliclona viscosa*. **Accepted for publication** 217

3. G. Schmidt, T. Mordhorst, M. Köck. Two Additional Haliclamines J and K from the Arctic Marine Sponge *Haliclona viscosa*. **Manuscript draft** .. 223

ARTICLE TYPE www.rsc.org/xxxxxx | XXXXXXXX

Systematic Investigation on the MS-Fragmentation of Haliclamines

Gesine Schmidt,[a] Christoph Timm,[a] Achim Grube,[a] Ellen Lichte[a] and Matthias Köck*[,a]

Received (in XXX, XXX) Xth XXXXXXXXX 200X, Accepted Xth XXXXXXXXX 200X
First published on the web Xth XXXXXXXXX 200X
DOI: 10.1039/b000000x

Haliclamines take up an exceptional position in the large and diverse family of 3-alkyl pyridinium alkaloids (3-APAs) isolated from natural sources. They are the only compounds among the 3-APAs that possess a tetrahydropyridine moiety and are only reported as macrocyclic dimers. We recently identified haliclamines E and F directly from the crude extract of a sponge. Since mass spectrometry plays an important role in the identification of these compounds, we initiated the present study on the MS-fragmentation of haliclamines as an extension of our study on the fragmentation of cyclostellettamines. Surprisingly, the singly charged molecular ion in haliclamines shows a distinctly different fragmentation in MS/MS experiments than the doubly charged molecular ion.

Introduction

The number of known 3-alkyl pyridinium and 3-alkyl piperidine alkaloids (3-APAs) from sponges of the order Haplosclerida is constantly growing.[1] The main structural element of these alkaloids is a pyridine moiety connected in position 3 and/or 1 to an alkyl chain of variable length. It can be arranged to cyclic or open monomers, dimers, trimers and polymers. A second structural element consists of a tetrahydropyridine moiety likewise connected to an alkyl chain of variable length. However, only macrocyclic tetrahydropyridine dimers are known, and to date only from sponges of the genus *Haliclona*. Hence, the number and diversity of 3-alkyl pyridinium compounds (cyclostellettamines,[2] amphitoxin,[3] cyclohaliclonamines,[4] poly-alkylpyridinium salts (Poly-APS),[5] pachychalines,[6] niphatoxines,[7] and many others) greatly exceeds the number of 3-alkyl tetrahydropyridine compounds known as haliclamines (Scheme 1).[8, 9] This suggests that the oxidation state of the six-membered azacycle plays an important role in the occurrence of the compounds.

The repetitive 3-APA unit in cyclostellettamines and haliclamines cause NMR spectra to show only one structural unit of the molecule and the large number of similar methylene units results in a strong overlap of the aliphatic protons. NMR spectra are thus not ideally suited to distinguish large numbers of structurally very similar compounds present e.g. in *Haliclona viscosa* from Arctic waters. In these cases it makes sense to use LCMS and LCMS/MS methods to identify the natural compounds, e.g. directly from the crude extract.[9] Mass spectrometric methods constitute a fast and easy way to identify haliclamines, cyclostellettamines and, potentially, also trimeric and polymeric 3-APAs.[4, 6] They deliver insight into the size of the molecule as well as the length of the alkyl chains and number of double bonds therein.

For a confident identification of natural products by MS or MS/MS it is necessary to know the fragmentation pathways. As an expansion of our studies on the fragmentation of the

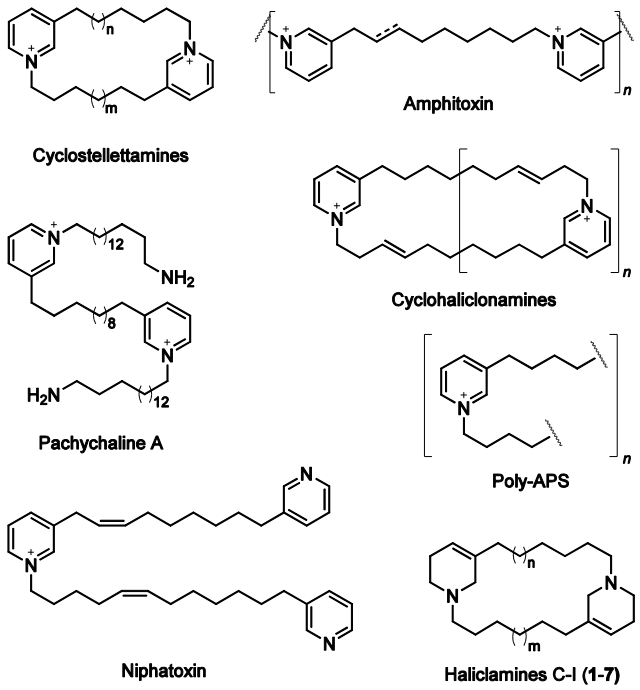

Scheme 1 3-Alkyl pyridinium/pyridine- and 3-alkyl tetrahydropyridine alkaloids reported from sponges of the order Haplosclerida.

cyclostellettamines[10] we present the fragmentation of haliclamines.

Under certain fragmentation conditions, haliclamines produce fragments that are equal in mass to fragments known from cyclostellettamines that possess the same chain lengths. Since the kind of fragments derived depend very much on the fragmentation mode and the molecular ion selected for fragmentation, these typical fragments can be used during identification studies. The survey comprises haliclamines with equal alkyl chain length and chain length differences of one, two and three methylene groups, respectively. We include haliclamines that have not yet been isolated from natural sources, i.e. haliclamines with alkyl chains of 12/12, 13/13 and 11/14 methylene groups.

Table 1 MS and in-source CID-MS/MS results for haliclamines C–I (**1-7**).

Haliclamine		HRMS $[M+H]^+$	HRMS $[M+2H]^{2+}$	in-source CID-MS/MS Frag. 1	in-source CID-MS/MS Frag. 2
C (**1**, 9/11)	calcd.	443.4360, $C_{30}H_{55}N_2$	222.2216, $C_{30}H_{56}N_2$	208.2059, $C_{14}H_{26}N$ (C_9)	236.2373, $C_{16}H_{30}N$ (C_{11})
	exper.	443.4364, Δm = 0.9 ppm	222.2216, Δm = 0.1 ppm	208.2050, Δm = 4.8 ppm	236.2359, Δm = 5.8 ppm
		FWHM: 0.0567	FWHM: 0.0380	FWHM: 0.0329	FWHM: 0.0359
D (**2**, 10/11)	calcd.	457.4516, $C_{31}H_{57}N_2$	229.2295, $C_{31}H_{58}N_2$	222.2216, $C_{15}H_{28}N$ (C_{10})	236.2373, $C_{16}H_{30}N$ (C_{11})
	exper.	457.4522, Δm = 1.2 ppm	229.2301, Δm = 3.0 ppm	222.2214, Δm = 1.0 ppm	236.2370, Δm = 1.1 ppm
		FWHM: 0.0581	FWHM: 0.0388	FWHM: 0.0351	FWHM: 0.0365
E (**3**, 9/10)	calcd.	429.4203, $C_{29}H_{53}N_2$	215.2138, $C_{29}H_{54}N_2$	208.2060, $C_{14}H_{26}N$ (C_9)	222.2216, $C_{15}H_{28}N$ (C_{10})
	exper.	429.4217, Δm = 3.3 ppm	215.2160, Δm = 10.1 ppm	208.2067, Δm = 3.3 ppm	222.2219, Δm = 1.2 ppm
		FWHM: 0.0571	FWHM: 0.0401	FWHM: 0.0326	FWHM: 0.0346
F (**4**, 11/11)	calcd.	471.4673, $C_{32}H_{59}N_2$	236.2373, $C_{32}H_{60}N_2$	236.2373, $C_{16}H_{30}N$ (2 × C_{11})	
	exper.	471.4664, Δm = 1.8 ppm	236.2364, Δm = 3.9 ppm	236.2355, Δm = 7.5 ppm	
		FWHM: 0.0557	FWHM: 0.0373	FWHM: 0.0366	
G (**5**, 12/12)	calcd.	499.4986, $C_{34}H_{63}N_2$	250.2529, $C_{34}H_{64}N_2$	250.2529, $C_{17}H_{32}N$ (2 × C_{12})	
	exper.	499.4967, Δm = 3.8 ppm	250.2527, Δm = 1.0 ppm	250.2524, Δm = 2.0 ppm	
		FWHM: 0.0598	FWHM: 0.0383	FWHM: 0.0376	
H (**6**, 13/13)	calcd.	527.5299, $C_{36}H_{67}N_2$	264.2686, $C_{36}H_{68}N_2$	264.2686, $C_{18}H_{34}N$ (2 × C_{13})	
	exper.	527.5283, Δm = 3.1 ppm	264.2690, Δm = 1.6 ppm	264.2685, Δm = 0.3 ppm	
		FWHM: 0.0643	FWHM: 0.0400	FWHM: 0.0393	
I (**7**, 11/14)	calcd.	513.5142, $C_{35}H_{65}N_2$	257.2608, $C_{35}H_{66}N_2$	236.2373, $C_{16}H_{30}N$ (C_{11})	278.2842, $C_{19}H_{36}N$ (C_{14})
	exper.	513.5121, Δm = 4.2 ppm	257.2610, Δm = 0.8 ppm	236.2630, Δm = 5.5 ppm	278.2833, Δm = 3.3 ppm
		FWHM: 0.0632	FWHM: 0.0406	FWHM: 0.0368	FWHM: 0.0413

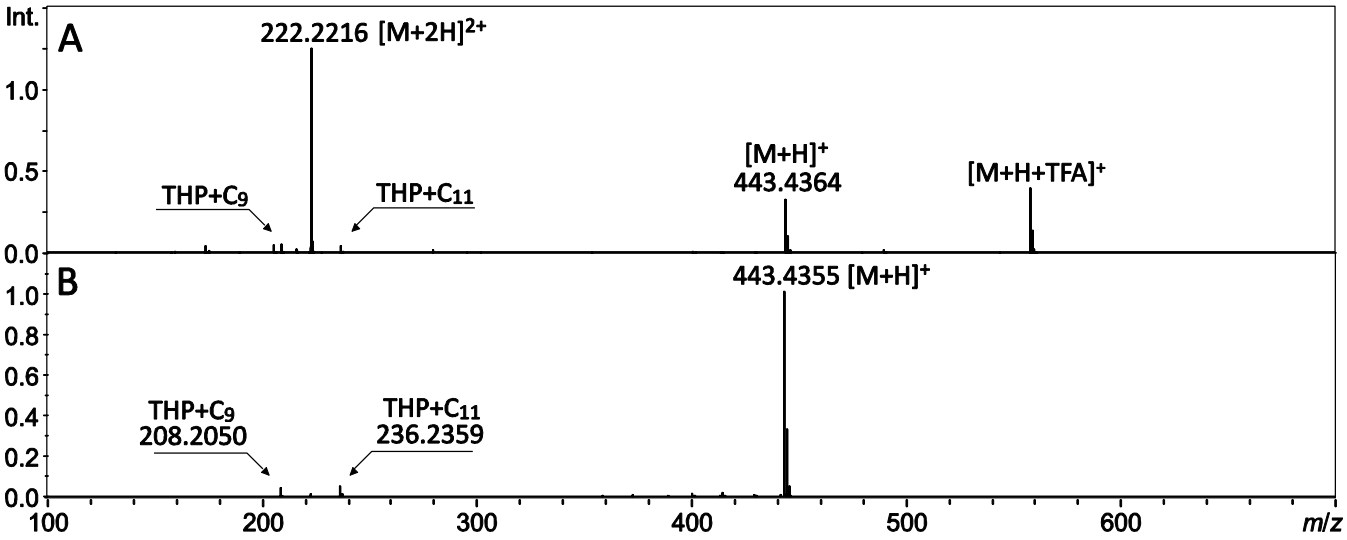

Fig. 1 High resolution mass spectrum (A) and HR-in-source-CID-MS/MS spectrum (B) of haliclamine C (**1**) (THP = tetrahydropyridine).

Results and Discussion

The synthetic haliclamines used within this investigation originate from reduction of synthetic cyclostellettamines that contain the desired chain lengths. This reduction provides haliclamines C (**1**, *m* = 4, *n* = 6), D (**2**, *m* = 5, *n* = 6), E (**3**, *m* = 4, *n* = 5), F (**4**, *m* = *n* = 6), G (**5**, *m* = *n* = 7), H (**6**, *m* = *n* = 8) and I (**7**, *m* = 6, *n* = 9)[9] and follows a procedure described by Baldwin et al.[11] Haliclamines G (**5**), H (**6**) and I (**7**) are not yet reported from natural sources but are purposely synthesized for this study. Since all haliclamines show the same fragmentation pattern under equal MS conditions, haliclamine C (**1**) serves as a general representative during the discussion of the fragmentation pattern.

The high resolution mass spectrum of haliclamine C (**1**) displays three major peaks: the singly charged molecular ion at *m*/*z* 443.4364, the doubly charged molecular ion at *m*/*z* 222.2216 and the TFA[12] adduct of haliclamine C (**1**) at *m*/*z* 557.4269 (Figure 1).

Two additional minor peaks at *m*/*z* 208.2050 and 236.2359 are visible in HR-MS of haliclamine C (**1**) and represent mass equivalents of fragments composed of e.g. a tetrahydropyridine (THP) moiety connected to a chain of 9 or 11 methylene groups, respectively (Table 1).

For fragmentation studies, the compounds receive two different treatments: (a) in-source CID-MS/MS (on a TOF mass spectrometer equipped with an ESI-source) as an omni-directional fragmentation method, and (b) CID-MS^n (on an Ion-trap mass spectrometer, likewise equipped with an ESI source) as a possibility to select different precursor ions for fragmentation.

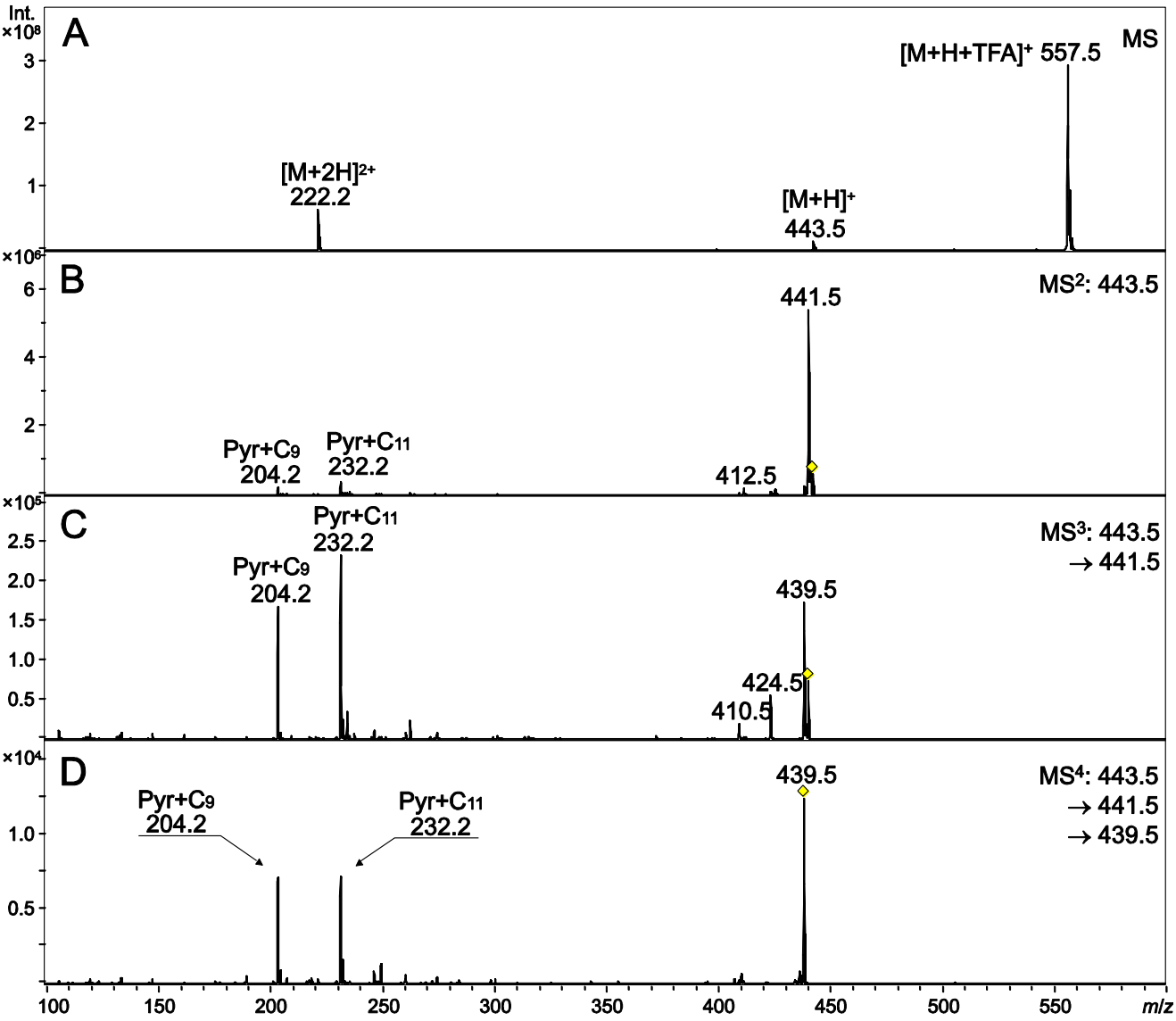

Fig. 2 CID-MS/MS spectra of haliclamine C (**1**) during fragmentation of the singly charged molecular ion. Diamonds mark the respective precursor ions (Pyr = pyridine).

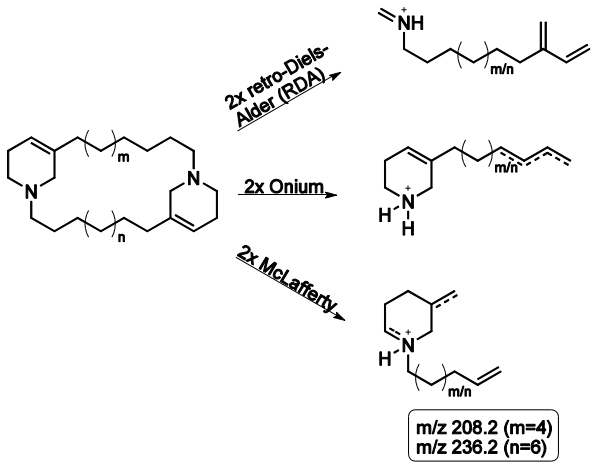

Scheme 2 Possible fragments derived from different fragmentation reactions of haliclamine C (**1**) assuming two equal simultaneous fragmentation reactions.

Fragmentation by in-source CID

Application of in-source CID-MS/MS conditions results in increased intensity of the singly charged molecular ion, a considerable decrease in intensity of the doubly charged molecular ion and the loss of the TFA adduct ion. At the same time, the intensity of the THP + alkyl chain type fragments, *m*/*z* 208.2 and *m*/*z* 236.2, increases slightly. A number of reactions are supposable for the formation of fragments with the mass *m*/*z* 208.2 and *m*/*z* 236.2; onium and retro-Diels-Alder reactions as well as McLafferty rearrangement (Scheme 2). However, with in-source CID-MS/MS being omni-directional, it is not possible in this step to distinguish or argue which reaction is more probable. A combination of them is most likely. Since fragments of the same mass also form under MS^n conditions, a suggestion for the predominant fragmentation reaction is discussed below.

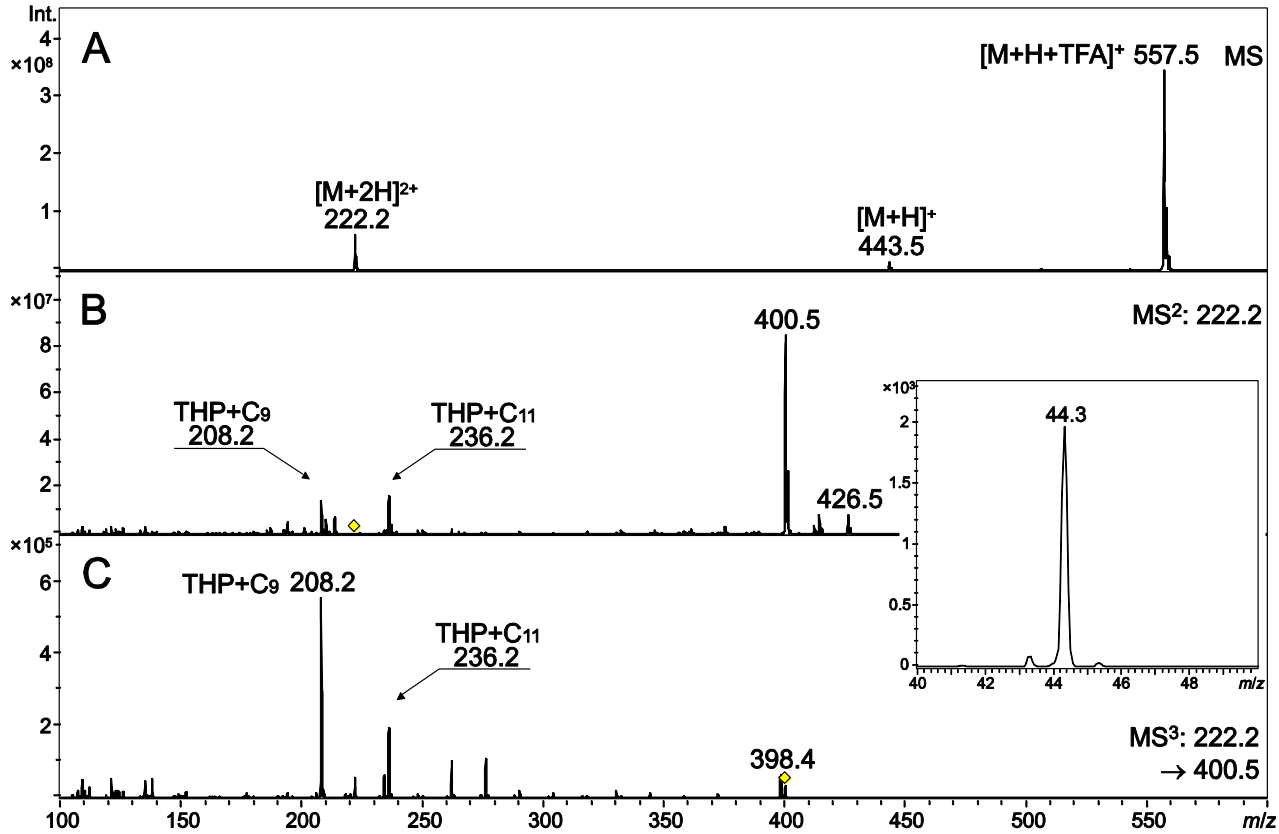

Fig. 3 CID-MS/MS spectra of haliclamine C (**1**) during fragmentation of the doubly charged molecular ion. The section shows a detail of the *m*/*z* 44 region during MS^2. Diamonds mark the respective precursor ions (THP = tetrahydropyridine).

Fragmentation by CID

Under CID-MS conditions on the Ion trap mass spectrometer, the two minor fragments that represent the THP + alkyl chain type fragments are not visible at considerable intensities which is probably due to slight differences in source geometry or other instrument parameters. For CID-MS^n experiments, both the singly and the doubly charged molecular ion serve as precursors for fragmentation experiments and result in two distinctly different fragmentation patterns.

Fragmentation of the singly charged molecular ion

The first pattern originates from isolation and fragmentation of the singly charged molecular ion. Here, a stepwise loss of 2 mass units at a time occurs in MS^2 and subsequently also in MS^3, resulting in a total of 4 mass units difference to the molecular ion (Figure 2). It is the result of a progressive oxidation of the THP rings in which each of the rings can be oxidized independently or one ring is fully oxidized to the pyridinium.

From the MS^n spectra it is clear that complete oxidation of one THP to the pyridinium is preferred (Scheme 3A). There are two indications for this: one is the appearance of two strong fragments at *m*/*z* 204.2 and 232.2 which stand for the mass equivalent of a pyridinium (Pyr) moiety connected to either alkyl chain [Pyr + $(CH_2)_9$ or Pyr + $(CH_2)_{11}$]; the other is the absence of a continued oxidation after the loss of four mass units which would be expected if neither ring was completely oxidized in this step. However, no pronounced mass peak at *m*/*z* 437.4 is present in the MS^4 experiment.

The oxidation of only one of the THP rings might be explained by considering that the fully unsaturated pyridine lends structural stability to the molecule while the THP easily fractures, e.g. in a retro-Diels-Alder reaction. With one ring existing as a pyridine and the other as THP, the compound can follow a fragmentation pattern as described for the cyclostellettamines. An onium reaction and McLafferty rearrangement both provide the fragments *m*/*z* 204.2 and 232.2 (Scheme 3B).

The phenomenon of oxidation to the pyridine also occurs during a high temperature NMR experiment in DMSO-d_6 under air. From approximately 353 K, four distinct signals appear in the range 8.0 to 9.5 ppm and a fifth signal at 4.6 ppm. They become increasingly stronger with higher temperature. The signals correspond in multiplicity and chemical shift to the cyclostellettamine aromatic protons and the methylene group attached to the pyridine nitrogen. Thus, the tetrahydropyridine ring in haliclamine is oxidized to a pyridine and the amount of pyridine increases with increasing temperature. The reaction does not happen under a protective gas or in $CDCl_3$-d_1.

In mass spectrometry, this oxidation happens in two steps under generation of a dihydropyridine. Dihydropyridines are known to decompose into pyridines and tetrahydropyridines when heated or on exposure to air.[13] However, in NMR there seems to be a direct oxidation from the THP to the pyridine

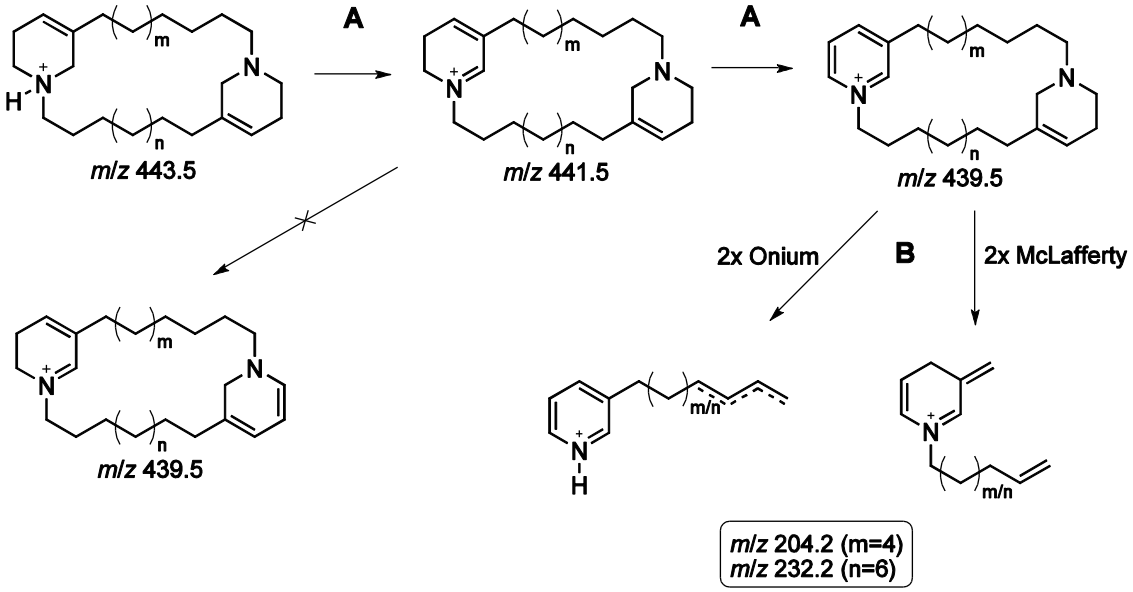

Scheme 3 Fragmentation of the singly charged molecular ion of haliclamine C (**1**). A: stepwise oxidation; B: fragmentation into the Pyr + alkyl chain type fragments.

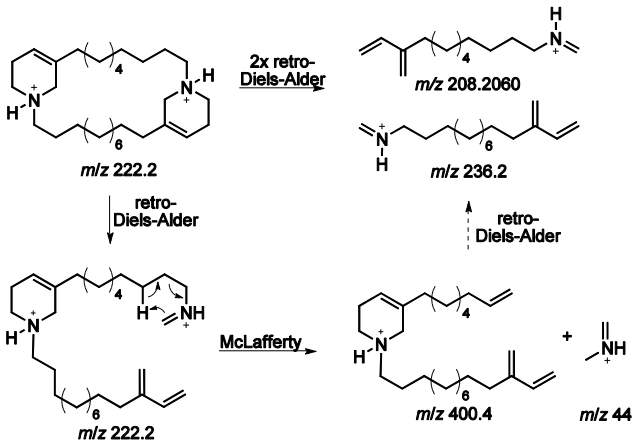

Scheme 4 Proposed fragmentation pathway of the doubly charged molecular ion of haliclamine C (**1**).

since none of the NMR signals correspond to a dihydropyridine. A ring opening as proposed for MS experiments does not seem to occur since the signals that correspond to a terminal methylene or imine group are missing. While it is not possible from the NMR spectrum to determine whether only one or possibly both THP rings in the molecule are oxidized, it is still clear that the THP ring is completely oxidized to the pyridinium. This strengthens the conclusion on complete oxidation of one THP ring instead of a partial oxidation to dihydropyridines in both THP rings made above for the MS fragmentation.

There are also some indications that the macro-cycle opens up, possibly during the ionization or in a multi-fragmentation process during MS^2; though at low intensity, MS^2 and MS^3 provide fragments that derive from a loss of *m*/*z* 17, correspondent to ammonia elimination, and *m*/*z* 31, the elimination of methanamine. To achieve this loss, the macro-cyclic and tetrahydropyridine ring structures must be open early. Ammonia loss from methylenediamines is described by Bosshardt and Hesse[14], but it seems to be a minor process in comparison to the formation of the Pyr + $(CH_2)_{9/11}$ fragments.

Fragmentation of the doubly charged molecular ion

The second fragmentation pattern under CID-MS^n conditions evolves when fragmenting the doubly charged molecular ion. Most obvious is the immediate loss of a charged fragment that includes one of the nitrogen atoms since all emerging fragments are singly charged and even numbered (Figure 3). For the loss of such a charged fragment a ring opening of both the macro-cycle and the THP ring has to occur. The loss of the charged fragment strongly indicates a retro-Diels-Alder (RDA) reaction for the initial ring opening which leads to a doubly charged methylene iminium ion (*m*/*z* 222.2, Scheme 4). Other reactions like α-cleavage and onium reactions open the macro-cycle but leave the THP intact, and therefore do not lead to an intermediate from which this charged fragment can be split.

The most pronounced fragment in MS^2 emerging from doubly charged haliclamine C (**1**) is *m*/*z* 400.5 (Δ *m*/*z* 44 to the precursor). Since both nitrogen atoms are protonated in the doubly charged compound, an onium reaction would lead to a charged fragment *m*/*z* 30 (Figure 3) and a second charged fragment at *m*/*z* 414. The latter is detected at low intensity while *m*/*z* 30 cannot be detected due to instrument limitations. A McLafferty-type rearrangement would result in the two charged fragments *m*/*z* 44 and *m*/*z* 400 (Scheme 4). Several authors have investigated the fragmentation of aliphatic iminium ions;[15] they conclude that the fragmentation mechanism, i.e. whether an onium reaction or a McLafferty rearrangement dominate the process, strongly depends on the length of the alkyl chain. Taking into account the length of the aliphatic chain in haliclamines, McLafferty rearrangement would be the prominent reaction. However, the authors examined aliphatic iminium ions that carried a single charge

while the haliclamine in the present fragmentation carries a double charge. Added to this, McLafferty rearrangement is defined as leading to a charged and a neutral particle. Since both fragments, *m*/*z* 44 and 400, retain their charge and are visible in MS^2 (Figure 3), with *m*/*z* 400 present at highest intensity, we must conclude that the underlying reaction is not a McLafferty rearrangement. If however the aliphatic chain of considerable length in haliclamines can be seen a pseudo-neutral isolator against the second charge present in the molecule, McLafferty rearrangement would be possible.

At the same time, THP + alkyl chain type fragments *m*/*z* 208.2 and 236.2 emerge during MS^2. This is in contrast to the Pyr + alkyl chain type fragments generated during fragmentation of the singly charged molecular ion but comparative to results from in-source CID-MS/MS experiments. A suitable explanation for the THP type fragments seems to be a second RDA reaction at the remaining THP ring leading to two long chain aliphatic methylene iminium ions that are the mass equivalent of a THP ring connected to an alkyl chain of 9 or 11 methylene groups in the case of haliclamine C (**1**).

During fragmentation of the *m*/*z* 400.5 ion in MS^3, we again observe the loss of *m*/*z* 2, correspondent to the generation of a double bond, along with the characteristic stepwise cleavage of the alkyl chain with mass differences of *m*/*z* 14 (Figure 4). However, this fragment *m*/*z* 398.4 is of low intensity and cannot be compared to the stepwise oxidation of the singly charged molecular ion as only one oxidation step can be observed.

Conclusions

The systematic investigation of the MS spectra of haliclamines expands the analysis of the fragmentation pathways of 3-alkyl pyridinium alkaloids which was initiated by our work on the cyclostellettamines. Most astonishingly in this respect are the different fragmentation patterns of singly and doubly charged haliclamine molecular ions. Whereas the fragmentation of the singly charged molecular ion leads to fragments corresponding in mass to a pyridinium moiety connected to an alkyl chain, the fragmentation of the doubly charged molecular ion results in tetrahydropyridine-type fragments. Fragmentation of the doubly charged molecular ion results in a similar fragmentation as reported from ESI-in-source-CID-MS/MS fragmentation. The presented investigation serves as a reference for future studies of these molecules.

Acknowledgments

We would like to thank Prof. J. J. Veith for valuable discussions on the project.

Notes and references

[a] *Alfred-Wegener-Institute, Am Handelshafen 12,27570 Bremerhaven, Germany. Fax: +49 (0) 471 4831 1425; Tel: +49 (0) 471 4831 1497; E-mail: mkoeck@awi.de*

† Electronic Supplementary Information (ESI) available: experimental conditions for synthesis, purification and compound data acquisition for haliclamines C-I (**1**-**7**) and precursors, compound data for haliclamines C-I (**1**-**7**) and precursors, HRMS and MS/MS spectra of haliclamines C-I (**1**-**7**), high temperature NMR spectra of haliclamine C (**1**) in DMSO-d_6. See DOI: 10.1039/b000000x/

‡ Mass spectra were acquired in positive mode after external calibration with sodium formiate cluster. HRMS and in-source CID-MS/MS spectra were recorded on a micrOTOF spectrometer (Bruker Daltonics) equipped with an ESI source (capillary exit = 100 V, skimmer 1 = 50 V). For in-source CID-conditions, the capillary exit voltage was set to 180 V while skimmer 1 remained at 50 V. MS^n spectra were recorded on an Esquire 3000^{plus} Ion-trap (Bruker Daltonics) equipped with an ESI source. High-temperature NMR experiments were recorded with a Bruker Avance 400 (400 MHz) spectrometer.

1. R. J. Andersen, R. W. M. van Soest and F. Kong, in *Alkaloids: Chemical and Biological Perspectives*, ed. S. W. Pelletier, Pergamon Press, 1st edn., 1996, vol. 10, pp. 301-355.
2. N. Fusetani, N. Asai, S. Matsunaga, K. Honda and K. Yasumuro, *Tetrahedron Lett.*, 1994, **35**, 3967-3970.
3. S. Albrizio, P. Ciminiello, E. Fattorusso, S. Magno and J. R. Pawlik, *J. Nat. Prod.*, 1995, **58**, 647-652.
4. T. Teruya, K. Kobayashi, K. Suenaga and H. Kigoshi, *J. Nat. Prod.*, 2006, **69**, 135-137.
5. K. Sepčić, G. Guella, I. Mancini, F. Pietra, M. Dalla Serra, G. Menestrina, K. Tubbs, P. Macek and T. Turk, *J. Nat. Prod.*, 1997, **60**, 991-996; K. Sepčić, V. Marcel, A. Klaebe, T. Turk, D. Šuput and D. Fournier, *Biochim. Biophys. Acta*, 1998, **1387**, 217-225.
6. R. Laville, O. P. Thomas, F. Berrue, F. Reyes and P. Amade, *Eur. J. Org. Chem.*, 2008, 121-125.
7. M. S. Buchanan, A. R. Carroll, R. Addepalli, V. M. Avery, J. N. A. Hooper and R. J. Quinn, *J. Nat. Prod.*, 2007, **70**, 2040-2041; R. Talpir, A. Rudi, M. Ilan and Y. Kashman, *Tetrahedron Lett.*, 1992, **33**, 3033-3034.
8. N. Fusetani, K. Yasumuro and S. Matsunaga, *Tetrahedron Lett.*, 1989, **30**, 6891-6894; C. A. Volk, H. Lippert, E. Lichte and M. Köck, *Eur. J. Org. Chem.*, 2004, 3154-3158.
9. G. Schmidt, C. Timm and M. Köck, *Org. Biomol. Chem.*, 2009, **7**, 3061-3064.
10. A. Grube, C. Timm and M. Köck, *Eur. J. Org. Chem.*, 2006, 1285-1295.
11. J. E. Baldwin, D. R. Spring, C. E. Atkinson and V. Lee, *Tetrahedron*, 1998, **54**, 13655-13680.
12. TFA was introduced during chromatographic purification of the synthetic compound.
13. R. F. Francis, C. D. Crews and B. S. Scott, *J. Org. Chem*, 1978, **43**, 3227-3230; N. Naiman, H. Rollema, E. Johnson and N. Castagnoli, Jr., *Chem. Res. Toxicol.*, 1990, **3**, 133-138; R. J. Sundberg, D. S. Grierson and H.-P. Housson, *J. Org. Chem*, 1984, **49**, 2400-2404.
14. H. Bosshardt and M. Hesse, *Angew. Chem. Int. Ed.*, 1974, **13**, 252-266.
15. H. Budzikiewicz and P. Bold, *Org. Mass. Spectrom.*, 1991, **26**, 709-712; C. Djerassi and C. Fenselau, *J. Am. Chem. Soc.*, 1965, **87**, 5752-5756; J. H. Gross and H. J. Veith, *Org. Mass. Spectrom.*, 1993, **28**, 867-872.

7.1.1 Supporting Information

Systematic Investigation of the MS-fragmentation of the Haliclamines

Gesine Schmidt, Christoph Timm, Achim Grube, Ellen Lichte and Matthias Köck*

*To whom correspondence should be addressed. mkoeck@awi.de

Synthetic pathway towards the haliclamines

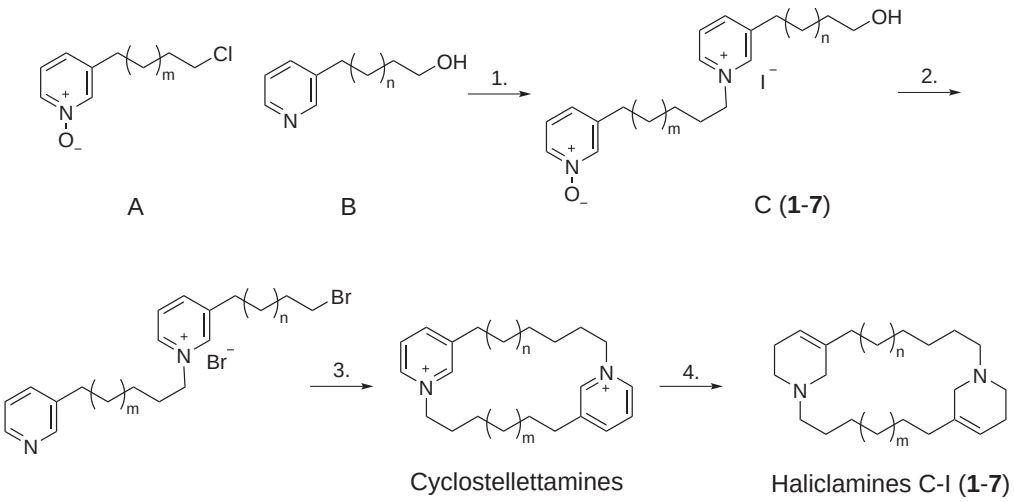

Figure 7.1 Pathway for synthesis of the haliclamines.

1. Synthesis of *N*-oxide dimers A mixture of 1.0 mmol *N*-oxide (**A**), 1.0 mmol alcohol (**B**), and 1.2 mmol NaI was dissolved in 25 mL butan-2-one and refluxed for 48 h. After cooling the solvent was removed and the residue was adsorbed on silica and purified via column chromatography. The starting material was synthesized following literature procedures.

2./3. Synthesis of Cyclostellettamines Within 10 minutes PBr_3 (0.39 mL, 4.0 mmol) was added to a cooled (0 °C) suspension of dimer **C** in 15 mL of $CHCl_3$ under an atmosphere of Argon. The mixture was stirred for 15 minutes at that temperature and then heated to reflux for 1 h. After cooling it was poured onto 50 mL of an ice/water mixture. The layers were separated and the water layer was extracted with CH_2Cl_2 (3 × 15 mL). The combined organic extracts were neutralized with 2 M Na_2CO_3 (3 × 15 mL), dried over $MgSO_4$, and the solvent was removed leaving about 1 mL bromide-containing solution. After diluting with 10 mL of butan-2-one it was added to a refluxing solution of NaI (0.33 g, 2.2 mmol) in 200 mL butan-2-one via a syringe pump at a rate of 0.5 mL h^{-1}. The mixture was refluxed for 4 days. Removal of the solvent yielded an oily residue which solidified upon trituration with Et_2O. The resulting solid was purified via recrystallisation.

4. Synthesis of Haliclamines A solution of the cyclostellettamine (**D**, 0.13 mmol) in 10 mL CH_2Cl_2/MeOH (1:1) was cooled to –40 °C and $NaBH_4$ (0.10 g, 2.63 mmol) was added. After stirring for two hours in the cold, the mixture was allowed to warm to room temperature, 5 mL of 2 M NaOH solution were added and it was stirred for an additional 15 minutes. It was then poured onto 15 mL water and extracted with CH_2Cl_2 (3 × 10 mL). Drying of the combined organic extracts over $MgSO_4$ and removal of the solvent yielded the crude product (**1**-**7**). The crude product was purified via preparative HPLC.

Experimental conditions

All solvents were purified by distillation, with the exception of THF which was distilled from sodium/benzophenone under argon. Column chromatography was performed on silica gel 60 (Merck, particle size 0.04–0.063 mm). Aluminum plates pre-coated with Merck silica 60 were used for TLC. Compounds were visualized by UV irradiation (254 nm) or dying with $KMnO_4$ solution (1 g $KMnO_4$, 6.6 g K_2CO_3, 2 mL 5 % NaOH solution in 100 mL H_2O). Purification of the synthetic compounds was performed on a Jasco 1500 series HPLC system. It was equipped with a Prontosil Eurobond RP_{18} column (20 × 250 mm, 5 μm, 40 °C) applying a MeCN/H_2O (0.1 % TFA) gradient [30 % MeCN / 70 % H_2O isocratic for 5 min; to 60 % MeCN / 40 % H_2O in 30 min; isocratic for 5 minutes; to 100 % MeCN in 10 min] with a flow rate of 8 mL min^{-1}. Analytical HPLC used a Kromasil RP_{18} column (4.6 × 250 mm, 5 μm, 40 °C), as before with a MeCN/H_2O (0.1 % TFA) gradient [from 100 % H_2O to 80 % MeCN / 20 % H_2O in 40 min; to 100 % MeCN in 5 min] at a flow rate of 1 mL min^{-1}. UV spectra were recorded during HPLC analyses with a DAD (Jasco). Melting points were obtained with a Kofler melting point apparatus and are uncorrected. NMR spectra were recorded with Bruker AM 250 (250 MHz), Bruker AM 300 (300 MHz), and Bruker Avance 400 (400 MHz) spectrometers. All experiments were performed at 300 K, with the exception of the high-temperature NMR experiment for which the temperatures are given in Figure SI 4. Chemical shifts are quoted in ppm and are referenced to the appropriate solvent signal. FT-IR spectra were recorded on a Perkin-Elmer 1600 series spectrometer. Absorption maxima are reported in wave numbers and the following abbreviations are used: s strong, m medium, w weak. Elemental analysis was performed on a

Heraeus CHN Rapid. Mass spectra were acquired in positive mode after external calibration with sodium formiate cluster. HRMS and in-source CID-MS/MS spectra were recorded on a micrOTOF spectrometer (Bruker Daltonics) equipped with an ESI source (capillary exit = 100 V, skimmer 1 = 50 V). For in-source CID-conditions, the capillary exit voltage was set to 180 V while skimmer 1 remained at 50 V. MS^n spectra were recorded on an Esquire 3000^{plus} Ion-trap (Bruker Daltonics) equipped with an ESI source.

Haliclamine C (**1**), 9/11

Compound data

3-(9hydroxynonyl)-1-[11-(*N*-oxidopyridine-3-yl)-undecyl]-pyridinium iodide (**1C**). 3-(11-chloroundecyl)-pyridine-*N*-oxide (**1A**, 1.50 g, 5.28 mmol), 9-(pyridine-3-yl)-nonane-1-ol (**1B**, 1.17 g, 5.28 mmol), and NaI (0.95 g, 6.34 mmol) were treated as described above (procedure 1.). Chromatography on silica (9:1 CH_2Cl_2/MeOH) yielded 1.83 g (58%) of the dimer as a yellow solid. — TLC R_f: 0.3 (9:1 CH_2Cl_2/MeOH). — ^{1}H-NMR (250 MHz, DMSO-d_6): δ = 1.09-1.73 (m, 30 H, 15 × CH_2), 1.93 (m, 2 H, NCH_2CH_2), 2.52 (t, J = 7.4 Hz, 2 H, 3-CH_2), 2.79 (t, J = 7.6 Hz, 2 H, 3'-CH_2), 3.36 (dt, J = 6.1 Hz, J = 4.8 Hz, 2 H, CH_2OH), 4.30 (t, J = 4.9 Hz, 1 H, OH), 4.56 (t, J = 7.3 Hz, 2 H, NCH_2), 7.19 (d, J = 7.9 Hz, 1 H, H4), 7.32 (dd, J = 7.8 Hz, J = 6.4 Hz, 1 H, H5), 7.99-8.18 (m, 3 H, H2, H6 and H5') 8.49 (d, J = 8.1 Hz, 1 H, H4'), 8.95 (d, J = 6.0 Hz, 1 H, H6'), 9.05 (s, 1 H, H2'). — ^{13}C-NMR (62.5 MHz, DMSO-d_6): δ = 25.2, 25.4, 28.2-28.8 (12 × CH_2), 29.6 (3'-CH_2CH$_2$), 29.8 (3-CH_2CH$_2$), 31.4 (3'-CH$_2$), 31.5 (3-CH$_2$), 32.4 (CH$_2$CH$_2$OH), 60.5 (NCH_2), 60.6 (CH$_2$OH), 125.3 (C4), 125.9 (C5), 127.4 (C5'), 136.1 (C6), 138.1 (C2), 141.3 (C3'), 142.1 (C6'), 142.9 (C3) 143.8 (C2') 145.0 (C4'). — IR (KBr, cm^{-1}): $\tilde{\nu}$ = 3416 s, 3096 m, 2924 s, 2851 s, 1630 w, 1604 w, 1568 w, 1505 m, 1467 s, 1438 m, 1370 w, 1308 w 1266 s, 1159 s, 1063 m, 1019 m, 962 m, 793 m, 760 m, 719 w, 679 s. — HRMS ((+)-ESI): m/z = 469.3761 (calcd. 469.3789 for $C_{30}H_{49}N_2O_2^+$ [M+H]$^+$).

Cyclostellettamine O (**1D**). Following the procedure 2./3., cyclostellettamine O (**1D**) was prepared from 3-(9-hydroxynonyl)-1-[11-(*N*-oxidopyridine-3-yl)-undecyl]-pyridinium iodide (**1C**) (1.50 g, 2.51 mmol), PBr_3 (0.97 mL, 10.06 mmol) and NaI (0.83 g, 5.53 mmol). Recrystallisation from MeOH/Et_2O yielded 1.24 g (71%) of a brown solid. — TLC bromide: R_f: 0.55 (free base, 9:1 CH_2Cl_2/MeOH); cyclostellettamine O (**1D**): R_f: 0.23 (9:1 CH_2Cl_2/MeOH). — ^{1}H-NMR (250 MHz, DMSO-d_6): δ = 0.84-1.43 (m, 24 H, 12 × CH_2), 1.43-1.79 (m, 4 H, 3-CH_2CH$_2$), 1.84-1.97 (m, 4 H, NCH_2CH$_2$), 2.81 (t, J = 6.9 Hz, 4 H, 3-CH_2), 4.60 (t, J = 5.8 Hz, 4 H, NCH_2), 8.10 (dd, J = 8.0 Hz, J = 6.0 Hz, 2 H, H5), 8.50 (d, J = 8.0 Hz, 2 H, H4), 8.96 (d, J = 6.0 Hz, 2 H, H6), 9.09 (s, 2 H, H2). — ^{13}C-NMR (62.5 MHz, DMSO-d_6): δ = 24.6, 25.0, 27.2, 27.6, 27.7, 28.1-28.9 and 29.3 (14 × CH_2), 29.8 and 30.1 (3-CH_2CH$_2$), 31.1 and 31.2 (3-CH$_2$), 60.3 and 60.5 (NCH_2), 127.7 (C5), 142.1 (C6), 142.6 (C3),

143.8 (C2), 145.3 (C4). — IR (KBr, cm^{-1}): $\tilde{\nu}$ = 3017 m, 2924 s, 2850 s, 1626 m, 1584 w, 1504 s, 1468 s, 1368 w, 1318 w, 1240 w, 1153 w, 920 w, 830 w, 807 w, 722 w, 694 m. — EA calcd. for $C_{30}H_{48}N_2I_2$ (690.52): C 52.18, H 7.01, N 4.06; calc. for $C_{30}H_{48}N_2I_2 \times 0.5\ H_2O$: C 51.51, H 7.06, N 4.00; found C 51.73, H 7.04, N 3.75. — UV (DAD): λ_{max} = 218, 270 nm; λ_{min} = 242 nm. — HRMS ((+)-ESI): m/z = 218.1903 (calcd. 218.1904 for $C_{30}H_{48}N_2{}^{2+}$ $[M+H]^{2+}$).

Haliclamine C (**1**). In the manner described above (procedure 4.), 100 mg of cyclostellettamine O (**1D**) were treated with 100 mg of $NaBH_4$. Purification of 58 mg of the crude product via HPLC yielded 27 mg (29%) haliclamine C (**1**) as TFA-salt. — TLC R_f: 0.43 (9:1 CH_2Cl_2/MeOH). — ^{1}H-NMR (400 MHz, $CDCl_3$): δ = 1.19-1.46 (m, 28 H, 14 × CH_2), 1.72-1.85 (m, 4 H, NCH_2CH_2), 2.01 (t, J = 6.4 Hz, 4 H, 3-CH_2), 2.14-2.37 (m, 2 H, H5'), 2.56-2.76 (m, 2 H, H5), 2.83-3.17 (m, 6 H, H6' and NCH_2), 3.30 (d, J = 15.6 Hz, 2 H, H2'), 3.41-3.62 (m, 2 H, H6), 3.83-3.97 (m, 2 H, H2), 5.62 (s, 2 H, H4), 11.95-12.30 (m, 2 H, NH). — ^{13}C-NMR (75.0 MHz, $CDCl_3$): δ = 21.5 and 21.8 (C5), 23.4 (NCH_2CH_2), 26.0, 26.2, 27.0, 27.1 and 28.0-29.0 (14 × CH_2), 34.5 and 34.6 (3-CH_2), 48.2 and 48.7 (C6), 51.4 and 51.8 (C2), 55.4 and 55.8 (CH_2N), 119.2 (C4), 131.1 (C3). — IR (KBr, cm^{-1}): $\tilde{\nu}$ = 2931 s, 2858 m, 1735 w, 1671 s, 1560 w, 1466 m, 1199 s, 1137 s, 798 w, 720 m. — HRMS ((+)-ESI): m/z = 443.4334 (calcd. 443.4360 for $C_{30}H_{55}N_2^+$ $[M+H]^+$); m/z = 222.2210 (calcd. 222.2217 for $C_{30}H_{56}N_2{}^{2+}$ $[M+H]^{2+}$).

Mass spectra

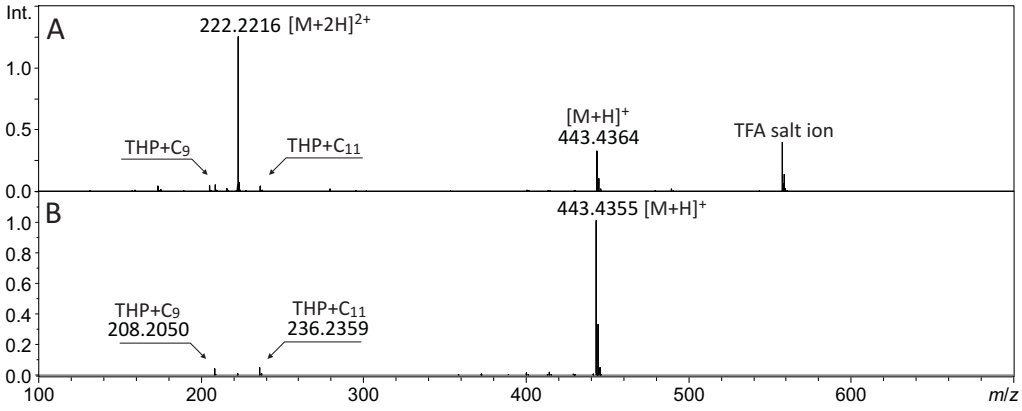

Figure 7.2 High-resolution mass spectrum of haliclamine C (**1**) under standard (top) and in-source CID-MS/MS condition (below). THP = tetrahydropyridine.

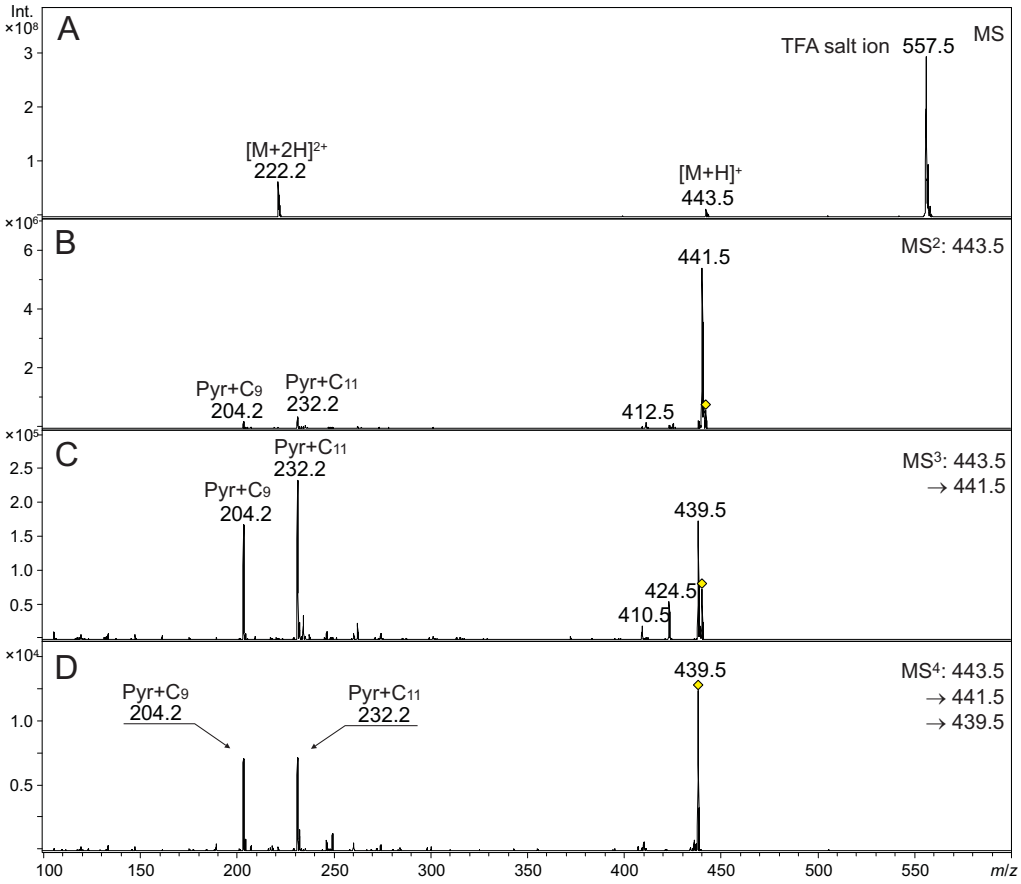

Figure 7.3 MS/MS-fragmentation of the singly charged molecular ion of haliclamine C (**1**) under ion trap conditions. Pyr = pyridine. Precursor ions for fragmentation are marked with a yellow diamond.

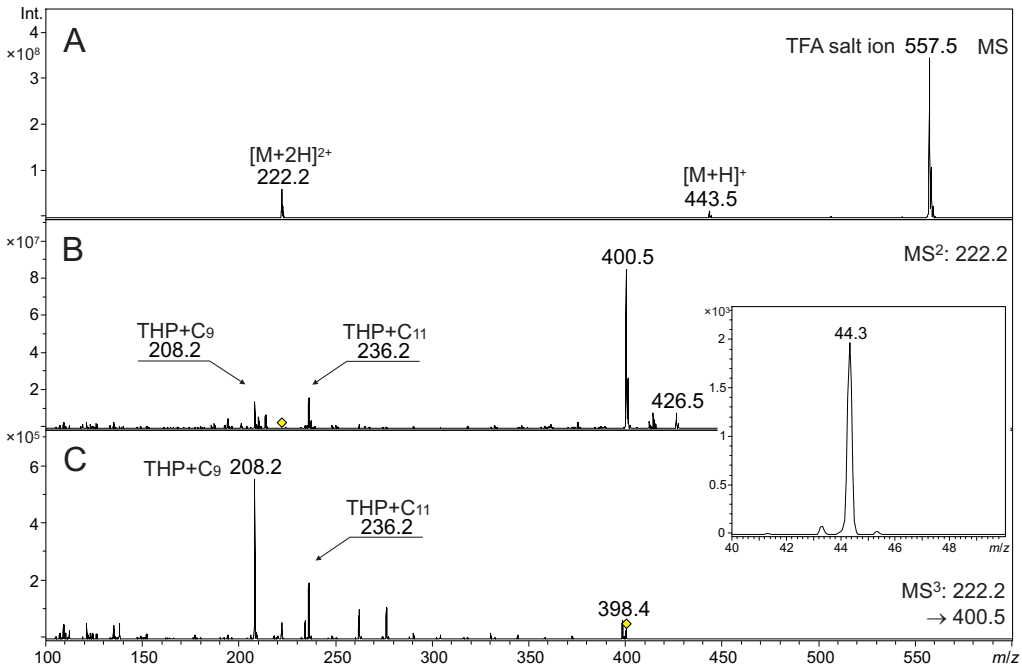

Figure 7.4 MS/MS-fragmentation of the doubly charged molecular ion of haliclamine C (**1**) under ion trap conditions. THP = tetrahydropyridine. Precursor ions for fragmentation are marked with a yellow diamond.

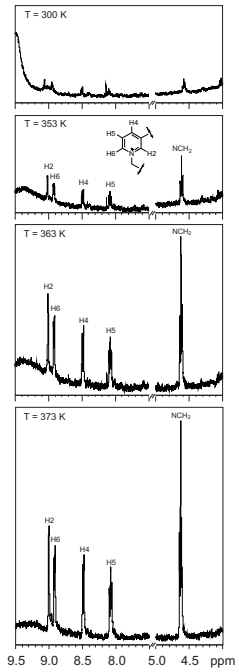

Figure 7.5 Details of the ^{1}H-NMR spectrum of haliclamine C (**1**) at different temperatures. Spectra are equally scaled.

Haliclamine D (**2**), 10/11

Compound data

3-(10-hydroxydecyl)-1-[11-(*N*-oxidopyridine-3-yl)-undecyl]-pyridinium iodide (**2C**). For preparation and compound data refer to Grube et al.[117]

Cyclostellettamine Q (**2D**). For preparation and compound data refer to Grube et al.[117]

Haliclamine D (**2**). In the manner described above (procedure 4.), 100 mg of cyclostellettamine Q (**2D**) were treated with 100 mg of $NaBH_4$. Purification of 56 mg of the crude product via HPLC yielded 31 mg (32%) haliclamine D (**2**) as TFA-salt. — TLC R_f: 0.43 (9:1 CH_2Cl_2/MeOH). — ^{1}H-NMR (300 MHz, $CDCl_3$): δ = 1.18-1.50 (m, 30 H, 15 × CH_2), 1.71-1.88 (m, 4 H, NCH_2CH_2), 1.97-2.09 (m, 4 H, 3-CH_2), 2.29 (d, J = 18.6 Hz, 2 H, H5'), 2.54-2.73 (m, 2 H, H5), 2.85-3.17 (m, 6 H, H6' and NCH_2), 3.27 (d, J = 15.5 Hz, 2 H, H2'), 3.46-3.60 (m, 2 H, H6), 3.85-3.99 (m, 2 H, H2), 5.63 (s, 2 H, H4), 12.34 (s, 2 H, NH). — ^{13}C-NMR (75.0 MHz, $CDCl_3$): δ = 21.5 and 21.7 (C5), 23.4 and 23.7 (NCH_2CH_2), 26.1, 26.3, 27.0, 27.1, 28.2, 28.3, 28.4, 28.6-28.8, 28.9 and 29.2 (15 × CH_2), 34.5 and 34.7 (3-CH_2), 48.4 and 48.8 (C6), 51.4 and 51.5 (C2), 55.4 and 55.9 (NCH_2), 119.2 (C4), 131.2 (C3). — IR (KBr, cm^{-1}): $\tilde{\nu}$ = 2929 s, 2857 m, 1672 s, 1531 w, 1465 w, 1414 w, 1308 w, 1198 s, 1135 s, 828 w, 798 w, 720 m. — The compound does not show UV absorption. — HRMS ((+)-ESI): m/z = 457.4508 (calcd. 457.4516 for $C_{31}H_{57}N_2^+$ $[M+H]^+$); m/z = 229.2287 (calcd. 229.2295 for $C_{31}H_{58}N_2^{2+}$ $[M+H]^{2+}$).

Mass spectra

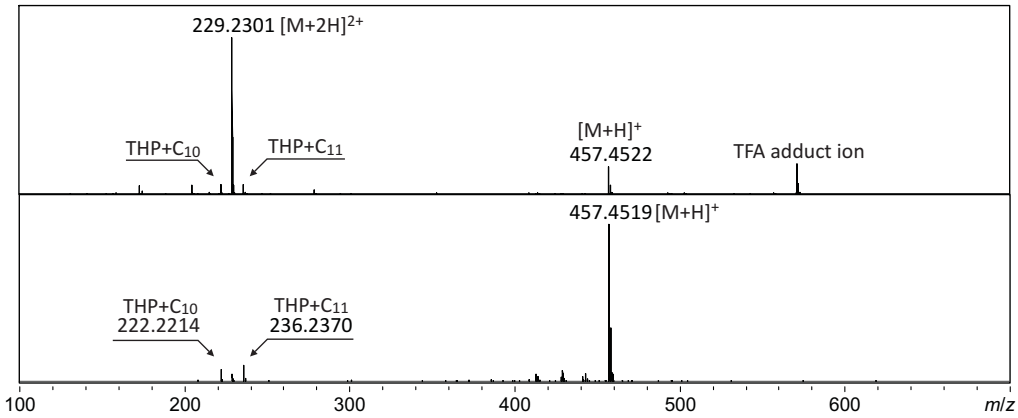

Figure 7.6 High-resolution mass spectrum of haliclamine D (**2**) under standard (top) and in-source CID-MS/MS condition (below). THP = tetrahydropyridine.

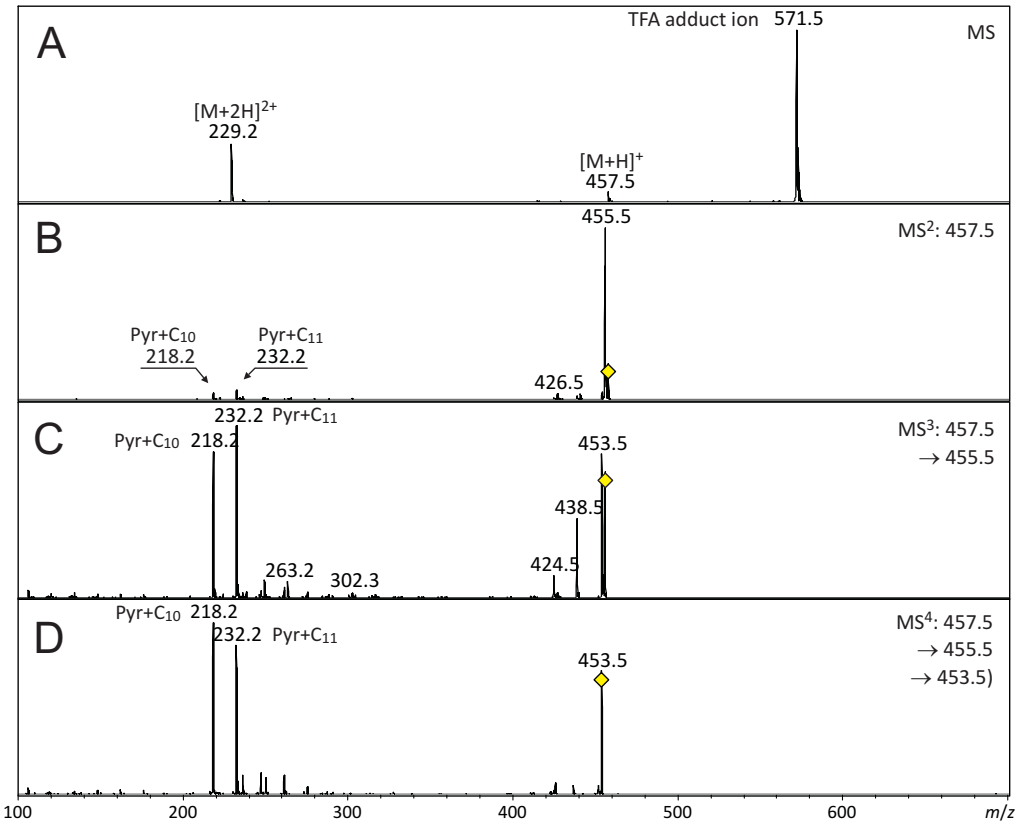

Figure 7.7 MS/MS-fragmentation of the singly charged molecular ion of haliclamine D (**2**) under ion trap conditions. Pyr = pyridine. Precursor ions for fragmentation are marked with a yellow diamond.

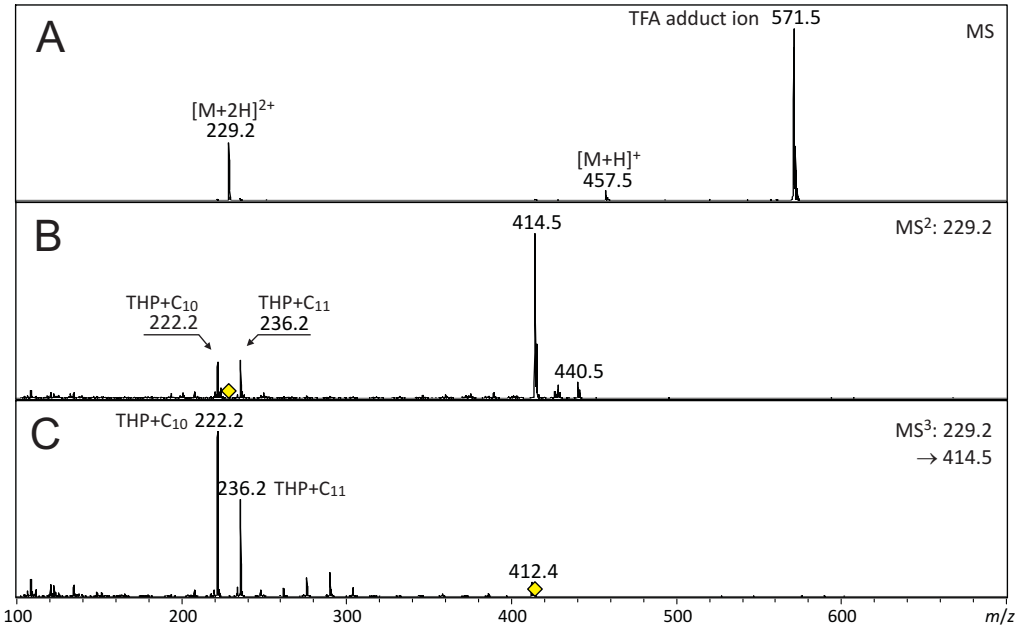

Figure 7.8 MS/MS-fragmentation of the doubly charged molecular ion of haliclamine D (**2**) under ion trap conditions. THP = tetrahydropyridine. Precursor ions for fragmentation are marked with a yellow diamond.

Haliclamine E (**3**), 9/10

Compound data

3-(10-hydroxydecyl)-1-[9-(*N*-oxidopyridine-3-yl)-nonyl]-pyridinium iodide (**3C**). 3-(9-chlorononyl)-pyridine-*N*-oxide (**3A**, 0.80 g, 3.13 mmol), 10-(pyridine-3-yl)-decane-1-ol (**3B**, 0.74 g, 3.13 mmol), and NaI (0.56 g, 3.76 mmol) were treated as described above (procedure 1.). Chromatography on silica (9:1 CH_2Cl_2/MeOH) yielded 0.59 g (33%) of the dimer as a brown solid. — TLC R_f: 0.22 (9:1 CH_2Cl_2/MeOH). — ^{1}H-NMR (250 MHz, DMSO-d_6): δ = 1.07-1.72 (m, 28 H, 14 × CH_2), 1.83-1.98 (m, 2 H, NCH_2CH_2), 2.45-2.59 (m, 2 H, 3-CH_2), 2.79 (t, J = 7.6 Hz, 2 H, 3'-CH_2), 3.29-3.44 (m, 2 H, CH_2OH), 4.33 (t, J = 5.1 Hz, 1 H, OH), 4.55 (t, J = 7.3 Hz, 2 H, NCH_2), 7.20 (d, J = 8.0 Hz, 1 H, H4), 7.32 (dd, J = 7.7 Hz, J = 6.5 Hz, 1 H, H5), 8.02-8.13 (m, 3 H, H2, H6 and H5'), 8.48 (d, J = 8.1 Hz, 1 H, H4'), 8.94 (d, J = 6.0 Hz, 1 H, H6'), 9.04 (s, 1 H, H2'). — ^{13}C-NMR (62.5 MHz, DMSO-d_6): δ = 25.3, 25.4, 28.2, 28.5-28.9 and 29.0 (11 × CH_2), 29.7 (3'-CH_2CH_2), 29.9 (3-CH_2CH_2), 30.5 (NCH_2CH_2), 31.5 (3-CH_2 and 3'-CH_2), 32.4 CH_2CH_2OH), 60.6 (NCH_2), 62.7 (CH_2OH), 125.5 (C4), 126.0 (C5), 127.5 (C5'), 136.2 (C6), 138.1 (C2), 141.4 (C3'), 142.1 (C6'), 143.0 (C3), 143.9 (C2'), 145.0 (C4'). — IR (NaCl, cm^{-1}): $\tilde{\nu}$ = 3416 s, 3027 w, 2926 s, 2854 s, 1734 w, 1630 m, 1503 m, 1443 s, 1355 w, 1260 m, 1163 s, 1052 w, 965 w, 802 w, 762 w, 722 w, 685 s. — HRMS ((+)-ESI): m/z = 455.3591 (calcd. 455.3632 for $C_{29}H_{47}N_2O_2^+$ $[M+H]^+$).

Cyclostellettamine N (**3D**). Following procedure 2./3., cyclostellettamine N (**3D**) was prepared from 3-(10-hydroxydecyl)-1-[9-(*N*-oxidopyridine-3-yl)-nonyl]-pyridinium iodide (**3C**) (0.50 g, 0.86 mmol), PBr_3 (0.32 mL, 3.44 mmol) and NaI (0.28 g, 1.19 mmol). Recrystallisation from MeOH/Et_2O gave 0.39 g (67%) of a yellow solid. TLC bromide: R_f: 0.65 (free base, 9:1 CH_2Cl_2/MeOH); cyclostellettamine N (**3D**): R_f: 0.41 (9:1 CH_2Cl_2/MeOH). — ^{1}H-NMR (250 MHz, DMSO-d_6): δ = 0.96-1.40 (m, 22 H, 11 × CH_2), 1.55-1.72 (m, 4 H, 3-CH_2CH_2), 1.82-1.99 (m, 4 H, NCH_2CH_2), 2.81 (t, J = 6.4 Hz, 4 H, 3-CH_2), 4.60 (t, J = 6.1 Hz, 4 H, NCH_2), 8.10 (dd, J = 7.8, J = 6.1 Hz, 2 H, H5), 8.50 (d, J = 7.9 Hz, 2 H, H4), 8.97 (d, J = 5.9 Hz, 2 H, H6), 9.11 (s, 2 H, H2). — ^{13}C-NMR (62.5 MHz, DMSO-d_6): δ = 24.5, 24.9, 27.0, 27.5, 27.8, 28.1-28.6, 29.0 and 29.2 (13 × CH_2), 29.9 and 30.0 (3-CH_2CH_2), 31.0 and 31.3 (3-CH_2), 60.4 and 60.5 (NCH_2), 127.7 (C5), 142.3 (C6), 142.6 (C3), 143.9 (C2),

145.3 (C4). — IR (KBr, cm^{-1}): $\tilde{\nu}$ = 3011 s, 2922 s, 2851 s, 1624 m, 1501 s, 1467 m, 1444 m, 1364 w, 1238 w, 1205 w, 1153 w, 930 w, 828 w, 697 s, 618 w. — UV (DAD): λ_{max} = 218, 270 nm; λ_{min} = 242 nm. — HRMS ((+)-ESI): m/z = 549.2682 (calcd. 549.2700 for $C_{29}H_{46}N_2I^+$ $[M+H]^+$); m/z = 211.1824 (calcd. 211.1825 for $C_{29}H_{46}N_2{}^{2+}$ $[M+H]^{2+}$).

Haliclamine E (**3**). In the manner described above (procedure 4.), 100 mg of cyclostellettamine N (**3D**) were treated with 100 mg of $NaBH_4$. Purification of 47 mg of the crude product via HPLC yielded 32 mg (35%) haliclamine (**3**) as TFA-salt. — TLC R_f: 0.43 (9:1 CH_2Cl_2/MeOH). — ^{1}H-NMR (300 MHz, $CDCl_3$): δ = 1.18-1.49 (m, 26 H, 13 × CH_2), 1.72-1.89 (m, 4 H, NCH_2CH_2), 2.20 (t, J = 6.6 Hz, 4 H, 3-CH_2), 2.27 (d, J = 17.3 Hz, 2 H, H5'), 2.51-2.69 (m, 2 H, H5), 2.87-3.16 (m, 6 H, NCH_2 and H6), 3.21-3.37 (m, 2 H, H2'), 3.43-3.55 (m, 2 H, H6), 3.90 (d, J = 15.7 Hz, 2 H, H2), 5.62 (s, 2 H, H4), 12.69 (br. s, 2 H, NH). — ^{13}C-NMR (75.0 MHz, $CDCl_3$): δ = 21.5 and 21.8 (C5), 23.5 and 23.8 (NCH_2CH_2), 26.0, 26.4, 27.0, 27.1, 27.2, 28.0-28.7 and 29.0 (13 × CH_2), 34.3 and 34.7 (3-CH_2), 47.9 and 48.7 (C6), 50.8 and 51.1 (C2), 54.8 and 55.5 (NCH_2), 119.1 (C4), 131.1 (C3). — IR (KBr, cm^{-1}): $\tilde{\nu}$ = 2932 m, 2860 m, 2623 w, 1685 s, 1465 w, 1406 w, 1198 s, 1162 s, 1133 s, 828 m, 797 m, 719 m. — The compound does not show UV absorption. — HRMS ((+)-ESI): m/z = 429.4161 (calcd. 429.4203 for $C_{29}H_{53}N_2{}^+$ $[M+H]^+$); m/z = 215.2129 (calcd. 215.2138 for $C_{29}H_{54}N_2{}^{2+}$ $[M+H]^{2+}$); m/z = 543.4057 (calcd. 543.4127 for $C_{29}H_{54}N_2{}^{2+}$ × $C_2F_3O_2{}^-$ $[M+H]^+$).

Mass spectra

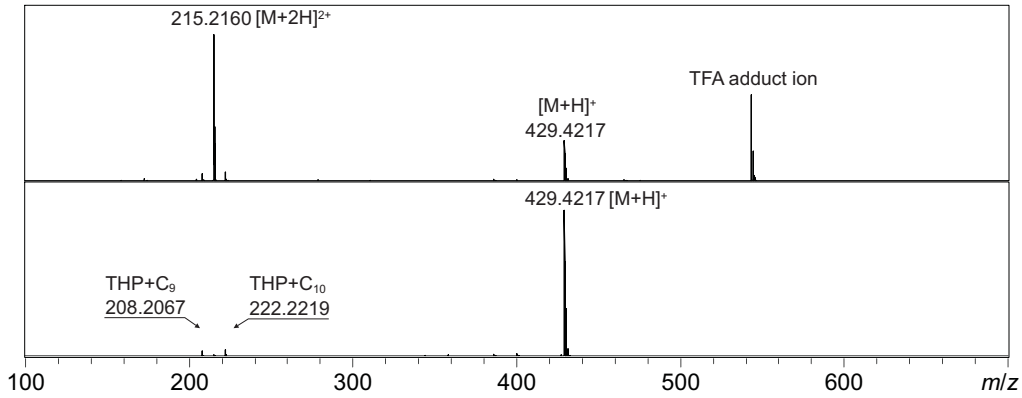

Figure 7.9 High-resolution mass spectrum of haliclamine E (**3**) under standard (top) and in-source CID-MS/MS condition (below). THP = tetrahydropyridine.

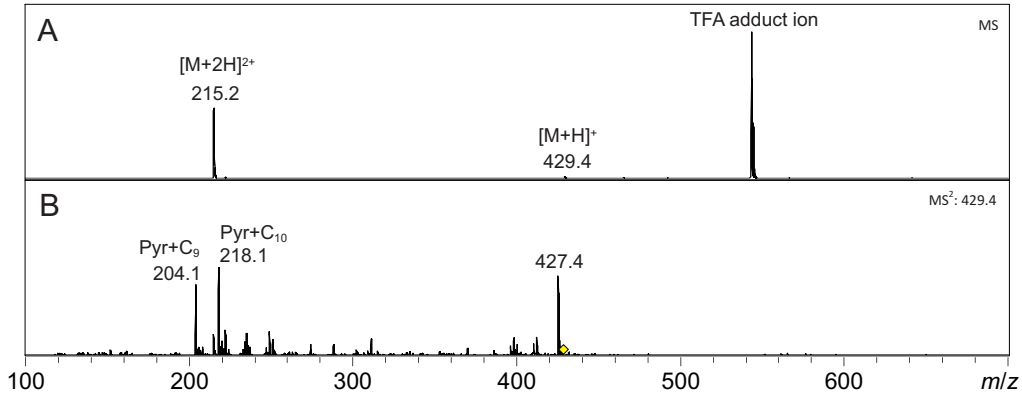

Figure 7.10 MS/MS-fragmentation of the singly charged molecular ion of haliclamine E (**3**) under ion trap conditions. Pyr = pyridine. Precursor ions for fragmentation are marked with a yellow diamond.

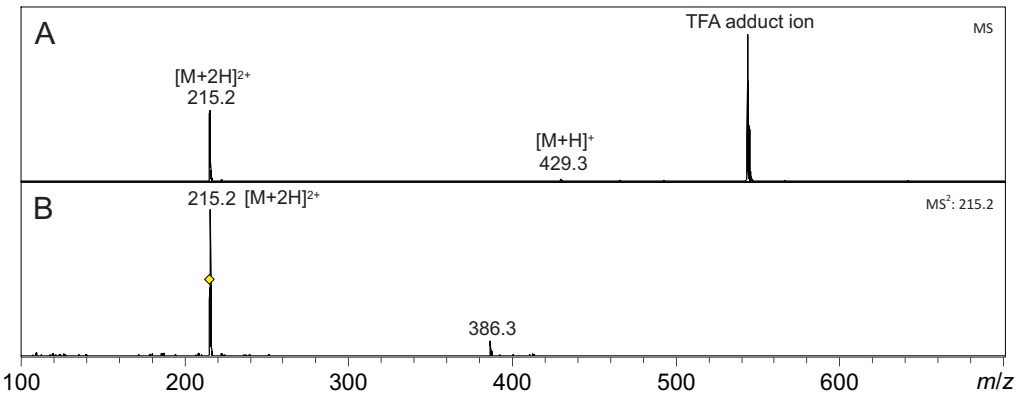

Figure 7.11 MS/MS-fragmentation of the doubly charged molecular ion of haliclamine E (**3**) under ion trap conditions. THP = tetrahydropyridine. Precursor ions for fragmentation are marked with a yellow diamond.

Haliclamine F (**4**), 11/11

Compound data

3-(11-hydroxyundecyl)-1-[11-(*N*-oxidopyridine-3-yl)-undecyl]-pyridinium iodide (**4C**). 3-(11-chloroundecyl)-pyridine-*N*-oxide (**4A**, 0.90 g, 3.17 mmol), 11-(pyridine-3-yl)-undecane-1-ol (**4B**, 0.79 g, 3.17 mmol), and NaI (0.57 g, 3.80 mmol) were treated as described above (procedure 1.). Chromatography on silica (9:1 CH_2Cl_2/MeOH) yielded 1.38 g (70%) of the dimer as a yellow solid. — TLC R_f: 0.42 (9:1 CH_2Cl_2/MeOH). — ^{1}H-NMR (250 MHz, DMSO-d_6): δ = 1.11-1.73 (m, 34 H, 17 × CH_2), 1.82-2.03 (m, 2 H, NCH$_2$CH_2), 2.53 (t, J = 7.8 Hz, 2 H, 3-CH_2), 2.79 (t, J = 7.6 Hz, 2 H, 3'-CH_2), 3.36 (dt, J = 6.6 Hz, J = 5.4 Hz, 2 H, CH_2OH), 4.30 (t, J = 5.1 Hz, 1 H, OH), 4.55 (t, J = 7.3 Hz, 2 H, NCH_2), 7.19 (d, J = 7.9 Hz, 1 H, H4), 7.31 (dd, J = 7.3 Hz, J = 6.7 Hz, 1 H, H5), 8.02-8.12 (m, 3 H, H2, H6, H5'), 8.48 (d, J = 8.0 Hz, 1 H, H4'), 8.93 (d, J = 6.0 Hz, 1 H, H6'), 9.02 (s, 1H, H2'). — ^{13}C-NMR (62.5 MHz, DMSO-d_6): δ = 25.2, 25.4 and 28.1-28.9 (14 × CH_2), 29.6 (3'-CH$_2$CH_2), 29.8 (3-CH$_2$CH_2), 30.5 (NCH$_2$CH_2), 31.4 (3'-CH_2), 31.5 (3-CH_2), 32.4 (CH_2CH$_2$OH), 60.6 (CH_2OH and NCH_2), 125.3 (C4), 125.9 (C5), 127.4 (C5'), 136.1 (C6), 138.1 (C2), 141.3 (C3'), 142.1 (C6'), 142.9 (C3), 143.8 (C2'), 145.0 (C4'). — IR (KBr, cm^{-1}): $\tilde{\nu}$ = 3405 m, 3059 w, 2922 s, 2849 s, 1735 w, 1628 w, 1600 w, 1560 w, 1468 m, 1430 w, 1268 w, 1156 m, 1049 w, 1014 w, 963 w, 802 w, 758 w, 720 w, 682 m. — HRMS ((+)-ESI): m/z = 497.4065 (calcd. 497.4102 for $C_{32}H_{53}N_2O_2^+$ [M+H]$^+$).

Cyclostellettamine R (**4D**). Following procedure 2./3., cyclostellettamine R (**4D**) was prepared from 3-(11-hydroxyundecyl)-1-[11-(*N*-oxidopyridine-3-yl)-undecyl]-pyridinium iodide (**4C**) (1.00 g, 1.60 mmol), PBr_3 (0.62 mL, 6.40 mmol) and NaI (0.53 g, 3.52 mmol). Recrystallisation from H_2O yielded 598 mg (52%) as a yellow solid. — TLC bromide: R_f: 0.6 (free base, 9:1 CH_2Cl_2/MeOH); cyclostellettamine R (**4D**): R_f: 0.15 (9:1 CH_2Cl_2/MeOH). — M. p. 228 ï¿½C. — ^{1}H-NMR (250 MHz, DMSO-d_6): δ = 0.96-1.33 (m, 28 H, 14 × CH_2), 1.51-1.76 (m, 4 H, 3-CH$_2$CH_2), 1.80-2.00 (m, 4 H, NCH$_2$CH_2), 2.81 (t, J = 6.7 Hz, 4 H, 3-CH_2), 4.64 (t, J = 6.2 Hz, 2 H, NCH_2), 8.10 (dd, J = 7.8 Hz, J = 6.1 Hz, 2 H, H5), 8.51 (d, J = 7.9 Hz, 2 H, H4), 9.05 (d, J = 5.8 Hz, 2 H, H6), 9.18 (s, 2 H, H2). — ^{13}C-NMR (75.0 MHz, DMSO-d_6): δ = 25.0, 27.5, 28.4, 28.7-29.0 and 29.3 (16 × CH_2), 30.1 (3-CH$_2$CH_2),

31.2 (3-CH_2), 60.4 (NCH_2), 127.7 (C5), 142.3 (C6), 142.5 (C3), 144.0 (C2), 145.3 (C4). — IR (KBr, cm^{-1}): $\tilde{\nu}$ = 3012 s, 2921 s, 2852 s, 1627 m, 1582 w, 1502 s, 1469 s, 1445 m, 1371 w, 1241 w, 1207 w, 1171 w, 1152 w, 953 w, 924 w, 846 w, 820 m, 759 w, 697 s. — EA calcd. for $C_{32}H_{52}N_2I_2$ (718.58): C 53.49, H 7.29, N 3.90; found C 53.34, H 7.29, N 3.73. — UV (DAD): λ_{max} = 218, 270 nm; λ_{min} = 242 nm. — HRMS ((+)-ESI): m/z = 232.2042 (calcd. 232.2060 for $C_{32}H_{52}N_2^{2+}$ $[M+H]^{2+}$).

Haliclamine F (**4**). In the manner described above (procedure 4.), 100 mg of cyclostellettamine R (**4D**) were treated with 100 mg of $NaBH_4$. Purification of 29 mg of the crude product via HPLC yielded 20 mg (20%) haliclamine F (**4**) as TFA-salt. — TLC R_f: 0.43 (9:1 CH_2Cl_2/MeOH). — ^{1}H-NMR (300 MHz, $CDCl_3$): δ = 1.18-1.49 (m, 32 H, 16 × CH_2), 1.70-1.85 (m, 4 H, NCH_2CH_2), 2.01 (t, J = 7.1 Hz, 4 H, 3-CH_2), 2.26 (d, J = 18.5 Hz, 2 H, H5'), 2.55-2.72 (m, 2 H, H5), 2.85-3.11 (m, 6 H, H6' and NCH_2), 3.25 (d, J = 16.0 Hz, 2 H, H2'), 3.46-3.58 (m, 2 H, H6), 3.89 (d, J = 15.8 Hz, 2 H, H2), 5.62 (s, 2 H, H4), 12.62 (s, 2 H, NH). — ^{13}C-NMR (75.0 MHz, $CDCl_3$): δ = 21.5 and 21.6 (C5), 23.5 (NCH_2CH_2), 26.4, 27.0, 27.1, and 28.3-29.0 (16 × CH_2), 34.4 and 34.6 (3-CH_2), 48.1 and 48.3 (C6), 51.4 and 51.5 (C2), 55.2 and 55.5 (NCH_2), 119.1 (C4), 131.1 (C3). — IR (KBr, cm^{-1}): $\tilde{\nu}$ = 2928 s, 2856 m, 1675 s, 1465 w, 1412 w, 1197 s, 1170 s, 1132 s, 828 w, 798 w, 720 m. — The compound does not show UV absorption. — HRMS ((+)-ESI): m/z = 236.2371 (calcd. 236.2373 for $C_{32}H_{60}N_2^{2+}$ $[M+H]^{2+}$).

Mass spectra

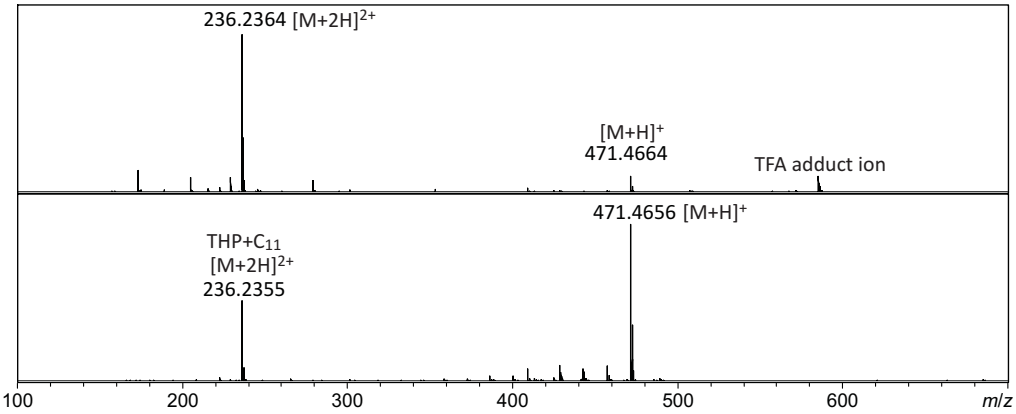

Figure 7.12 High-resolution mass spectrum of haliclamine F (**4**) under standard (top) and in-source CID-MS/MS condition (below). THP = tetrahydropyridine.

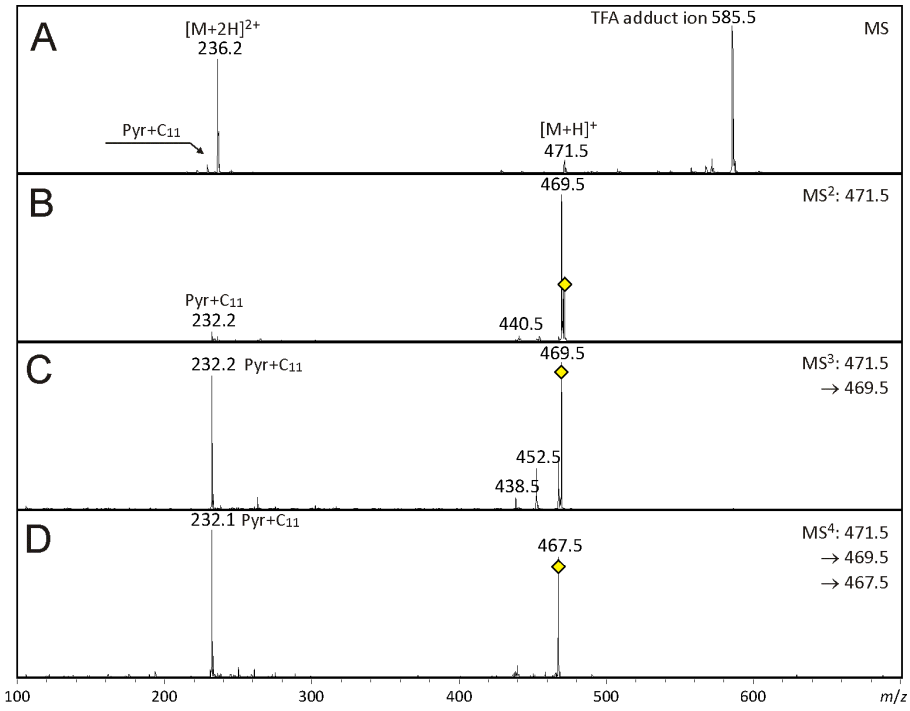

Figure 7.13 MS/MS-fragmentation of the singly charged molecular ion of haliclamine F (**4**) under ion trap conditions. Pyr = pyridine. Precursor ions for fragmentation are marked with a yellow diamond.

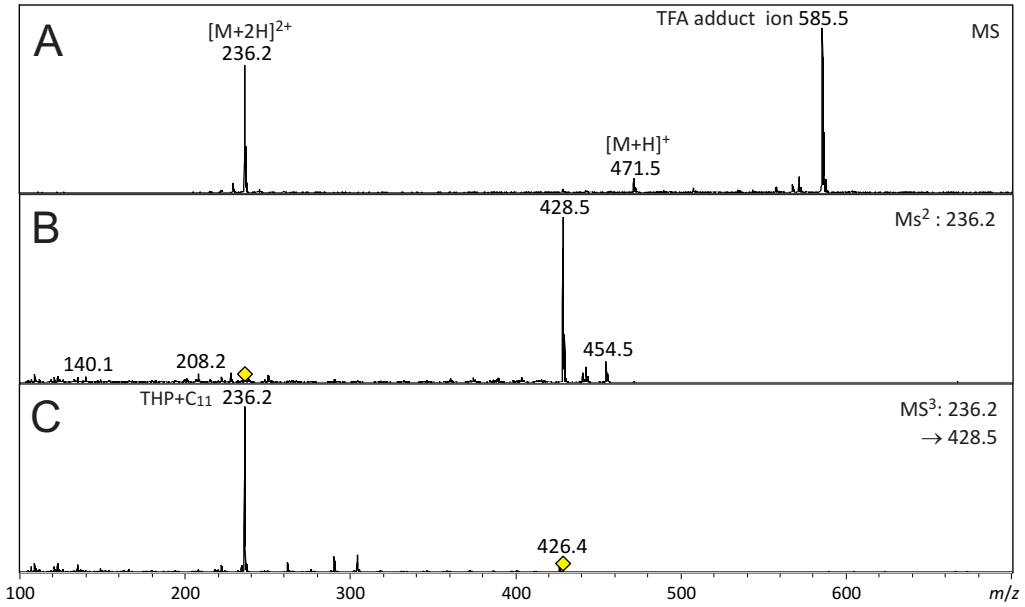

Figure 7.14 MS/MS-fragmentation of the doubly charged molecular ion of haliclamine F (**4**) under ion trap conditions. THP = tetrahydropyridine. Precursor ions for fragmentation are marked with a yellow diamond.

Haliclamine G (**5**), 12/12

Compound data

3-(12-hydroxydodecyl)-1-[12-(*N*-oxidopyridine-3-yl)-dodecyl]-pyridinium iodide (**5C**). 3-(12-chlorododecyl)-pyridine-*N*-oxide (**5A**, 0.89 g, 3.35 mmol), 12-(pyridine-3-yl)-dodecane-1-ol (**5B**, 1.00 g, 3.35 mmol), and NaI (0.60 g, 4.00 mmol) were treated as described above (procedure 1.). Chromatography on silica (9:1 CH_2Cl_2/MeOH) yielded 1.99 g (91%) of the dimer as a light yellow solid. — TLC R_f: 0.34 (9:1 CH_2Cl_2/MeOH) — ^{1}H-NMR (250 MHz, DMSO-d_6): δ = 1.13-1.72 (m, 38 H, 19 × CH_2), 1.82-2.00 (m, 2 H, NCH_2CH_2), 2.50-2.56 (m, 2 H, 3-CH_2), 2.80 (t, J = 7.5 Hz, 2 H, 3'-CH_2), 3.33-3.40 (m, 2 H, CH_2OH), 4.37 (t, J = 5.0 Hz, 1 H, OH), 4.59 (t, J = 7.3 Hz, 2 H, NCH_2), 7.20 (d, J = 8.2 Hz, 1 H, H4), 7.29-7.37 (m, 1 H, H5), 8.02-8.14 (m, 3 H, H2, H6, H5'), 8.49 (d, J = 8.3 Hz, 1 H, H4'), 8.99 (d, J = 6.0 Hz, 1 H, H6'), 9.10 (s, 1 H, H2') — ^{13}C-NMR (62.5 MHz, DMSO-d_6): δ = 25.3, 25.5 and 28.2-29.1 (16 × CH_2), 29.7 (3'-CH_2CH_2), 29.9 (3-CH_2CH_2), 30.6 (NCH_2CH_2), 31.5 (3'-CH_2 and 3-CH_2), 32.5 (CH_2CH_2OH), 60.6 (CH_2OH and NCH_2), 125.5 (C4), 126.1 (C5), 127.6 C5'), 136.3 (C6), 138.1 (C2), 141.5 (C3'), 142.1 (C6'), 143.0 (C3), 143.9 (C2'), 145.1 (C4') — IR (KBr, cm^{-1}): $\tilde{\nu}$ = 3346 s, 3041 m, 2916 s, 2850 s, 1654 w, 1630 w, 1599 w, 1560 w, 1501 w, 1481 w, 1470 s, 1438 m, 1325 w, 1270 s, 1203 w, 1157 s, 1048 m, 1014 m, 940 w, 885 w, 855 w, 811 m, 760 w, 716 w, 680 m — HRMS ((+)-ESI): m/z = 525.4368 (calcd. 525.4415 for $C_{34}H_{57}N_2O_2^+$ [M+H]$^+$).

Cyclostellettamine A (**5D**). For preparation and compound data refer to Baldwin et al.[203]

Haliclamine G (**5**). In the manner described above (procedure 4.), 100 mg of cyclostellettamine A (**5D**) were treated with 100 mg of $NaBH_4$. Purification of 45 mg of the crude product via HPLC yielded 31.1 mg (32%) haliclamine G (**5**) as TFA-salt. — TLC R_f: 0.51 (9:1 CH_2Cl_2/MeOH) — ^{1}H-NMR (250 MHz, $CDCl_3$): δ = 1.14-1.48 (m, 40 H, 20 × CH_2), 1.70-1.89 (m, 4 H, NCH_2CH_2), 2.01 (t, J = 7.1 Hz, 4 H, 3-CH_2), 2.26 (d, J = 18.3 Hz, 2 H, H5'), 2.55-2.69 (m, 2 H, H5), 2.87-3.12 (m, 6 H, H6' and NCH_2), 3.23 (d, J = 16.0 Hz, 2 H, H2'), 3.43-3.56 (m, 2 H, H6), 3.89 (d, J = 15.8 Hz, 2 H, H2), 5.62 (s, 2 H, H4), 12.87 (s, 2 H, NH) — ^{13}C-NMR (150 MHz, $CDCl_3$): δ = 21.2 and 21.3 (C5), 23.8(NCH_2CH_2), 26.5, 27.0 and 27.2, 28.6,

28.8-29.1 and 29.2 (20 × CH_2), 34.6 (3-CH_2), 48.1 (C6), 51.3 (C2), 55.3 (NCH_2), 119.0 (C4), 131.1 (C3) — IR (KBr, cm^{-1}): $\tilde{\nu}$ = 2929 s, 2855 m, 2593 w, 1735 w, 1670 s, 1467 m, 1420 w, 1194 s, 1175 s, 1149 s, 831 m, 799 m, 719 m — The compound does not show UV absorption. — HRMS ((+)-ESI): m/z = 264.2676 (calcd. 264.2686 for $C_{36}H_{68}N_2{}^{2+}$ $[M+2H]^{2+}$).

Mass spectra

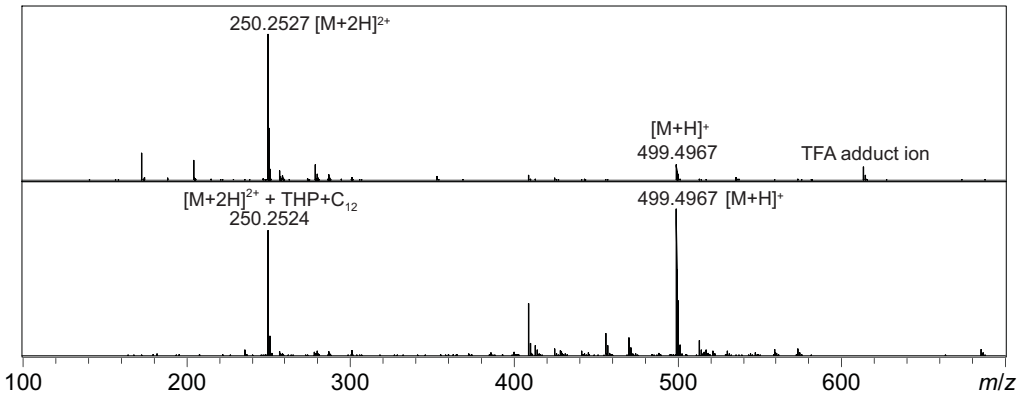

Figure 7.15 High-resolution mass spectrum of haliclamine G (**5**) under standard (top) and in-source CID-MS/MS condition (below). THP = tetrahydropyridine.

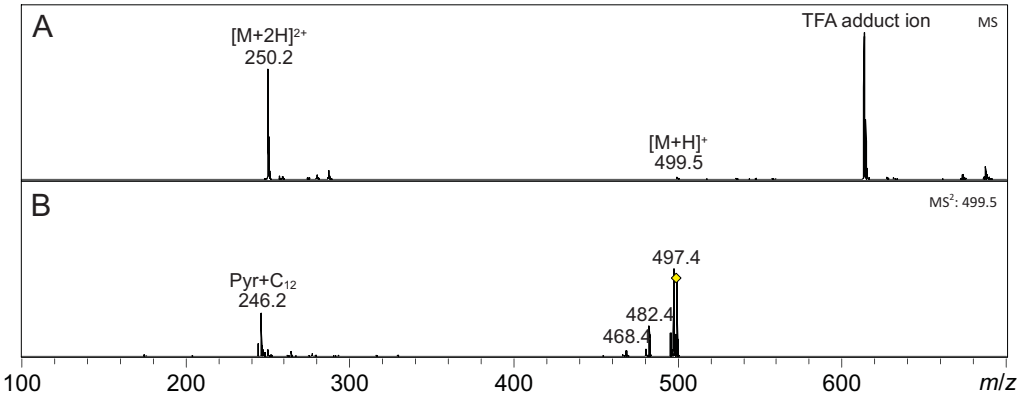

Figure 7.16 MS/MS-fragmentation of the singly charged molecular ion of haliclamine G (**5**) under ion trap conditions. Pyr = pyridine. Precursor ions for fragmentation are marked with a yellow diamond.

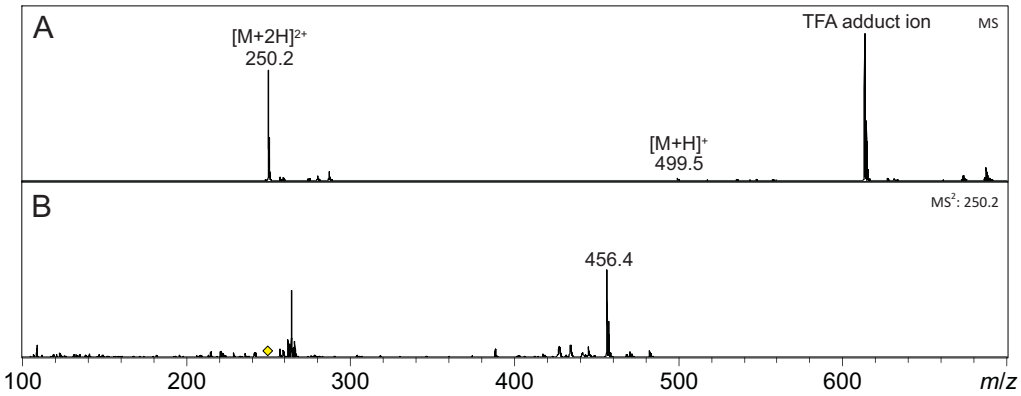

Figure 7.17 MS/MS-fragmentation of the doubly charged molecular ion of haliclamine G (**5**) under ion trap conditions. THP = tetrahydropyridine. Precursor ions for fragmentation are marked with a yellow diamond.

Haliclamine H (**6**), 13/13

Compound data

3-(13-hydroxytridecyl)-1-[13-(*N*-oxidopyridine-3-yl)-tridecyl]-pyridinium iodide (**6C**). 3-(13-chlorotridecyl)-pyridine-*N*-oxide (**6A**, 0.30 g, 1.08 mmol), 13-(pyridine-3-yl)-tridecane-1-ol (**6B**, 0.34 g, 1.08 mmol), and NaI (0.19 g, 1.30 mmol) were treated as described above (procedure 1.). Chromatography on silica (9:1 CH_2Cl_2/MeOH) yielded 475 mg (65%) of the dimer as a light yellow solid. — TLC R_f: 0.44 (5:1 CH_2Cl_2/MeOH) — ^{1}H-NMR (250 MHz, MeOD-d_4): δ = 1.13-1.83 (m, 42 H, 21 × CH_2), 1.96-2.11 (m, 2 H, NCH_2CH_2), 2.68 (t, J = 7.6 Hz, 2 H, 3-CH_2), 2.90 (t, J = 7.6 Hz, 2 H, 3'-CH_2), 3.53 (t, J = 6.5 Hz, 2 H, CH_2OH), 4.64 (t, J = 7.3 Hz, 2 H, NCH_2), 7.44-7.58 (m, 2 H, H4 and H5), 8.03 (dd, J = 7.4 Hz, J = 6.3 Hz 1 H, H5'), 8.15-8.27 (m, 2 H, H2 and H6), 8.47 (d, J = 7.9 Hz, 1 H, H4'), 8.87 (d, J = 5.7 Hz, 1 H, H6'), 8.98 (s, 1 H, H2') — ^{13}C-NMR (62.5 MHz, MeOD-d_4): δ = 27.0, 27.2, 30.1 and 30.4-30.8 (18 × CH_2), 31.6 (3'-CH_2CH_2), 31.7 (3-CH_2CH_2), 32.5 (NCH_2CH_2), 33.5 (3'-CH_2) 33.6 (3-CH_2), 33.7 (CH_2CH_2OH), 63.0 (CH_2OH and NCH_2), 127.7 (C4), 129.0 (C5), 131.6 (C5'), 137.9 (C6), 140.0 (C2), 143.4 (C3'), 144.4 (C6'), 145.3 (C3), 145.8 (C2'), 146.7 (C4') — IR (KBr, cm^{-1}): $\tilde{\nu}$ = 3396 s, 3075 m, 2919 s, 2848 s, 1702 w, 1627 m, 1601 m, 1560 m, 1498 w, 1469 s, 1436 s, 1371 w, 1298 m, 1269 s, 1217 m, 1155 s, 1052 s, 1013 s, 962 s, 905 w, 865 w, 810 m, 793 m, 759 m, 718 s, 682 s — HRMS ((+)-ESI): m/z = 553.4711 (calcd. 553.4728 for $C_{36}H_{61}N_2O_2^+$ $[M+H]^+$).

Cyclostellettamine C (**6D**). For preparation and compound data refer to Baldwin et al.[203]

Haliclamine H (**6**). In the manner described above (procedure 4.), 100 mg of cyclostellettamine C (**6D**) were treated with 100 mg of $NaBH_4$. Purification of 44 mg of the crude product via HPLC yielded 27.8 mg (29%) haliclamine H (**6**) as TFA-salt. — TLC R_f: 0.51 (9:1 CH_2Cl_2/MeOH) — ^{1}H-NMR (250 MHz, $CDCl_3$): δ = 1.21-1.45 (m, 36 H, 18 × CH_2), 1.71-1.84 (m, 4 H, NCH_2CH_2), 2.01 (t, J = 7.0 Hz, 4 H, 3-CH_2), 2.27 (d, J = 18.4 Hz, 2 H, H5'), 2.51-2.69 (m, 2 H, H5), 2.89-3.12 (m, 6 H, H6' and NCH_2), 3.24 (d, J = 16.3 Hz, 2 H, H2'), 3.44-3.56 (m, 2 H, H6), 3.90 (d, J = 16.1 Hz, 2 H, H2), 5.62 (s, 2 H, H4), 12.75 (s, 2 H, NH) — ^{13}C-NMR

(150 MHz, $CDCl_3$): δ = 21.3 (C5), 23.9 (NCH_2CH_2), 26.3, 27.2, 28.6, 28.7-29.0, 29.1 (18 × CH_2), 34.5 (3-CH_2), 48.1 (C6), 51.4 (C2), 55.0 (NCH_2), 118.9 (C4), 131.1 (C3) — IR (KBr, cm^{-1}): $\tilde{\nu}$ = 2928 s, 2854 s, 2579 w, 1671 s, 1467 m, 1414 w, 1196 s, 1173 s, 1143 s, 830 m, 800 w, 720 m — The compound does not show UV absorption. — HRMS ((+)-ESI): m/z = 250.2519 (calcd. 250.2530 for $C_{34}H_{64}N_2{}^{2+}$ $[M+2H]^{2+}$).

Mass spectra

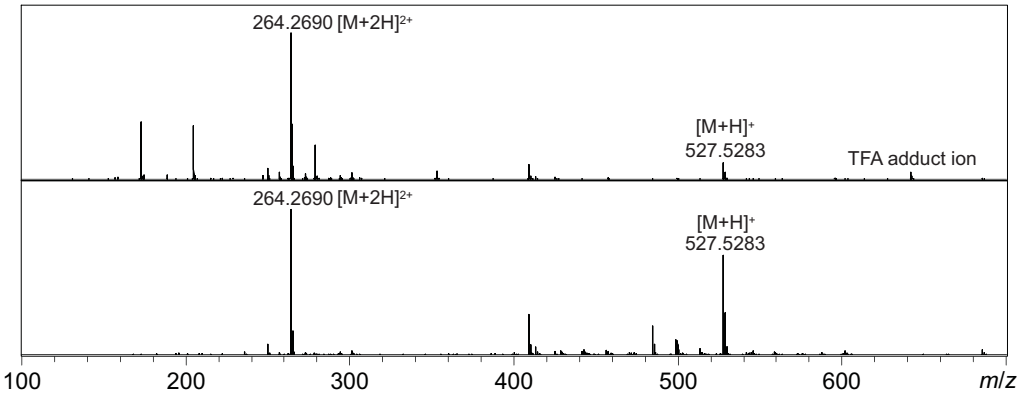

Figure 7.18 High-resolution mass spectrum of haliclamine H (**6**) under standard (top) and in-source CID-MS/MS condition (below). THP = tetrahydropyridine.

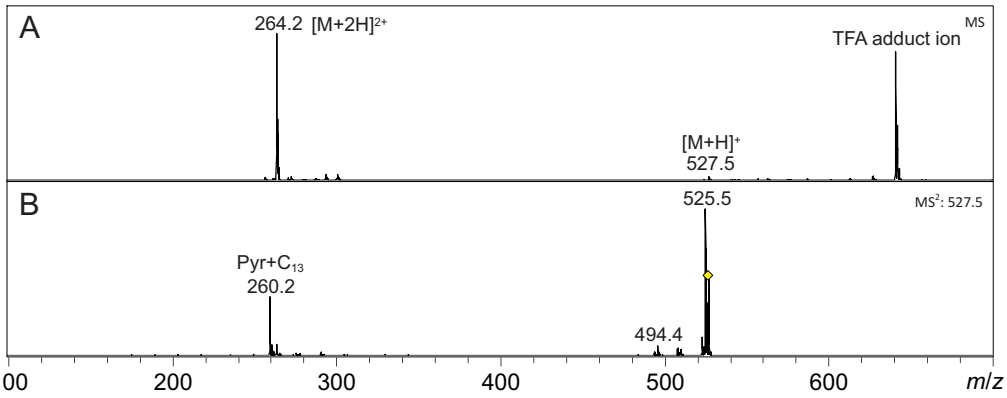

Figure 7.19 MS/MS-fragmentation of the singly charged molecular ion of haliclamine H (**6**) under ion trap conditions. Pyr = pyridine. Precursor ions for fragmentation are marked with a yellow diamond.

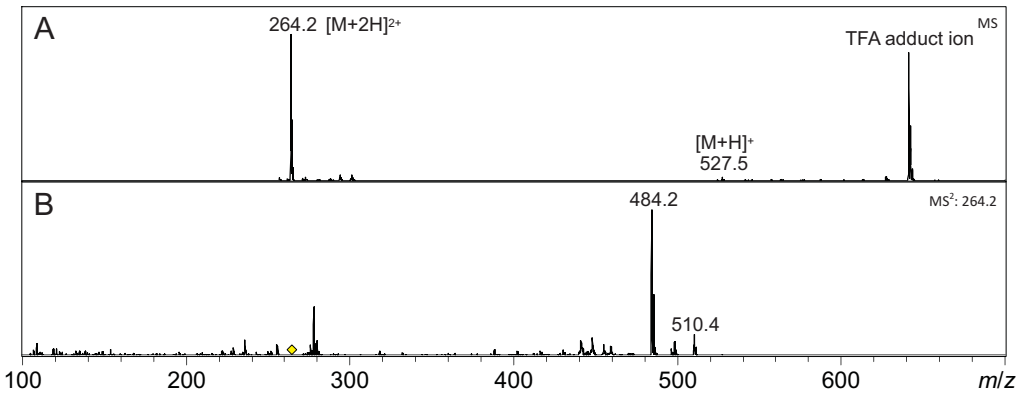

Figure 7.20 MS/MS-fragmentation of the doubly charged molecular ion of haliclamine H (**6**) under ion trap conditions. THP = tetrahydropyridine. Precursor ions for fragmentation are marked with a yellow diamond.

Haliclamine I (**7**), 11/14

Compound data

3-(14-hydroxytetradecyl)-1-[11-(*N*-oxidopyridine-3-yl)-undecyl]-pyridinium iodide (**7C**). For preparation and compound data refer to Grube et al.[117]

Cyclostellettamine L (**7D**). For preparation and compound data refer to Grube et al.[117]

Haliclamine I (**7**). In the manner described above (procedure 4.), 100 mg of cyclostellettamine L (**6D**) were treated with 100 mg of $NaBH_4$. Purification of 67 mg of the crude product via HPLC yielded 37 mg (39%) haliclamine I (**7**) as TFA-salt. — TLC R_f: 0.51 (9:1 CH_2Cl_2/MeOH) — ^{1}H-NMR (250 MHz, $CDCl_3$): δ = 1.21-1.48 (m, 38 H, 19 × CH_2), 1.69-1.88 (m, 4 H, NCH_2CH_2), 1.96-2.10 (m, 4 H, 3-CH_2), 2.27 (d, J = 18.1 Hz, 2 H, H5'), 2.51-2.70 (m, 2 H, H5), 2.88-3.11 (m, 6 H, H6' and NCH_2), 3.24 (d, J = 16.1 Hz, 2 H, H2'), 3.44-3.57 (m, 2 H, H6), 3.90 (d, J = 16.0 Hz, 2 H, H2), 5.62 (s, 2 H, H4), 12.73 (s, 2 H, NH) — ^{13}C-NMR (150 MHz, $CDCl_3$): δ = 21.3 and 21.4 (C5), 23.7 and 23.8 (NCH_2CH_2), 26.4, 27.1, 28.6-29.1 (19 × CH_2), 34.5 and 34.6 (3-CH_2), 48.1 and 48.2 (C6), 51.4 and 51.5 (C2), 55.0 and 55.1 (NCH_2), 118.9 and 119.0 (C4), 131.0 (C3) — IR (KBr, cm^{-1}): $\tilde{\nu}$ = 2929 s, 2855 s, 2441 w, 1670 s, 1468 m, 1418 w, 1196 s, 1142 s, 830 m, 800 m, 720 s — The compound does not show UV absorption. — HRMS ((+)-ESI): m/z = 257.2590 (calcd. 257.2608 for $C_{35}H_{66}N_2^{2+}$ $[M+2H]^{2+}$).

Mass spectra

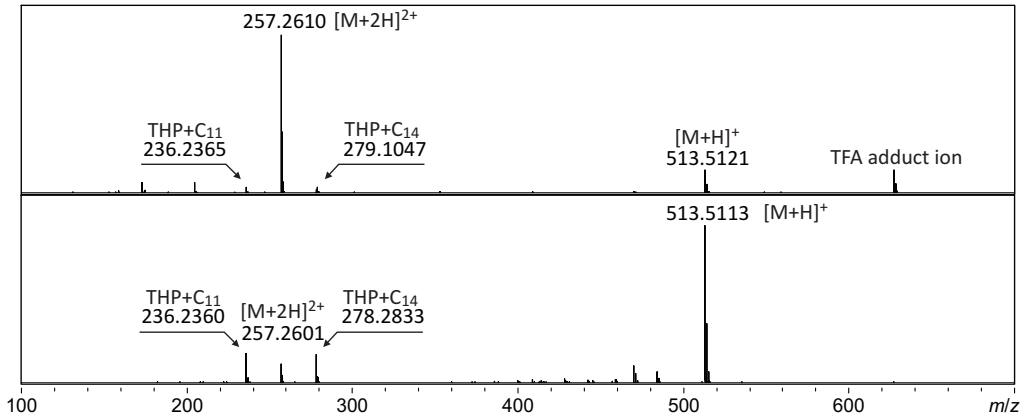

Figure 7.21 High-resolution mass spectrum of haliclamine I (**7**) under standard (top) and in-source CID-MS/MS condition (below). THP = tetrahydropyridine.

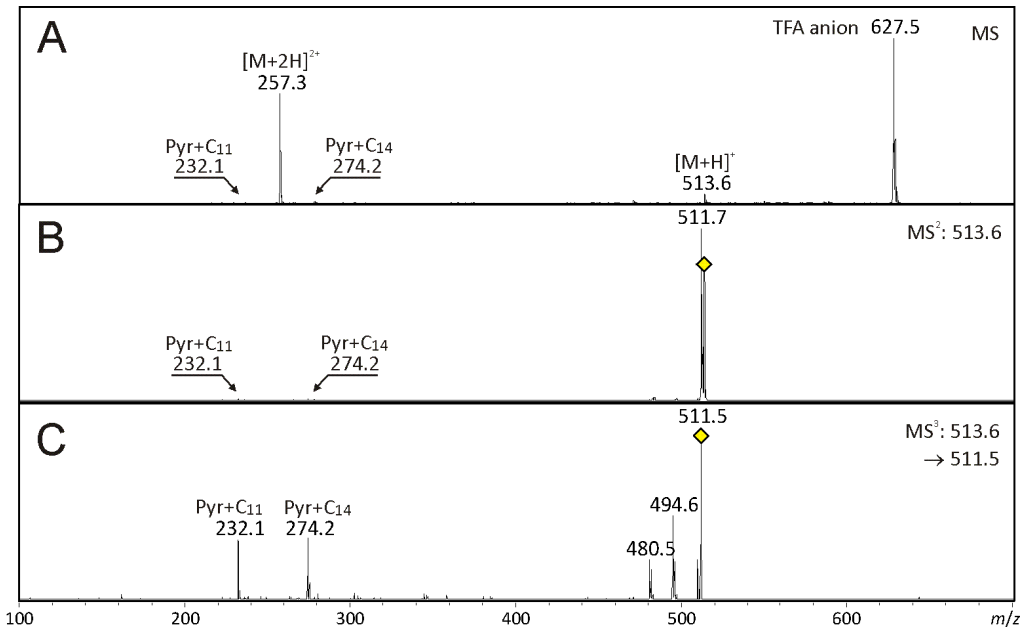

Figure 7.22 MS/MS-fragmentation of the singly charged molecular ion of haliclamine I (**7**) under ion trap conditions. Pyr = pyridine. Precursor ions for fragmentation are marked with a yellow diamond.

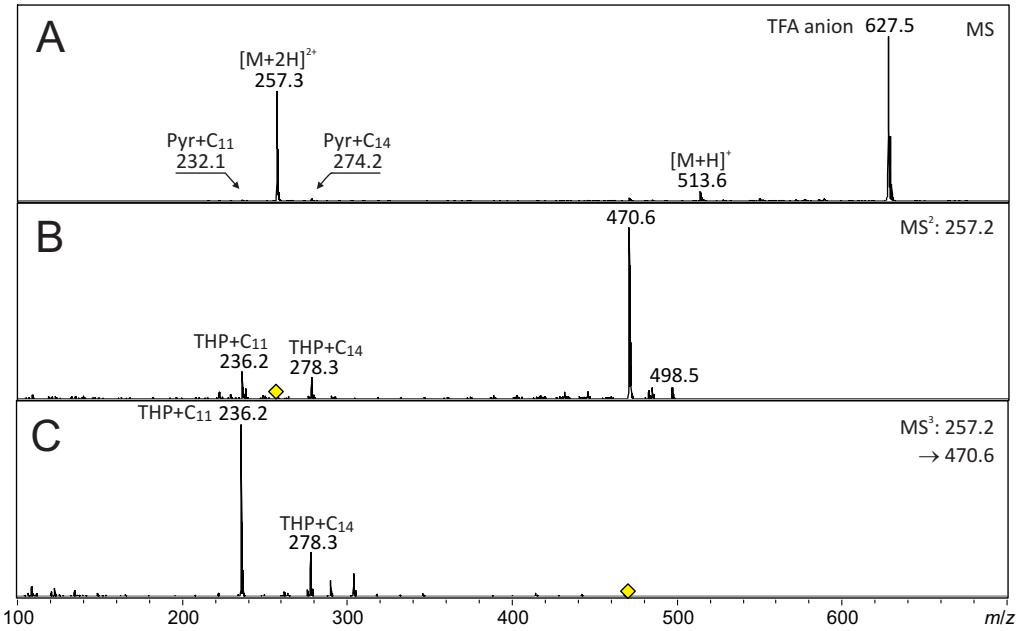

Figure 7.23 MS/MS-fragmentation of the doubly charged molecular ion of haliclamine I (**7**) under ion trap conditions. Pyr = pyridine, THP = tetrahydropyridine. Precursor ions for fragmentation are marked with a yellow diamond.

Haliclocyclin C, a new monomeric 3-alkyl pyridinium alkaloid from the Arctic marine sponge *Haliclona viscosa*

Gesine Schmidt,[a] Christoph Timm[a] and Matthias Köck*[a]

Received (in XXX, XXX) Xth XXXXXXXXX 200X, Accepted Xth XXXXXXXXX 200X
First published on the web Xth XXXXXXXXX 200X
DOI: 10.1039/b000000x

For the first time, the macrocyclic monomeric 3-alkyl pyridinium alkaloid with an alkyl chain of 13 methylene groups, haliclocyclin C (**1**) could be identified from a natural source in the crude extract of the Arctic sponge *Haliclona viscosa*. Structure elucidation based on the comparison of the natural product with the corresponding synthetic compound.

In recent years, a number of novel 3-alkyl pyridinium alkaloids were identified from the crude extract of the Arctic marine sponge *Haliclona viscosa*.[1-2, 3] The material available from this sponge is limited by the small size of the individuals, their slow growth rate and the effort to sample substainably in the Arctic ecosystem. A new refinement of the spectroscopic methods led to improved resolution of the compound peaks in HPLC experiments and consequently also in the coupled mass spectrometric analyses. As a result, we were able to identify a new monomeric 3-alkyl pyridinium alkaloid (**1**, Scheme 1) by HPLC-HRMS experiments. The compound could not be isolated in sufficient quantity and purity to allow NMR studies.

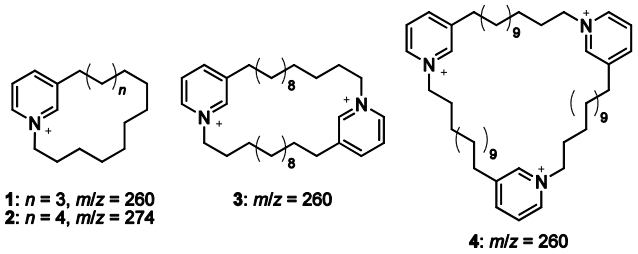

Scheme 1 Cyclic monomeric, dimeric and trimeric and a linear 3-alkyl pyridinium alkaloid isolated from the Arctic sponge *Haliclona viscosa*.

Compound **1** elutes at a retention time of 15.5 min in the crude extract of *H. viscosa*. It shows a singly charged molecular ion of *m*/*z* = 260.2368 which suggests a molecular formula of $C_{18}H_{30}N$ (Δm = 1.8 ppm, Fig. 1). Apart from a partly overlapping, unidentified compound, the mass spectrum of the natural compound does not show other molecular-, fragment- or adduct-ions. The molecular mass is by 14 mass units smaller than the mass of the known cyclic monomeric 3-alkyl pyridinium compound 2[3] which elutes at 17.9 min in the same sponge extract and also shows only a singly charged molecular ion. The crude extract of *H. viscosa* contains a number of compounds that are structurally very similar but differ in the length of the alkyl chains and the degree of oligomerisation. Cyclostellettamine C (**3**) at a retention time of 16.5 min also shows a molecular ion at *m*/*z* = 260, but it can be differentiated from the molecular ion of **1** by being doubly charged. Another molecular ion of *m*/*z* = 260 is found for viscosamine C (**4**)[4] which elutes at 17.1 min, but the molecular ion of **4** is triply charged, and the spectrum shows additional fragment and adduct masses.[1]

Therefore, it seems reasonable to propose that **1** is the structural analogue of **2** and contains an alkyl chain that is shortened by one methylene group in comparison to **2**. Compound **1** has previously been synthesized during the development of the total synthesis of cyclostellettamine C (**3**)[5] as well as for cytotoxicity studies[3] and is therefore available for chromatographic comparisons between the natural compound and the synthetic compound.

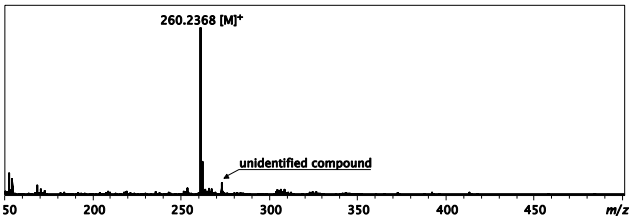

Fig. 1. High-resolution mass spectrum of natural haliclocyclin C (**1**) resulting from a chromatographic separation of the crude extract.

The synthetic compound **1** elutes at the same retention time as the natural compound **1** in the crude extract. The HPLC-HRMS analysis of the synthetic compound **1** yields the mass *m*/*z* = 260.2360 (Fig. 2) which corresponds to the molecular formula $C_{18}H_{30}N$ with a mass accuracy of 4.9 ppm and fits very well to the observed mass of the natural compound **1**. As before in the natural compound **1**, the mass spectrum of the synthetic compound **1** does not show additional fragment- or adduct-ions. The chromatographic analysis of a mixture of the crude extract and the synthetic **1** results in increased intensity of the compound peak in the crude extract (Fig. 3). It can therefore be concluded that the natural compound **1** has the same structure as the synthetic 1.

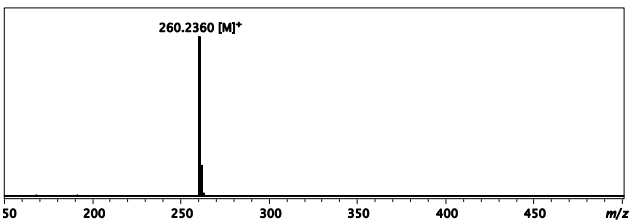

Fig. 2. High-resolution mass spectrum (direct injection) of synthetic haliclocyclin C (**1**).

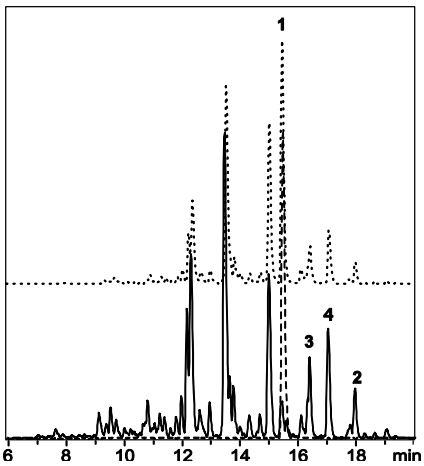

Fig.3 Overlay of the HPLC-HRMS base peak chromatogram of the crude extract of a *Haliclona viscosa* sample from 2000 (black), the synthetic haliclocyclin C (**1**, dashed line), and a mixture of both (dotted line). The chromatogram peaks of haliclocyclin F (**2**), cyclostellettamine C (**3**), and viscosamine C (**4**) are indicated by the appropriate number.

Although Schmitz et al. (1978)[6] and Davies-Coleman et al. (1993)[7] describe chloride as the predominant, if not exclusive natural counterion of halitoxin and the cyclostellettamines, we do not find evidence for chloride as the counterion in the 3-alkyl pyridinium alkaloids contained in the crude extract of the Arctic *Haliclona viscosa*. Instead, MALDI-TOF investigations of the crude extract show a different ion of yet unknown structure (unpublished results). This first report of haliclocyclin C (**1**) from a natural source completes the set of oligomers with equidistant alkyl chains (C_{13}) isolated or identified in the Arctic sponge *Haliclona viscosa*. An interesting aspect is the progression of the bioactivity between the monomeric haliclocyclin C (**1**), dimeric cyclostellettamine C (**3**) and trimeric viscosamine (**4**).[8] The monomeric compound shows the highest whereas the trimeric compound shows the lowest antimicrobial activity.[9] The cytotoxic activity in volumetric concentrations is almost identical for all three while in molar concentrations viscosamine C (**4**) shows the strongest and haliclocyclin C (**1**) the lowest cytotoxic activity.[10] While the monomer with a C_{14} alkyl chain, haliclocyclin F (**2**), also exists in the crude extract, the corresponding dimer and trimer with C_{14} alkyl chains, cyclostellettamine F and viscosamine F, have not been identified yet. On the other hand, a viscosamine in which at least one C_{14} alkyl chain is present was recently identified in *Haliclona viscosa* (unpublished results).

With the appearance of additional cyclic monomeric 3-alkyl pyridinium alkaloids we suggest that the to-date unnamed compound **2** should be renamed to haliclocyclin F; this suggestions follows the nomenclature of cyclostellettamines, where cyclostellettamine F contains two C_{14} alkyl chains.[11] Accordingly, compound **1** should be named haliclocyclin C (**1**) in analogy to cyclostellettamine C (**3**) and viscosamine C (**4**) both of which contain alkyl chains with 13 methylene groups.

Notes and references

[a] *Alfred-Wegener-Institute for Polar and Marine Research, Am Handelshafen 12, 27570 Bremerhaven, Germany. Fax: +49 (0) 471 4831 1425; Tel: +49 (0) 471 4831 1497; E-mail: mkoeck@awi.de*

† Electronic Supplementary Information (ESI) available: instrumentation information, experimental data and high resolution mass spectra of **1** obtained from LCMS of the crude extract and the pure, synthetic compound. See DOI: 10.1039/b000000x/

1. C. A. Volk and M. Köck, *Org. Lett.*, **2003**, *5*, 3567-3569.
2. C. A. Volk and M. Köck, *Org. Biomol. Chem.*, **2004**, *2*, 1827-1830; C. A. Volk, H. Lippert, E. Lichte and M. Köck, *Eur. J. Org. Chem.*, **2004**, 3154-3158; G. Schmidt, C. Timm and M. Köck, *Org. Biomol. Chem.*, **2009**, *7*, 3061-3064.
3. C. Timm, C. Volk, F. Sasse and M. Köck, *Org. Biomol. Chem.*, **2008**, *6*, 4036-4040.
4. Viscosamine C (**4**) was originally published under the name viscosamine.[1] It was recently renamed to viscosamine C[8] to account for the presence of additional viscosamines with different chain lengths. The name follows the nomenclature of the cyclostellettamines.
5. H. Anan, N. Seki, O. Noshiro, K. Honda, K. Yasumuro, T. Ozasa and N. Fusetani, *Tetrahedron*, **1996**, *52*, 10849-10860.
6. F. J. Schmitz, K. H. Hollenbeak and D. C. Campbell, *J. Org. Chem.*, **1978**, *43*, 3916-3922.
7. M. T. Davies-Coleman, D. J. Faulkner, G. M. Dubowchik, G. P. Roth, C. Polson and C. Fairchild, *J. Org. Chem.*, **1993**, *58*, 5925-5930.
8. C. Timm, T. Mordhorst and M. Köck, *Mar. Drugs*, **2010**, *8*, 483-497.
9. Antibacterial activity was tested against Escherichia coli tolC and Staphylococcus aureus. Results were obtained from an agar diffusion test with a test concentration of 20 µg. The diameter of growth inhibition is given in mm: **1** (19/16), **3** (12/11), **4** (8/9).
10. The cytotoxicity was tested against mouse fibroblasts L929. The IC50 values in µg mL 1 are: **1** (1.2), **3** (1.0), **4** (1.2). The molar activities (µM) are: **1** (4.62), **3** (1.92), **4** (1.54).
11. J. E. Baldwin, D. R. Spring, C. E. Atkinson and V. Lee, *Tetrahedron*, **1998**, *54*, 13655-13680.

7.2.1 Supporting Information

Haliclocyclin C, a new monomeric 3-alkyl pyridinium alkaloid from the Arctic marine sponge *Haliclona viscosa*

Gesine Schmidt, Christoph Timm and Matthias Köck*

*To whom correspondence should be addressed. mkoeck@awi.de

Extraction and analysis of the natural compound **1**

The sponge was collected in summer 2003 by the AWI scientific diving team using SCUBA in the Kongsfjord, Spitsbergen, at a depth of aproximately 15 m. One part of the sponge was conserved in ethanol for taxonomic identification, which was performed by Wallie H. de Weerdt at the Zoölogisch Museum Amsterdam (voucher MAK301). The remaining sponge tissue was frozen at –20 °C and transported back to Bremerhaven where it was freeze-dried. Freeze-dried sponge tissue (4.18 g) was exhaustively extracted at room temperature with a 1:1 mixture of methanol and dichloromethane (4 × 80 mL).

The resulting crude extract was investigated by HR-LCMS on an Agilent 1100 HPLC system equipped with a Waters XTerra RP_{18} column (3.0 × 150 mm, 3.5 µm) applying an ACN/H_2O (0.1 % HCOOH) gradient at 35 °C; 0 min and a flow rate of 0.4 mL min^{-1}: 20 % ACN/80 % H_2O; 25 min: 55 % ACN/45 % H_2O; 27 min: 100 % ACN. UV spectra were recorded during HPLC analysis with a DAD (Agilent). Mass spectra were acquired on-line with a coupled Bruker Daltonics microTOF_{LC} mass

spectrometer. The instrument was externally calibrated using sodium formiate cluster. TLC used prefabricated, silica coated aluminum sheets (Merck, silica 60) and a liquid phase of CH_2Cl_2/MeOH (9:1). NMR spectra were recorded on a Bruker Avance 250 MHz spectrometer at 298 K in DMSO-d_6. Melting points were determined using a Kofler melting point apparatus and are uncorrected. Chemical shifts are quoted in ppm and are referenced to the appropriate solvent signal. FT-IR spectra were recorded on a Perkin-Elmer 1600 series spectrometer. Absorption maxima are reported in wave numbers and the following abbreviations are used: s strong, m medium, w weak.

Experimental data for the synthetic Haliclocyclin C (**1**)

Synthesis followed the method described by Timm & Köck (2008)[1] and produced a yellow solid (60% synthesis yield). TLC: $R_f = 0.25$ (9:1 CH_2Cl_2/MeOH on Merck silica 60) — mp: 151 °C — ^{1}H-NMR (250 MHz, DMSO-d_6): δ = 0.97-1.34 (m, 18 H, 9 × CH_2), 1.67-1.82 (m, 2 H, 3-CH_2CH_2), 1.90-2.06 (m, 2 H, pyCH_2CH_2), 2.87 (t, J = 6.3 Hz, 2 H, 3-CH_2), 4.64 (t, J = 6.0 Hz, 2 H, pyCH_2), 8.12 (dd, J = 7.9 Hz, J = 6.2 Hz, 1 H, H5), 8.53 (d, J = 8.0 Hz, 1 H, H4), 8.98 (d, J = 6.0 Hz, 1 H, H6), 9.14 (s, 1 H, H2) — ^{13}C-NMR (62.5 MHz, DMSO-d_6): δ = 23.4, 25.5, 25.6, 25.8, 25.9, 26.2, 26.4, 26.6, 28.1, 28.8 (10 × CH_2), 29.3 (3-CH_2CH_2), 30.5 (3-CH_2), 60.3 (CH_2N), 127.6 (C5), 142.3 (C6), 142.6 (C3), 143.8 (C2), 145.5 (C4) — IR (NaCl, cm^{-1}): 3018 m, 2927 s, 2857 s, 1624 m, 1508 m, 1463 m, 1442 m, 1383 w, 1229 w, 1154 w, 931 w, 842 w, 814 w, 793 w, 717 w, 690 w — HRMS (ESI, direct injection): m/z = 260.2332 (calcd. for $C_{18}H_{30}N^+$ m/z = 260.2373).

1 C. Timm, C. Volk, F. Sasse and M. Köck, *Org. Biomol. Chem.*, **2008**, *6*, 4036-4040.

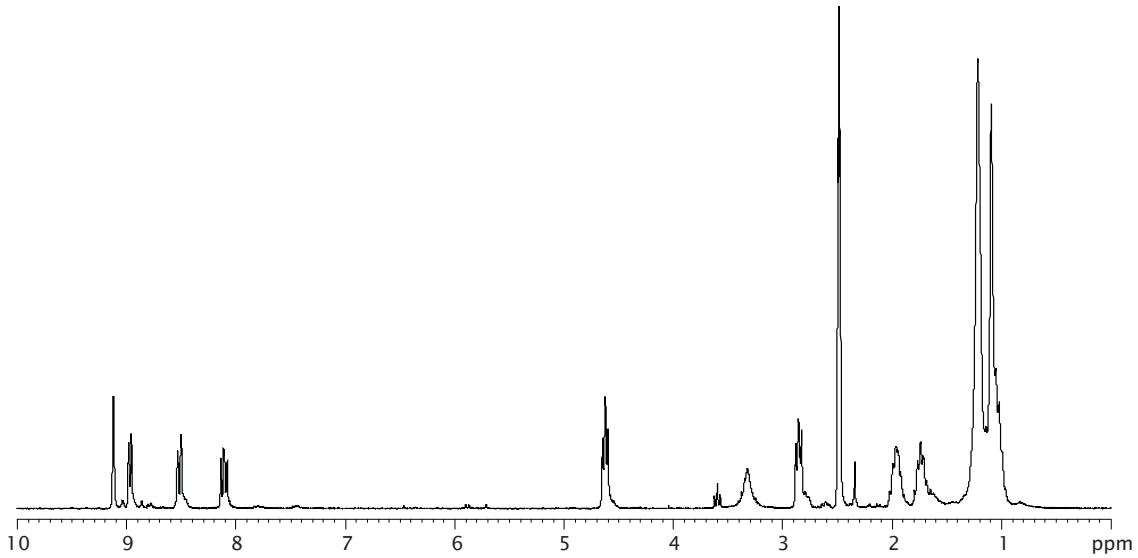

Figure 7.24 ^{1}H-NMR spectrum of the synthetic Haliclocyclin C (**1**) in DMSO-d_6.

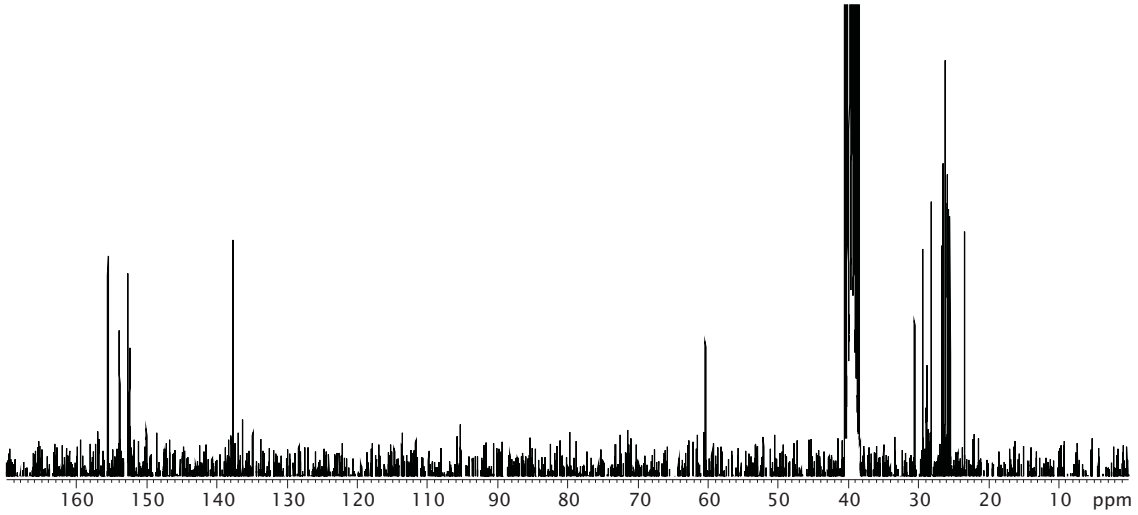

Figure 7.25 ^{13}C-NMR spectrum of the synthetic Haliclocyclin C (**1**) in DMSO-d_6.

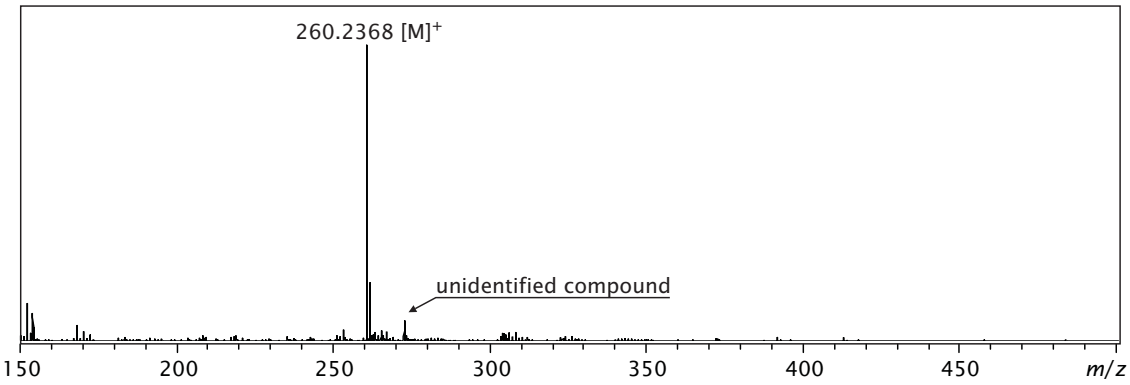

Figure 7.26 HRMS spectrum of the natural compound **1** obtained from LC-MS analysis of the crude extract.

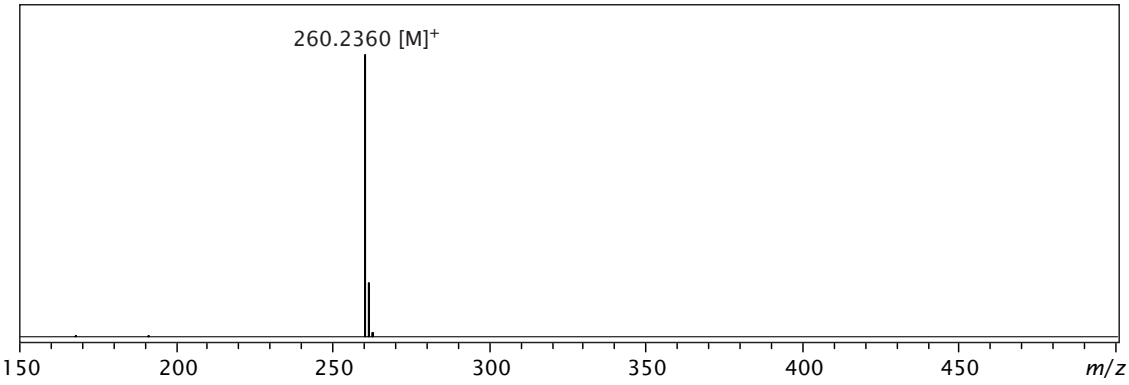

Figure 7.27 HRMS spectrum of the synthetic compound **1** obtained from LC-MS analysis of the pure, synthetic compound.

Two additional haliclamines, J and K, from the Arctic marine sponge *Haliclona viscosa*

Gesine Schmidt,[a] Thorsten Mordhorst[a] and Matthias Köck*[a]

Received (in XXX, XXX) Xth XXXXXXXXX 200X, Accepted Xth XXXXXXXXX 200X
First published on the web Xth XXXXXXXXX 200X
DOI: 10.1039/b000000x

Refined spectroscopic methods and a detailed knowledge about the behaviour of haliclamines during mass spectrometric experiments led to the identification of two new haliclamines, haliclamine J (1) with two equal alkyl chains of 10 methylene groups and haliclamine K (2) with alkyl chains of 10 and 12 methylene groups, directly from the crude extract of the sponge *Haliclona viscosa*.

Haliclamines are cyclic dimeric 3-alkyl tetrahydropyridine alkaloids where two tetradydropyridine moieties (THP) are interconnected in 1- and 3-position[1] by alkyl chains of variable length. They are integrated into the large and diverse group of 3-alkyl pyridinium alkaloids (3-APAs).[2] Mono-, di-, tri-, and polymeric 3-alkyl pyridinium compounds have been identified in six different sponge families of the order Haplosclerida from around the world. In contrast, only dimeric haliclamines have to date only been reported from two locations, Hiburi-jima, Japan, and the Svalbard archipelago, and only from the sponge genus *Haliclona*.[3, 4] As such they take up an exceptional position within the 3-APA compound class.

Only recently, the comparison of the crude extract of the Arctic sponge *Haliclona viscosa* with retention times and spectrometric data of two synthetic haliclamines led to the identification of the two new haliclamines E and F.[4] The subsequent systematic investigation of the MS-fragmentation of haliclamines[5] laid the basis for further detailed HPLC-HRMS examinations of crude extracts of *H. viscosa*.

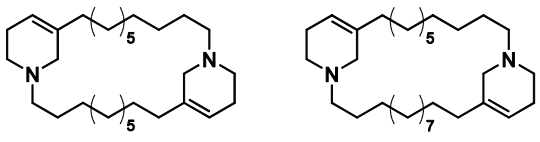

1 **2**

Fig. 1 Haliclamine J (**1**) and K (**2**)

The knowledge about haliclamine behavior in mass spectrometry now enabled us to identify two more haliclamines, haliclamine J (**1**, 10/10) and K (**2**, 10/12), from the same crude extract that had yielded the haliclamines E and F. Isolation of the compounds was not possible due to the limited amount of sponge material available. The two new compounds were not recognized in earlier HPLC-HRMS analyses since they co-eluted with haliclamines C and F. A refinement of the spectroscopic method split both the haliclamine C and the haliclamine F peak into two and thus allowed to distinguish the known and the new compound.

Compound **1** at a retention time of 13.8-14.0 min shows a singly charged pseudomolecular ion $[M+H]^+$ at m/z = 443.4370 and a doubly charged pseudomolecular ion $[M+2H]^{2+}$ at m/z = 222.2225 corresponding to the molecular formula $C_{30}H_{55}N_2$ The same molecular formula and similar masses are assigned to haliclamine C (**3**), but **3** elutes at a retention time of 14.0-14.2 min. Haliclamine C (**3**) contains two alkyl chains of 9 and 11 methylene groups, respectively. The high resolution mass spectrum of haliclamine C shows mass peaks of two fragments at m/z = 208.2090 and m/z = 236.2331 which represent the mass equivalent of a THP moitey connected to either alkyl chain. In constrast, the mass spectrum of compound **1** does not show obvious fragments. The different retention time to haliclamine C (**3**) and the absence of fragment masses suggests the alkyl chains to be of equal length of 10 methylene groups. This is supported by the isotope peak intensity of the doubly charged molecular ion and the observed isotope pattern that indicates a superimposed singly charged mass. While the calculated peak intensity (PI) is 100 : 33.3 : 5.5, the observed PI is 100 : 31.1 : 10.4 (Figure A). The X+2 isotope peak of an overlying singly charged fragment lies at m/z = 224.2244. Both results suggest that compound **1** should be a haliclamine with saturated alkyl chains of ten methylene groups, each. Evidence by comparison to synthetic compounds is in progress.

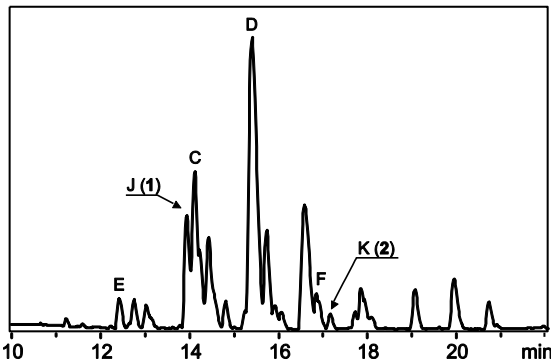

Fig 2 Base peak chromatogram of a crude extract of Haliclona viscosa. Known haliclamines are marked

Compound **2** which elutes at 17.0–17.3 min shows a singly charged pseudomolecular ion $[M+H]^+$ at m/z = 471.4699 and a doubly charged pseudomolecular ion $[M+2H]^{2+}$ at m/z = 236.2385. This corresponds to a molecular formula of $C_{32}H_{60}N_2$ (Δm = 5.5 ppm for $[M+H]^+$ and Δm = 5.2 ppm for $[M+2H]^{2+}$), the same as has been established for haliclamine F

which elutes at a retention time of 16.8–17.0 min. With the alkyl chains of haliclamine F being of equal length of 11 methylene groups the fragments that represent the THP moiety connected to an alkyl chain concur with the doubly charged molecular ion. In the mass spectrum of compound **2** however, two fragment peaks are visible at m/z = 222.2218 and m/z = 250.2538. They correspond to fragments that carry alkyl chains of 10 and 12 methylene groups, respectively. Evidence by comparison to synthetic compounds is in progress.

Conclusions

The resolution obtained by spectroscopic methods has a large impact on the resolution of coupled spectrometric analyses. The detailed knowledge about the behavior of haliclamines in different mass spectrometric experiments yielded relevant information for the identification of new compounds directly from the crude extract as is required by the small sample sizes of Arctic sponges.

Notes and references

[a] *Alfred-Wegener-Institute for Polar and Marine Research, Am Handelshafen 12, 27570 Bremerhaven, Germany. Fax: +49 (0) 471 4831 1425; Tel: +49 (0) 471 4831 1497; E-mail: mkoeck@awi.de*

† Electronic Supplementary Information (ESI) available: Chromatographic and spectrometric data. See DOI: 10.1039/b000000x/

1. According to IUPAC nomenclature, the tetrahydropyridines in haliclamines are 1,5-disubstituted 1,2,3,6-tetrahydropyridines. For reasons of their structural proximity to the cyclostellettamines and other 3-alkyl pyridinium alkaloids and for the habitual use in previous publications they are termed 1,3-disubstituted in this context.
2. K. Sepčić, *J. Toxicol. - Toxin Rev.*, 2000, **19**, 139-160.
3. N. Fusetani, K. Yasumuro and S. Matsunaga, *Tetrahedron Lett.*, 1989, **30**, 6891-6894; C. A. Volk, H. Lippert, E. Lichte and M. Köck, *Eur. J. Org. Chem.*, 2004, 3154-3158.
4. G. Schmidt, C. Timm and M. Köck, *Org. Biomol. Chem.*, 2009, **7**, 3061-3064.
5. G. Schmidt, C. Timm, A. Grube, E. Lichte and M. Köck, *Org. Biomol. Chem.*, 2010, **submitted**.

Bibliography

[1] *Römpp Online*, http://www.roempp.com, **2010**.

[2] K. Felix, *Klin. Wochenschr.* **1927**, *6*, 1878–1879.

[3] G. Löffler, *Basiswissen Biochemie mit Pathobiochemie*, Springer, **2003**.

[4] G. Michal, *Biochemical pathways: an atlas of biochemistry and molecular biology*, Wiley, **1999**.

[5] D. Erpenbeck, R. van Soest, *Mar. Biotechnol.* **2007**, *9*, 2–19.

[6] G. Habermehl, P. E. Hammann, H. C. Krebs, *Naturstoffchemie — Eine Einführung*, Springer, **1992**.

[7] K. Hiller, M. F. Melzig, *Lexikon der Arzneipflanzen und Drogen*, Springer, **2003**.

[8] S. Grabley, R. Thiericke (Eds.), *Drug Discovery from Nature*, Springer Verlag Berlin, Heidelberg, **1999**.

[9] S. Lee, M. Tomizawa, J. E. Casida, *J. Agr. Food Chem.* **2003**, *51*, 2646–2652.

[10] T. D. Wyatt, *Pheromones and Animal Behavior — Communication by Smell and Taste*, Cambridge University Press, **2003**.

[11] P. Howse, J. Stevens, O. Jones, *Insect Pheromones and Their Use in Pest Management*, Chapman & Hall, **1997**.

[12] F. Kempken, R. Kempken, *Gentechnik bei Pflanzen*, Springer, **2000**.

[13] L. A. Buchner, *Arch. Pharm.* **1887**, *225*, 889–906.

[14] F. W. Sertürner, *J. Pharmacol.* **1806**, *14*, 47–93.

[15] T. S. Kaufman, E. A. Rúveda, *Angew. Chem. Int. Ed.* **2005**, *44*, 854–885.

[16] A. Niemann, *Arch. Pharm.* **1860**, *153*, 129–155.

[17] A. Fleming, *Brit. J. Exp. Pathol.* **1929**, *10*, 226–236.

[18] S. Smith, *J. Chem. Soc.* **1930**, 508–510.

[19] Schröder, Prinzhorn, Kraut, *Ann. Chem. Pharm.* **1869**, *150*, 1–20.

[20] S. Moncada, S. H. Ferreira, J. R. Vane, *Eur. J. Pharmacol.* **1975**, *31*, 250–260.

[21] D. J. Faulkner, *Nat. Prod. Rep.* **2000**, *17*, 1–6.

[22] D. J. Faulkner, *Tetrahedron* **1977**, *33*, 1421–1433.

[23] D. J. Faulkner, *Antonie van Leeuwenhoek* **2000**, *77*, 135–145.

[24] D. J. Faulkner, M. K. Harper, M. G. Haygood, C. E. Salomon, E. W. Schmidt in *Drugs from the Sea*, N. Fusetani (Ed.), Karger, **2000**, pp. 107–119.

[25] Y.-B. Ahn, S.-K. Rhee, D. E. Fennell, L. J. Kerkhof, U. Hentschel, M. M. Häggblom, *Appl. Env. Microbiol.* **2003**, *69*, 4159–4166.

[26] P. Proksch, R. Ebel, R. A. Edrada, P. Schupp, W. H. Lin, Sudarsono, V. Wray, K. Steube, *Pure Appl. Chem.* **2003**, *75*, 343–352.

[27] M. Mitova, S. Popov, , S. De Rosa, *J. Nat. Prod.* **2004**, *67*, 1178–1181.

[28] M. G. Haygood, E. W. Schmidt, S. K. Davidson, D. J. Faulkner, *J. Molec. Microbiol. Biotechnol.* **1999**, *1*, 33–43.

[29] B. M. Olivera, J. M. McIntosh, L. J. Cruz, F. A. Luque, W. R. Gray, *Biochemistry* **1984**, *23*, 5087–5090.

[30] B. M. Olivera, J. M. McIntosh, C. Clark, D. Middlemas, W. R. Gray, L. J. Cruz, *Toxicon* **1985**, *23*, 277–282.

[31] A. E. Wright, D. A. Forleo, G. P. Gunawardana, S. P. Gunasekara, F. E. Koehn, O. J. McConnell, *J. Org. Chem.* **199**, *55*, 4508–4512.

[32] K. L. Rinehart, T. G. Holt, N. L. Fregeau, J. G. Stroh, P. A. Keifer, F. Sun, L. H. Li, D. G. Martin, *J. Org. Chem.* **1990**, *55*, 4512–4515.

[33] B. Haefner, *Drug Discovery Today (DDT)* **2003**, *8*, 536–544.

[34] J. W. Blunt, B. R. Copp, M. H. G. Munro, P. T. Northcote, M. R. Prinsep, *Nat. Prod. Rep.* **2005**, *22*, 15–61.

[35] J. Vacelet, N. Boury-Esnault, *Nature* **1995**, *373*, 333–335.

[36] J. Vacelet, E. Duport, *Zoomorphology* **2004**, *123*, 179–190.

[37] P. R. Bergquist, *Sponges*, University of California Press, **1978**.

[38] P. Hayward, T. N. Smith, C. Shields, *Sea Shore of Britain and Europe*, HarperCollins Publishers London, **1996**.

[39] A. C. Jones, J. E. Blum, J. R. Pawlik, *J. Exp. Mar. Biol. Ecol.* **2005**, *322*, 67–81.

[40] E. Burns, M. Ilan, *Mar. Ecol. Progr. Ser.* **2003**, *252*, 115–123.

[41] E. Burns, I. Ifrach, S. Carmeli, J. R. Pawlik, M. Ilan, *Mar. Ecol. Progr. Ser.* **2003**, *252*, 105–114.

[42] J. W. Blunt, B. R. Cropp, M. H. G. Munro, P. T. Northcote, M. R. Prinsep, *Nat. Prod. Rep.* **2009**, *27*, 165–237.

[43] W. Fenical, *Mar. Biotechnol.* **1997**, *15*, 339–341.

[44] S. R. Kelly, E. Garo, P. R. Jensen, W. Fenical, J. R. Pawlik, *Aquat. Microb. Ecol.* **2005**, *40*, 191–203.

[45] U. Bickmeyer, A. Grube, K.-W. Klings, J. R. Pawlik, M. Köck, *Mar. Biotechnol.* **2010**, *12*, 267–272.

[46] R. Ruzicka, D. F. Gleason, *Oecologia* **2008**, *154*, 785–794.

[47] G. J. Bakus, G. Green, *Science* **19743**, *185*, 951–953.

[48] D. J. Faulkner, *Nat. Prod. Rep.* **1984**, *1*, 251–280.

[49] M. E. Hay, W. Fenical, *Annu. Rev. Ecol. Syst.* **1988**, *19*, 111–145.

[50] M. A. Becerro, R. W. Thacker, X. Turon, M. J. Uriz, V. J. Paul, *Oecologia* **2003**, *135*, 91–101.

[51] J. Rovirosa, M. de la Luz Vasquez, A. San-Martin, *Biochem. Syst. Ecol.* **1990**, *18*, 53–55.

[52] J. Hooper, R. Capon, C. Keenan, D. Parry, N. Smit, *Invertebr. Taxon.* **1992**, *6*, 261–301.

[53] J. Fromont, S. Kerr, R. Kerr, M. Riddle, P. Murphy, *Biochem. Syst. Ecol.* **1994**, *22*, 735–752.

[54] S. Albrizio, P. Ciminiello, E. Fattorusso, S. Magno, *Tetrahedron* **1994**, *50*, 783–788.

[55] P. Ciminiello, V. Costantino, E. Fattorusso, S. Magno, A. Mangoni, M. Pansini, *J. Nat. Prod.* **1994**, *57*, 705–712.

[56] P. Ciminiello, E. Fattorusso, S. Magno, *J. Nat. Prod.* **1994**, *57*, 1564–1569.

[57] P. Ciminiello, E. Fattorusso, S. Magno, *J. Nat. Prod.* **1995**, *58*, 689–696.

[58] P. Ciminiello, E. Fattorusso, S. Magno, M. Pansini, *Biochem. Syst. Ecol.* **1996**, *24*, 105–113.

[59] P. Ciminiello, C. Dell'Aversano, E. Fattorusso, S. Magno, *Tetrahedron* **1996**, *52*, 9863–9868.

[60] P. Ciminiello, E. Fattorusso, M. Forino, S. Magno, *Tetrahedron* **1997**, *53*, 6565–6572.

[61] P. Ciminiello, C. Dell'Aversano, E. Fattorusso, S. Magno, M. Pansini, *J. Nat. Prod.* **1999**, *62*, 590–593.

[62] P. Ciminiello, C. Dell'Aversano, E. Fattorusso, S. Magno, M. Pansini, *J. Nat. Prod.* **2000**, *63*, 263–266.

[63] M. Page, L. West, P. Northcote, C. Battershill, M. Kelly, *J. Chem. Ecol.* **2005**, *31*, 1161–1174.

[64] M. A. Becerro, V. J. Paul, *Mar. Ecol. Progr. Ser.* **2004**, *280*, 115–128.

[65] D. Kelman, Y. Benayahu, Y. Kashman, *J. Chem. Ecol.* **2000**, *26*, 1123–1133.

[66] G. J. Bakus, N. M. Targett, B. Schulte, *J. Chem. Ecol.* **1986**, *12*, 951–987.

[67] M. J. Uriz, D. Martin, X. Turon, E. Ballesteros, R. Hughes, C. Acebal, *Mar. Ecol. Progr. Ser.* **1991**, *70*, 175–188.

[68] C. Ferretti, S. Vacca, C. De Ciucis, B. Marengo, A. R. Duckworth, R. Manconi, R. Pronzato, C. Domenicotto, *Mar. Ecol.* **2009**, *30*, 327–336.

[69] N. Lindquist, M. E. Hay, *Ecol. Monogr.* **1996**, *66*, 431–450.

[70] J. B. McClintock, B. J. Baker, *Mar. Ecol. Progr. Ser.* **1997**, *154*, 121–131.

[71] T. Gerrodette, A. O. Flechsig, *Mar. Biol.* **1979**, *55*, 103–110.

[72] H. Lippert, K. Iken, C. Volk, M. Köck, E. Rachor, *J. Exp. Mar. Biol. Ecol.* **2004**, *310*, 131–146.

[73] C. Timm, T. Mordhorst, M. Köck, *Mar. Drugs* **2010**, *8*, 483–497.

[74] C. A. Volk, M. Köck, *Org. Biomol. Chem.* **2004**, *2*, 1827–1830.

[75] W. H. de Weerdt, *Beaufortia* **1985**, *35*, 61–91.

[76] W. H. de Weerdt, *Beaufortia* **1986**, *36*, 81–165.

[77] M. W. de Laubenfels, *Syst. Zool.* **1957**, *6*, 156–159.

[78] R. W. M. Van Soest, N. Boury-Esnault, J. N. A. Hooper, K. Rützler, N. J. de Voogd, B. Alvarez, E. Hajdu, A. Pisera, J. Vacelet, R. Manconi, C. Schoenberg, D. Janussen, K. R. Tabachnick, M. Klautau, *World Porifera Database*, http://www.marinespecies.org/porifera, **2010**.

[79] M. Köck, *Die Haliclona viscosa Story*, Presentation, **2006**, GKSS/AWI CO-Symposium.

[80] F. J. Schmitz, K. H. Hollenbeak, D. C. Campbell, *J. Org. Chem.* **1978**, *43*, 3916–3922.

[81] J. C. Braekman, D. Daloze, P. Macedo de Abreu, C. Piccinni-Leopardi, G. Germain, M. Van Meerssche, *Tetrahedron Lett.* **1982**, *23*, 4277–4280.

[82] M. Nakagawa, M. Endo, N. Tanaka, L. Gen-Pei, *Tetrahedron Lett.* **1984**, *25*, 3227–3230.

[83] R. Sakai, T. Higa, C. W. Jefford, G. Bernardinelli, *J. Am. Chem. Soc.* **1986**, *108*, 6404–6405.

[84] C. Timm, Ph.D. thesis, Johann Wolfgang Goethe-Universität Frankfurt/Main, Germany, **2007**.

[85] K. Sepčić, G. Guella, I. Mancini, F. Pietra, M. Dalla Serra, G. Menestrina, K. Tubbs, P. Macek, T. Turk, *J. Nat. Prod.* **1997**, *60*, 991–996.

[86] A. Casapullo, O. C. Pinto, S. Marzocco, G. Autore, R. Riccio, *J. Nat. Prod.* **2009**, *72*, 301–303.

[87] C. Timm, C. Volk, F. Sasse, M. Köck, *Org. Biomol. Chem.* **2008**, *6*, 4036–4040.

[88] G. Koren-Goldshlager, Y. Kashman, M. Schleyer, *J. Nat. Prod.* **1998**, *61*, 282–284.

[89] Y. Kashman, G. Koren-Goldshlager, M. D. G. Gravalos, M. Schleyer, *Tetrahedron Lett.* **1999**, *40*, 997–1000.

[90] H. Sorek, A. Rudi, M. Aknin, E. M. Gaydou, Y. Kashman, *J. Nat. Prod.* **2010**, *73*, 456–458, DOI 10.1021/np900500c.

[91] C. A. Volk, H. Lippert, E. Lichte, M. Köck, *Eur. J. Org. Chem.* **2004**, 3154–3158.

[92] G. Schmidt, C. Timm, M. Köck, *Org. Biomol. Chem.* **2009**, *7*, 3061–3064.

[93] N. Fusetani, K. Yasumuro, S. Matsunaga, *Tetrahedron Lett.* **1989**, *30*, 6891–6894.

[94] T. Teruya, K. Kobayashi, K. Suenaga, H. Kigoshi, *J. Nat. Prod.* **2006**, *69*, 135–137.

[95] R. Laville, G. Genta-Jouve, C. Urda, R. Fernández, O. P. Thomas, F. Reyes, P. Amade, *Molecules* **2009**, *14*, 4716–4724.

[96] C. A. Volk, M. Köck, *Org. Lett.* **2003**, *5*, 3567–3569.

[97] M. Jaspars, V. Pasupathy, P. Crews, *J. Org. Chem.* **1994**, *59*, 3253–3255.

[98] R. D. Charan, M. J. Garson, I. M. Brereton, A. C. Willis, J. N. A. Hooper, *Tetrahedron* **1996**, *52*, 9111–9120.

[99] R. J. Clark, K. L. Field, R. D. Charan, M. J. Garson, I. M. Brereton, A. C. Willis, *Tetrahedron* **1998**, *54*, 8811–8826.

[100] S. Aratake, A. Trianto, N. Hanif, N. J. de Voogd, J. Tanaka, *Mar. Drugs* **2009**, *7*, 523–527.

[101] K. H. Jang, G. W. Kang, J. Jeon, C. Lim, H. Lee, C. J. Sim, K. Oh, J. Shin, *Org. Lett.* **2009**, *11*, 1713–1716.

[102] G. Cimino, R. Puliti, G. Scognamiglio, A. Spinella, E. Trivellone, C. A. Mattia, L. Mazzarella, *Pure & Appl. Chem.* **1989**, *61*, 535–538.

[103] R. Sakai, S. Kohmoto, T. Higa, C. W. Jefford, G. Bernardinelli, *Tetrahedron Lett.* **1987**, *28*, 5493–5496.

[104] M. Kobayashi, Y.-J. Chen, S. Aoki, Y. In, T. Ishida, I. Kitagawa, *Tetrahedron* **1995**, *51*, 3727–3736.

[105] G. Cimino, S. De Stefano, G. Scognamiglio, G. Sodano, E. Trivellone, *Bull. Soc. Chim. Belg.* **1986**, *95*, 783–800.

[106] G. Cimino, A. Spinella, E. Trivellone, *Tetrahedron Lett.* **1989**, *30*, 133–136.

[107] G. Cimino, C. A. Mattia, L. Mazzarella, R. Puliti, G. Scognamiglio, A. Spinella, E. Trivellone, *Tetrahedron* **1989**, *45*, 3863–3872.

[108] H. Lippert, Ph.D. thesis, University of Bremen, **2003**.

[109] T. Turk, K. Sepčić, I. Mancini, Graziano, *3-Alkylpyridinium and 3-alkylpyridine compounds from marine sponges, their synthesis, biological activity and potential use*, Atta-ur-Rahman (Ed.), Elsevier, **2008**, chapter 6, pp. 355–397.

[110] C. Timm, M. Köck, *Biological activity of synthetic 3-alkyl pyridinium alkaloids*, manuscript in preparation, **2010**.

[111] H. Anan, N. Seki, O. Noshiro, K. Honda, K. Yasumuro, T. Ozasa, N. Fusetani, *Tetrahedron* **1996**, *52*, 10849–10860.

[112] R. Scott, A. Whyment, A. Foster, K. Gordon, B. Milne, M. Jaspars, *J. Membrane Biol.* **2000**, *176*, 119–131.

[113] R. G. S. Berlinck, C. A. Ogawa, A. M. P. Almeida, M. A. A. Sanchez, E. L. A. Malpezzi, L. V. Costa, E. Hajdu, J. C. de Freitas, *Comp. Biochem. Physiol.* **1996**, *115C*, 155–163.

[114] C. Volk, Ph.D. thesis, Johann Wolfgang Goethe-Universität Frankfurt/Main, Germany, **2004**.

[115] A. Grube, C. Timm, R. Berlinck, M. Köck, *3-Alkylpyridinium Alkaloide aus marinen Schwämmen: Anwendung massenspektrometrischer Verfahren zur Strukturaufklärung*, Presentation Bruker Daltonics User Meeting, **2005**.

[116] J. H. H. L. de Oliveira, A. Grube, M. Köck, R. G. S. Berlinck, M. L. Macedo, A. G. Ferreira, E. Hajdu, *J. Nat. Prod.* **2004**, *67*, 1685–1689.

[117] A. Grube, C. Timm, M. Köck, *Eur. J. Org. Chem.* **2006**, *2006*, 1285–1295.

[118] J. H. Gross, *Mass spectrometry. A textbook*, Springer, **2004**.

[119] C. Pepe, H. Sayer, J. Dagaut, R. Couffignal, *Rap. Comm. Mass Spectrom.* **1997**, *11*, 919–921.

[120] C. Pepe, K. Dif, *Rap. Comm. Mass Spectrom.* **2001**, *15*, 97–103.

[121] R. Laville, O. P. Thomas, F. Berrue, F. Reyes, P. Amade, *Eur. J. Org. Chem.* **2008**, 121–125.

[122] F. W. McLafferty, F. Tureček, *Interpretation of mass spectra*, University Science Books, **1993**.

[123] *Viscosalines $B_{1,2}$ and $E_{1,2}$ — New 3-Alkylpyridinium Alkaloids from the Marine Sponge Haliclona viscosa*, title, manuscript in preparation.

[124] C. Villiers, J.-P. Dognon, R. Pollet, P. Thuéry, M. Ephritikhine, *Angew. Chem., Int. Ed.* **2010**, *122*, 3543–3546.

[125] M. T. Davies-Coleman, D. J. Faulkner, G. M. Dubowchik, G. P. Roth, C. Polson, C. Fairchild, *J. Org. Chem.* **1993**, *58*, 5925–5930.

[126] H. Kaczmarek, M. Włodarska-Kowalczuk, J. Legeżyńska, M. Zajączowski, *Poln. Pol. Res.* **2005**, *26*, 137–155.

[127] H. Hop, T. Pearson, E. N. Hegseth, K. M. Kovacs, C. Wiencke, S. Kwasniewski, K. Eiane, F. Mehlum, B. Gulliksen, M. Wlodarska-Kowalczuk, C. Lydersen, J. M. Weslawski, S. Cochrane, G. W. Gabrielsen, R. J. G. Leakey, O. J. Lønne, M. Zajaczkowski, S. Falk-Petersen, M. Kendall, S.-Å. Wängberg, K. Bischof, A. Y. Voronkov, N. A. Kovaltchouk, J. Wiktor, M. Poltermann, G. di Prisco, C. Papucci, S. Gerland, *Pol. Res.* **2002**, *21*, 167–208.

[128] W. Walkusz, S. Kwaśniewski, S. Falk-Petersen, H. Hop, V. Tverberg, P. Wieczorek, J. M. Weslawski, *Pol. Res.* **2009**, 1–27.

[129] H. Svendsen, A. Beszczynska-Møller, J. O. Hagen, B. Lefauconnier, V. Tverberg, S. Gerland, J. B. Ørbæk, K. Bischof, C. Papucci, M. Zajaczkowski, R. Azzolini, O. Bruland, C. Wiencke, J. Winther, W. Dallmann, *Pol. Res.* **2002**, *21*, 133–166.

[130] P. Schlichtholz, I. Goszczko, *Deep-Sea Res. I* **2006**, *53*, 7608–626.

[131] F. R. Cottier, F. Nilsen, M. E. Inall, S. Gerland, V. Tverberg, H. Svendsen, *Geophys. Res. Lett.* **2007**, *34*, L10607, DOI: 10.1029/2007GL029948.

[132] S. Gerland, A. H. H. Renner, *Ann. Glaciol.* **2007**, *46*, 435–442.

[133] K. J. Willis, F. R. Cottier, S. Kraśniewski, *Pol. Res.* **2008**, *31*, 475–481.

[134] K. Lüning, M. J. Dring, *Helgoländer Wiss. Meeresunters.* **1979**, *32*, 403–424.

[135] K. Lüning, *Meeresbotanik. Verbreitung, Ökophysiologie und Nutzung der marinen Makroalgen*, Georg Thieme Verlag, **1985**.

[136] M. Assmann, *Ber. Polarforsch.* **2004**, *492*, 86–90.

[137] *OSPAR Regional Quality Status Report – Greater North Sea. Chapter 2: Geography, Hydrography and Climate*, http://www.ospar.org/eng/doc/pdfs/R2C2.pdf, **2000**.

[138] P. Naylor, *Great British Marine Animals 2nd ed.*, Sound Diving Publications, **2005**.

[139] H. Zanker, Ph.D. thesis, Johann Wolfgang Goethe Universität Frankfurt/Main, **2004**.

[140] J. Fromont, M. Garson, *Coral Reefs* **1999**, *18*, 340.

[141] I. Nagelkerken, L. Aerts, L. Pors, *Reef Encounter* **2000**, *28*, 14–15.

[142] R. E. Grant, *Edinburgh New Philosoph. J.* **1826**, *2*, 203–204.

[143] L. M. Lambe, *Trans. R. S. C.* **1892**, *Sec. IV*, 67–78.

[144] J. Ott, *Meereskunde 2nd ed.*, UTB für Wissenschaft and Ulmer Eugen Verlag, **1996**.

[145] J. P. Bryant, T. P. Clausen, P. B. Reichardt, M. C. McCarthy, R. A. Werner, *Oecologia* **1987**, *73*, 513–517.

[146] M. Gallo, E. Katz, *J Bacteriol.* **1972**, *109*, 659–667.

[147] G. Hobbs, C. M. Frazer, D. C. J. Gardner, F. Flett, S. G. Oliver, *J. Gen. Microbiol.* **1990**, *136*, 2291–2296.

[148] G. J. Clark, D. Langley, M. E. Bushell, *Microbiol.* **1995**, *141*, 663–669.

[149] B. G. Fleury, J. Coll, E. Tentori, S. Duquesne, L. Figueiredo, *Mar. Biol.* **2000**, *136*, 63–68.

[150] C. Duque, A. Martínez, G. Peñuela, *Rev. Colomb. Chim.* **1985**, *14*, 81–88.

[151] P. Chaurand, J. L. Norris, D. S. Cornett, J. A. Mobley, R. M. Caprioli, *J. Proteome Res.* **2006**, *5*, 2889–2900.

[152] D. J. Harvey, *Mass Spectrom. Rev.* **2006**, *25*, 595–662.

[153] E. Nordhoff, M. Schürenberg, G. Thiele, C. Lübbert, K.-D. Kloeppel, D. Theiss, H. Lehrach, J. Gobom, *Int. J. Mass Spectrom.* **2003**, *226*, 163–180.

[154] G. Montaudo, F. Samperi, M. S. Montaudo, *Progr. Polym. Res.* **2006**, *31*, 277–357.

[155] D. N. Dickinson, M. T. L. Duc, M. Satomi, J. D. Winefordner, D. H. Powell, K. Venkateswaran, *J. Microbiol. Meth.* **2004**, *58*, 1–12.

[156] M. Erhard, H. von Döhren, P. Jungblut, *Nat. Biotechnol.* **1997**, *15*, 906–909.

[157] A. Grube, T. Maier, M. Kostrzewa, M. Köck, *Z. Naturforsch.* **2007**, *62b*, 600–604.

[158] L. H. Cohen, A. I. Gusev, *Anal. Bioanal. Chem.* **2002**, *373*, 571–586.

[159] R. Knochenmuss, F. Dubois, M. J. Dale, R. Zenobi, *Rapid Comm. Mass Spectrom.* **1996**, *10*, 871–877.

[160] R. Knochenmuss, V. Karbach, U. Wiesli, K. Breuker, R. Zenobi, *Rapid Comm. Mass Spectrom.* **1998**, *12*, 529–534.

[161] G. McCombie, R. Knochenmuss, *Anal. Chem.* **2004**, *76*, 4990–4997.

[162] P. D. N. Hebert, M. Y. Stoeckle, T. S. Zemlak, C. M. Francis, *PLoS Biol.* **2004**, *2*, e312 (3657–3663).

[163] *National Center for Biotechnology Information*, http://www.ncbi.nlm.nih.gov/, **2010**.

[164] G. Schmidt, L. Gallego, H. Angermeier, U. Hentschel, M. Köck, *Phylogenetic Relationship of Arctic and Temperate Sponges of the Genus Haliclona*, manuscrips in preparation, **2010**.

[165] B. E. Picton, C. C. Morrow, *Encyclopedia of Marine Life of Britain and Ireland*, www.habitas.org.uk, **2007**.

[166] S. Zea, T. P. Henkel, J. R. Pawlik, *The Sponge Guide: a picture guide to Caribbean sponges*, www.spongeguide.org, **2009**.

[167] M. Assmann, Ph.D. thesis, Johann Wolfgang Goethe Universität Frankfurt am Main, **2000**.

[168] A. Grube, Ph.D. thesis, TU Carolo Wilhelmina zu Braunschweig, **2007**.

[169] G. Schmidt, A. Grube, M. Köck, *Eur. J. Org. Chem.* **2007**, 4103–4110.

[170] D. J. Craik, *Science* **2006**, *311*, 1563–1564.

[171] M. Trabi, D. J. Craik, *Trends Biochem. Sci.* **2002**, *27*, 132–138.

[172] O. Saether, D. J. Craik, I. D. Campbell, K. Sletten, J. Juul, D. G. Norman, *Biochemistry* **1995**, *34*, 4147–4158, sequence *cyclo*-(SWPVCTRNGLPVCGETCVGGTCNTPGCTC).

[173] D. G. Barry, N. L. Daly, R. J. Clark, L. Sando, D. J. Craik, *Biochemistry* **2003**, *42*, 6688–6695.

[174] G. R. Pettit, C. L. Herald, M. R. Boyd, J. E. Leet, C. Dufresne, D. L. Doubek, J. M. Schmidt, R. L. Cerny, J. N. A. Hooper, K. C. Rützler, *J. Med. Chem.* **1991**, *34*, 3339–3340.

[175] G. R. Pettit, R. Tan, M. D. Williams, L. P. Tackett, J. M. Schmidt, *Bioorg. Med. Chem. Lett.* **1993**, *3*, 2869–2874.

[176] G. R. Pettit, F. Gao, R. L. Cerny, D. L. Doubek, L. P. Tackett, J. M. Schmidt, J.-C. Chapuis, *J. Med. Chem.* **1994**, *37*, 1165–1168.

[177] O. Mechnich, G. Hessler, H. Kessler, M. Bernd, B. Kutscher, *Helv. Chim. Acta* **1997**, *80*, 1338–1354.

[178] A. Randazzo, F. Dal Piaz, S. Orrù, C. Debitus, C. Roussakis, P. Pucci, L. Gomez-Paloma, *Eur. J. Org. Chem.* **1998**, 2659–2665.

[179] J. Vicente, B. Vera, A. D. Rodríguez, I. Rodríguez-Escudero, R. Raptis, *Tetrahedron Lett.* **2009**, *50*, 4571–4574.

[180] B. Vera, J. Vicente, A. D. Rodríguez, *J. Nat. Prod.* **2009**, *72*, 1555–1562.

[181] J. Kobayashi, M. Tsuda, T. Nakamura, Y. Mikami, H. Shigemori, *Tetrahedron* **1993**, *49*, 2391–2402.

[182] A. Napolitano, I. Bruno, P. Rovero, R. Lucas, M. Payàï¿½ Peris, L. Gomez-Paloma, R. Riccio, *Tetrahedron* **2001**, *57*, 6249–6255.

[183] M. Tsuda, H. Shigemori, Y. Mikami, J. Kobayashi, *Tetrahedron* **1993**, *49*, 6785–6796.

[184] J. Kobayashi, T. Nakamura, M. Tsuda, *Tetrahedron* **1996**, *52*, 6355–6360.

[185] R. Fernández, S. Omar, M. Feliz, E. Quinoá, R. Riguera, *Tetrahedron Lett.* **1992**, *33*, 6017–6020.

[186] G. R. Pettit, Z. Cíchacz, J. Barkoczy, A.-C. Dorsaz, D. L. Herald, M. D. Williams, D. L. Doubek, J. M. Schmidt, L. P. Tackett, D. C. Brune, R. L. Cerny, J. N. A. Hooper, G. J. Bakus, *J. Nat. Prod.* **1993**, *56*, 260–267.

[187] A. Napolitano, M. Rodriquez, I. Bruno, S. Marzocco, G. Autore, R. Riccio, L. Gomez-Paloma, *Tetrahedron* **2003**, *59*, 10203–10211.

[188] O. Mechnich, H. Kessler, *Lett. Peptide Sci.* **1997**, *4*, 21–28.

[189] J. N. Tabudravu, M. Jaspars, L. A. Morris, J. J. Kettenes-van den Bosch, N. Smith, *J. Org. Chem.* **2002**, *67*, 8593–8601.

[190] G. R. Pettit, M. R. Rhodes, R. Tan, *J. Nat. Prod.* **1999**, *62*, 409–414.

[191] G. R. Pettit, J.-P. Xu, Z. Cíchacz, M. D. Williams, A.-C. Dorsaz, D. C. Brune, M. R. Boyd, R. L. Cerny, *Bioorg. Med. Chem. Lett.* **1994**, *4*, 2091–2096.

[192] G. R. Pettit, B. E. Toki, J.-P. Xu, D. C. Brune, *J. Nat. Prod.* **2000**, *63*, 22–28.

[193] G. R. Pettit, J. ping Xu, Z. A. Cíchacz, M. D. Williams, J.-C. Chapuis, R. L. Cerny, *Bioorg. Med. Chem. Lett.* **1994**, *4*, 2677–2682.

[194] W.-L. Li, Y.-H. Yi, H.-M. Wu, Q.-Z. Xu, H.-F. Tang, D.-Z. Zhou, H.-W. Lin, Z.-H. Wang, *J. Nat. Prod.* **2003**, *66*, 146–148.

[195] F. Kong, D. L. Burgoyne, R. J. Andersen, T. M. Allen, *Tetrahedron Lett.* **1992**, *33*, 3269–3272.

[196] R. Mohammed, J. Peng, M. Kelly, M. T. Hamann, *J. Nat. Prod.* **2006**, *69*, 1739–1744.

[197] C. Cychon, M. Köck, *J. Nat. Prod.* **2010**, *73*, 738–742.

[198] G. R. Pettit, J. K. Srirangam, D. L. Herald, K. L. Erickson, D. L. Doubek, J. M. Schmidt, L. P. Tackett, G. J. Bakus, *J. Org. Chem.* **1992**, *57*, 7217–7220.

[199] G. R. Pettit, S. R. Taylor, *J. Org. Chem.* **1996**, *61*, 2322–2325.

[200] J. Tabudravu, L. A. Morris, J. J. Kettenes-van den Bosch, M. Jaspars, *Tetrahedron Lett.* **2001**, *42*, 9273–9276.

[201] B. L. Schwartz, M. M. Bursey, *Biol. Mass Spectrom.* **1992**, *21*, 92–96.

[202] M. Laroche, C. Imperatore, L. Grozdanov, V. Costantino, A. Mangoni, U. Hentschel, E. Fattorusso, *Marine Biology* **2007**, *151*, 1365–1373.

[203] J. E. Baldwin, D. R. Spring, C. E. Atkinson, V. Lee, *Tetrahedron* **1998**, *54*, 13655–13680.

[204] B. E. Picton, C. Morrow, R. W. B. van Soest, *Sponges of Britain and Ireland - A colour guide and working document*, Marine Conservation Society, **2007**.

[205] É. Topsent, Ph.D. thesis, Faculté des Sciences de Paris, **1888**.

[206] W. Lundbeck, *The Danish Ingolf Expedition*, *Vol. 6*, H. Hagerup, **1902**, chapter Porifera (Part I). Homorrhaphidae and Heterorrhaphidae, pp. 1–108.

[207] E. Hentschel, *Kungl. Svenska Vetenskapakademiens Handlingar* **1916**, *54*, 1–18.

[208] L. M. Lambe, *Trans. R. S. C.* **1893**, *Sec. IV*, 25–43.

[209] N. Oku, K. Nagai, N. Shindoh, Y. Terada, R. W. M. van Soest, S. Matsunaga, N. Fusetani, *Bioorg. Med. Chem. Lett.* **2004**, *14*, 2617–2620.

[210] S. Matsunaga, K. Shinoda, N. Fusetani, *Tetrahedron Lett.* **1993**, *34*, 5953–5954.

[211] N. Fusetani, N. Asai, S. Matsunaga, K. Honda, K. Yasumuro, *Tetrahedron Lett.* **1994**, *35*, 3967–3970.

[212] J. Kobayashi, T. Murayama, Y. Ohizumi, T. Sasaki, T. Ohta, S. Nozoe, *Tetrahedron Lett.* **1989**, *30*, 4833–4836.

[213] H. Nakamura, S. Deng, J. Kobayashi, Y. Ohizumi, Y. Tomotake, T. Matsuzaki, Y. Hirata, *Tetrahedron Lett.* **1987**, *28*, 621–624.

[214] J. Kobayashi, T. Murayama, S. Kosuge, F. Kanda, M. Ishibashi, H. Kobayashi, Y. Ohizumi, T. Ohta, S. Nozoe, T. Sasaki, *J. Chem Soc. Perkin Trans. 1* **1990**, 3301–3303.

[215] J. Kobayashi, C. Zeng, M. Ishibashi, H. Shigemori, T. Sasaki, Y. Mikami, *J. Chem. Soc. Perkin Trans. 1* **1992**, 1291–1294.

[216] M. Tsuda, K. Naoko, J. Kobayashi, *Tetrahedron Lett.* **1994**, *35*, 4387–4388.

[217] M. Tsuda, K. Naoko, J. Kobayashi, *Tetrahedron* **1994**, *50*, 7957–7960.

[218] J. Kobayashi, M. Tsuda, N. Kawasaki, T. Sasaki, Y. Mikami, *J. Nat. Prod.* **1994**, *57*, 1737–1740.

[219] M. Tsuda, K. Inaba, N. Kawasaki, K. Honma, J. Kobayashi, *Tetrahedron* **1996**, *52*, 2319–2324.

[220] M. Tsuda, D. Watanabe, J. Kobayashi, *Tetrahedron Lett.* **1998**, *39*, 1207–1210.

[221] T. Ichiba, R. Sakai, S. Kohmoto, G. Saucy, T. Higa, *Tetrahedron Lett.* **1988**, *29*, 3083–3086.

[222] Y. Takahasi, T. Kubota, J. Fromont, J. Kobayashi, *Org. Lett.* **2009**, *11*, 21–24.

[223] K. Kondo, H. Shigemori, Y. Kikuchi, M. Ishibashi, T. Sasaki, J. Kobayashi, *J. Org. Chem.* **1992**, *57*, 2480–2483.

[224] M. Kobayashi, K. Kawazoe, I. Kitigawa, *Chem. Pharm. Bull.* **1989**, *37*, 1676–1678.

[225] M. Kobayashi, K. Kawazoe, I. Kitigawa, *Tetrahedron Lett.* **1989**, *30*, 4149–4152.

[226] A. R. Carroll, P. J. Scheuer, *Tetrahedron* **1990**, *46*, 6637–6644.

[227] B. Harrison, S. Talapatra, E. Lobkovski, J. Clardy, P. Crews, *Tetrahedron Lett.* **1996**, *37*, 9151–9154.

[228] J. I. Jiménez, G. Goetz, C. M. S. Mau, W. Y. Yoshida, P. J. Scheuer, R. T. Williamson, M. Kelly, *J. Org. Chem.* **2000**, *65*, 8465–8469.

[229] J. C. Braekman, D. Daloze, N. Defay, D. Zimmermann, *Bull. Soc. Chim. Belg.* **1984**, *93*, 941–944.

[230] F. Kong, P. J. Andersen, T. M. Allen, *Tetrahedron Lett.* **1994**, *35*, 1643–1646.

[231] F. Kong, P. J. Andersen, T. M. Allen, *Tetrahedron* **1994**, *50*, 6137–6144.

[232] F. Kong, P. J. Andersen, T. M. Allen, *J. Am. Chem. Soc.* **1994**, *116*, 6007–6008.

[233] F. Kong, R. J. Andersen, *Tetrahedron* **1995**, *51*, 2895–2906.

[234] J. Rodríguez, B. M. Peters, L. Kurz, R. C. Schatzman, D. McCarley, L. Lou, P. Crews, *J. Am. Chem. Soc.* **1993**, *115*, 10436–10437.

[235] J. Rodríguez, P. Crews, *Tetrahedron Lett.* **1994**, *35*, 4719–4722.

[236] D. E. Williams, P. Lassota, R. J. Andersen, *J. Org. Chem.* **1998**, *63*, 4838–4841.

[237] E. Quiñoà, P. Crews, *Tetrahedron Lett.* **1987**, *28*, 2467–2468.

[238] J.-C. Quirion, T. Sevenet, H.-P. Husson, B. Weniger, C. Debitus, *J. Nat. Prod.* **1992**, *55*, 1505–1508.

[239] M. S. Buchanan, A. R. Carroll, R. Addepalli, V. M. Avery, J. N. A. Hooper, R. J. Quinn, *J. Nat. Prod.* **2007**, *70*, 2040–2041.

[240] S. Albrizio, P. Ciminiello, E. Fattorusso, S. Magno, J. R. Pawlik, *J. Nat. Prod.* **1995**, *58*, 647–652.

[241] S. Sakemi, L. E. Totton, H. H. Sun, *J. Nat. Prod.* **1990**, *53*, 995–999.

[242] D. B. Stierle, D. J. Faulkner, *J. Nat. Prod.* **1991**, *54*, 1134–1136.

[243] Y. R. Torres, R. G. S. Berlinck, A. Magalhães, A. B. Schefer, A. G. Ferreira, E. Hajdu, G. Muricy, *J. Nat. Prod.* **2000**, *63*, 1098–1105.

[244] R. Talpir, A. Rudi, M. Ilan, Y. Kashman, *Tetrahedron Lett.* **1992**, *33*, 3033–3034.

[245] Y. Venkatesvarlu, M. Venkata Rami Reddy, J. Venkateswara Rao, *J. Nat. Prod.* **1994**, *57*, 1283–1285.

A
Haliclona

Haliclona viscosa

The species descriptions is taken from the book "Sponges of Britain and Ireland - A colour guide and working document" [204]

Form Variable, depending on microhabitat, but typically from spreading cushions with mamillate oscular chimneys, to massive lobose forms with tall, rugose, volcano-like oscular chimneys. These oscular chimneys tend to be arranged in irregular rows in cushion forms. The rows can become ill-defined ridges, caused by the oscular chimneys anastomosing for up to 3/4 of their height. In large forms the oscular projections can be mammiform, or chimneys, which become bulbous for the first 2/3 of their height, narrowing more sharply in the upper 1/3. The oscular rows may appear as tassels, or as repent branches. More information is required on growth forms, and their relationships with habitat types. Specimens may be large, with a spread of up to 30 cm, and height to 5 cm.

Colour Typically purple, but can verge to pink or brown in some specimens. The colour is normally deeper on the higher portions of the sponge (i.e. oscular chimneys), becoming a washed-out fawn/grey away from the extremities. The depth of colour probably reduces.

Smell None.

Slime May be present in considerable amounts, especially when crushed or torn apart.

Consistency Firm, compressible, friable.

Surface Smooth and punctate (from the inhalant pores). Large specimens become rugose, caused by irregular tuberculate projections of variable size and position, giving a distinctive warty appearance. The projections can form surface ridges, giving the sponge an "angular" appearance. Some specimens display an initially moderate friction, but quickly become slimy as pressure is applied.

Apertures The oscules are formed on chimneys, as described under 'Form'. The openings are large, up to 1cm in diameter, and remain open after collection and preservation. Inhalant pores show through the surface, and are closely packed and conspicuous.

Contraction None.

Skeleton Primary tracts are 3 to 6 spicules in diameter, with single inter-connecting spicules which are not differentiated into secondary tracts. There is no ectosomal skeleton. Spongin is scarce, nodal.

Spicules Oxea, typically slightly curved, but varying from straight to fairly abruptly bent in the middle. 140-160 $\times$ 4.5-7 µm. Larger oxea (up to 170 µm?) are rare. Oxea in the range 95-140 $\times$ 1-5.5 µm are occasionally found.

Habitat This sponge is typically found from the upper circalittoral downwards, but less well developed specimens occur in shallower water and on the shore. It mainly occurs on vertical rock faces, in silt free areas of considerable water movement, e.g. gullies and/or areas exposed to wave action and tidal currents.

Distribution Recently known from W. coast of Ireland; Northern Ireland (Antrim; Strangford Lough); W. coast of Scotland (Mull; Coll; Tiree; Oban; Lewis); SW Britain (Salcombe, Devon, Eddystone, Hard Deeps; Scilly Isles; Lundy).

Similar Species

Key Identification Features The purplish colour, giant volcano-like oscules, rugose appearance and slime are characteristic. Less well developed specimens could be confused with other Chalinids. This description is compiled largely from 11 specimens in the collection of G. Ackers. Other specimens may differ slightly in detail.

Table A.1 *Haliclona viscosa* samples obtained from the Kongsfjord between 1999 and 2009. Spgn. = Spitsbergen, KFN = Kongsfjordneset, HNC = Hansneset Cave, Sec.Met. = secondary metabolites.

Year	1999	2000	2001	2003	2009	
ID	HAVI 025	CV 217	CV 218	MAK 301	09/23	09/27
Origin	Kongsfjord	Kongsfjord	Kongsfjord	KFN	KFN	HNC
Depth	15-25 m	15-25 m	15-25 m	12 m	16 m	2 m
Date/Season	May-June	Summer	Summer	20 June	June	June
Voucher[a]	16591	17008	17009		in Bremerhaven	
published	Chalinasterol	**43**	**43**	**29**, **30**	**61**, **62**	
	Cholesterol	**18**	**18**	**61**, **62**		
	27, **28**					

[a] Reference number of vouchers deposited at the Zoölogisch Museum Amsterdam

Table A.2 Key parameters of the type descriptions of different *Haliclona* sponges. *H.* = *Haliclona*, *R.* = *Reniera*, prim. = primary, sec. = secondary, paucisp. = paucispicular, unisp. = unispicular, ↓ = away from the extremities.

	H. viscosa Topsent 1888 [205]	*H. rosea* Bowerbank 1866	*H. indistincta* Bowerbank	*R. laxa* Lundbeck 1902 [206]
Consistency	firm, friable	soft, fragile	soft, friable	soft, fragile looser than *tubulosa*
Slime	very slimy			
Ectoskeleton	none	none	none	none
Surface		shiny, smooth		
Oscula	1-5 mm	0.5-2 mm 0.5-1 mm	1.5-3 mm	2-4 mm
	on ridges	few, scattered	sharp edges	round, flush
Prim. tracts	paucisp.	paucisp., wavy	paucisp.	paucisp.
Sec. tracts	unisp.	unisp.	unisp.	unisp.
Spongin	little	scarce, at nodes	little, at nodes	some, at nodes
Oxea length	110-150 µm	150-220 µm	110-150 µm	180-205 µm
Oxea width	3-8 µm	4-12 µm	3-8 µm	11 µm
Choanosome	disorderly ↓ confused	orderly	many spicules confused	orderly
Collected	0-50 m Shetlands- Mediterranean	0-200 m Arctic-Boreal	intertidal Britain, France, USA	80-180 m Iceland

Table A.3 Key parameters of the type descriptions of different *Haliclona* sponges. *R.* = *Reniera*, prim. = primary, sec. = secondary, paucisp. = paucispicular, unisp. = unispicular, polysp. = polyspicular, ↓ = away from the extremities.

	R. heterofibrosa Lundbeck 1902 [206]	*R. glacialis* Hentschel 1916 [207]	*R. mollis* Lambe 1893 [208]	*R. rufescens* Lambe 1892 [143]
Consistency				
Slime				
Ectoskeleton	none	none	none	none
Surface				
Oscula	1-2 mm	4 mm	5 mm	2 mm
Prim. tracts	paucisp.	paucisp.	paucisp.	unisp.
Sec. tracts	polysp.	unisp.	unisp.	unisp.
Spongin	some, at nodes	copious, at nodes		
Oxea lenght	160-178 µm	144-168 µm	196-262 µm	144 µm
Oxea width	5-10 µm	6-8 µm	13 µm	13 µm
Choanosome	disorderly ↓	disorderly ↓		
Collected	12 m	15-45 m	36-45 m	
	Iceland	Svalbard	Vancouver Is.	Kamtchatka

Table A.4 Key parameters of the type descriptions of different *Haliclona* sponges. *H.* = *Haliclona*, *R.* = *Reniera*, prim. = primary, sec. = secondary, paucisp. = paucispicular, unisp. = unispicular, ↑ = towards the extremities.

	R. tubulosa Fristedt 1902	*H. cinerea* Grant 1826	*R. calamus* Lundbeck 1902 [206]
Consistency	soft, firm	soft, fragile, compressible	hard, firm
Slime		slime strands	
Ectoskeleton	none	present, unisp.	none
Surface			
Oscula	2-4 mm		not always present
Prim. tracts	polysp.	unisp.	polysp.
Sec. tracts	unisp.	unisp.	unisp.
Oxea length	170-208 µm	80-140 µm	235-268 µm (straight) 107-150 µm (curved)
Oxea width	5-8 µm	3-8 µm	11/7 µm (straight/curved)
	varying ends	hastate, stylote	
Choanosome		disorderly ↑	rather irregular
Collected	18-55 m	inter-, subtidal	1 000-1 600 m
	Greenland, Iceland	NE Atlantic (Orkney-	Iceland
	Farøer	W Mediterranean)	

3-APAs from Haplosclerid sponges (except *Haliclona*)

Table A.5 3-Alkyl pyridinium and 3-alkyl tetrahydropyridine alkaloids isolated from different sponge genera.

Nr	Geographic region	Compound	Sponge
1	JPN, Shishi-shima	Cyclostellettamine A, G [209]	*Xestospongia* sp.
		Dehydrocyclostellettamine D, E [209]	*Xestospongia* sp.
2	JPN, Hachijo-jima	Cribrochalinamin oxide A, B [210]	*Cribrochalina* sp.
3	JPN, Sata, Shikoku Is.	Cyclostellettamine A–F [211]	*Stelletta maxima*
	JPN, Unten Bay	Theonelladins A–D [212]	*Theonella swinhoei*
	JPN, Kerama Is.	Manzamine A, B [213]	*Pellina* sp.
		Niphatesines A–D [214]	*Niphates* sp.
		Niphatesines E–H [215]	*Niphates* sp.
		Keramaphidine C [216]	*Amphimedon* sp.
		Keramamine C [216]	*Amphimedon* sp.
		Ircinol A, B [217]	*Amphimedon* sp.
		Manzamine A–C [217]	*Amphimedon* sp.
		Ircinal A, B [217]	*Amphimedon* sp.
		6-Hydoxymanzamine A [218]	*Amphimedon* sp.
		3,4-Dihydroxymanzamine A [218]	*Amphimedon* sp.
		Manzamine L [219]	*Amphimedon* sp.
		Ma'eganedin A [220]	*Amphimedon* sp.
	JPN, Miyako Is.	Manzamine E, F [221]	*Xestospongia* sp.
	JPN, Seragaki Is.	Zamamides A, B [222]	*Amphimedon* sp.
	JPN, Kise Is.	Ircinal A, B [223]	*Ircinia* sp.
	JPN, Aragusuku-jima	Araguspongines A–H, J [224]	*Xestospongia* sp.
		Aragupetrosine A [225]	*Xestospongia* sp.
	JPN, Iriomote Is.	Manzamine A, E, F, X [104]	*Xestospongia* sp.
		Xestomanzamine A, B [104]	*Xestospongia* sp.
5	FSM, Ant Atoll	Ikimines A–D [226]	unidentified sponge
	FSM, Pohnpei	Halitoxin, unbranched [125]	*Callyspongia fibrosa*
6	IDN, Sangihe Is.	Halicyclamine B [227]	*Xestospongia* sp.
7	IDN, Derawan Is.	Upenamide [228]	*Echinochalina* sp.
8	PNG, Laing Is.	Petrosin [81]	*Petrosia seriata*
		Petrosin A, B [229]	*Petrosia seriata*
	PNG, Madang	Ingamine A, B [230]	*Xestospongia ingens*
		Ingenamine [231]	*Xestospongia ingens*
		Mandangamine A [232]	*Xestospongia ingens*
		Ingenamine B–F [233]	*Xestospongia ingens*
9	PNG, Milne Bay	Xestocyclamine A [234]	*Xestospongia* sp.

		Xestocyclamine B [235]	*Xestospongia* sp.
	PNG, Motupore Is.	Motuporamine A–C [236]	*Xestospongia exigua*
10	FJI, Vitu Levu	Niphatynes A, B [237]	*Niphates* sp.
11	NCL, Baie de Prony	Xestospongin B, D [238]	*Xestospongia* sp.
		Araguspongine F [238]	*Xestospongia* sp.
		Demethylxestospongin B [238]	*Xestospongia* sp.
12	AUS, Capricorn Is.	Niphatoxin C [239]	*Callyspongia* sp.
13	AUS	Xestospongin A–D [82]	*Xestospongia exigua*
14	BHS, San Salvador Is.	Amphitoxin [240]	*Amphimedon compressa*
	BHS, Acklin Is.	Xestamines A–C [241]	*X. wiedenmayeri*
		Xestamines A, B, D–H [242]	*Calyx podatypa*
15	PRI, Isla Maguayez	Halitoxin, branched [80]	*Amphimedon compressa*
16	MTQ	Pachychalines A–C [121]	*Pachychalina* sp.
17	BRA, Ilha do Pai	Ingenamine G [116]	*Pachychalina* sp.
		Cyclostellettamine G–I, K, L [116]	*Pachychalina* sp.
	BRA, Búzios	Haliclonacyclamine E [243]	*Arenosclera brasiliensis*
		Arenosclerin A–C [243]	*Arenosclera brasiliensis*
18	ISR, Gulf of Eilat	Niphatoxin A, B [244]	*Niphates* sp.
19	IND, Andaman Is.	Araguspongin C, D, E [245]	*Xestospongia exigua*
		Xestospongin D [245]	*Xestospongia exigua*
		3α-Methylaraguspongin [245]	*Xestospongia exigua*

Country Codes: AUS = Australia, BRA = Brasil, BHS = Bahamas, FJI = Fiji, FSM = Micronesia, IDN = Indonesia, ISR = Israel, IND = India, JPN = Japan, MTQ = Martinique, NCL = New Caledonia, PNG = Papua New Guinea, PRI = Puerto Rico.

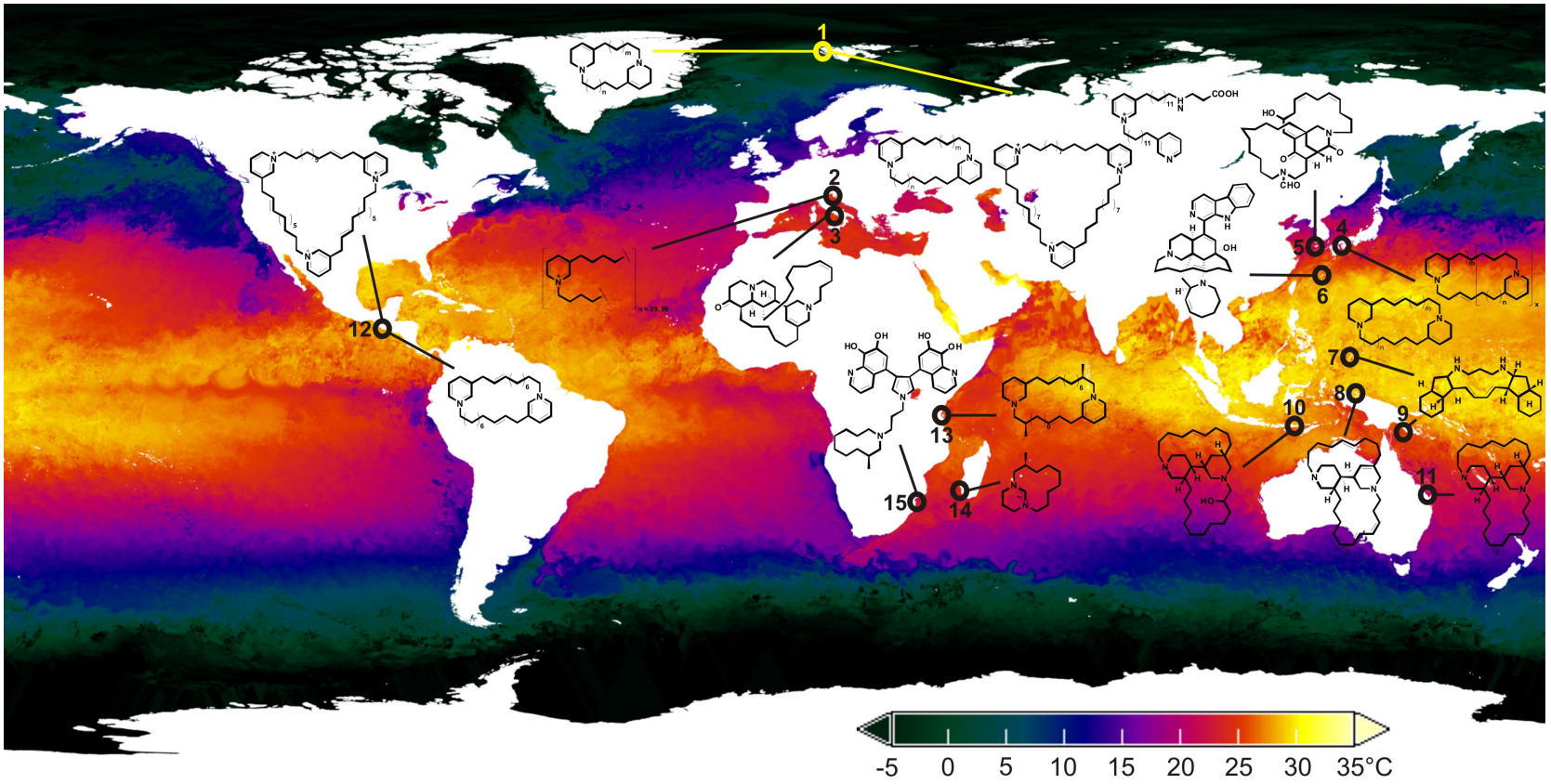

Figure A.1 World map of sea surface temperatures representing Northern hemisphere summer conditions (June 30, 2005). Numbers denote geographic regions as given in Table 3.1. Changed from NASA/Goddard Space Flight Center Scientific Visualization Studio http://svs.gsfc.nasa.gov/goto?3191.

Acknowledgements

For the joy of working under excellent conditions and the freedom to decide which way to go with my thesis I am deeply indebted to my coach, PD Dr. Matthias Köck. He always found the time to discuss my work and offer a different perspective. He always supported my plans to travel to distant islands knowing how much it means to a PhD student to be able to associate with otherwise dusty or slimy samples. But a PhD thesis is nothing without a proper committee; Prof. Dr. Thomas Lindel kindly assumed mentorship for this thesis and Prof. Dr. Uwe Schröder kindly acted as chairman for the defense.

This work was not possible without the help of many collaborators: I would like to thank Prof. Dr. Ute Hentschel, Hilde Angermeier, Laura Gallego (University of Würzburg) and Prof. Dr. Bininda-Emonds (University of Oldenburg) who helped with DNA and RNA analyses; Prof. Dr. Andreas Prange, Dipl.-Ing. Stephan Lassen, and Dr. Jürgen Gandraß (GKSS, Geesthacht) who enabled the MALDI-TOF-MS experiments; Dr. Andreas Jakob (Bruker Daltonics, Bremen) who supported me with Q-TOF measurements; Prof. Dr. Stefan Frickenhaus (AWI) who assisted in the world of computer models and Dr. Christoph Timm (University of Frankfurt) who provided synthetic compounds.

Expeditions are an exceptional time in the life of a researcher; to Prof. Dr. J. R. Pawlik and Prof. Dr. C. Schütt I am very thankful for the great opportunity to participate in their research cruises, their help and interest in my research. I am also very grateful to Dr. Michael Assmann whose sponge collections formed the basis of my work; to Prof. Dr. Rob W. M. van Soest for sharing his knowledge about sponge taxonomy; to Max Schwanitz who provided many of the underwater photographs used in this thesis; and the other members of the diving teams, Stefan,

Timo, Hannah, Sebastian, Marco, Mark, Sandra, Ireen, Tiff, Steve and Tim who were usually first to spot "the" sponge.

My collegues Dr. Achim Grube, Christine Cychon, Ellen Lichte, Dr. Sven Meyer, Dr. Thorsten Mordhorst and Qun Göthel have furnished our small working group with nice atmosphere, joyous, social activities, great discussions and mutual support. I especially would like to thank Christine for her help during the expeditions to Ny-Ålesund and trips to Geesthacht and Ellen for analytical and preparative HPLC measurements. And thank you, Achim - you filled my PhD student years with laughter and austerity, encouragement and friendship.

My friends who are not in science had to endure a great deal of chat about oceans and what treasures lie hidden in them. Dear Anne, Tobi, Zazie and Katharina, thank you for your patience with me, your refreshing friendship and for infecting me with your passion for high latitudes and deserted altitudes. Thanks to Franci, Fre, Geli, Katharina, Max, Marcus and Steffi for the good times, distraction from scientific thinking and your reassurance. There will always be a cold beer (if need be Jägermeister Tonic) in my fridge for you!

Dear Terje, thank you so much for the last years, your love, help, support and encouragement!

Ekki and Gorks – you are the ones who more than 22 years ago set the way. Without your courage, patience, constant reassurance and ever challenging inquisitiveness, the teenager with enthusiasm for oceans would probably have chosen to study something more "solid".